Durham University

Durham E-Theses

RS-invariant resummations of QCD perturbation theory

Tonge, Darrell Graham

How to cite:

Tonge, Darrell Graham (1997) *RS-invariant resummations of QCD perturbation theory*, Durham theses, Durham University. Available at Durham E-Theses Online: http://etheses.dur.ac.uk/4964/

Use policy

The full-text may be used and/or reproduced, and given to third parties in any format or medium, without prior permission or charge, for personal research or study, educational, or not-for-profit purposes provided that:

- a full bibliographic reference is made to the original source
- a link is made to the metadata record in Durham E-Theses
- the full-text is not changed in any way

The full-text must not be sold in any format or medium without the formal permission of the copyright holders.

Please consult the full Durham E-Theses policy for further details.

Academic Support Office, The Palatine Centre, Durham University, Stockton Road, Durham, DH1 3LE
e-mail: e-theses.admin@durham.ac.uk Tel: +44 0191 334 6107
http://etheses.dur.ac.uk

RS-Invariant Resummations of QCD Perturbation Theory

A thesis submitted for the degree of
Doctor of Philosophy
by

Darrell Graham Tonge

The copyright of this thesis rests with the author. No quotation from it should be published without the written consent of the author and information derived from it should be acknowledged.

Centre for Particle Theory
University of Durham
September 1997

- 3 APR 1998

Abstract

We propose a renormalon-inspired resummation of QCD perturbation theory based on approximating the renormalization scheme (RS) invariant effective charge (EC) beta-function coefficients by the portion containing the highest power of $b = (11N\text{–}2N_f)/6$, the first beta-function coefficient, for SU(N) QCD with N_f quark flavours. This can be accomplished using exact large-N_f all-orders results. The resulting resummation is RS-invariant and the exact next-to-leading order (NLO) and next-to-NLO (NNLO) coefficients in any RS are included. This improves on a previously employed naive leading-b resummation which is RS-dependent.

The RS-invariant resummation is used to assess the reliability of fixed-order perturbation theory for the e^+e^- R-ratio, hadronic tau-decay ratio R_τ, and Deep Inelastic Scattering (DIS) sum rules, by comparing it with the exact NNLO results in the EC RS. For R and R_τ, where large-order perturbative behaviour is dominated by a leading ultra-violet renormalon singularity, the comparison indicates fixed-order perturbation theory to be very reliable. For DIS sum rules, which have a leading infra-red renormalon singularity, the performance is rather poor.

We show that QCD Minkowski observables such as the R and R_τ are completely determined by the EC beta-function, $\rho(x)$, corresponding to the Euclidean QCD vacuum polarization Adler D-function, together with the NLO perturbative coefficient of D. An efficient numerical algorithm is given for evaluating R, R_τ from a weighted contour integration of $D(s\epsilon^{i\theta})$ around a circle in the complex squared energy s-plane, with $\rho(x)$ used to evolve in s around the contour.

The difference between the R, R_τ constructed using the NNLO and leading-b resummed versions of $\rho(x)$ provides an estimate of the uncertainty due to the uncalculated higher order corrections. We estimate that at LEP energies ideal data on the R-ratio could determine $\alpha_s(M_Z^2)$ to three-significant figures. For R_τ we estimate a theoretical uncertainty $\delta\alpha_s(m_\tau^2) \simeq 0.01$, corresponding to $\delta\alpha_s(M_Z^2) \simeq 0.002$. This encouragingly small uncertainty is much less than has recently been deduced from comparison with the analogous naive all-orders resummation, which we demonstrate to be extremely RS dependent and hence misleading.

Acknowledgements

I would especially like to thank my supervisor, Chris Maxwell, for his guidance and support throughout my three years in Durham. I am very grateful for the privilege and opportunity of working and collaborating with him.

My thanks go to Matt for putting up with me in the confined office space over the last three years, and to David 'the complete theoretical physicist' and Andrew 'the complete cynic' for always finding some form of humour (however sick) in the most dire situations. Beyond this I wish to express my thanks to all my fellow students, to numerous to mention, for making the Centre for Particle Theory such a pleasant place to work.

My gratitude goes to all the staff in the particle physics group here in Durham. To Nigel Glover, Valya Khoze, Alan Martin, Mike Pennington, James Stirling, and Mike Whalley, thank you all for giving me the opportunity to be part of the group.

Can I also thank all my friends outside CPT: the lads from Astrophysics who never let scientific discovery impinge upon valuable drinking time; the girls from archaeological conservation — they know who they are; and the original crew from Palatine House (in alphabetical order) — Dave, Gail, Jason, Peter, Phil and Rob. Most of all can I thank Ania, for her friendship, encouragement and support in my final year at Durham.

I would like to acknowledge PPARC for funding this research.

Most importantly, I would like to thank my parents and family, for always being there for me, and for their support and encouragement over the years. I dedicate this Ph.D. thesis to them.

This thesis is dedicated to my family,
to Mum and Dad
with all my love.

Declaration

I declare that no material presented in this thesis has previously been submitted for a degree at this or any other university.

The research described in this thesis has been carried out in collaboration with Dr. C.J. Maxwell and has been published as follows:

- RS-invariant all-orders renormalon resummations for some QCD observables, C.J. Maxwell and D.G. Tonge, Nucl. Phys. **B481** (1996) 681.
- The uncertainty in $\alpha_s(M_Z^2)$ determined from hadronic tau decay measurements, C.J. Maxwell and D.G. Tonge, Durham Preprint DTP/97/30 [hep-ph/9705314].

© The copyright of this thesis rests with the author.

Contents

Preface

Quantum Chromodynamics is the quantized gauge field theory of the strong interaction. It describes how the quanta of the strong interaction, *quarks* (massive fractionally-charged spin-$\frac{1}{2}$ fermions) and *gluons* (massless spin-1 gauge bosons) interact to form hadrons.

The theory of the strong interaction requires the introduction of a new quantum number – called *colour*. The quark fields are vectors in a three dimensional *colour space*, existing in three different colour states – red, green or blue; antiquarks in one of the corresponding anticolours. Since vectors are coordinate independent, the labelling is an arbitrary coordinate choice and it is possible to make a co-ordinate rotation in this colour space, intermixing the definitions of red, green and blue, without changing the physical content. This *global colour symmetry* can be described by the *non-abelian* group of SU(3). Observed hadrons can then only be formed from *colour singlet* (colourless) combinations of quarks and antiquarks: baryons consist of three quarks with different colours, mesons of a quark–antiquark pair with identical colours. Individual quarks cannot be colourless and are therefore not observed as free particles.

Global gauge invariance, however, requires rotation parameters to be propagated from one point in space to another arbitrarily quickly, which is unnatural. A much stronger restriction requires *local gauge invariance*. That is, a colour space rotation can be performed which varies at each space-time point. Enforcing quark-quark and quark-gluon interactions to conserve colour in a locally SU(3) invariant manner naturally leads to a idea of *Yang-Mills* theory of the strong interaction. The discovery that a Yang-Mills theory can incorporate masses while preserving renormalizability paved the way for QCD to take its place as one pillar of the *Standard Model* of elementary particle physics.

Quantum field theories such as QCD are not exactly solvable, the interaction of the underlying fields making the field equations intractable. In order to make physical predictions we use *renormalized perturbation theory*, an approximate method found to be extraordinarily successful for QED.

Considerable progress in understanding the strong interaction has been achieved through the application of perturbation theory to the more sophisticated theory of QCD. There are, however, important differences between the two theories of QED and QCD. The non-abelian structure of the colour group SU(3) is more complicated than the structure of the electromagnetic abelian group U(1); while QED only requires one uncharged gauge boson, the photon, QCD has 8 gluons which carry different combinations of colour charge. Apart from a coupling between gluons and quarks, QCD predicts the self-coupling of gluons. The profound consequence of this is that Yang-Mills theories, such as QCD, have the property of *asymptotic freedom.* Asymptotic freedom predicts that the coupling of quarks and gluons will diminish at high energies so that the quarks and gluons behave as free particles, which can be identified as the partons of deep inelastic scattering (DIS) experiments. At low energies the coupling grows, consequently one expects the quarks and gluons to be bound inside hadrons. At macrosopic distances, *confinement* effects dominate, and non-perturbative techniques become necessary.

In both QED and QCD we calculate the expansion coefficients exactly as a series in the coupling using Feynman diagrammatics; nonetheless computational difficulties limit the order in perturbation theory to a single figure. In QED the coupling is small enough to mean the this truncation of the expansion does not greatly affect our ability to predict physical quantities. In contrast the coupling in QCD is sufficiently large to create scope for non-negligible differences in predictions due to both neglected higher order terms in the perturbative expansion and ambiguities from an arbitrary choice of renormalization scheme. Our inability to disentagle these two factors is further complicated by non-perturbative effects and the interpretation of perturbation theory as an asymptotic series.

Thesis outline

This thesis will discuss a selection of ideas from renormalized QCD perturbation theory. These aspects will then be used to develop a formalism which will allow us to objectively assess the reliability of perturbative QCD predictions for a selection of phenomenologically interesting observables.

In Chapter 1 we assemble some of the ideas essential to an understanding of the subsequent chapters. After a description of the QCD Lagrangian we consider how the renormalization inevitably leads to the the introduction of a renormalization scheme (RS). The requirement that observables be independent of the RS leads directly to the central ideas of the renormalization group (RG) and running coupling. The non-trivial implications of these

two concepts are then discussed: dimensional transmutation, RG-improved perturbation theory, asymptotic freedom, and confinement. To link with the non-perturbative QCD we consider the operator product expansion (OPE), introduce the observables to be considered in later chapters and, finally, discuss the measurement of the coupling α_s and scale parameter Λ.

In Chapter 2 we focus on the problem of renormalization scheme (RS) dependence. We start by considering how the RS can be parameterized by a set of mutually independent variables to give an explicit realisation of the RG. Using this parameterization to identify RS-invariant quantities we exhibit the RS dependence of fixed-order perturbation theory. We then introduce a number of renormalization schemes to be encountered in later chapters and some proposed solutions to the RS dependence problem. Finally we detail the RG-invariant effective charge (EC) formalism, that allows the non-perturbative identification of each observable with an effective charge.

Chapter 3 focusses on the study of perturbation theory at large-orders. We start with a brief resume on the reasons why perturbation theory is expected to be divergent at large-orders, not just for QED but as a general property of quantum field theories. Interpreting the perturbative expansion as a asymptotic series we introduce the Borel transform to sum the series. Using the example of the vacuum polarization function and the idea of an expansion in a large number of quark flavours we isolate a class of diagrams that lead to the divergence of the perturbative theory in QED and QCD. Applying the Borel transform this behaviour leads to renormalon singularities in the Borel plane. The IR renormalons are then related to non-perturbative condensates using the OPE.

In Chapter 4 we motivate the use of a new expansion in the first beta-function coefficient for QCD. We review recent results in the application of this expansion to perform all-orders Borel resummations of QCD perturbation theory. The renormalization scheme dependence of the resulting expressions motivates the central idea of the chapter. We propose to incorporate fixed-order perturbation theory and resummation into a single expression which is explicitly invariant under the RG. To achieve this we apply the EC formalism. The resulting RS-invariant resummation is used to assess the reliablility of perturbation theory for a number of QCD observables, and assess the uncertainty in α_s and Λ. We discuss various possible improvements to the RS-invariant resummation.

In Chapter 5 we enhance this RS-invariant resummation procedure for Minkowski observables by incorporating to all-orders known analytical continuation terms. We assess the difference between the contour-improved RS-invariant resummation and the contour-

improved NNLO EC resummation to determine the uncertainty in α_s and Λ from hadronic tau decay. We provide simple numerical parametrizations to facilitate these fits. Our results are then compared with recent work which suggests a much larger uncertainty.

In Chapter 6 we present some concluding remarks on the thesis.

Chapter 1

A theoretical overview of QCD

1.1 Introduction

In this introductory chapter we give a brief overview of those elements of QCD theory which are essential to subsequent chapters. Beginning with the QCD Lagrangian we move on to consider renormalization in QCD. This naturally leads to the central ideas of the chapter: the renormalization scheme, renormalization group and running coupling α_s. The implications of these concepts are then discussed: the introduction of a mass scale Λ into massless QCD through dimensional transmutation, RG-improved perturbation theory, and asymptotic freedom. To link the perturbative and non-perturbative regions of QCD we then introduce the operator product expansion. Finally we define the QCD observables relevant to later chapters and consider the measurement of the strong coupling α_s and scale parameter Λ.

A detailed discussion of QCD theory and phenomenology can be found in references [1–4]. A historical background to the development of QCD can be found in reference [5].

1.2 The QCD Lagrangian

The theory is completely described by the minimal local SU(N) gauge invariant QCD Lagrange density given by

$$\mathcal{L}_{QCD} = \mathcal{L}_{classical} + \mathcal{L}_{gauge-fixing} + \mathcal{L}_{ghost} \,. \tag{1.1}$$

This is dependent on the quark fields, ψ_f, of flavour f, the gluon field, A^a_μ, and the ghost field, ω. We start by considering the colour symmetry group SU(N).

1.2.1 Colour SU(N)

Consider a set of Dirac four-component quark spinor fields, denoted ψ — vectors in a N dimensional *colour space*. The fields ψ transform under a irreducible representation of the non-abelian *Lie group* SU(N). SU(N) is then the group of local symmetry transformations,

$$\psi \longrightarrow \psi' = U(x)\psi \ , \tag{1.2}$$

where U are $N \times N$ *unitary* matrices, $U^\dagger U = UU^\dagger = 1$, with determinant one, $\det|U| = 1$. U has $N^2 - 1$ parameters and can be written,

$$U(x) = e^{i\Theta_a(x)T^a} \ , \tag{1.3}$$

where the repeated index implies summation over $a = 1 \ldots (N^2-1)$. The $N \times N$ hermitian matrices T^a are the *generators* of SU(N), and Θ_a are the parameters of the transformation. In the case of SU(3), T^a are known as the *colour matrices*. They obey the commutation relation

$$\left[T^a, T^b\right] = if^{abc}T^c, \tag{1.4}$$

where f^{abc} are the *structure constants* of QCD, which are real and antisymmetric. The set of T^a's satisfying the commutation relation is called the *Lie algebra* of the Lie group. Also, since $\det|U| = \det\left|e^{i\Theta_a T^a}\right| = e^{i\Theta_a Tr(T^a)}$, it follows that T^a are traceless. We may choose a normalization so that the colour matrices give the following relations:

$$Tr(T^aT^b) = T_F\delta^{ab} \quad \Longrightarrow \quad T_F = \frac{1}{2} \tag{1.5}$$

$$\sum_a T^a_{\alpha\beta}T^a_{\beta\gamma} = C_F\,\delta_{\alpha\gamma} \quad \Longrightarrow \quad C_F = \frac{N^2-1}{2N} \tag{1.6}$$

$$\sum_{c,d} f^{acd}f^{bcd} = C_A\delta_{ab} \quad \Longrightarrow \quad C_A = N \ . \tag{1.7}$$

T_F, C_A, C_F are *colour factors*, the eigenvalues of the SU(N) invariant Casimir operators.

1.2.2 The classical QCD Lagrangian

$\mathcal{L}_{classical}$ describes the dynamics of QCD — the interaction of massive spin-$\frac{1}{2}$ quarks and massless spin-1 gluons — and is given by,

$$\mathcal{L}_{classical} = \sum_f \bar{\psi}_f \left(i\,\not{D}^\mu - m_f\right)\psi_f - \frac{1}{4}F^a_{\mu\nu}F_a^{\mu\nu}. \tag{1.8}$$

Here the sum is over N_f quark flavours and m_f is the quark mass. The metric is given by $g^{\mu\nu} = \mathrm{diag}(1,-1,-1,-1)$ and the gamma matrices satisfy the anticommutation relations

$\{\gamma^\mu, \gamma^\nu\} = 2g^{\mu\nu}$. $\mathcal{D}$ is the covariant derivative acting on both triplet and octet fields, defined by,

$$\mathcal{D}^\mu = \partial^\mu + igA_a^\mu T^a, \tag{1.9}$$

where g is the coupling strength of the interaction between coloured quarks and gluons. The field strength tensor, $F_a^{\mu\nu}$ is given by,

$$F_a^{\mu\nu} = \partial^\mu A_a^\nu - \partial^\nu A_a^\mu + g f_{abc} A_b^\mu A_c^\nu. \tag{1.10}$$

where the colour indices a, b, c run over the eight colour degrees of freedom of the gluon field A_μ^a. From Eq.(1.9) and (1.10) one can obtain the commutation relation

$$[\mathcal{D}_\mu, \mathcal{D}_\nu] = igT^a F_a^{\mu\nu} \,. \tag{1.11}$$

1.2.3 Local gauge invariance

The Lagrangian $\mathcal{L}_{classical}$ is invariant under local SU(N) gauge transformations. One can thus redefine the quark fields independently at every point in space-time without changing the physical content of the theory. Formally, the quark spinor fields and covariant derivative transform as the fundamental representation under a local SU(N) gauge transformation

$$\psi(x) \longrightarrow \psi'(x) \equiv U(x)\psi(x) \tag{1.12}$$

$$\mathcal{D}_\mu\psi(x) \longrightarrow \mathcal{D}'_\mu\psi'(x) \equiv U(x)\mathcal{D}_\mu\psi(x)\,. \tag{1.13}$$

Eqs.(1.11–1.13) can be used to fix the transformation properties of the covariant derivative, gluon field and non-abelian field strength tensor

$$\begin{aligned} \mathcal{D}_\mu \longrightarrow \mathcal{D}'_\mu &= U\mathcal{D}_\mu U^\dagger \\ T_a A_\mu^a \longrightarrow T_a A_\mu^{a\prime} &= UT_a A_\mu^a U^\dagger + \frac{i}{g}(\partial_\mu U)U^\dagger \\ T^a F_a^{\mu\nu} \longrightarrow T^a F_a^{\mu\nu\prime} &= UT^a F_a^{\mu\nu} U^\dagger \,. \end{aligned} \tag{1.14}$$

One sees that the gluon field transforms as the adjoint representation and the field strength tensor transforms in the same manner as the quark field. In analogy with QED there is no gauge invariant method by which one can obtain a mass for the gluon since a term $m^2 A^a A_a$ violates gauge invariance.

Decomposing the classical Lagrangian into separate pieces:

$$\mathcal{L}_{classical} = -\frac{1}{4}(\partial^\mu A_a^\nu - \partial^\nu A_a^\mu)(\partial_\mu A_\nu^a - \partial_\nu A_\mu^a) + \sum_f \bar{\psi}_f \left(i\gamma^\mu\partial_\mu - m_f\right)\psi_f$$

$$- g\, A_a^\mu \sum_f \bar{\psi}_f \gamma_\mu T^a \psi_f \tag{1.15}$$

$$+ \frac{g}{2} f^{abc} \left(\partial^\mu A_a^\nu - \partial^\nu A_a^\mu\right) A_\mu^b A_\nu^c - \frac{g^2}{4} f^{abc} f_{ade} A_b^\mu A_c^\nu A_\mu^d A_\nu^e ,$$

some properties of this Lagrange density are immediately apparent

- All interactions are given in terms of a single universal coupling g, which is called the *strong coupling constant.* g is the only free parameter in the Lagrangian.
- The first line contains the kinetic terms for the different fields, giving rise to the corresponding propagators.
- The colour interaction between quarks and gluons is given by the second line; it involves the SU(3) matrices T^a.
- Owing to the non-abelian structure of the SU(3) colour group, the term quadratic in the gluon field A_a^μ in $F_a^{\mu\nu}$ generates cubic and quartic gluon self-interactions in the $F_a^{\mu\nu} F_{\mu\nu}^a$ term, as shown in the last line; the strength of these three and four point interactions is given by the same coupling g which appears in the fermionic piece of the Lagrangian. Therefore the *gluon carries a colour charge.*

The existence of self-interactions among the gauge fields is a new feature that was not present in QED. The presence of glue-glue interactions leads to the property of asymptotic freedom and presumably is also responsible for confinement.

1.2.4 Gauge fixing and ghost fields

The fields A_a^μ have 4 Lorentz degrees of freedom (polarizations) while a massless spin-1 gluon has 2 physical polarizations only. Although gauge invariance makes these additional degrees of freedom irrelevant, they give rise to technical complications when quantizing the theory.

The canonical momentum associated with A_a^μ, $\pi_\mu^a(x) \equiv \delta\mathcal{L}/\delta(\partial_0 A_a^\mu) = A_{\mu 0}^a$, vanishes identically for $\mu = 0$. The standard commutation relation is then meaningless for $\mu = \nu = 0$. In fact, the field A_a^0 is just a classical quantity, since it commutes with all the other fields. This is expected since we know that there are 2 unphysical components of the gluon field which should not be quantized.

Gauge-fixing

In order to prevent this a *gauge-fixing* term must be added. An arbitrary choice can be made as to how the gauge should be fixed, and all physical quantities should be independent of this choice. One can impose a Lorentz-invariant gauge condition, such as $\partial_\mu A^\mu_a = 0$. The simplest way to implement this is to add to the Lagrangian the gauge-fixing term

$$\mathcal{L}_{gauge-fixing} = -\frac{1}{2\xi}(\partial^\mu A^a_\mu)(\partial_\nu A^\nu_a) \tag{1.16}$$

where ξ is the so-called gauge parameter. Setting $\xi = 1$ ($\xi = 0$) in Eq.(1.16) we obtain the *Feynman gauge* (*Landau gauge*). The 4 Lorentz components of the canonical momentum $\pi^a_\mu(x) \equiv \delta\mathcal{L}/\delta(\partial_0 A^\mu_a) = A^a_{\mu 0} - \frac{1}{\xi} g_{\mu 0}(\partial^\nu A^a_\nu)$ are then non-zero, and one can develop a covariant quantization formalism [1].

Ghost fields

In covariant gauges the gluon propagator still contains 4 polarization components. To ensure gauge-fixing does not violate the unitarity of the S-matrix we must add a Faddeev–Popov *ghost* Lagrangian

$$\mathcal{L}_{ghost} = -\partial_\mu \bar{\omega}_a \mathcal{D}^\mu \omega^a , \qquad \mathcal{D}^\mu \omega^a \equiv \partial^\mu \omega^a - g f^{abc} \omega^b A^\mu_c , \tag{1.17}$$

where ω^a, $\bar{\omega}^a$ ($a = 1, \ldots, N^2 - 1$) is a set of anticommuting, massless, hermitian, scalar fields. These additional *ghost fields*, provided with the necessary coupling to the gluon field and obeying the wrong statistics, exactly cancel unphysical probabilities from scalar and longitudinal gluon polarizations propagating along the internal lines of loop diagrams. The exact mechanism giving rise to the Faddeev–Popov term can be understood using the path-integral formalism (for more details see [6]).

1.3 Renormalized QCD perturbation theory

In analogy with QED, we make physical predictions in QCD by calculating the S-matrix using perturbation theory, computing the expansion coefficients using Feynman diagrammatics. As in QED, the integrals associated with Feynman diagrams are divergent. There-

[1] An alternative choice is provided by axial gauges, $\mathcal{L}_{gauge-fixing} = -\frac{1}{2\xi}(n^\mu A^a_\mu)(n_\nu A^\nu_a)$. Ghost fields are not then unnecessary but the form of the gluon propagator is more complicated and additional unphysical poles exist at $n \cdot p = 0$.

fore to obtain physical meaning from a priori meaningless divergent quantities requires the use of regularization and renormalization.

1.3.1 The perturbative expansion of the S-matrix

For particles of definite momenta the probability of quantum transitions from initial to final states is given by the S-matrix. The S-matrix is mathematically constructed from physical principles: analyticity as a mathematical formulation of microscopic causality, unitarity as probability conservation, crossing symmetry as a general property of Feynman diagrams, and the position and character of the cut in the complex energy plane as a description of the properties of the particle spectrum. This S-matrix can be formally linked to the Lagrange density given in Eq.(1.1) using Feynman's *Path Integral* formalism (for more details see [6]). Furthermore, when the strong coupling constant is small, a perturbative expansion of the S-matrix can be made and the usual QCD Feynman rules derived. These allow S-matrix elements to be calculated by drawing all topologically distinct Feynman diagrams, of the appropriate order, linking initial and final states. These diagrams are then translated into mathematical formulae using the Feynman rules.

The Feynman rules are defined from the action operator

$$S = i \int \mathrm{d}^4 x \mathcal{L}(x) \; . \tag{1.18}$$

The inverse propagators are obtained from $-S_0$ and the interactions, to be considered as perturbations, from S_I. Separating the Lagrangian density into a free piece $\mathcal{L}_0$ and interacting piece $g\mathcal{L}_I$ the Feynman rules can then be determined. Equations (1.8), (1.16) and (1.17) are sufficient to derive these Feynman rules in a covariant gauge (see for example [4]). The Feynman rules, in a covariant gauge, can be found in [3].

The Feynman rules allow us to define *Green functions* in momentum space. These are vacuum expectation values of time-ordered products of fields

$$(2\pi)^4 \delta(q_1 + \cdots + q_n) \Gamma_{\alpha_1 \cdots \alpha_n}(q_1 \cdots q_n) = \prod_{i=1}^{n} \int \mathrm{d}^4 x \mathrm{e}^{-iq\cdot x} \langle 0 | T(\phi_{\alpha_1}(x_1) \ldots \phi_{\alpha_n}(x_n) | 0 \rangle \; . \tag{1.19}$$

where α_i represent space-time and group indices of the fields denoted by $\phi(x)$. The Green function Γ is the sum of all Feynman diagrams. All of the information of the theory is contained in the Green functions.

In practical terms the inverse quark and gluon propagators can be obtained from the the free piece, $\mathcal{L}_0$, of the QCD Lagrangian. We make the identification $\partial^\mu = -iq^\mu$

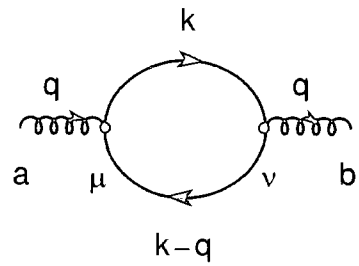

Figure 1.1: Contribution to the gluon self-energy diagram.

for an incoming field, the inverse quark propagator in momentum space is found to be $-i\delta_{ab}(\not{q} - m)$. The quark propagator is then

$$\Delta^{(2)}_{ab}(q) = \delta_{ab}\left(\frac{i}{\not{q} - m + i\epsilon}\right) . \tag{1.20}$$

Similarly, the gluon propagator is given by

$$\Delta^{(2)}_{\{ab,\,\mu\nu\}}(q) = \delta_{ab}\frac{i}{q^2 + i\epsilon}\left[-g_{\mu\nu} + (1-\xi)\frac{q_\mu q_\nu}{q^2 + i\epsilon}\right] . \tag{1.21}$$

Without a gauge fixing term it is impossible to define the gluon propagator in a covariant gauge.

Higher-order perturbative corrections to tree-level results in QCD involve Feynman diagrams containing closed particle loops. These loop diagrams translate to give divergent integrals which can be classified into two types:

- *Ultra-Violet divergences*: caused by the divergent behaviour of the integrand as the loop momenta becomes large. One can interpret these loop integrals as probing the very short distance region of space-time (or high momenta region of momentum space). They are removed by a redefinition of the quark-gluon coupling, absorbing the infinity, in a process known as *renormalization.*

- *Infra-Red divergences*: caused by the divergent behaviour of the integrand as the loop momenta becomes small, such divergences have been shown to cancel at all orders in perturbation theory for physical observables [8].

As an example consider the one-loop correction given by the inclusion of a fermion in the gluon propagator (contributing to the gluon self-energy) in Figure 1.1. The corresponding

contribution in momentum space can be easily obtained, using Feynman rule methods:

$$i\Pi^{\mu\nu}_{ab}(q) = -g^2\delta_{ab}N_f T_F \int \frac{\mathrm{d}^4k}{(2\pi)^4} \frac{\mathrm{Tr}[\gamma^\mu \not{k}\gamma^\nu(\not{k}-\not{q})]}{k^2(k-q)^2} \tag{1.22}$$

The result is proportional to g^2, because there are two $q\bar{q}g$ vertices, and there is a trivial colour factor, $T_F = \frac{1}{2}$. Momentum conservation is insufficient to constrain the momenta flowing around the loop, and as a result the momentum must be integrated over.

The problem appears in the unconstrained momentum integration. The integral is clearly logarithmic divergent due to the behaviour of the integrand for large k

$$i\Pi^{\mu\nu}_{ab}(q) \sim \int \frac{\mathrm{d}^4k}{k^4} \sim \int \frac{k^3\mathrm{d}k}{k^4} \int \mathrm{d}\Omega \sim \infty \,, \tag{1.23}$$

where Ω is a solid angle.

1.3.2 Regularization

The manipulation of divergent integrals is not well defined, so we require a method of rendering each integral, order by order, finite. The introduction of a suitable convergence device is generically termed *regularization*. After rearranging the perturbative series so that the divergent terms are collected into the physical parameters we remove the regulator to recover our physical theory. The resulting theory must be independent of the regularization method since it is a purely mathematical device required to define the theory at the quantum level.

For QCD the most versatile method is *dimensional regularization* (DR) [9]. The idea of DR is to render the divergent integral finite by reducing the number of multiple integrals. This is achieved by changing the number of space-time dimensions from 4 to $n < 4$. Explicitly making momentum integrations we obtain an analytic expression as a function of n. Analytically continuing to $n = 4$ the divergence exhibits itself in the expression as a pole at $n = 4$.

For example consider using DR with $n = 4 - 2\epsilon$ dimensions to regulate the UV divergence in the integral of Eq.(1.22). To preserve the dimensions of the coupling and fields (g must remain dimensionless in $4 - 2\epsilon$ dimensions) we introduce a scale μ with $g \longrightarrow g\mu^\epsilon$ so that

$$g^2\frac{\mathrm{d}^4k}{2\pi^4} \longrightarrow g^2\mu^{2\epsilon}\frac{\mathrm{d}^{4-2\epsilon}k}{2\pi^{4-2\epsilon}} \,. \tag{1.24}$$

In practice the pole at $\epsilon = 0$ always appear in the combination

$$\frac{\Gamma(1+\epsilon)}{\epsilon}(4\pi)^\epsilon = \frac{1}{\epsilon} + \ln(4\pi) - \gamma_E + O(\epsilon) \,. \tag{1.25}$$

where the Γ function is defined in Eq.(A.1).

Making a Lorentz decomposition and using a Feynman parametrization to carry out the integration we then have

$$\Pi^{\mu\nu}_{ab}(q^2) = \delta_{ab}(-q^\mu q^\nu + g^{\mu\nu}q^2)\Pi(q^2)\,, \tag{1.26}$$

with

$$\Pi(q^2) = \frac{4}{3}N_f T_f \frac{g^2}{16\pi^2}\mu^{2\epsilon}\left(\frac{1}{\epsilon} - \gamma_E + \ln 4\pi + \ln -\frac{q^2}{\mu^2} + \frac{5}{3} + O(\epsilon)\right)\,. \tag{1.27}$$

where $\gamma_E = 0.57722\ldots$ is the Euler-Mascheroni constant.

Unlike other forms of regularization, which violate many of the underlying physical features, DR preserves all properties of the original action which are independent of the dimensions of space-time, such as Ward-Takahashi identities; thus the regularized theory is Lorentz invariant, gauge invariant and unitary.

1.3.3 Renormalization

Given a regularized set of divergences we are in a position to renormalize the theory. A common method by which to do this is *multiplicative renormalization* (MR), briefly mentioned below. For a complete discussion of the theory of regularization and renormalization see reference [10].

Multiplicative renormalization

Multiplicative renormalizability (MR) ensures that for every *bare* (unrenormalized) operator there exists a regulator dependent multiplicative factor Z, the *renormalization constant*, that makes the operator independent of the regulator when expressed in terms of renormalized quantities. MR involves summing the infinite series of loop diagrams for some fixed number of external lines. This divergent sum is then absorbed into a redefinition of the coupling constant and the mass in the bare Lagrangian, under the assumption that the bare coupling g_B and mass are unmeasurable quantities.

For example in QCD we redefine the fields and parameters by

$$\begin{aligned}
&\psi_B = Z_\psi^{1/2}\psi\,, \quad A^A_{\mu\,B} = Z_A^{1/2}A^A_\mu\,, \quad \omega^A_B = Z_\omega^{1/2}\omega^A \\
&g_B = Z_g g\,, \quad m_B = Z_m m\,, \quad \xi_B = Z_A\xi\,,
\end{aligned} \tag{1.28}$$

where B denotes the bare operator. A renormalizable theory will require only a finite number of Z's to render it finite to any order. An important property of gauge theories, such as QED or QCD, is that the underlying gauge invariance guarantees the renormalizability of the theory by reducing the number of renormalization constants required. Specifically, only one Z_ψ is required for all quark fields and only one Z_A for both the gauge parameter and gluon field. The 3-point ($\bar{\psi}\psi A_\mu$, $A_\mu A_\nu A^\mu$), four-point ($A_\mu A_\nu A^\mu A^\nu$) and ghost-gluon interactions ($\bar{\omega}\omega A_\mu$) involve the same Z_g hence only a single renormalized coupling is required [2].

Returning to the Eq.(1.27) we absorb the divergent one-loop correction into the definition of the coupling

$$g^2(\mu^2) = g_B^2 \mu^{2\epsilon} \left\{ 1 - g_B^2 \mu^{2\epsilon} N_f \frac{T_f}{12\pi^2} \left[\frac{1}{\epsilon} + \text{finite} \right] + \ldots \right\} , \tag{1.29}$$

where the constant 'finite' denotes the different finite terms in Eq.(1.29). We renormalize at the spacelike momenta $Q^2 \equiv -q^2$ so as to avoid particle thresholds. The redefinition Eq.(1.29) is meaningful, provided that it can be done in a self-consistent way: all ultraviolet divergent contributions to all possible scattering processes should be eliminated through the same redefinition of the coupling (and the fields).

The scattering amplitude for the gluon self-energy is of the form $\mathcal{R}(Q^2) \sim g^2 [1 - \Pi + \cdots]$. Making the redefinition Eq.(1.29), the scattering amplitude is finite and gives rise to a definite prediction for the observable, which can be compared with experiment; thus, one actually measures the *dressed* (renormalized) coupling g^2. We then have

$$\begin{aligned} \mathcal{R}(Q^2) &\sim g^2 \left\{ 1 - \Pi_{\mathcal{R}}(Q^2/\mu^2) \right\} \\ &\sim g^2 \left\{ 1 - g^2(\mu^2) N_f \frac{T_f}{12\pi^2} \left(\ln \left(\frac{Q^2}{\mu^2} \right) + \text{finite} \right) + \ldots \right\} . \end{aligned} \tag{1.30}$$

Renormalization schemes

According to the renormalization program we subtract all the divergences from the Green functions systematically order-by-order in perturbation theory. While the infinities are removed uniquely, there still exists a two-fold arbitrariness in this procedure:

- The arbitrariness of fixing the *renormalization scale*, μ. Regularization of loop integrals introduces an arbitrary mass scale μ, the point at which the subtractions

[2] The proof of these statements involves using Slavnov-Taylor (generalized Ward-Takahashi) identities; these identities guarantee the universality of the renormalized coupling g, see reference [1].

to remove the UV divergences are performed. The Green functions, such as $g^2(\mu^2)$ and the renormalized self-energy correction $\Pi_{\mathcal{R}}(Q^2/\mu^2)$, are dependent on our choice of μ, but the physical observable $\mathcal{R}(Q^2)$ is of course μ-independent.

- The arbitrariness of choosing the *renormalization prescription* set up to subtract divergences. There is a choice in how to define a divergent piece in a Green function i.e. how much of the finite piece is to be subtracted together with the infinity. For example, the convention used to split the self-energy contribution $\Pi_{\mathcal{R}}(Q^2/\mu^2)$ into a divergent piece and a finite term, including the Q^2 dependence, is ambiguous because the finite Q^2-independent contributions can be separated in many different ways. Note, however, that the logarithmic Q^2-dependence is always the same.

In a broader sense these two arbitrary choices can be termed the *renormalization scheme* (RS). Just as the renormalization scale can be characterized by the parameter μ, it is also possible to give an explicit parameterization for the renormalization prescription. A discussion of the renormalization scheme dependence and its parameterization is the focus of Chapter 2.

1.4 The renormalization group

The arbitrary choice of RS means that we have many possible expressions for a physical observable. As these expressions are obtained for a single physical observable starting from a unique Lagrangian they must be equivalent. This independence of the physical parameters from changes in the RS is mathematically expressed in terms of the *renormalization group* (RG).

To see how this can come about we will restrict ourselves to considering the invariance of physical observables under changes of renormalization scale, μ. This invariance under the Gell-Mann-Low renormalization group [11] is a simple subset of the general Stueckelberg and Petermann renormalization group transformations [12]. A discussion of the more general RG transformations is considered in Chapter 2.

We consider a generic Green function Γ (say the coupling or mass) in two RS's, barred and unbarred. If Γ_B is the bare quantity and Γ is the renormalized quantity then

$$\Gamma = Z\Gamma_B\,, \qquad \bar{\Gamma} = \bar{Z}\bar{\Gamma}_B\,. \tag{1.31}$$

A transformation from the unbarred to barred scheme is effected by a renormalization

$$\bar{\Gamma} = z\Gamma \,, \qquad z = \frac{\bar{Z}}{Z} \,, \tag{1.32}$$

where z is a *finite* renormalization, since the divergent part in $\bar{Z}$ cancels with that of Z owing to its multiplicative nature. Eq.(1.32) defines a set of finite renormalizations $\{z(\bar{\mu}, \mu)\}$ for varying scale $\mu, \bar{\mu}$ which we may regard as transformations that possess group properties.

Since all the possible expressions for a physical observable are connected via a finite renormalization of Eq.(1.32), the uniqueness of the physical prediction implies that the observable $\mathcal{R}$ is invariant under a finite renormalization.

$$\bar{\mathcal{R}}(q, \bar{g}, \bar{m}, \bar{\mu}) = \mathcal{R}(q, g, m, \mu) \,, \tag{1.33}$$

where g, $\bar{g}$ and m, $\bar{m}$ are the renormalized coupling and mass in the two schemes with renormalization scales μ, $\bar{\mu}$. Though the functional form of $\mathcal{R}$ and $\bar{\mathcal{R}}$ may be different, the numerical values are identical. Unfortunately, we do not have the exact expression for $\mathcal{R}$. Instead we calculate $\mathcal{R}$ through a perturbation series in g^2 which is truncated at order g^{2n}, neglecting higher-order terms. One then finds that $\mathcal{R}$ and $\bar{\mathcal{R}}$ differ by $O(g^{2n+2})$. This is the source of the RS dependence discussed in Chapter 2.

1.4.1 The renormalization group equation

For an infinitesimal change in the scale μ the transformations of the renormalization group are expressible in terms of a differential equation – the *renormalization group equation* (RGE). The RGE appropriate for changes of scale μ is based on the observation that the physical theory cannot depend on our arbitrary choice of μ. In order to keep the physics invariant, changes in scale μ must be offset by compensating changes in other renormalized physical parameters, such as the masses and coupling.

We can understand how this feature arises in MR since we have a multiplicative relation between the Green functions of the bare theory and renormalization theory. However, the bare theory is totally independent of the scale μ; we can express this as

$$\mu \frac{\mathrm{d}}{\mathrm{d}\mu} \Gamma_B^{(n)} = 0 \,. \tag{1.34}$$

Thus, to ensure the bare Green function is independent of the μ, there must be a non-trivial relation between the renormalization Green function and the renormalization constant Z; a relation that is expressed by the RGE.

To be more precise consider a generic dimensionless QCD observable $\mathcal{R}(Q)$ where Q denotes the single dimensionful scale on which it depends (typically the centre of mass energy $\sqrt{s}$). We assume massless QCD — valid if the scale Q is much greater than all other dimensionful parameters such as quark masses and if $\mathcal{R}$ has a defined massless limit. For later convenience we rewrite the strong coupling in the form [3]

$$a = \frac{\alpha_s}{\pi} = \frac{g^2}{4\pi^2} \,. \tag{1.35}$$

Then from Eq.(1.34) we see then that if we hold the bare coupling fixed, the physical observable $\mathcal{R}$ cannot depend on our choice for μ. Since $\mathcal{R}$ is dimensionless, it can only depend on the ratio Q/μ and the renormalized coupling α_s. Mathematically, we express this μ independence of $\mathcal{R}$ as

$$\mu\frac{d}{d\mu}\mathcal{R}(Q/\mu, a) \equiv \left[\mu\frac{\partial}{\partial\mu} + \beta(a)\frac{\partial}{\partial a}\right]\mathcal{R}(Q/\mu, a) = 0 \,, \tag{1.36}$$

where

$$\beta(a) = \mu\frac{\partial a}{\partial\mu} \,. \tag{1.37}$$

Eq.(1.36) is the *renormalization group equation* (RGE). Eq.(1.37) is a renormalization group function termed the *beta-function*. The differentiation in the definition of Eq.(1.37) is performed at fixed bare coupling.

1.4.2 The running coupling

The RGE represents a powerful constraint on the renormalized Green functions of any quantum field theory, yielding important consequences. For our purpose the most important is the *running coupling*. In order to introduce this concept we rewrite Eq.(1.36) in the form

$$\left[-\frac{\partial}{\partial t} + \beta(a)\frac{\partial}{\partial a}\right]\mathcal{R}(e^t, a) = 0 \,, \quad t = \ln\left(\frac{Q}{\mu}\right) \,. \tag{1.38}$$

We solve Eq.(1.38) by implicitly defining a running coupling $\alpha_s(Q)$, as follows

$$\beta(a(Q)) = \frac{\partial a(Q)}{\partial t} \,, \tag{1.39}$$

Integrating Eq.(1.39) we have

$$t = \int_a^{\bar{a}} \frac{dx}{\beta(x)}, \quad a(\mu) \equiv a \,, \quad a(Q) \equiv \bar{a}. \tag{1.40}$$

[3] This is defined in analogy with the fine structure constant in QED.

Formally we have applied the RGE to obtain

$$\mathcal{R}(e^t, a(\mu)) = \mathcal{R}(1, a(Q)) \,. \tag{1.41}$$

and hence we see that $\mathcal{R}(a(Q))$ is a solution of Eq.(1.38). All of the scale dependence in $\mathcal{R}$ enters through the running of the coupling constant $\alpha_s(Q)$, so that, given a perturbative calculation of $\mathcal{R}$, its variation with Q can be determined by solving Eq.(1.40).

1.5 The QCD beta-function

Before moving on to consider the beta-function equation in more detail, we will make as small digression to consider the phenomena of dimensional transmutation.

1.5.1 Dimensional transmutation

Let use consider the observable $\mathcal{R}(Q)$ in massless QCD. Naive scaling would suggest that because there is a single large scale, $\mathcal{R}$ should have a constant value independent of Q. This result is not correct in a renormalizable quantum field theory. Renormalization introduces a second mass scale μ so that $\mathcal{R}$ depends in general on the ratio Q/μ and is therefore not constant.

The running behaviour of $\mathcal{R}$ with Q can be written as

$$Q\frac{\mathrm{d}\mathcal{R}}{\mathrm{d}Q} = \rho(\mathcal{R}) \,. \tag{1.42}$$

Integrating Eq.(1.42) yields

$$\ln Q + \textit{finite constant} = \int_{\infty}^{\mathcal{R}} \frac{\mathrm{d}x}{\rho(x)} \equiv f(\mathcal{R}(Q)) \,. \tag{1.43}$$

The definition of the observable $\mathcal{R}$ is non-unique since it contains an integration constant to be specified. The choice of integration limit at infinity ensures a unique specification of the r.h.s of Eq.(1.43), so that the l.h.s contains all arbitrariness.

Since $f(\mathcal{R})$ must be dimensionless, we introduce the arbitrary unphysical mass parameter μ in order to compensate for the dimensionful quantity Q. Q is then measured in arbitrary units of μ. Since all physical observables must be independent of the units in which we measure them, $f(\mathcal{R})$ cannot depend upon μ, implicitly or explicitly. We therefore introduce the ansatz

$$\text{finite constant} = f(\mathcal{R}(\mu)) - \ln \mu \,, \tag{1.44}$$

so that

$$f(\mathcal{R}(Q)) = \ln \frac{Q}{\mu} - f(\mathcal{R}(\mu)) \; . \tag{1.45}$$

To obtain the observable $\mathcal{R}(Q)$ we invert $f(\mathcal{R}(Q))$

$$\mathcal{R}(Q) = f^{-1}\left(\ln \frac{Q}{\mu} - f(\mathcal{R}(\mu)) \right) \; . \tag{1.46}$$

By definition $\mathcal{R}(Q))$ can only depend on Q, so to eliminate the dependence on μ in the argument of f^{-1} we set

$$f(\mathcal{R}(\mu)) = \ln \frac{\mu}{\Lambda} \; . \tag{1.47}$$

So finally

$$\mathcal{R}(Q) = f^{-1}\left(\ln \frac{Q}{\Lambda} \right) \; . \tag{1.48}$$

Crucially we see that $\mathcal{R}(Q)$ is a now a function of Q and Λ.

Starting with the running behaviour of a dimensionless quantity in a massless field theory (QCD), one has introduced an arbitrary mass scale μ necessary by dimensional analysis arguments. As a direct result, and to compensate for this scale, a massive parameter Λ has been 'discovered'.

Eq.(1.48) is exact and does not show any dependence upon μ. However, in perturbation theory the function $\rho(\mathcal{R}(Q))$ will be expanded as a power series in $\mathcal{R}$ and truncated at order n. The renormalized coupling α_s and perturbative coefficients will then depend on the choice made for the scale μ. Integrating this truncated equation renders only an approximate result, dependent on μ, that only asymptotically ($Q \to \infty$) reaches the exact result of Eq.(1.48). The dependence of truncated perturbation theory upon the unphysical μ is one part of the larger problem of renormalization scheme dependence.

1.5.2 The beta-function equation and Λ parameter

Massless perturbative QCD is a theory with only one free parameter — the bare coupling g_B in the classical Lagrangian. Quantizing the classical Lagrangian results in an infinite coupling that must be renormalized. In the renormalized theory the one free parameter manifests itself as an absence of a boundary condition for the beta-function equation.

In QCD the beta-function is a perturbatively calculable quantity

$$\mu \frac{\partial a}{\partial \mu} = -ba^2 + O(a^3) \equiv \beta(a) \; , \tag{1.49}$$

where the beta-function coefficients are extracted from loop corrections to the bare vertices of the theory. The first beta-function coefficient is [13]

$$b = \frac{(11C_A - 2N_f)}{6} . \tag{1.50}$$

Truncating the series in Eq.(1.49) at leading-order and solving the resulting differential equation for $\alpha_s(Q)$ gives the solution

$$a(Q) = \frac{a(\mu)}{1 + a(\mu)b\ln(Q/\mu)} . \tag{1.51}$$

This gives the relation between $a(Q)$ and $a(\mu)$, allowing the strong coupling constant to be written independently of the scale μ.

Rearranging Eq.(1.51) gives

$$\frac{1}{a(Q)} - b\ln Q = \frac{1}{a(\mu)} - b\ln\mu \equiv -b\ln(\Lambda) . \tag{1.52}$$

since the left and right hand sides of the above are of identical form and therefore must be independent of both Q and μ. Here Λ is the *universal dimensional transmutation mass parameter* of QCD. Λ efficiently parametrizes the missing boundary condition information in Eq.(1.49). It is therefore convenient to regard Λ as the fundamental QCD parameter which must be fitted to experiment.

The introduction of Λ allows us to write the asymptotic solution for α_s in terms of this parameter. Again, neglecting terms of $O(a^3)$ we can perform the integration in Eq.(1.49) to obtain

$$a(Q) = \frac{1}{b\ln(Q/\Lambda)} . \tag{1.53}$$

This allows a determination of $a(Q)$ for a given value of Λ. Naively Λ is the scale at which the beta-function would diverge if extrapolated far outside its domain of validity. We will discuss the problem of the RS dependence of α_s and Λ and how there are defined at higher-orders in perturbation theory in Chapter 2.

1.5.3 RG-improved perturbation theory

Consider the effective quark-gluon vertex in Figure 1.2. Assuming $\alpha_s \ll 1$ we may calculate this vertex perturbatively. To NLO we must add the contributions of Figure 1.2. Each loop gives an additional α_s and $\ln Q^2/\mu^2$. Schematically one has

$$a(Q) = a(\mu) - \frac{1}{2}ba^2(\mu)\left(\ln\frac{Q^2}{\mu^2} + \text{finite}\right) + O\left(a^3(\mu)\ln^2\frac{Q^2}{\mu^2}\right) . \tag{1.54}$$

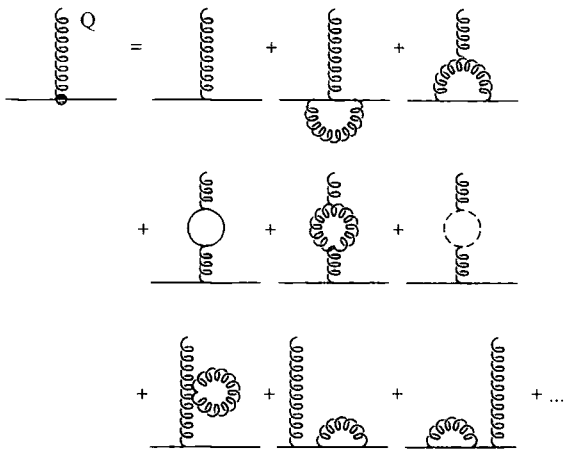

Figure 1.2: The effective quark-gluon coupling is the bare coupling plus loop corrections; only one-loop (NLO) corrections are shown above.

Even though $\alpha_s \ll 1$ the expansion is still potentially divergent since μ is arbitrary. Instead we must require that $\alpha_s \ln Q^2/\mu^2 \ll 1$. This, however, is unsatisfactory if we wish to consider the high-momenta behaviour of the theory.

To solve this problem we use the renormalization group. Expanding Eq.(1.51) as a series in $\alpha_s(\mu)$

$$a(Q) = a(\mu) - \frac{1}{2}ba^2(\mu)\ln\left(\frac{Q^2}{\mu^2}\right) + O\left(a^3(\mu)\ln^2\frac{Q^2}{\mu^2}\right) . \tag{1.55}$$

We can then observe that Eq.(1.51) contains the resummed expression of Eq.(1.54). The coupling $\alpha_s(Q)$ is *renormalization group improved.*

Returning to the QCD observable $\mathcal{R}$, we can now see the importance of the running coupling. We assume $\mathcal{R}$ has the perturbative expansion

$$\mathcal{R}(a(Q)) = \mathcal{R}_{PARTON} + r_0(a(Q) + \cdots) , \tag{1.56}$$

where $\mathcal{R}_{PARTON}$ is the parton level term and r_0 is the leading-order term, both independent of α_s. $\mathcal{R}(\alpha_s(Q))$ can then be re-expressed in terms of $\alpha_s(\mu)$ using Eq.(1.51)

$$\begin{aligned} \mathcal{R}(\alpha_s(Q)) &= \mathcal{R}_{PARTON} + r_0 a(\mu)\sum_{i=0}^{\infty}\left[-\frac{1}{2}ba(\mu)\ln\frac{Q^2}{\mu^2}\right]^i \\ &= \mathcal{R}_{PARTON} + r_0 a(\mu)\left[1 - \frac{1}{2}ba(\mu)\ln\frac{Q^2}{\mu^2} + \frac{1}{4}b^2a^2(\mu)\ln^2\frac{Q^2}{\mu^2} + \cdots\right] \end{aligned} \tag{1.57}$$

Thus order-by-order the running coupling is automatically resumming logarithms of Q^2/μ^2.

Eq.(1.51) only resums the leading logarithms of the form $\alpha_s^n(\ln Q^2/\mu^2)^n$. In principle the logarithms can be resummed to all-orders. By including the the NLO correction

to the beta-function in Eq.(1.49) we can resum next-to-leading logarithms of the form $\alpha_s^n(\ln Q^2/\mu^2)^{n-1}$. For the NLO perturbative coefficient $r_1 a^2$ this would give $r_1 a(\mu)^2(1 - a(\mu^2)b\ln(Q^2/\mu^2) + \ldots)$ — one less logarithm in each term. Generally the higher-order terms in $\mathcal{R}$ when expanded will give terms with less logarithms per power of α_s. The replacement of $\alpha_s(\mu)$ by $\alpha_s(Q)$ resums an infinite set of Feynman diagrams — those required to make the result independent of the scale μ. It is now possible to study the high-momenta behaviour of QCD observables. The perturbative expansion for $\mathcal{R}$ is said to be *renormalization group improved.*

1.6 Asymptotic freedom and confinement

For $N = 3$, and assuming $N_f \leq 33/2$, we can determine from Eq.(1.50) that the first beta-function coefficient of QCD, b, is positive. Two characteristic features of QCD can then be read off:

- *Asymptotic freedom* [13]: At the energy scale Q increases the QCD coupling becomes smaller, as would be expected from Eq.(1.53). The approach to zero is rather slow since α_s only decreases like an inverse power of $\ln Q$. For sufficiently large energy scales, $Q \gg \Lambda$, this feature allows us to obtain a good approximation to a physical process by calculating a truncated perturbative expansion in α_s. [4].

- Confinement: As Q decreases the running coupling $\alpha_s(Q)$ increases. The colour force becomes stronger and may well be enough to hold quarks and gluons permanently together in *infrared slavery.* This would explain why the quark and gluon states are not observed over macroscopic distances. For low energy scales, $Q \sim \Lambda$, $\alpha_s > 1$ and perturbation theory is not valid. Non-perturbative methods must then be implemented.

In the region intermediate between these the high and low energy scales one can use the perturbative expansion with care. One must ask how closely the truncated fixed-order series approximates the physical observable and to what degree non-perturbative information contributes. This idea will be taken up in further in Chapter 3.

This behaviour may be compared with that of QED. For QED the first beta-function coefficient is negative ($b = -2/3N_f$), so that the coupling would increase at large Q.

[4] We do not imply that the perturbative series is convergent. In Chapter 3 we see that formally we have an asymptotic series.

QED is therefore a *non-asymptotically* free theory. The fact that the b coefficients in QED and QCD have the opposite sign for $N_f \leq 33/2$ is thus crucial. This difference in behaviour can be traced back to their different group structures — the effect of the non-Abelian glue-glue self interactions in QCD is to make b positive for $N_f \leq 33/2$.

1.7 The operator product expansion (OPE)

A standard method to investigate the interplay of perturbative and non-perturbative effects is the *operator product expansion* (OPE) [14, 15].

In any renormalizable quantum field theory one finds that the time-ordered product of two-field operators $T[A(x)B(y)]$ does not have a well-defined limit as the separation of the two fields in coordinate space goes to zero. The OPE, as implemented in reference [15], enables one to attach some quantitative meaning to the limit $x - y \to 0$. We expand the product of two fields as a series of well-defined operators localized at $x - y = 0$. Formally, we write

$$T[A(x)B(y)] \simeq \lim_{(x-y)\to 0} \sum_i \mathcal{C}_i(x-y)\mathcal{O}_i\left(\frac{x+y}{2}\right) . \tag{1.58}$$

Here the sum is over a set of non-singular local renormalized composite field operators, $\mathcal{O}_i$. The *Wilson coefficients*, $\mathcal{C}_i$'s, are complex coefficient c-number functions of x, singular at $x - y = 0$. The local operator $\mathcal{O}_i$ is regular in the sense that the singularity of the product of $T[A(x)B(y)]$ is fully contained in the coefficient function $\mathcal{C}_i$. The operators $\mathcal{O}_i$ are ordered according to their canonical dimensions, and their quantum numbers must match those of AB. As a consequence, the coefficients $\mathcal{C}_i$ are ordered according to their decreasing singularity degree, and only a finite number of them are singular functions infinite at the origin, while the remainder of the expansion is finite or tends to zero with vanishing distance. To any finite order in $x - y$, only a finite number of terms contribute.

A specific example of the application of the OPE in QCD (or QED) relevant to later chapters is provided by a generic current correlator in momentum space [16].

1.7.1 The Adler D-function

We shall be interested in the SU(N) QCD vacuum polarization function, the transverse part of the correlator of two vector (electromagnetic) currents $j_\mu = \sum_i Q_i \bar{\psi}_i \gamma_\mu \psi_i$ ($i =$

$u, d, s, \ldots$) in the Euclidean region, with N_f active flavours of massless quarks,

$$\Pi(q^2)(q_\mu q_\nu - g_{\mu\nu}q^2) = i\int d^4x\, \mathrm{e}^{iq\cdot x}\langle 0|T\{j_\mu(x)j_\nu^\dagger(0)\}|0\rangle\ . \tag{1.59}$$

We neglect electroweak corrections and assume massless quarks. In order to avoid an unspecified constant, we shall actually focus on the related Adler D-function,

$$D(-Q^2) = -12\pi^2 Q^2 \frac{\mathrm{d}}{\mathrm{d}Q^2}\Pi(Q^2)\ , \tag{1.60}$$

where $Q^2 = -q^2 > 0$ is the spacelike Euclidean squared momentum transfer. The Adler D-function is a formally RG-invariant quantity, in contrast to $\Pi(q^2)$ which does not satisfy the homogeneous RGE. As such D may be considered a physical quantity despite the fact that it cannot be directly measured experimentally.

In SU(N) QCD perturbation theory $D(Q^2)$ is calculable for spacelike momenta and can be written in the form

$$D(Q^2) = N\sum_f Q_f^2\left(1 + \frac{3}{4}C_F\tilde{D}\right) + \left(\sum_f Q_f\right)^2 \tilde{\tilde{D}}\ , \tag{1.61}$$

where Q_f denotes the electric charge of the quarks and the summation is over the flavours accessible at a given energy.

The perturbative correction to the parton model result has the expansion

$$\tilde{D} = a + d_1 a^2 + d_2 a^3 + \cdots + d_k a^{k+1} + \cdots\ , \tag{1.62}$$

with $a = \alpha_s(\mu^2)/\pi$ the RG-improved coupling which will evolve with renormalization scale μ^2 according to the beta-function equation (1.49). The flavour singlet contribution $\tilde{\tilde{D}}$ first enters at $O(a^3)$ due to the existence of diagrams of the "light-by-light" type (see Figure 1.3) and is given by

$$\tilde{\tilde{D}} = \left(\frac{55}{216} - \frac{5}{9}\zeta_3\right)a^3 + \cdots\ . \tag{1.63}$$

Its contribution is numerically small.

For the Adler D-function the first two coefficients, d_1 and d_2, have been computed [17, 18]; and the result using the $\overline{\mathrm{MS}}$ scheme with renormalization scale $\mu^2 = Q^2$ is

$$d_1 = \left(-\frac{11}{12} + \frac{2}{3}\zeta_3\right)N_f + C_A\left(\frac{41}{8} - \frac{11}{3}\zeta_3\right) - \frac{1}{8}C_F \tag{1.64}$$

$$\begin{aligned} d_2 = {} & \left(\frac{151}{162} - \frac{19}{27}\zeta_3\right)N_f^2 + C_A\left(-\frac{970}{81} + \frac{224}{27}\zeta_3 + \frac{5}{9}\zeta_5\right)N_f \\ & + C_F\left(-\frac{29}{96} + \frac{19}{6}\zeta_3 - \frac{10}{3}\zeta_5\right)N_f + C_A^2\left(\frac{90445}{2592} - \frac{2737}{108}\zeta_3 - \frac{55}{18}\zeta_5\right) \\ & + C_A C_F\left(-\frac{127}{48} - \frac{143}{12}\zeta_3 + \frac{55}{3}\zeta_5\right) + C_F^2\left(-\frac{23}{32}\right)\ . \end{aligned} \tag{1.65}$$

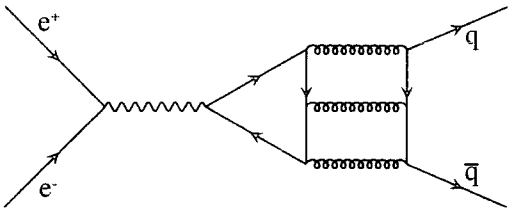

Figure 1.3: "Light-by-light" type contribution to $D(Q^2)$.

Here ζ_p denotes the Riemann zeta function, defined in Eq.(A.5).

We can apply a short-distance OPE to $D(Q^2)$ to systematically organize the perturbative and non-perturbative contributions into an expansion in powers of $1/Q^2$. This yields the representation,

$$D(Q^2) = \sum_n \sum_{dim\mathcal{O}=2n} \frac{\mathcal{C}(Q^2,\mu^2)\langle\mathcal{O}(\mu^2)\rangle}{(Q)^{2n}} . \tag{1.66}$$

The inner sum is over local gauge-invariant scalar operators of dimension $0, 2, 4, \ldots$. The $n = 0$ term, the unit operator, corresponds to perturbative corrections $\hat{D}$. Leading quark-mass corrections appear by treating running quark masses as operators so that $D = 2$ operators are of the form $m_i(\mu^2)m_j(\mu^2)$. Dynamical operators $D = 4, 6, \ldots$ give the non-perturbative physics. The scale invariant D=4 operators are the quark condensate $\langle m_j\bar{\psi}_i\psi_i\rangle$ and gluon condensate $\langle(\alpha_s/\pi)GG\rangle$. At D=6 scale-dependent 4-quark operators appear. The parameter μ is is an arbitrary factorization scale separating long-distance non-perturbative effects from short distance perturbative effects. The long-distance dynamics due to logarithms of the light quark masses is absorbed into the vacuum matrix elements $\langle\mathcal{O}(\mu^2)\rangle$; these are fixed phenomenologically. Short-distance effects absorbed into the Wilson coefficients $\mathcal{C}(Q^2,\mu^2)$, dimensionless functions of Q^2 and μ^2, can then be computed perturbatively as an expansion in $\alpha_s(\mu)$.

We make use the OPE in the next section in relation to the observable R_τ and meet it again in Chapter 3 to consider its connection to large-order perturbation theory.

1.8 QCD observables of interest

In addition to the Adler D-function defined in the last section we will wish to consider the following observables in later chapters.

1.8.1 The e^+e^- R-ratio

The production of hadrons in e^+e^- annihilation has long been considered a good test of perturbative QCD. Hadronic production occurs through the mechanism, $e^+e^- \to \gamma^*, Z^* \to$ hadrons and is totally inclusive. The details of hadronization are then irrelevant removing the need to define jets, since unitarity means that all partons turn into hadrons with unit probability.

The experimentally relevant R-ratio for e^+e^- annihilation is the observable

$$R \equiv \frac{\sigma(\mathrm{e^+e^-} \to \text{hadrons})}{\sigma(\mathrm{e^+e^-} \to \mu^+\mu^-)} \,. \tag{1.67}$$

In SU(N) QCD perturbation theory

$$R(s) = N \sum_f Q_f^2 \left(1 + \frac{3}{4} C_F \tilde{R}\right) + \left(\sum_f Q_f\right)^2 \tilde{\tilde{R}} \,, \tag{1.68}$$

where $s = Q^2 = -q^2 > 0$ is the physical timelike Minkowski squared momentum transfer ($\sqrt{s}$ is the e^+e^- c.m. energy).

Here $\tilde{R}$ denotes the perturbative corrections to the parton model result and has the formal expansion

$$\tilde{R}(s) = a + r_1 a^2 + r_2 a^3 + \cdots + r_k a^{k+1} + \cdots \,. \tag{1.69}$$

We assume the $\overline{\mathrm{MS}}$ scheme with $\mu^2 = s$. $\tilde{\tilde{R}}$ first enters at $O(a^3)$ due to the existence "light-by-light" diagrams. The first two perturbative coefficients r_1 and r_2 have been calculated [17, 18] and, as we will now show, may be directly related, to the coefficients d_1 and d_2, Eq.(1.64) and Eq.(1.65) respectively, of the Adler D-function.

To relate the $\mathrm{e^+e^-}$ R-ratio to the QCD vacuum polarization function, we start by integrating Eq.(1.60)

$$\Pi(s) - \Pi(\hat{s}) = -\frac{1}{12\pi^2} \int_{\hat{s}}^{s} \mathrm{d}t \frac{D(-t)}{t} \,, \tag{1.70}$$

where $\hat{s}$ is a reference timelike momentum. Taking $s = Q^2$, $R(s)$ and $\Pi(s)$ may be related using the optical theorem supplemented by analyticity.

$$R(s) = 12\pi \mathrm{Im}\, \Pi(s + i\epsilon) = \frac{6\pi}{i} [\Pi(s + i\epsilon) - \Pi(s - i\epsilon)] \,. \tag{1.71}$$

Using Eq.(1.70) and Eq.(1.71) we can relate $R(s)$ and $D(s)$ succinctly by

$$R(s) = -\frac{1}{2\pi i} \int_{s-i\epsilon}^{s+i\epsilon} \mathrm{d}t \frac{D(-t)}{t} \,. \tag{1.72}$$

Using Cauchy's theorem this can be converted into a contour integral running counter-clockwise around the circle $t = s$ in the complex energy plane, cut along the positive real axis. Choosing

$$t = -s\mathrm{e}^{\mathrm{i}\theta} , \tag{1.73}$$

the contour integral can be expressed as

$$R(s) = \frac{1}{2\pi}\int_{-\pi}^{\pi} \mathrm{d}\theta D(s\mathrm{e}^{i\theta}) \tag{1.74}$$

To recover the conventional expression Eq.(1.69) for the perturbative contribution $\check{R}$, we insert the series Eq.(1.62) for $\check{D}$ under the contour integral, and expand $a(s\mathrm{e}^{\mathrm{i}\theta})$ in terms of $a(s)$

$$a(s\mathrm{e}^{i\theta}) = a(s) - \frac{b}{2}i\theta a(s)^2 + \left[-\frac{b}{2}i\theta + \left(-\frac{b}{2}i\theta \right)^2 \right] a(s)^3 \cdots . \tag{1.75}$$

Evaluating the θ integrals one obtains

$$r_1 = d_1 , \qquad r_2 = d_2 - \frac{1}{12}\pi^2 b^2 . \tag{1.76}$$

The π^2 term arises due to the analytical continuation. In Chapter 5 we return to consider the contour integral representation for the R-ratio in more detail.

1.8.2 Hadronic tau decay ratio R_τ

The ratio R_τ is defined, analogously to the R-ratio, using the total τ hadronic width normalized to the leptonic width as

$$R_\tau \equiv \frac{\Gamma(\tau \to \nu_\tau + \text{hadrons})}{\Gamma(\tau \to \nu_\tau e^- \overline{\nu}_e)} . \tag{1.77}$$

The inclusive character of the total hadronic decay rate makes a theoretical calculation of R_τ possible, opening up a wide range of interesting studies [19].

R_τ can be theoretically separated into contributions from specific quark currents, namely, vector (V) and axial-vector (A) $\bar{u}d$- and $\bar{u}s$-quark currents. Experimentally, however, contributions are resolved into only three categories: non-strange decays, split into vector and axial vector contributions, and strange decays. The corresponding naive predictions then become $R_{\tau,V,A} \simeq N/2|V_{ud}|^2$ and $R_{\tau,S} \simeq N|V_{us}|^2$ where V_{ud} and V_{us} are CKM mixing matrix elements with $|V_{ud}|^2 + |V_{us}|^2 \approx 1$. Hence for $N = 3$ QCD $R_\tau \simeq 3$.

To evaluate R_τ the theoretical analysis starts with the two-point correlation functions for the vector $j^\mu_{ij,V} = \bar{\psi}_j \gamma^\mu \psi_i$ and axial-vector $j^\mu_{ij,A} = \bar{\psi}_j \gamma^\mu \gamma_5 \psi_i$ colour singlet quark currents

$(i,j = u,d,s)$

$$\Pi^{\mu\nu}_{ij,V/A}(q^2) \equiv i\int d^4x\, e^{iq\cdot x}\langle 0|T\{j^{\mu}_{ij,V/A}(x)j^{\nu}_{ij,V/A}(0)^{\dagger}\}|0\rangle \quad (1.78)$$

$$= \Pi^{(1)}_{ij,V/A}(q^2)(q^{\mu}q^{\nu} - g^{\mu\nu}q^2) + q^{\mu}q^{\nu}\Pi^{(0)}_{ij,V/A}(q^2)\,, \quad (1.79)$$

where we have made a Lorentz decomposition. The superscript $(J = 0,1)$ denotes the angular momentum in the hadronic rest frame.

Since the imaginary parts of the two-point correlators are proportional to the spectral functions for hadrons, the hadronic τ decay rate can be written as an integral of these spectral functions over the invariant mass $s = -q^2 > 0$ of the final state hadrons [22]

$$R_{\tau} = 12\pi\int_0^{m_{\tau}^2}\frac{\mathrm{d}s}{m_{\tau}^2}(1-\frac{s}{m_{\tau}^2})^2\left[(1+2\frac{s}{m_{\tau}^2})\mathrm{Im}\Pi^{(1)}(\mathrm{s}) + \mathrm{Im}\Pi^{(0)}(\mathrm{s})\right]\,, \quad (1.80)$$

with the correlator combinations according to the decomposition

$$\Pi^{(J)}(s) \equiv |V_{ud}|^2(\Pi^{(J)}_{ud,V} + \Pi^{(J)}_{ud,A}) + |V_{us}|^2(\Pi_{us,V+A})\,. \quad (1.81)$$

Unfortunately, hadronic spectral functions are sensitive to QCD non-perturbative effects — the lower integration limit corresponds to the threshold for hadronic production, m_{π} (zero in massless QCD), a region where confinement effects dominate. As a result the integrand cannot be reliably calculated from QCD. Nonetheless, the analytic property of the correlator $\Pi(s)$ can be exploited. $\Pi(s)$ is an analytic function of complex s with the exception of the positive real s axis, where the imaginary part has singularities. In a manner analogous to that of the R-ratio the integral, Eq.(1.80), can be expressed as a contour integral in the complex s plane running counter-clockwise around the circle $s = m_{\tau}^2$ from $s = m_{\tau}^2 - i\epsilon$ to $s = m_{\tau}^2 + i\epsilon$

$$R_{\tau} = 6\pi i\oint_{|s|=m_{\tau}^2}\frac{\mathrm{d}s}{m_{\tau}^2}(1-\frac{s}{m_{\tau}^2})^2\left[(1+2\frac{s}{m_{\tau}^2})\Pi^{(1+0)}(s) - 2\frac{s}{m_{\tau}^2}\Pi^{(0)}(s)\right]\,. \quad (1.82)$$

Unlike Eq.(1.80), Eq.(1.82) requires correlators only for complex $s \sim m_{\tau}^2$, which is large enough to expect only small contributions from non-perturbative effects. In analogy to Eq.(1.66) one can then apply a short-distance OPE to organize the perturbative and non-perturbative contributions to the correlators into an expansion in powers of $1/s$ [20, 21, 22]. Possible uncertainties associated with the use of the OPE near the time-like axis are absent, because the integrand includes a factor $(1 - s/m_{\tau}^2)^2$, a double zero at $s = m_{\tau}^2$, effectively suppressing the contribution near the branch cut. Choosing the factorization scale $\mu^2 = m_{\tau}^2$ avoids large logarithms $\ln(s/\mu^2)$ in the perturbative expansion of $C(s,\mu^2)$. Inserting the OPE expansion into Eq.(1.82) and evaluating the contour

integral, R_τ can be expressed as an expansion in powers of $1/m_\tau^2$ with coefficients that depend only logarithmically on m_τ.

Incorporating all known corrections to the naive contribution, the total ratio R_τ can then be cast in the form

$$R_\tau = N(|V_{ud}|^2 + |V_{us}|^2)\, S_{EW} \left[1 + \frac{3}{4} C_F \tilde{R}_\tau + \delta_{EW} + \delta_{PC}\right] . \tag{1.83}$$

$\tilde{R}_\tau$ is the dimension-0 perturbative correction, neglecting quark masses. Power corrections, δ_{PC}, are split into leading quark-mass corrections ($D = 2$) δ_{MASS} and non-perturbative corrections ($D = 4, 6, \ldots$) δ_{NP}. The factors S_{EW} and δ_{EW} are electroweak corrections.

Perturbative corrections

In the massless chiral limit, ($m_u = m_d = m_s = 0$), both vector and axial-vector currents are conserved so that $s\Pi^{(0)}(s) = 0$; perturbative corrections do not contribute to the longitudinal self-energy function. Furthermore, the chiral invariance of massless QCD implies that $\Pi^{(0+1)}_{ij,V} = \Pi^{(0+1)}_{ij,A} \equiv \Pi(s)$ ($i \neq j$). This implies that only the transverse correlator $\Pi^{(0+1)}(s)$ contributes to Eq.(1.82).

Replacing $\Pi(s)$ by the Adler D-function and integrating Eq.(1.82) by parts yields

$$R_\tau = \frac{1}{2\pi i} \oint_{|s|=m_\tau^2} \frac{\mathrm{d}s}{s} \left(1 - 2\frac{s}{m_\tau^2} + 2\frac{s^3}{m_\tau^6} - \frac{s^4}{m_\tau^8}\right) D(-s) . \tag{1.84}$$

Choosing the contour $s = -m_\tau^2 \mathrm{e}^{i\theta}$ we obtain [20]

$$R_\tau = \frac{1}{2\pi} \int_{-\pi}^{\pi} \mathrm{d}\theta\, (1 + 2\mathrm{e}^{i\theta} - 2\mathrm{e}^{3i\theta} - \mathrm{e}^{4i\theta}) D(m_\tau^2 \mathrm{e}^{i\theta}) . \tag{1.85}$$

$\tilde{R}_\tau$ has a perturbative expansion of the form of Eq.(1.69) with coefficients which we shall denote r_k^τ. Since the energy scale, $s = m_\tau^2$, of the process lies below the threshold for charmed hadron production only three flavours u, d, s, are active. There are no "light-by-light" corrections for R_τ since $(\Sigma Q_f)^2 = 0$ for u, d, s active quark flavours.

The first two perturbative coefficients r_1^τ and r_2^τ have been calculated [17, 18] and can, in a manner analogous to R, be expressed in terms of d_1 and d_2. To recover the conventional expression for the perturbative contribution, $\tilde{R}_\tau$ the series for $\tilde{D}(m_\tau^2 \mathrm{e}^{i\theta})$ is inserted. One then expands $a(m_\tau^2 \mathrm{e}^{i\theta})$ in terms of $a(m_\tau^2)$. Denoting the terms due to analytical continuation by g_n, we can evaluate the θ integrals to obtain [17, 18]

$$r_1^\tau = d_1 + g_1 = 5.2023 \tag{1.86}$$

$$r_2^\tau = d_2 + g_2 = 26.366 , \tag{1.87}$$

for $N_f = 3$, where

$$g_1 = \frac{19}{24}b = 3.5625 \tag{1.88}$$

$$g_2 = \frac{19}{24}(2d_1 + c)b + \left(\frac{265}{288} - \frac{1}{12}\pi^2\right)b^2 = 19.995\ . \tag{1.89}$$

One can note that g_1 and g_2 are far larger than d_1 and d_2. This stems from the long running along the circle $s = m_\tau^2 e^{i\theta}$ and gives rise to a sizeable RS dependence. There is no physical reason to truncate the contour integral at $O(a^3)$ for either $\tilde{R}$ or $\tilde{R}_\tau$. One could instead numerically evaluate the contour integral, hence resumming the analytical continuation terms to all-orders in $a(s)$; a subject we will return to in Chapter 5.

Non-perturbative corrections

The non-perturbative corrections to R_τ from dimension-D operators in the OPE can be expressed in the form [22]

$$\delta_{PC} = -16\frac{\overline{m^2}}{m_\tau^2} + 32\pi^4\frac{m\overline{\psi}\psi}{m_\tau^4} + \frac{11\pi^2}{4}(a(m_\tau^2))^2\frac{\langle\alpha_s/\pi GG\rangle}{m_\tau^4} - 2\frac{\langle\overline{\psi}\Gamma\psi\overline{\psi}\Gamma\psi\rangle}{m_\tau^6} + \cdots \tag{1.90}$$

where $\overline{m^2}$ is a weighted average of the running quark masses m_u^2, m_d^2, and m_s^2 evaluated at the scale m_τ^2.

The leading quark mass correction term $\overline{m^2}$ (dimension-2 operator) in Eq.(1.90) has been calculated to $O(\alpha_s^2)$ [23] for R_τ. For the up quark and down quark the mass corrections are negligible, ($\sim -0.08\%$). The correction from the strange quark-mass, however, is significant, giving a total mass correction $\delta_{MASS} = -(0.9 \pm 0.2)\%$.

Neglecting the logarithmic dependence of the Wilson coefficients $\mathcal{C}(s, \mu^2)$ on s (since it is an $O(\alpha_s)$ effect), one can evaluate the contour integrals using Cauchy's residue theorem, to find they are non-zero only for D =2, 4, 6, and 8. In the massless chiral limit the $D = 2$ correction vanishes due to the absence of a dimension-2 operator. The $D = 4$ operator vanishes due to kinematical effects in the integrand. $D = 6, 8$ are then the only non-zero contributions.

If one incorporates the logarithmic dependence of the Wilson coefficients on s then operators of dimensions other than 6 and 8 contribute, though suppressed by $(\alpha_s(m_\tau^2))^2$. Since the four-quark ($D = 6$) operators have no such suppression they generate the largest power corrections. Using a phenemenological fit their size was estimated to be [22] $\delta_{NP} \simeq -(0.7 \pm 0.4)\%$. The small numerical value derives from a large cancellation

between vector and axial-vector contributions combined with the fact that they fall off like $1/m_\tau^6$.

Since the actual evaluation of the power corrections combines experimental and theoretical considerations which are to an extent model dependent it is better to directly measure the non-perturbative contribution from the τ decay data. Moments of the invariant-mass distribution of the final state hadrons in τ decay are used to perform the analysis [94]. The most recent analysis gives [24] $\delta_{NP} = -(0.5 \pm 0.7)\%$. The total power correction contribution can thus be estimated to be $\delta_{PC} = \delta_{MASS} + \delta_{NP} = -(1.4 \pm 0.9)\%$.

Electroweak corrections

The leading electroweak correction is a RG-summation of higher order $\alpha^n \ln^n(M_Z/m_\tau)$ terms, representing a short-distance correction to the low-energy effective four-fermion coupling [26]

$$S_{EW} = \left(\frac{\alpha(m_b^2)}{\alpha(m_\tau^2)}\right)^{\frac{9}{19}} \left(\frac{\alpha(M_W^2)}{\alpha(m_b^2)}\right)^{\frac{9}{20}} \left(\frac{\alpha(M_Z^2)}{\alpha(M_W^2)}\right)^{\frac{36}{17}} \simeq 1.0194 \ . \tag{1.91}$$

with $\alpha_{m_b} \simeq 1/132.05$, $\alpha_{M_W} \simeq 1/127.97$ and $\alpha_{M_Z} \simeq 1/127.93$. The small next-to-leading non-logarithmic correction is [27] $\delta_{EW} = \frac{5}{12}\frac{\alpha(m_\tau^2)}{\pi} \simeq 0.001$ where $\alpha(m_\tau^2) \simeq 1/133.29$ denotes the QED running coupling.

Experimental value of $\tilde{R}_\tau$

Experimentally, R_τ can be obtained from measurements of the leptonic branching ratio of the τ and also from τ-lifetime measurements [25]. In the following chapters we will take the experimental value of $R_\tau = 3.64 \pm 0.014$ [79] corresponding to an average of these two determinations. Correcting for the small estimated power corrections and mass corrections discussed above, and taking into account the small electroweak corrections this corresponds to a value of $\tilde{R}_\tau = 0.205 \pm 0.006$.

1.8.3 Deep inelastic scattering (DIS) sum rules

We will be interested in three DIS sum rules; the polarized and unpolarized Bjorken sum rules, and the Gross-Llewellyn Smith sum rule.

Polarized Bjorken Sum Rule (PBjSR)

First we consider the polarized Bjorken sum rule (PBjSR) [30]:

$$\begin{aligned} K_{PBj} &\equiv \int_0^1 g_1^{\text{ep-en}}(x,Q^2)\mathrm{d}x \\ &= \frac{1}{3}\left|\frac{g_A}{g_V}\right|\left(1-\frac{3}{4}C_F\hat{K}\right) . \end{aligned} \tag{1.92}$$

with g_V and g_A the nucleon vector and axial vector couplings, respectively. Here $\hat{K}$ denotes the perturbative corrections to the zeroth order parton model sum rule,

$$\hat{K} = a + K_1 a^2 + K_2 a^3 + \cdots + K_k a^{k+1} + \cdots . \tag{1.93}$$

The exact K_1 and K_2 are known [28, 29]; assuming the $\overline{\text{MS}}$ scheme with renormalization scale $\mu^2{=}Q^2$

$$K_1 = -\frac{1}{3}N_f + \left(\frac{23}{12}C_A - \frac{7}{8}C_F\right) , \tag{1.94}$$

$$\begin{aligned} K_2 &= \left(\frac{115}{648}\right)N_f^2 + C_A\left(-\frac{3535}{1296} - \frac{\zeta_3}{2} + \frac{5}{9}\zeta_5\right)N_f + C_F\left(\frac{133}{864} + \frac{5}{18}\zeta_3\right)N_f \\ &\quad + C_A^2\left(\frac{5437}{648} - \frac{55}{18}\zeta_5\right) + C_A C_F\left(-\frac{1241}{432} + \frac{11}{9}\zeta_3\right) + C_F^2\left(\frac{1}{32}\right) . \end{aligned} \tag{1.95}$$

Unpolarized Bjorken Sum Rule (BjSR)

We can also consider the (unpolarized) Bjorken Sum Rule (BjSR)

$$\begin{aligned} U_{Bj} &\equiv \int_0^1 \mathrm{d}x F_1^{\bar{\nu}p-\nu p}(x,Q^2) \\ &= 1 - \frac{1}{2}C_F\hat{U} . \end{aligned} \tag{1.96}$$

$\hat{U}$ has perturbative corrections to the zeroth order parton model sum rule of the form of Eq.(1.93) with coefficients which we shall denote U_k. The perturbative coefficients U_1 and U_2 are known [31, 32]; we assume the $\overline{\text{MS}}$ scheme with renormalization scale $\mu^2{=}Q^2$

$$U_1 = -\frac{4}{9}N_f + \left(\frac{91}{36}C_A - \frac{11}{8}C_F\right) , \tag{1.97}$$

$$\begin{aligned} U_2 &= \left(\frac{155}{648}\right)N_f^2 + C_A\left(-\frac{4235}{1296} + \frac{7}{6}\zeta_3 - \frac{5}{3}\zeta_5\right)N_f + C_F\left(\frac{335}{288} - \frac{1}{6}\zeta_3\right)N_f \\ &\quad + C_A^2\left(\frac{8285}{648} + 5\zeta_3 - 10\zeta_5\right) + C_A C_F\left(-\frac{2731}{144} - \frac{91}{3}\zeta_3 + \frac{95}{2}\zeta_5\right) \\ &\quad + C_F^2\left(\frac{313}{32} + \frac{47}{2}\zeta_3 - 35\zeta_5\right) . \end{aligned} \tag{1.98}$$

Gross-Llewellyn Smith Sum Rule (GLSSR)

Finally we consider the GLS sum rule [33]

$$\begin{aligned} K_{GLS} &\equiv \frac{1}{6}\int_0^1 F_3^{\bar{\nu}\mathrm{p}+\nu\mathrm{p}}(x,Q^2)\mathrm{d}x \\ &= \left(1-\frac{3}{4}C_F\hat{K}+\hat{\tilde{K}}\right) . \end{aligned} \tag{1.99}$$

The perturbative corrections, $\hat{K}$, are the same as for the PBj; but there are additional corrections of "light-by-light" type, $\hat{\tilde{K}}$, analogous to $\hat{\tilde{D}}$ of Eq.(1.61). These will similarly enter at $O(a^3)$ and are found to be small.

1.9 Measuring Λ and the strong coupling α_s

Presently, all precision QCD phenemenology is performed at next-to-leading order (NLO) or next-to-NLO (NNLO) in RG-improved perturbation theory. By comparing such theoretical calculations with high-statistics experimental data one hopes to be able to extract the renormalized QCD coupling α_s or the fundamental QCD parameter Λ.

Since α_s and Λ are both RS-dependent, neither are physical observables. Presently, the conventional reference scheme for the coupling is $\alpha_s^{\overline{\mathrm{MS}}}(M_Z)$, the $\overline{\mathrm{MS}}$ scheme with renormalization scale set at the Z^0 boson mass. Since Λ is dependent on the number of flavours it is customary therefore to consider $\Lambda_{\overline{\mathrm{MS}}}^{(5)}$. We will comment further on the $\overline{\mathrm{MS}}$ scheme in Chapter 2. For values of α_s extracted at lower energies it is necessary to evolve $\alpha_s(Q)$ from the measured scale Q to M_Z. The method for this is considered in the next section.

Global average of $\alpha_s(M_Z)$ measurements

A wide range of observables and methods are now used to measure $\alpha_s(M_Z)$. Evolving all of these measurements to $Q = M_Z$, we obtain a 'global average' [34]

$$\alpha_s(M_Z^2) = 0.118 \pm 0.005 . \tag{1.100}$$

This corresponds to a value of $\Lambda_{\overline{\mathrm{MS}}}^{(5)} = 239^{+74}_{-60}\mathrm{MeV}$.

Theoretical ambiguities in the determination of α_s and $\Lambda_{\overline{\mathrm{MS}}}$

Our intention to accurately determine α_s or Λ is unfortunately hampered due to a number of factors, some of which we mention below.

- The truncation of perturbation theory at NLO or NNLO due to the technical difficulties of calculating Feynman diagrams. For observables at low energy scales there is the possibility that unknown higher-order corrections, negligible at higher energies where α_s is small, become important.

- The asymptotic nature of perturbation theory. If the series is divergent, the next order may represent no improvement with respect to the lower-order result. On the contrary, at a certain order it will lead to deterioration. Chapter 3 discusses this further.

- The dependence of truncated QCD perturbative calculations on the renormalization scale, at NLO, and renormalization scheme (RS) at higher orders. We consider this problem in Chapter 2.

- Sources of non-perturbative power corrections, particularly of the form $1/Q^{2n}$, for low energy observables. We make contact with this problem in Chapter 3.

- The effects of quark masses; these include finite quark mass corrections for intermediate energy observables, and the need to evolve α_s through flavour thresholds (which we discuss in the next section).

In Chapter 4 and 5 we will combine the discussion of RS dependence and the asymptotic nature of perturbation theory to assess the reliability of α_s and $\Lambda_{\overline{\rm MS}}$ determinations.

1.9.1 Evolving α_s through quark mass thresholds

The recent calculation of NNLO perturbative coefficients for a variety of observables has allowed precise estimates of $\alpha_s^{\overline{\rm MS}}(M_Z)$ to be made. Of particular use have been estimates of α_s from low and intermediate energy observables. However, in order to test the compatibility of these results one crucially relies on the evolution $\alpha_s^{\overline{\rm MS}}(Q) \to \alpha_s^{\overline{\rm MS}}(M_Z)$ governed by the beta function equation. A difficulty arises from the evolution through quark mass thresholds. Since $\overline{\rm MS}$ schemes are mass-independent, that is the higher-order c_k beta-function coefficients are independent of the quark masses, the required decoupling of heavy quarks is not manifest in each order of perturbation theory [35].

To obtain decoupling in QCD for the $\overline{\rm MS}$ scheme one builds in the decoupling region, $\mu \ll m_f(\mu)$, where $m_f(\mu)$ is the mass of the heavy quark with flavour f, an effective field theory with only the $f-1$ active light quark flavours. The value of N_f increases by one unit as we pass from the effective theory to the full theory and so the beta-function

changes, altering the running of α_s. Calculating the process in the $\overline{\text{MS}}$ scheme one obtains a matching condition connecting the parameters of the low energy effective Lagrangian to the full theory. The decoupling theorem [35] means that one can calculate the process in the 'light' $f-1$ theory up to terms of order $1/m$. The coupling of the effective theory can then be expressed as a power series in the coupling of the full theory with coefficients which are polynomials of degree n in $x = \ln(\mu^2/m(\mu)^2)$, and independent of both the gauge and the light quark masses.

The matching of α_s has been calculated to order a_f^3 [36] [5],

$$a_{f-1}(\mu) = a_f(\mu) - \frac{1}{6}x a_f(\mu)^2 + \left(\frac{1}{36}x^2 - \frac{19}{24}x + \frac{11}{72}\right)a_f(\mu)^3 \,. \tag{1.101}$$

where a_{f-1} and a_f denote the running coupling for a specific variant of the MS scheme in the $f-1$ and f flavour QCD theories, respectively. The structure of Eq.(1.101) is dictated by the renormalization group. Note that we should in addition consider the matching of the running mass m_μ, however, we will omit this for simplicity.

The coupling and light quark masses in the f and $f-1$ flavour theories are matched at the scale $\mu = \mu_M$. The matching scale μ_M is chosen so that perturbative expansions can be kept under control. Hence, the criterion for the scale μ_M is that $|x|$ must not become very much greater than one. Beyond that the choice of scale is somewhat arbitrary. The most important point is the consistency of the calculation in the full theory ($Q \gg m$) and the calculation performed in an effective theory ($Q \ll m$). Since the expressions for $a_f(Q)$ and $a_{f-1}(Q)$ are only valid for $Q \gg m$ and $Q \ll m$, respectively, any physical argument about the expressions at $Q \sim m$ (for example requiring continuity of the coupling) is not strictly valid.

1.10 Summary and conclusions

In this chapter we have reviewed some of the ideas central to an understanding of QCD. To calculate QCD observables we are required to make an approximation – a perturbative expansion in powers of the coupling. The inevitable need to renormalize these calculations introduces ambiguities through their dependence on the renormalization scale and renormalization prescription; collectively termed the renormalization scheme.

By imposing the condition that physical observables are invariant under the renormalization group a running coupling $\alpha_s(Q)$ was introduced, the evolution of which is governed by

[5] There is a numerically insignificant misprint in the original paper by Bernreuther and Wetzel. The coefficient "7/72" of α_s^3 in the matching condition was corrected by Larin et. al. to "11/72".

the beta-function equation. The integration of the beta-function leads to the introduction of a dimensional transmutation mass parameter, Λ, to ensure the correct dimensionality and parameterize the missing boundary condition information. Λ can be regarded as the free parameter of QCD that must be fitted to experiment.

The introduction of a running coupling allowed us to RG-improve the perturbative series, resumming logarithms which would otherwise destroy the perturbative expansion, and naturally uncover the property of asymptotic freedom, justifying our original use of a perturbative expansion for large energy scales. At low energy scales, however, the increasing size of the coupling requires non-perturbative techniques. We introduced the idea of an operator product expansion (OPE), and applied it to the vacuum polarization function and hadronic tau-decay ratio R_τ. Finally we briefly mentioned some of the existing obstacles to an accurate measurement of α_s and Λ.

Chapter 2

Renormalization scheme dependence

2.1 Introduction

In the last chapter we saw how the divergences of Green functions in QCD were disposed of by the standard technique of renormalization. The renormalization procedure is not a unique process, since the divergences can be removed in a number of ways, with the result that Green functions are dependent on the renormalization scale μ, and more generally, on the renormalization prescription in higher-orders. This arbitrary choice of scale and prescription can be termed the renormalization scheme (RS). In general the coupling and perturbative coefficients in a theory are RS dependent. For example, the RS dependence of the coupling is directly associated with it being a Green function at specific values of its arguments.

Physical observables in QCD, or any quantum field theory, however, are unique and unambiguous. Mathematically, this requires the invariance of physical observables under the full renormalization group (RG) [12]. Hence, theoretical predictions derived from the Green functions should be independent of the renormalization scheme; symbolically

$$\frac{\mathrm{d}}{\mathrm{d}(RS)}\Gamma^{(n)}(p_1,p_2,\ldots,p_n) = \left(\frac{\partial}{\partial(RS)} + \frac{\mathrm{d}\alpha_s}{\mathrm{d}(RS)}\frac{\partial}{\partial\alpha_s}\right)\Gamma^{(n)}(p_1,p_2,\ldots,p_n) = 0\,. \qquad (2.1)$$

This occurs for a complete calculation of the perturbative series summed to all-orders since the dependence on the RS cancels between different orders to leave an RS independent result. It is our reliance on truncating the perturbative series at fixed-order to obtain an approximate expression for the physical observable that creates a source for the RS dependence. Two results at $O(\alpha_s^n)$, calculated in two RS's, will in general differ by a term

of $O(\alpha_s^{n+1})$.

RS dependence is a general phenomenon in other quantum field theories such as QED, but the practical effect depends on the particular theory. In QED the coupling is small over a wide range of renormalization scales so the problem of RS dependence is of less interest. In contrast the coupling in QCD is sufficiently large to cause non-negligible differences in theoretical predictions due to both neglected higher order terms in the perturbative expansion and ambiguities from an arbitrary choice of RS. One cannot readily disentangle these two effects, and as a result the RS dependence of QCD perturbative calculations is a very real problem. It is therefore essential to have an objective means of of resolving the RS ambiguity to allow perturbative approximations to have quantitative meaning.

The response in the literature to this 'renormalization scheme dependence' problem has mainly been to advocate that some particular choice of scale and/or RS is the 'best' one. This is in the face of the central fact that the scale and RS are arbitrary unphysical quantities. Unsurprisingly, no particular scheme or scale commands universal support. In response to this confusion experimentalists have expanded the error bars associated with measurements to include a 'theoretical uncertainty', sacrificing unambiguous clarity and limiting the extent of detailed investigations of QCD.

Many proposed approaches to solve the RS dependence problem have been attempts to make educated guesses at uncalculated higher-order terms in the perturbative series; in a sense that a particular choice of RS will give a prediction as if we knew the full series. Another widespread belief is that the severity of the RS dependence for a particular observable is somehow related to the size of the unknown corrections in higher-orders. This overlooks the problem that the size of higher order corrections is itself an RS dependent concept. For example, the uncalculated corrections to a RS dependent NNLO prediction must also depend on the RS so that their sum does not. Of course there is a RS where there are no higher order corrections at all!

The resolution of the RS dependence problem in QCD is not a matter of finding a 'good' expansion parameter. There is a false assumption, deriving from QED where a traditional 'on-shell' RS has been used almost exclusively, that the same RS – hence expansion parameter – must be used for every observable. That this assumption is incorrect has been implicit since the introduction of the running coupling.

The solution to the RS dependence problem is not found in the study of Feynman diagrammatics; and while the idea of renormalization is crucial, its technicalities are irrelevant. The most important themes are the concepts of RG-invariance, which is best understood

without invoking the machinery of renormalization itself, and perturbative approximation theory. Essentially, we have two types of information about a physical observable.

- The first few terms in the perturbative expansion in some RS. The higher order terms are simply unknown.
- The knowledge that the exact result is independent of the RS since physical quantities are invariant under the renormalization group. We therefore require an RG-invariant approximation.

Note that both these points restrict our attention to the aim of deciding what it is actually possible to learn about the uncalculated terms from the information at our disposal.

The plan of the chapter is as follows. Section 2.2 considers how renormalization scheme dependence can be parametrized and exhibits the explicit scheme dependence at $\mathrm{N^nLO}$. In Section 2.3 we take a brief look at some common RS's and in Section 2.4 review three proposed solutions to the scheme dependence problem. Section 2.5 looks in detail at one further proposed solution – the Effective Charge (EC) formalism. Section 2.6 summarises the chapter.

2.2 The scheme dependence problem

We begin this chapter by reviewing the renormalization scheme (RS) dependence of the coupling 'α_s' and the perturbative coefficients r_k. We refer the reader to references [37, 38] for more details.

2.2.1 Parametrizing RS dependence

Consider a generic dimensionless QCD observable $\mathcal{R}(Q)$ where Q denotes the single dimensionful scale on which it depends. In renormalization group (RG) improved perturbation theory we can write without loss of generality

$$\mathcal{R}(Q) = a + r_1 a^2 + r_2 a^3 + \cdots + r_k a^{k+1} + \cdots , \tag{2.2}$$

where $a \equiv \alpha_s(\mu)/\pi$ denotes the RG-improved coupling. By dividing any observable depending only on a single dimensionful scale by its (possibly) dimensionful tree-level perturbative coefficient and raising to a suitable power we can always arrange that the

formal perturbation series for $\mathcal{R}(Q)$ assumes the form (2.2) representing a dimensionless $\mathcal{R}(Q)$ [1].

Using the notation introduced by Stevenson [37] the dependence of the coupling a on the scale μ is specified by a beta-function equation

$$\frac{\mathrm{d}a}{\mathrm{d}\ln\tau} = -a^2(1 + ca + c_2a^2 + \cdots + c_ka^k + \cdots) \equiv \frac{\beta(a)}{b} , \tag{2.3}$$

where

$$\tau \equiv b\ln\frac{\mu}{\Lambda} , \tag{2.4}$$

with μ the renormalization scale and Λ the dimensional transmutation mass parameter of QCD. The boundary condition on Eq.(2.3) is not provided by the theory but may be expressed in terms the, μ independent but RS dependent, scale parameter Λ which is fitted by experiment.

We shall consider SU(N) QCD with N_f flavours of massless quark, and assume that the first beta-function coefficient b is positive ($b > 0$ or $N_f < 33/2$ for $N = 3$ QCD). The first and second universal RS-invariant beta-function coefficients, are then given by [13, 39]

$$\begin{aligned} b &= \frac{(11C_A - 2N_f)}{6} , \\ c &= \left[-\frac{7}{8}\frac{C_A^2}{b} - \frac{11}{8}\frac{C_AC_F}{b} + \frac{5}{4}C_A + \frac{3}{4}C_F\right] , \end{aligned} \tag{2.5}$$

where C_A=N and C_F=$(N^2$–$1)/2N$.

We will restrict our discussion to physical observables in massless QCD. By considering only physical quantities the two RS's will only be distinguishable if they correspond to different definitions of the coupling, that is different definitions of the finite part of the renormalization constant Z in the relation $a = Za_B$, with a_B the bare coupling. To be more explicit consider two RS's, barred and unbarred couplings a, $\bar{a}$, respectively. The two calculations of the renormalized coupling start from the same bare coupling a^B,

$$a = Za^B , \qquad \bar{a} = \bar{Z}a^B . \tag{2.6}$$

The infinite parts of Z and $\bar{Z}$ must be equal to all-orders in perturbation theory. Thus the two constants must be related by a finite renormalization z

$$a(\mu) = z\bar{a}(\mu) = \bar{a}(\mu)(1 + \nu_1\bar{a}(\mu) + \nu_2\bar{a}^2(\mu) + \cdots + \nu_k\bar{a}^k(\mu) + \cdots) , \tag{2.7}$$

[1] For our purpose Eq.(2.2) is no less general than $\mathcal{R}(Q) = \mathcal{R}_{PARTON} + r_0a^M(1 + r_1a + r_2a^2 + \cdots)$; the parton model term $\mathcal{R}_{PARTON}$ and leading-order coefficient r_0 are RS-invariants and the analysis will generalize for arbitrary positive M.

where we have expanded z as a series in a. This relation is written with the renormalization scale parameters having the same value, but not necessarily the same meaning in the two RS's. The connection between corresponding couplings a and $\bar{a}$ will then be such that

$$\bar{\beta}(\bar{a}) = \beta(a)\frac{\mathrm{d}\bar{a}}{\mathrm{d}a} \,. \tag{2.8}$$

Different definitions for other renormalization constants will be irrelevant since while they affect the Green functions, the differences will cancel order-by-order in physical quantities. We assume massless quarks since different ways of renormalizing the mass terms in the theory could affect calculations of observables. For massive quarks, however, the RS dependence discussion will go through in any mass-independent RS i.e. one in which $c_2, c_3, \ldots, c_k, \ldots$ do not depend on the fermion masses. For discussion of the special considerations required for gauge theories see reference [37].

The perturbative coefficients r_k and coupling a are in general RS dependent. Only the parton model term $\mathcal{R}_{PARTON}$, leading-order coefficient r_0 (set to zero and unity in Eq.(2.2), respectively), b, and c are RS independent. The higher order coefficients $c_2, c_3, \ldots, c_k, \cdots$ are RS dependent. Turning this statement around implies that different RS's are characterized by different $c_2, c_3, \cdots, c_k, \ldots$. As shown by Stevenson [37] one may consistently use the parameters $\tau, c_2, c_3, \ldots, c_k, \ldots$ to label the renormalization scheme. Conventionally when retaining terms up to and including $r_n a^{n+1}$ in Eq.(2.2) one truncates Eq.(2.3) retaining terms up to and including $c_n a^{n+2}$. On integrating up Eq.(2.3) one can define $a^{(n)}(\tau, c_2, \ldots, c_n)$ and correspondingly find for the consistency of perturbation theory the following dependence of the r_k on the RS parameters $\tau, c_2, c_3, \ldots, c_k, \ldots$: $r_1(\tau)$, $r_2(\tau, c_2)$, $r_3(\tau, c_2, c_3)$, ..., $r_k(\tau, c_2, c_3, \ldots, c_k)$, ... In this way the n^{th} order truncated approximant is labelled by the scheme variables, $\mathcal{R}^{(n)}(\tau, c_2, \ldots, c_n)$. When summed to all-orders this dependence cancels to obtain a formally RS-invariant sum.

The formal consistency of perturbation theory requires that if we truncate the perturbative series at order n, i.e. $O(a^{n+1})$, there remains a difference of order a^{n+2},

$$\bar{\mathcal{R}}^{(n)}(\bar{\tau}, \bar{c_2}, \cdots, \bar{c_n}) - \mathcal{R}^{(n)}(\tau, c_2, \cdots, c_n) = k a^{n+2} + O(a^{n+3}) \,, \tag{2.9}$$

so that differences between results in the two different RS's are formally effects one order higher in perturbation theory. k depends on $\tau, c_2, \ldots, c_n$ and $\bar{\tau}, \bar{c_2}, \ldots, \bar{c_n}$ and may well not be a small coefficient. Note that the self-consistency equation (2.9) requires that there is a partial cancellation between the RS dependence of a and the coefficients r_k, which fixes the functional dependence of the r_k on the parameters $\tau, c_2, c_3, \ldots, c_k, \cdots$. We will demonstrate this in Section 2.2.3.

2.2.2 RS dependence at NLO

Before exhibiting the explicit scheme dependence at $O(a^{n+1})$, we consider the simpler NLO case. The NLO RS parameter is τ, Eq.(2.4). It should be emphasised that even at NLO it is not sufficient to specify that one has chosen the renormalization scale μ to specify the RS. The renormalization scheme is specified by τ which incorporates Λ as well.

At NLO we have

$$\mathcal{R}^{(1)}(\tau) = a^{(1)}(\tau) + r_1(\tau)(a^{(1)}(\tau))^2 \,, \tag{2.10}$$

where $a^{(1)}(\tau)$ is obtained by integrating up the NLO truncation of Eq.(2.3)

$$\frac{\mathrm{d}a}{\mathrm{d}\tau} = -a^2(1+ca) \,. \tag{2.11}$$

With a boundary condition $a^{(1)}(0) = \infty$ one obtains

$$\tau = \frac{1}{a^{(1)}(\tau)} + c\ln\left(\frac{ca^{(1)}(\tau)}{1+ca^{(1)}(\tau)}\right) . \tag{2.12}$$

To determine how $r_1(\tau)$ depends on τ explicitly we use Eq.(2.7) and Eq.(2.8) to relate the renormalized coupling and beta function in scheme RS to that in $\overline{\mathrm{RS}}$. Integrating up the beta-functions as in Eq.(2.12) and taking the difference we find

$$\tau - \bar{\tau} = \frac{1}{a} + c\ln\left(\frac{ca^{(1)}(\tau)}{1+ca^{(1)}(\tau)}\right) + O(a) - \frac{1}{\bar{a}} - c\ln\left(\frac{c\bar{a}^{(1)}(\tau)}{1+c\bar{a}^{(1)}(\tau)}\right) - O(\bar{a}) \,, \tag{2.13}$$

where $O(a)$ and $O(\bar{a})$ terms reflect contributions beyond NLO in the beta-function. Since the argument is true for all μ we can take $\mu \to \infty$ so that the $O(a)$ terms tend to zero by asymptotic freedom. Inserting Eq.(2.7) into Eq.(2.2) for the two RS's and equating coefficients one finds

$$r_1 = \nu_1 + \bar{r}_1 \,. \tag{2.14}$$

Using Eq.(2.7) and equating coefficients of corresponding powers of a gives

$$\tau - \bar{\tau} = \nu_1 \,. \tag{2.15}$$

Eliminating ν_1 in Eq.(2.14) and Eq.(2.15) gives

$$\bar{r}_1 - r_1 = \bar{\tau} - \tau \,. \tag{2.16}$$

This implies that

$$r_1(\tau) = \tau + r_1(0) \,. \tag{2.17}$$

Since $\mathcal{R}(Q)$ is a function of the single dimensionful scale Q we can identify this with the RS-invariant combination

$$\rho_0(Q) = \tau - r_1(\tau) \equiv b \ln \frac{Q}{\overline{\Lambda}} \tag{2.18}$$

with $\rho_0(Q)$ and $\overline{\Lambda}$ RS-invariants. $\overline{\Lambda}$ is only dependent on the particular observable $\mathcal{R}$. These quantities are RG-invariant which strongly suggests they should have physical significance, as opposed to RS-dependent quantities $r_1(\tau)$ and $a(\tau)$ which depend on unphysical parameters. The goal of a Feynman diagram calculation at NLO is therefore to determine ρ_0.

Since ρ_0 is an RS-invariant and recalling the definition of τ, Eq.(2.4), we see that for two different renormalization schemes RS and $\overline{\text{RS}}$ we have the exact Celmaster-Gonslaves relation [40]

$$\Lambda_{\overline{RS}} = \Lambda_{RS} \exp\left[\frac{r_1^{RS}(\mu) - r_1^{\overline{RS}}(\mu)}{b}\right], \tag{2.19}$$

with $r_1^{RS}(\mu)$ denoting the NLO calculation is some RS and $r_1^{RS}(\mu) \equiv r_1(\tau)$. In particular from Eq.(2.18) with $\mu = Q$ we find that

$$\overline{\Lambda} = \Lambda_{RS} \exp\left[\frac{r_1^{RS}(\mu = Q)}{b}\right], \tag{2.20}$$

Note that $r_1^{RS}(\mu = Q)$ is a Q-independent quantity. The observable-dependent $\overline{\Lambda}$ is then directly connected to the Λ_{RS} the universal dimensional transmutation parameter of QCD, given a NLO calculation in some RS.

The important implication of Eq.(2.19) is that it does not matter which Λ_{RS} we choose to try to extract from the data. The exponent is a universal μ independent constant exactly relating the Λ's in the two schemes, given NLO calculations in these two RS's. If the RS is mass-independent then Λ_{RS} will be universal and can be exactly related to $\Lambda_{RS'}$ in any other scheme by a universal factor given a NLO calculation for any observable in both RS's.

We can exhibit the explicit scheme dependence of $\mathcal{R}^{(1)}(\tau)$ on τ, by considering the dependence on $a(\tau)$. Using Eq.(2.18) and Eq.(2.12) to write $r_1(\tau)$ in terms of ρ_0 and $a^{(1)}(\tau)$ in terms of τ, respectively, we find

$$\mathcal{R}^{(1)}(\tau) = a^{(1)}(\tau) + \left[\frac{1}{a} + c \ln\left(\frac{c a^{(1)}(\tau)}{1 + c a^{(1)}(\tau)}\right) - \rho_0(Q)\right](a^{(1)}(\tau))^2 . \tag{2.21}$$

Plainly we see that perturbative approximations are not polynomials in the coupling. However, when plotted against $a^{(1)}(\tau)$, $\mathcal{R}^{(1)}$ has a approximately inverted parabolic shape provided $\rho_0 > 0$. From Eq.(2.18) this holds true if $Q > \overline{\Lambda}$. $\mathcal{R}^{(1)}(\tau)$ has a maximum at

$a(\tau) \simeq 1/\rho_0$ ($\tau \simeq \rho_0$) where $\mathcal{R}^{(1)}(\rho_0) \simeq 1/\rho_0$. $\mathcal{R}^{(1)}(\tau)$ vanishes at $a = 0$ ($\tau = \infty$) and at $a(\tau) \simeq 2/\rho_0$ ($\tau \simeq \rho_0/2$).

Let us now discuss how use Eq.(2.21) to extract Λ_{RS} or $\alpha_s(M_Z)$ in the scheme RS. Notice first that the curve $\mathcal{R}^{(1)}(\tau)$ of Eq.(2.21) is a universal function of τ and ρ_0, where the value of the invariant ρ_0 depends on the particular observable $\mathcal{R}$. If ρ_0 is sufficiently small that the maximum $\mathcal{R}^{(1)} \simeq 1/\rho_0$ lies above the data then the curve will cut the measured data at two scales τ_1, τ_2. Conversely, if ρ_0 is made larger the curve will be below the data line. Thus an infinite set of τ, ρ_0 pairs fit the data perfectly. If we wish to measure ρ_0 (and hence Λ_{RS}) we must specify τ. This is the NLO scheme dependence problem.

2.2.3 RS dependence at N^{n}LO

Let us complete our discussion by examining the explicit scheme dependence of the higher perturbative coefficients $r_k(\tau, c_2, \cdots, c_k)$.

Integrating up Eq.(2.3) truncated at n^{th} order and imposing asymptotic freedom, $a(\tau) \to 0$ as $\tau \to \infty$, one finds that

$$\tau = \int_0^a \frac{\mathrm{d}x}{\beta(x)} + (\text{infinite constant}) \,. \tag{2.22}$$

The particular choice of infinite constant corresponds to a definition of Λ. The infinite constant has the form

$$(\text{infinite constant}) = -\int_0^\infty \frac{\mathrm{d}x}{\kappa(x)} \,, \tag{2.23}$$

where $\kappa(x)$ is *any* function with the same singularity structure as $1/\beta(x)$ as $x \to 0$. Since the beta-function has the universal $x \to 0$ behaviour $\beta(x) = -bx^2(1 + cx)$ we choose

$$\kappa(x) = -bx^2(1 + cx) \,. \tag{2.24}$$

With this choice in Eq.(2.23), we split the integration range into (0,a) and (a,∞), and substitute into Eq.(2.23) to obtain the transcendental equation.

$$\tau = \frac{1}{a^{(n)}} + c \ln \frac{ca^{(n)}}{1 + ca^{(n)}} + \int_0^{a^{(n)}} \mathrm{d}x \left[-\frac{1}{x^2 B(x)} + \frac{1}{x^2(1 + cx)} \right] \,, \tag{2.25}$$

where $B(x) \equiv (1 + cx + c_2x^2 + c_3x^3 + \cdots + c_nx^n)$. $a^{(n)}(\tau, c_2, c_3, \cdots, c_n)$ is the solution of this transcendental equation. At NLO the r.h.s reduces to the first two terms as expected from Eq.(2.12). In the above analysis we implicitly assumed that, even though we integrate at constant c_k, the integration constant is independent of c_k. This can be verified by a more detailed discussion [37].

Note that we use the definition of Λ due to Stevenson [37] throughout our discussion. This differs from the conventional definition [41] by a N_f-dependent, but RS-invariant factor, such that

$$\Lambda(Stevenson) = \left(\frac{2c}{b}\right)^{-\frac{c}{b}} \Lambda(conventional) \,. \tag{2.26}$$

The numerical value of the factor $(2c/b)^{-c/b}$ varies from 1.10 ($N_f = 3$) to 1.18 ($N_f = 6$).

The explicit functional dependence of the r_k on the RS is conveniently obtained by considering the special RS, the effective charge (EC) scheme [42], in which $r_1 = r_2 = \cdots = r_n = \ldots = 0$ so that $a^{(n)} = \mathcal{R}^{(n)}$ is an effective charge i.e. the renormalized coupling is the observable itself. From Eq.(2.18) this RS will correspond to the choice of parameter $\tau{=}\rho_0$ (ensuring $r_1 = 0$). To determine the remaining parameters, $c_2^{EC}{=}\rho_2$, $c_3^{EC}{=}\rho_3$, ..., $c_k^{EC}{=}\rho_k$, ..., characterizing the EC RS, one proceeds as follows. If we choose the barred scheme in Eq.(2.8) to be the EC scheme

$$\overline{\beta}(\overline{a}) = \rho(\overline{a}) = \overline{a}^2(1 + \rho_1\overline{a} + \rho_2\overline{a}^2 + \cdots + \rho_k\overline{a}^k + \cdots) \,, \tag{2.27}$$

with $\overline{a}{=}\mathcal{R}$. Then Eq.(2.8) gives [38]

$$\rho(\mathcal{R}) = \beta(a(\mathcal{R}))\frac{\mathrm{d}\mathcal{R}}{\mathrm{d}a} \,, \tag{2.28}$$

where $a(\mathcal{R})$ is the inverted perturbation series.

By expanding both sides of Eq.(2.28) as power series in $\mathcal{R}$ and equating coefficients one obtains [43, 44]

$$\begin{aligned} \rho_1 &= c \\ \rho_2 &= c_2 + r_2 - cr_1 - r_1^2 \\ \rho_3 &= c_3 + 2r_3 - 4r_1r_2 - 2r_1\rho_2 - cr_1^2 + 2r_1^3 \\ &\vdots \quad\quad \vdots \end{aligned} \tag{2.29}$$

Rearranging Eq.(2.29) we exhibit the explicit $\tau, c_2, c_3, \ldots$ dependence of the perturbative coefficients

$$\begin{aligned} r_1(\tau) &= \tau - \rho_0 \\ r_2(\tau, c_2) &= (\tau - \rho_0)^2 + c(\tau - \rho_0) + (\rho_2 - c_2) \\ r_3(\tau, c_2, c_3) &= (\tau - \rho_0)^3 + \frac{5}{2}c(\tau - \rho_0)^2 + (3\rho_2 - 2c_2)(\tau - \rho_0) + \frac{1}{2}(\rho_3 - c_3) \\ &\vdots \quad\quad \vdots \end{aligned} \tag{2.30}$$

The result for $r_n(\tau, c_2, \cdots, c_n)$ is a polynomial of degree n in $\tau - \rho_0$ with coefficients involving ρ_n,ρ_{n-1},$\cdots$,c and c_2,c_3,$\cdots$,c_n; such that $r_n(\rho_0, \rho_2, \rho_3, \cdots, \rho_n) = 0$. The $\rho_2, \rho_3, \cdots, \rho_n, \cdots$, are process-dependent RS-invariants which completely characterise the QCD observable $\mathcal{R}$. They are independent of the energy scale Q but do depend on the number of active quark flavours, N_f. Given just these numbers the perturbative coefficients in any RS can be obtained from Eq.(2.30). As we shall see in Section 2.5, $\rho_2, \rho_3, \cdots, \rho_n, \ldots$ have physical significance, while the RS-dependent r_k and c_k should be considered intermediate quantities to be eventually eliminated in favour of these RS-invariants.

At N^{n}LO one has a $n-1$ dimensional surface $\mathcal{R}^{(n)}(\tau, c_2, \ldots, c_n)$ and to extract ρ_0 one would need to specify τ, c_2, ..., c_n. At least in NLO for a given value of ρ_0 there is a maximum possible $\mathcal{R}^{(1)}$. In NNLO and higher one can show [45] that for a given value of ρ_0 there exists a choice of τ, c_2, ..., c_n such that $\mathcal{R}^{(n)}$ has any desired positive value. Choosing an RS is equivalent to choosing a point on the $n-1$ dimensional surface defined by $\mathcal{R}^{(n)}$. Thus, for any Λ_{RS} we can choose a sequence of schemes such that $\mathcal{R}^{(2)} = \mathcal{R}^{(3)} = \ldots = \mathcal{R}^{(n)} = \mathcal{R}_{exp}$, the experimentally measured value.

2.3 Common renormalization schemes

Before considering some proposed solutions to the RS dependence problem we introduce some more commonly used RS's.

2.3.1 Minimal subtraction and variants

The first of these is the minimal subtraction (MS) renormalization scheme [9]. As an example consider the renormalization of the gluon self-energy diagram, Figure 1.1. Returning to Eq.(1.27) we saw that using dimensional regularization we obtain an expression which has a $1/\epsilon$ pole. In the MS scheme we simply remove this pole. Note that this does not define a unique scheme; there is still a choice of renormalization point to be made.

More commonly used is the modified minimal subtraction scheme ($\overline{\text{MS}}$) [46]. In MS the $1/\epsilon$ pole always appears in conjunction with a group of constants, $\ln 4\pi - \gamma_E$, where γ_E=0.57722... is the Euler-Mascheroni constant. In $\overline{\text{MS}}$ these factors are removed along with the pole. The MS scheme and variants are defined purely in terms of a calculational procedure, with the advantage of providing a gauge and vertex independent, albeit physically unintuitive, definition of the coupling. The relative ease of calculation has led

to almost universal popularity amongst phenomenologists but it should be stressed that there is no compelling physical argument to suggest that it should be preferred over any other scheme. Notice that whilst we are free to choose the beta-function as we please and consider any RS, we do not a priori know which calculational procedure corresponds to such a general RS.

To relate MS and $\overline{\rm MS}$ RS's we note that for any observable and independent of μ [47]

$$r_1^{MS}(\mu) - r_1^{\overline{\rm MS}}(\mu) = \frac{b}{2}(\ln(4\pi) - \gamma_E) \; . \tag{2.31}$$

So using Eq.(2.19) we have

$$\Lambda_{\overline{\rm MS}} = 2.66\Lambda_{\rm MS} \; . \tag{2.32}$$

The relation is independent of N or N_f, and the higher-order beta-function coefficients in MS and $\overline{\rm MS}$ are identical, $c_k^{MS} = c_k^{\overline{\rm MS}}$ $(k \geq 2)$. The only difference is definition of the renormalization scale μ, deriving from the difference in the subtraction procedure. Hence a choice of scale μ using MS corresponds to the same RS as the use of the $\overline{\rm MS}$ procedure with scale 2.66μ. However, from Eq.(2.19) we see there is no non-trivial residual scheme dependence implied in a convenient choice of $\Lambda_{\overline{\rm MS}}$ as the fundamental QCD dimensional mass transmutation parameter we want to extract.

The beta-function coefficients in the $\overline{\rm MS}$ are known to four-loops [48, 49]

$$c_2^{\overline{\rm MS}} = \frac{\left[\frac{2857}{2} - \frac{5033}{18}N_f + \frac{325}{54}N_f^2\right]}{16(11 - \frac{2}{3}N_f)} \tag{2.33}$$

$$c_3^{\overline{\rm MS}} = \frac{\left[\frac{1093}{729}N_f^3 + \left(\frac{6472}{81}\zeta_3 + \frac{50065}{162}\right)N_f^2 - \left(\frac{6508}{27}\zeta_3 + \frac{1078361}{162}\right)N_f + \left(3564\zeta_3 + \frac{149753}{6}\right)\right]}{128(11 - \frac{2}{3}N_f)} \tag{2.34}$$

where the Riemann zeta function is defined in Eq.(A.5).

2.3.2 Momentum space subtraction (MOM) scheme

We shall in Chapters 3 and 4 refer to the momentum space subtraction (MOM) scheme [40]. This is based on the renormalization of a vertex (for example, the triple-gluon or quark-quark-gluon vertex) rather than of a self-energy. MOM schemes are defined so that radiative corrections to a particular vertex are absorbed into the coupling when the incoming momentum have particular values characterized by μ. The idea is that one will obtain a well-behaved series with such a definition of the coupling if μ is chosen to be the 'typical momentum' flowing through the relevant diagrams. Since the choice μ is the only ambiguity at NLO, and often the most serious problem at higher orders in perturbation

theory, the argument of MOM is basically correct but the method leaves the choice of μ to intuition.

We can relate MOM to the $\overline{\rm MS}$ scheme, with scale $\mu = {\rm e}^{u+v/b}Q$. MOM based on the *ggg* vertex at a symmetric subtraction point $\mu^2{=}Q^2$ [40] corresponds to $\overline{\rm MS}$ with $u{=}2.56$ and $v{=}C_A f(\xi)$, where f is a cubic polynomial in the gauge parameter ξ. For the Landau gauge, $\xi{=}0$, $v{=}{-}2.49C_A$. For other versions of MOM based on the *qqg* or ghost vertices, v will involve C_A and C_F. Notice that we consider MOM in two different gauges as separate RS's. This is because MOM is a gauge non-invariant RS. The values of the coefficients $\tau, c_2, \ldots$ are different for different choices of the gauge parameters ξ and thus correspond to distinct RS's. By comparison $\overline{\rm MS}$ is a gauge invariant RS since the gauge parameter ξ cancels order-by-order before one labels the RS [37].

2.3.3 Finite schemes

In fixed order perturbative calculations one can truncate the beta-function to define the coupling a. For all-orders resummations we require an all-orders definition of the coupling. One therefore requires a finite scheme where $B(x)$ has a finite radius of convergence and can be summed.

An extreme example is the so-called 't Hooft scheme [50] where $c_2{=}c_3{=}\cdots{=}c_k{=}\ldots{=}0$, $B(x){=}1+cx$. This results in the all-orders definition of the coupling,

$$b\ln\frac{\mu}{\Lambda} = \frac{1}{a} + c\ln\frac{ca}{1+ca}\,. \tag{2.35}$$

Of course we do not know how to calculate directly in this RS.

2.4 Proposed solutions to RS dependence

There have been many proposed solutions to the problem of renormalization scheme dependence. Many concentrate on the problem of finding an 'optimum scale' μ. We will consider three popular proposed solutions in the literature.

2.4.1 Physical scale

The argument in this approach is based around the idea that the renormalization scale should be chosen to be the physical scale $\mu = Q$. This viewpoint is motivated by the fact

that perturbative coefficients in higher orders will be polynomials in $\ln \mu/Q$

$$r_n = \sum_{i=0}^{n} K_{ni} \left(b \ln \frac{\mu}{Q} \right)^i . \tag{2.36}$$

By setting $\mu \simeq Q$ one therefore avoids large logarithms. If predictions in the vicinity of $\mu = Q$ are strongly μ-dependent then this is supposedly an indication that the perturbation series is intrinsically badly behaved.

The flaw in this argument is that it implicitly assumes that the NLO RS dependence is completely given by the dependence on the renormalization scale μ. As we have previously shown $r_n(\tau, c_2, \ldots, c_n)$ so the NLO RS-dependence is parametrized by $\tau = b \ln Q/\Lambda_{RS}$; so the coefficients depend on Λ_{RS} in addition to μ. The meaning of μ depends on the RS; this is evident in Eq.(2.32) where we observed that $\mu_{MS} = 2.66 \mu_{\overline{\rm MS}}$.

To demonstrate the error in the physical scale argument more explicitly we have from Eq.(2.21)

$$r_n = \sum_{i=0}^{n} \bar{K}_{ni} (\tau - \rho_0)^i , \tag{2.37}$$

where the coefficients $\bar{K}_{ni}$ do not depend on the NLO RS choice, but only on $c, c_2, \ldots, c_i$ and the RS-invariants $\rho_2, \rho_3, \ldots, \rho_i$. Therefore to avoid large terms one should choose $\tau \simeq \rho_0$, the effective charge scheme. To relate Eq.(2.37) to Eq.(2.36) we write

$$(\tau - \rho_0) = b \ln \frac{\mu}{Q} + r_1^{RS}(Q) = b \ln \left[\frac{\mu}{Q} \mathrm{e}^{r_1^{RS}/b} \right]^i , \tag{2.38}$$

where $r_1^{RS} = r_1^{RS}(\mu = Q)$. Then we write Eq.(2.37) as

$$r_n = \sum_{i=0}^{n} \bar{K}_{ni} \left[b \ln \left(\frac{\mu}{Q} \mathrm{e}^{r_1^{RS}/b} \right) \right] . \tag{2.39}$$

In Eq.(2.37) and Eq.(2.39) the $\bar{K}_{ni}$ coefficients do not depend on the NLO RS choice, whereas in Eq.(2.36) we see that since the K_{ni} depend on the NLO coefficient r_1^{RS} they will have an implicit dependence on the NLO RS choice. Following the same argument for Eq.(2.39) as that used to motivate $\mu \simeq Q$ from Eq.(2.36) we see that one should set $\mu \simeq Q \mathrm{e}^{r_1^{RS}/b} = \mu_{EC}$, the effective charge scale.

The conclusion is that in order to avoid large logarithms and correctly parametrize the NLO RS dependence one should choose the effective charge scheme, $\tau = \rho_0$.

2.4.2 BLM scale fixing

Brodsky, Lepage and Mackenzie (BLM) [51], motivated by physical considerations in QED, proposed to select the scale μ so that the NLO coefficient r_1 is independent of

the number of flavours N_f. The flavour-dependent part of r_1 is then absorbed into the coupling a. The linearly N_f-dependent part of r_1 appears in the calculated Feynman diagrammatics due to the insertion of a one-loop fermion bubble correction to the photon propagator [2]. BLM applies at NLO and assumes that Λ is always the same. Attempts to extend BLM to higher orders have been made [52], but for simplicity we consider the NLO case.

To be more precise, consider a physical observable, defined in two RS's, one the BLM scheme and the other arbitrary. The perturbative expansion in the two schemes will be

$$\begin{aligned} \mathcal{R} &= a + r_1 a^2 \\ \mathcal{R}^{BLM} &= a_{BLM} + r_1^{BLM} a_{BLM}^2 \end{aligned} \tag{2.40}$$

In general for both r_1 and b we can separate linearly N_f-dependent and N_f-independent contributions

$$\begin{aligned} r_1 &= r_1^{(1)} N_f + r_1^{(0)} \\ b &= b_{(1)} N_f + b_{(0)} \, . \end{aligned} \tag{2.41}$$

The two couplings can be related via Eq.(2.14)and Eq.(2.16). Using Eq.(2.41) the BLM perturbative coefficient will then be

$$r_1^{BLM} = r_1^{(1)\,BLM} N_f + r_1^{(0)\,BLM} + (b_{(1)} N_f + b_{(0)}) \ln(\mu_{BLM}/\mu) \, , \tag{2.42}$$

where μ_{BLM} and μ are the renormalization scales in the respective schemes.

BLM requires that the two N_f-dependent parts of Eq.(2.42) cancel each other exactly; thus we have

$$\mu_{BLM} = \mu \exp(-r_1^{(1)}/b_{(1)}) \tag{2.43}$$

$$r_1^{BLM} = r_1^{(0)} - \frac{b_{(0)}}{b_{(1)}} r_1^{(1)} \, . \tag{2.44}$$

The BLM approximant for $\mathcal{R}$ then reads

$$\mathcal{R}^{BLM} = a_{BLM} + (r_1^{(0)} - \frac{b_{(0)}}{b_{(1)}} r_1^{(1)}) a_{BLM}^2 \, , \tag{2.45}$$

where $a_{BLM} = a_{BLM}(\mu_{BLM})$.

[2] A generalization of this property has been exploited in QCD and termed "naïve non-abelianization"; in QCD there will be additional gluon and ghost loop corrections relevant in the running of α_s. We consider this in more detail in Chapter 3.

The BLM procedure is not RS-independent. Starting from two different initial schemes one can obtain different answers for $\mathcal{R}^{BLM}$. To observe the exact restrictions consider the observable, denoted $\bar{\mathcal{R}}$, in a second arbitrary scheme; we have

$$\bar{\mathcal{R}} = \bar{a} + \bar{r}_1 \bar{a}^2 \,, \tag{2.46}$$

with $a = \bar{a} + \bar{\nu}_1 \bar{a}^2$. From Eq.(2.14) we have that

$$\begin{aligned} \bar{r}_1 &= \bar{r}_1^{(1)} N_f + \bar{r}_1^{(0)} \\ &= (r_1^{(1)} + \bar{\nu}_1^{(1)} N_f) + (r_1^{(0)} + \bar{\nu}_1^{(0)}) \,. \end{aligned} \tag{2.47}$$

In this scheme $\mathcal{R}^{BLM}$ will have the NLO coefficient $\bar{r}_{BLM}$ given by

$$\bar{r}_1^{BLM} = (r_1^{(1)} N_f + \bar{\nu}_1^{(1)} N_f) + (r_1^{(0)} + \bar{\nu}_1^{(0)}) + (b_{(1)} N_f + b_{(0)}) \ln \mu_{BLM}/\bar{\mu} \,. \tag{2.48}$$

Applying the BLM criterion requires that

$$\mu_{BLM} = \bar{\mu} \exp(-(r_1^{(1)} + \bar{\nu}_1^{(1)})/b_{(1)}) \tag{2.49}$$

$$\bar{r}_1^{BLM} = r_1^{(0)} + \bar{\nu}_1^{(0)} - \frac{b_{(0)}}{b_{(1)}} (r_1^{(1)} + \bar{\nu}_1^{(1)}) \,. \tag{2.50}$$

For $\bar{r}_1^{BLM} = r_1^{BLM}$, it follows from Eq.(2.43–2.44) and Eq.(2.49–2.50) that we have the condition

$$\bar{\mu} = \mu \exp(C) \,, \qquad C \equiv \frac{\bar{\nu}_1^{(1)}}{b_{(1)}} = \frac{\nu_1^{(0)}}{b_{(0)}} \,. \tag{2.51}$$

where C is a constant, independent of N_f. Therefore scale transformations between the barred and unbarred schemes must be flavour independent.

The BLM scale setting procedure can only give scheme-invariant results within classes of schemes that can be transformed into each other via flavour-independent scale transformations. For instance, as discussed in Section 2.3.2, MOM schemes with different gauge or vertex choices are related to each other by flavour-dependent scale transformations and will hence give differing BLM results. This is rather unhelpful since we have no external criteria to choose the class of schemes that specifies the flavour-dependence of r_1 optimally. Nor do we have any physical reason to make us believe that such classes of schemes are the 'best'.

The basic misunderstanding in both the physical scale and BLM argument is the assumed existence of an 'optimal' scale μ. This is meaningless since there is no such thing as an optimal μ. There is, however, an optimal value of the ratio μ/Λ since this is exactly the variable that embodies the RS ambiguity at NLO.

2.4.3 The principle of minimum sensitivity (PMS)

The principle of minimum sensitivity (PMS) [37] is based on the fundamental notion of RG invariance. The principle [37] is that since the exact all-orders result is independent of the unphysical parameters $\tau, c_2, c_3, \cdots, c_k, \cdots$ we should choose the $O(a^{n+1})$ approximation $\mathcal{R}^n(\tau, c_2, \cdots, c_n)$ to mimic this property by minimizing its sensitivity to small variations in those parameters.

Mathematically PMS is formulated as a variational principle; we arrange that

$$\left.\frac{\partial \mathcal{R}^{(n)}}{\partial \tau}\right|_{\tau=\bar{\tau}} = \left.\frac{\partial \mathcal{R}^{(n)}}{\partial c_2}\right|_{c_2=\bar{c_2}} = \cdots = \left.\frac{\partial \mathcal{R}^{(n)}}{\partial c_n}\right|_{c_n=\bar{c_n}} = 0 \ . \tag{2.52}$$

The PMS scheme is then specified by $\bar{\tau}, \bar{c_2}, \cdots, \bar{c_n}$.

To give an example of PMS we consider NLO. We rewrite RG-invariance condition in terms of the parameters that label the RS dependence, in this case τ. We solve

$$\left.\frac{\partial \mathcal{R}^{(n)}}{\partial \tau}\right|_{\tau=\bar{\tau}} = \left(\left.\frac{\partial}{\partial \tau}\right|_a + \frac{\beta(a)}{b}\frac{\partial}{\partial a}\right)\mathcal{R}^{(n)} = 0 \ . \tag{2.53}$$

This leads to

$$a^2\frac{\partial r_1}{\partial \tau} - a(1+ca_1)(1+2r_1a) = 0 \ . \tag{2.54}$$

The $O(a^2)$ terms must cancel for the formal consistency of perturbation theory. The PMS criterion requires the remaining terms of Eq.(2.54) to vanish at $\tau = \bar{\tau}$

$$2\bar{r}_1(1+c\bar{a}) + c = 0 \ , \tag{2.55}$$

where $\bar{r}_1 \equiv r_1(\bar{\tau})$, $\bar{a} \equiv a(\bar{\tau})$. Eliminating $\bar{r}_1$ in Eq.(2.10) using Eq.(2.55) we then obtain the solution in terms of $\bar{a}$

$$\mathcal{R}^{(1)}_{PMS} = \frac{\bar{a}(1+\frac{1}{2}c\bar{a})}{(1+c\bar{a})} \ . \tag{2.56}$$

To determine the stationary point in terms of τ we rewrite Eq.(2.54) as the corresponding transcendental equation

$$\rho_0 = \frac{1}{a} + c\ln\left[\frac{ca}{1+ca}\right] + \frac{1}{2}\frac{c}{1+ca} \ . \tag{2.57}$$

We see that $\bar{a}$ and hence $\mathcal{R}^{(1)}_{PMS}$ is an RS-invariant. This is also true for higher order optimized approximants. If $\mathcal{R}(a)$ and all derivatives are monotonic then the perturbative approximant is irredeemably ambiguous since there is no objective means for choosing μ at which to evaluate the coupling. This happens in lowest order $\mathcal{R}(a) = a$, which therefore gives at best semi-quantitative results.

Unlike BLM or physical scale arguments, PMS correctly attempts to optimize μ/Λ. The disadvantages of the PMS method are that the coupling and the beta-function are unphysical quantities and that given the complex nature of the coupled equations which must be solved it is unclear whether their all-orders versions are defined.

2.5 The effective charge (EC) formalism

In the following section we give a detailed review of a generalization of Grunberg's effective charge approach [42] which will be central to the RS-invariant resummations to be discussed in Chapter 4 and 5. We refer the reader to references [38, 53] for full details.

2.5.1 The effective charge beta-function

We begin by considering a generic dimensionless QCD observable $\mathcal{R}(Q)$, with a formal perturbation series of the form (2.2). We shall refer to observables defined in this way as *effective charges*. Such effective charges satisfy several important properties.

For the dimensionless QCD observable $\mathcal{R}(Q)$ we can define the evolution equation for the Q-dependence of $\mathcal{R}$

$$\frac{\mathrm{d}\mathcal{R}(Q)}{\mathrm{d}\ln Q} \equiv \xi(\mathcal{R}) \,. \tag{2.58}$$

$\mathrm{d}\mathcal{R}/\mathrm{d}\ln Q$ and hence $\xi(\mathcal{R}(Q))$ are in principle experimentally observable quantities. To make contact with QCD perturbation theory we note that Eq.(2.58) is the beta-function equation in the effective charge (EC) scheme where the coupling is an effective charge:

$$a = \mathcal{R}(Q) \quad \Longrightarrow \quad r_1 = r_2 = \cdots = r_n = \cdots = 0 \,. \tag{2.59}$$

So we have

$$\frac{d\mathcal{R}(Q)}{d\ln Q} \equiv -b\rho(\mathcal{R}(Q)) \,, \tag{2.60}$$

where

$$\rho(\mathcal{R}(Q)) = -\mathcal{R}^2(1 + c\mathcal{R} + \rho_2\mathcal{R}^2 + \cdots + \rho_n\mathcal{R}^n + \cdots) \,, \tag{2.61}$$

where the effective charge beta-function coefficients ρ_n are Q-independent (but process-dependent) RS-invariant combinations of the r_i, c_i $(i \leq n)$, as shown in Section 2.2.3. The effective charge beta-function $\rho(\mathcal{R}(Q))$ is a key ingredient of the EC formalism and can be regarded as a physical observable to be reconstructed from the measured running of $\mathcal{R}(Q)$ e.g. at a next-linear collider. As measured from data it will include a resummation of

the (asymptotic) formal perturbation series together with non-perturbative $e^{-1/\mathcal{R}}$ terms which are invisible in perturbation theory [3].

2.5.2 The non-perturbative integrated beta-function

To obtain $\mathcal{R}(Q)$ we need to integrate Eq.(2.58). We use the assumption of asymptotic freedom as the necessary boundary condition. AF is equivalent to the statement that for any effective charge $\mathcal{R}(Q)$,

$$\lim_{Q\to\infty} \mathcal{R}(Q) = 0 \,. \tag{2.62}$$

This corresponds to the requirement that $\xi(R(Q)) < 0$ for $Q > Q_0$, with Q_0 some suitably low energy. (Equivalently, $\rho(\mathcal{R}(Q)) > 0$ for $Q > Q_0$).

Integrating up Eq.(2.60) and imposing AF as a boundary condition we obtain,

$$\ln \frac{Q}{\Lambda_{\mathcal{R}}} = \int_0^{\mathcal{R}(Q)} \frac{1}{\xi(x)} dx + (\text{infinite constant}) \tag{2.63}$$

where $\Lambda_{\mathcal{R}}$ is a finite constant of integration which depends on the way the infinite constant is chosen. The infinite constant can be chosen to be

$$(\text{infinite constant}) = -\int_0^{\infty} \frac{dx}{\eta(x)}, \tag{2.64}$$

where $\eta(x)$ is *any* function which has the same $x \to 0$ behaviour as $\xi(x)$. We know from Eq.(2.60) that $\xi(x)$ has the universal $x \to 0$ behaviour $\xi(x) = -b\rho(x) \approx -bx^2(1+cx)$ so we choose $\eta(x) = -bx^2(1+cx)$. Inserting this choice for $\eta(x)$ and rearranging Eq.(2.63) we find

$$b \ln \frac{Q}{\Lambda_{\mathcal{R}}} = \int_{\mathcal{R}(Q)}^{\infty} \frac{dx}{x^2(1+cx)} + \int_0^{\mathcal{R}(Q)} dx \left[-\frac{1}{\rho(x)} + \frac{1}{x^2(1+cx)} \right]. \tag{2.65}$$

Recognising the first integral on the right hand side of Eq.(2.65) as just Eq.(2.12) for the EC scheme, this then yields

$$\begin{aligned} F(\mathcal{R}(Q)) &= b \ln \frac{Q}{\Lambda_{\mathcal{R}}} - \int_0^{\mathcal{R}(Q)} dx \left[-\frac{1}{\rho(x)} + \frac{1}{x^2(1+cx)} \right] \\ &\equiv b \ln \frac{Q}{\Lambda_{\mathcal{R}}} - \Delta\rho_0(Q) \,, \end{aligned} \tag{2.66}$$

where

$$F(x) = \frac{1}{x} + c \ln \left(\frac{cx}{1+cx} \right) \,, \tag{2.67}$$

[3] To be more rigorous $\rho(\mathcal{R}) = -\mathcal{R}^2(1 + c\mathcal{R} + \rho_2\mathcal{R}^2 + \cdots + \rho_n\mathcal{R}^n + \cdots) + e^{-S/\mathcal{R}}\mathcal{R}^{\delta}(K_0 + K_1\mathcal{R} + \cdots)$, with $S, \delta, K_0, K_1, \ldots$ observable-dependent constants which we do not specify further [54].

Notice that the integrand of $\Delta\rho_0$ is regular at $x = 0$ and that in arriving at Eq.(2.66) we did not need to refer to perturbation theory, except to assume the asymptotic $x \to 0$ ($Q \to \infty$) behaviour $\xi(\mathcal{R}(Q)) \approx -b\mathcal{R}^2(1 + c\mathcal{R})$.

Rearranging Eq.(2.66) and assuming AF ($Q \to \infty$, $\mathcal{R}(Q) \to 0$), in which limit $\Delta\rho_0(Q) \to 0$, one finds that, asymptotically, for any effective charge $\mathcal{R}(Q)$

$$\lim_{Q\to\infty} Q\mathcal{F}(\mathcal{R}(Q)) = \Lambda_{\mathcal{R}} \ , \tag{2.68}$$

Here $\Lambda_{\mathcal{R}}$ is a observable-dependent scaling constant with the dimensions of energy, and we have defined a universal QCD scaling function

$$\mathcal{F}(x) \equiv e^{-1/bx}(1 + 1/cx)^{c/b} \ , \tag{2.69}$$

with

$$F(x) \equiv -b \ln \mathcal{F}(x) \tag{2.70}$$

The property (2.68) may be termed *asymptotic scaling* [53]. Given sufficiently large values of Q this property can evidently serve as a test of QCD, but since $\Lambda_{\mathcal{R}}$ is not universal it cannot usefully be applied at fixed values of Q.

As we will now show, the constant $\Lambda_{\mathcal{R}}$ obtained with the particular choice $\eta(x) = -bx^2(1+cx)$ is precisely the $\overline{\Lambda}$ introduced in Eq.(2.18). Consider the coupling a with scale $\mu = Q$ using the $\overline{\rm MS}$ subtraction procedure in NLO, and with the higher order beta-function coefficients zero ('t Hooft scheme [50]). This defines an all-orders coupling with

$$F(a) = b \ln \frac{Q}{\Lambda_{\overline{\rm MS}}} \ . \tag{2.71}$$

With $a \to 0$ as $Q \to \infty$, one has

$$R \simeq a + r_1^{\overline{\rm MS}}(Q)a^2 + \cdots \ , \tag{2.72}$$

so asymptotically,

$$F \simeq F(a) - r_1^{\overline{\rm MS}}(Q)a^2 + \cdots \ , \tag{2.73}$$

where the ellipsis denote terms which vanish as $Q \to \infty$. Inserting Eq.(2.73) into Eq.(2.68) and using Eq.(2.71) we obtain for $Q \to \infty$ the exact Celmaster-Gonslaves relation [40]

$$\Lambda_{\mathcal{R}} e^{-r_1/b} = \Lambda_{\overline{MS}} \ . \tag{2.74}$$

Comparing Eq.(2.20) and (2.74) we have that $\Lambda_{\mathcal{R}} = \overline{\Lambda}$.

If the next-to-leading order (NLO) perturbative coefficient $r_1 \equiv r_1^{\overline{MS}}(\mu = Q)$ has been calculated (in the $\overline{MS}$ scheme with scale $\mu^2 = Q^2$ for instance), then $\Lambda_{\mathcal{R}}$ can be converted

into a *universal* scaling constant $\Lambda_{\overline{MS}}$ via the *exact* relation (2.74). Use of different subtraction procedures results in different constants which, however, are still *universal.*

Using the exact Eq.(2.74) and Eq.(2.68) one finds that, asymptotically, for any effective charge $\mathcal{R}(Q)$

$$\lim_{Q\to\infty} Q\mathcal{F}(\mathcal{R}(Q))e^{-r_1/b} = \Lambda_{\overline{MS}} \,. \tag{2.75}$$

This property may be termed *universal asymptotic scaling* [53], and can be used to test QCD at fixed Q by looking at the scatter in $Q\mathcal{F}(\mathcal{R}(Q))e^{-r_1/b}$ for various observables [38]. Furthermore, one can then identify $b\ln(Q/\Lambda_{\mathcal{R}})$ with the NLO RS-invariant $\rho_0(Q)$ [38] using Eq.(2.18)

$$b\ln\frac{Q}{\Lambda_{\mathcal{R}}} = \rho_0(Q) \equiv b\ln\frac{Q}{\Lambda_{\overline{\rm MS}}} - r_1^{\overline{\rm MS}}(\mu = Q) \,, \tag{2.76}$$

One can see that $\Lambda_{\mathcal{R}}$ and ρ_0 are connected with the asymptotic dependence of $\mathcal{R}$ on Q i.e. $\lim_{Q\to\infty}\mathcal{R}(Q) \sim 1/\rho_0$. In principle $\Lambda_{\mathcal{R}}$ or ρ_0 could be measured given unlimited accelerator energies.

Finally, using Eq.(2.76) we can rewrite Eq.(2.66) as

$$\begin{aligned} F(\mathcal{R}(Q)) &= b\ln\frac{Q}{\Lambda_{\overline{\rm MS}}} - r_1^{\overline{MS}}(Q) - \Delta\rho_0(Q) \\ &= \rho_0(Q) - \Delta\rho_0(Q) \,. \end{aligned} \tag{2.77}$$

As stressed by [38] Eq.(2.77) holds *beyond perturbation theory* for the measured observable $\mathcal{R}(Q)$ and $\Delta\rho_0(Q)$ constructed from the measured running of $\mathcal{R}(Q)$, $\mathrm{d}\mathcal{R}(Q)/\mathrm{d}\ln Q = -b\rho(\mathcal{R}(Q))$. No reference was made to perturbation theory except to assume AF. That is, we can write a *non-perturbative* closed expression *exactly* relating the universal QCD dimensional mass transmutation parameter $\Lambda_{\overline{MS}}$ to physical observables.

2.5.3 The effective charge scheme

One could, of course, write down Eq.(2.77) perturbatively in the EC scheme by using the integrated beta-function Eq.(2.25) with $a^{(n)} = \mathcal{R}^{(n)}$, $\tau^{EC} = \rho_0$ and $B^{(n)} = \rho^{(n)} = 1 + cx + \rho_2 x^2 + \cdots + \rho_n x^n$. The scheme parameters are then the RS-invariant quantities $\rho_0, \rho_2, \rho_3, \cdots, \rho_n$.

The ρ_k can be calculated in any convenient scheme. For example ρ_2, the NNLO EC beta-function coefficient, can be calculated in the $\overline{\rm MS}$ RS given the NLO and NNLO perturbative coefficients, $r_1^{\overline{\rm MS}}$ and $r_2^{\overline{\rm MS}}$

$$\rho_2 = c_2^{\overline{\rm MS}} + r_2^{\overline{\rm MS}} - cr_1^{\overline{\rm MS}} - r_1^{\overline{\rm MS}\ 2} \,, \tag{2.78}$$

with $c_2^{\overline{\rm MS}}$ the three-loop $\overline{\rm MS}$ beta-function coefficient. This can be inserted into the integrated beta-function Eq.(2.77) and solved for $a^{(n)} = \mathcal{R} = \mathcal{R}^{data}$ to evaluate ρ_0.

In low orders of perturbation theory there is a close connection between the EC and PMS methods, and they give practically identical results. For example at NLO we have $F(a) = \rho_0$ (EC) and $F(a) + \frac{1}{2}\frac{c}{1+ca} = \rho_0$ (PMS). In both cases ρ_0 is then adjusted to give $\mathcal{R}^{(1)}_{PMS/EC} = \mathcal{R}^{(1)}_{data}$.

As we will discuss further in Chapter 3, it is believed that perturbation theory gives only asymptotic series which diverge at high orders. However, in optimized schemes such as PMS and EC one cannot regard perturbation theory as a conventional power series expansion in a fixed parameter. As noted in Section 2.2.2 and 2.2.3 perturbative approximants written in terms of RS-invariants are not polynomials in the coupling. The effects of optimization at higher orders and their possible convergence or divergence is thus of interest, and it has been suggested that optimized schemes may converge [53, 55].

2.6 Summary and conclusions

Stevenson's [37] parametrization of the RS offers an explicit realisation of the RG in massless QCD. For perturbation theory truncated at $O(a^{n+1})$ we require n independent parameters, $\tau, c_2, c_3, \ldots, c_n$, to label the RS dependence of the coupling and perturbative coefficients. Crucially we can construct RG-invariant quantities $\rho_0, \rho_2, \ldots$ from perturbative Feynman diagram calculations which together completely determine the physical observable. At NLO this leads to the exact Celmaster-Gonslaves equation, relating two Λ's in two RS's exactly given only the NLO perturbative coefficients in the two schemes. Using these RS-invariants the perturbative coefficients in any RS can be obtained.

To exploit these RS-invariants we introduced the EC formalism, which is a refinement and extension of RG-improved perturbation theory, and therefore different from the conventional concept of a power-series expansion in a fixed-parameter. One non-perturbatively identifies each observable as an all-orders coupling, with both coupling and beta-function experimental observables. We emphasise that the non-perturbative derivation of the EC formalism makes it more general than the adoption of a specific scheme. Given $\rho(x)$ and $\Lambda_{\overline{\rm MS}}$, $\mathcal{R}$ is unambiguously fixed by Eq.(2.77). Our knowledge of $\rho(x)$ can be increased from perturbation theory and independently from measurements of the running of $\mathcal{R}$, and then their consistency checked. These advantages will make the EC formalism a cornerstone for the ideas in Chapter 4 and Chapter 5.

Chapter 3

Perturbation theory at large-orders

3.1 Introduction

The subject of large-order perturbation theory (LOPT) has aroused new interest in the last decade, with particular attention paid to the power corrections to QCD predictions for hard scattering processes. One can point out two reasons for this growing interest in the large-order behaviour of the perturbative expansion coefficients in QCD:

- The theoretical problem of how physical observables can be reconstructed from their (often divergent) power series expansions. The discovery that for most practical quantum field theories the perturbative expansions demonstrate divergent behaviour at large orders must cause concern since it is our best tool for extracting phenomenological predictions.
- The practical need to assess the usefulness of evaluating multi-loop Feynman diagrams in QCD. Considerable effort has been devoted to the computation of higher-order QCD perturbative corrections; in some cases NNLO approximants are known, and we now seem to be at the limit of what can be achieved analytically or numerically. If the series is divergent, the next order may represent no improvement with respect to the lower-order result. On the contrary, at a certain order it will lead to deterioration — an effect exacerbated if the energy scale is low.

In this chapter we review the means by which perturbation theory, as applied to quantum field theory (QFT), has been investigated at large orders, and the insights and interpretations which have been consequently gained. We start in Section 3.2 by presenting Dyson's argument for the divergence of QED. To clarify how it is that the application of

fixed order perturbation theory to QFT gives such spectacular agreement with experiment when it appears to ignore an infinite number of divergent higher order terms we introduce the concept of an asymptotic series and the method of Borel summation in Sections 3.3 and 3.4. We move on in Section 3.5 to consider the large-N_f expansion as a method to resum the subset of Feynman diagrams which cause the divergence of the perturbative theory in QED and QCD. Section 3.6 considers the application of Borel transform technology to encode the divergent behaviour of the expansion coefficients in the form of renormalon singularities in the Borel plane. Briefly mentioning instanton singularities in Section 3.7, we move on in Section 3.8 to discuss the progress made in understanding the link between renormalons and non-perturbative power corrections, emphasising the role of operator product expansion in phenomenological calculations. Section 3.9 contains concluding remarks. For a more detailed review of LOPT see [56, 57].

3.2 The divergence of the QED perturbation theory

A physically intuitive argument to show that perturbative expansions in QED would diverge was presented by F.J. Dyson in 1952 [58]. To illustrate the mechanism we start by considering the perturbative expansion for a generic physical quantity f, in renormalized QED perturbation theory

$$f(e^2) = f_0 + f_1 e^2 + f_2 e^4 + \cdots = \sum_{k=0}^{\infty} f_k (e^2)^k \,, \tag{3.1}$$

where e is the electron charge and f_k is calculated using Feynman diagram methods. Let us assume that the series in Eq.(3.1) is the Taylor expansion of $f(e^2)$, uniquely determining $f(e^2)$, with radius of convergence $\rho > 0$ centred at the origin in the complex e^2 plane. Then $f(e^2)$ is analytic $\forall |e| < \rho$. Given this assumption, then, for sufficiently small values of e, $f(-|e^2|)$ will also be an analytic function with a convergent power series expansion.

Consider a 'gedanken' universe in which $e^2 = -\epsilon^2 < 0$, so that on a macroscopic scale the Coulomb interaction is opposite to that in our universe: like charges attract, unlike charges repel. Field theoretical fluctuations in the quantum vacuum continually result in the spontaneous creation and annihilation of electron-positron pairs. If enough electrons spontaneously appear in the vicinity of our system it will cause the energy of the system to decrease [1]. Moreover with enough pair production this decrease will be greater than the energy required to create all the lepton pairs. Pair production becomes energetically

[1] We do not take into account the Pauli principle which forbids us to put an arbitrary number of fermions in the same quantum state. The argument is only really valid for charged bosons.

favourable and manifests itself as a real process. Real electrons materialize from out of the vacuum and a pathological situation develops as it becomes ever more favourable for the vacuum to decay. Once this state is realised, an irreversible process of pair creation will set in until an infinite number of pairs has been created. With a finite probability for the required pair-creation, the disintegration of the vacuum is inevitable.

Therefore for $e^2 < 0$ the physical quantity f cannot be well-defined. Thus the series in Eq.(3.1) must have a zero radius of convergence and our observable $f(e^2)$ can at best be analytic in the complex e^2 plane with a singularity at $e^2 = 0$ and the negative real axis excluded. We conclude that the quantum tunneling instability between the vacua of the real universe and gedanken universe introduces a cut in the amplitude on the negative real axis, leading to the divergence of perturbation theory. As we will demonstrate in Section 3.6 one finds that LOPT has a generic factorial type divergence.

This conjecture has been questioned [55]. Eq.(3.1) can only generate a series in positive powers of the coupling. All analytic functions, however, are expressible as a Laurent expansion, which includes negative as well as positive powers of the expansion parameter. The perturbation expansion of a field theoretic quantity is therefore inherently incomplete, and incapable of providing all the information we require to construct the functional form of a physical observable. A physical observable is determined by its perturbative expansion plus *non-perturbative effects*. For example, the term e^{-1/e^2} is non-perturbative and would not contribute to the expansion on the right hand side of Eq.(3.1) – it is invisible in perturbation theory. It is possible for the perturbative expansion to converges to some well-behaved analytic function and that it is the non-perturbative part of the function $f(e^2)$ that has an essential singularity at the origin. The latter is then wholly responsible for the singular nature of $f(e^2)$ and it is not possible to deduce anything about the divergence of the perturbative expansion from Dyson's argument.

Despite the fact that Dyson's analysis is not entirely rigorous the general conclusion that QED perturbative series have zero radius of convergence raises important considerations. We must explain exactly how truncated perturbative series still have meaning when the series themselves formally diverge for any physical value of the expansion parameter.

3.3 Asymptotic series

To answer this question we assume that perturbative series in QFT's are in general asymptotic expansions. In our example this means that the sum on the right hand side of Eq.(3.1)

does not necessarily reproduce $f(e^2)$ uniquely but rather it converges asymptotically towards $f(e^2)$ for a finite number of terms, after which it begins to diverge.

Definition of an asymptotic series

Formally let us consider a general function $f(g)$ which is analytic in the domain $\mathcal{D}$, where $\mathcal{D}$ is a subset of the complex plane having the origin as an accumulation point. Perturbation theory (PT) is based on expressing $f(g)$ in the form of the power series at the origin

$$f(g) = \sum_{n=0}^{\infty} f_n g^n, \tag{3.2}$$

where g, the expansion parameter (usually the coupling in QFT), is considered to be a small numerical quantity.

A formal series (3.2) is called *asymptotic* to $f(g)$ on the domain $\mathcal{D}$ if the sequence of *remainders* $R_N(g)$ satisfies [59],

$$R_N(g) = \mid f(g) - f_N(g) \mid \leq C_{N+1}|g|^{N+1} \qquad \forall N, \forall g \in \mathcal{D} \tag{3.3}$$

where $f_N(g) = \sum_{n=0}^{N} f_n g^n$ is the N^{th} partial sum. That is, the right hand side of Eq.(3.2) diverges $\forall\ g \neq 0$ and in $\mathcal{D}$ it satisfies the bound Eq.(3.3) $\forall\ N$.

The optimum order of an asymptotic series

The bound on $R_N(g)$ supplies the method by which we can make sense of a divergent series. It informs us that if we choose to truncate the series after the first N terms we can obtain an approximation to $f(g)$ which for any N improves as $|g| \to 0$, with a discrepancy that is of one order higher then the approximant itself.

We note that if a small enough $|g|$ is inserted into the divergent series, then there will be an initial period of convergence before eventual divergence. One may define the *accuracy* $\epsilon(g)$ of the remainder function evaluated at N_{opt}, where N_{opt} is such as to minimise the remainder function. As $|g|$ increases from zero, period of convergence of the series (given by N) diminishes monotonically from infinity, reaching zero at a critical value $|g| = |g_c|$; then there is instant divergence. Correspondingly $\epsilon(g)$ will increase monotonically from zero. Furthermore for $|g| < |g_c|$, N_{opt} should give the point at which the period of convergence ends.

So, despite the fact that the infinite series is divergent for all non-zero values of g, the partial sum of N terms can be used to estimate $f(g)$ providing $|g|$ is small. For a particular fixed value of $|g|$ we can minimize the bound on the error in this estimate by minimizing the right hand side of Eq.(3.3) with respect to N. Hence we can find the optimum number of terms, $N_{\rm opt}$, to take in the partial sum. For QED the expansion parameter is the fine structure constant, $\alpha \simeq 1/137$. Assuming the expansion coefficients grow as $n!$, minimizing $f_n\alpha^n$ gives $N_{\rm opt} \sim 1/\alpha \sim 137$. Thus QED starts to diverge only at $\sim$137th order in the perturbative expansion, far beyond the present (or future) state-of-the-art in Feynman diagrams calculations.

Let us consider a slightly more general choice of form for the coefficients, f_n, which will lead to similar behaviour; that is, convergence of the partial sum up to $N_{\rm opt}$ terms, and divergence of the series beyond $N_{\rm opt}$ terms. So, for example,

$$C_N = AC^{-N}N! \,. \tag{3.4}$$

We can then write down a function of g which will characterize the maximum accuracy of the partial sum to N terms:

$$\begin{aligned} \epsilon(g) &= \min_{\{N\}} \left(f_N |g|^N \right) \\ &= f_{N_{\rm opt}} |g|^{N_{\rm opt}} \,. \end{aligned} \tag{3.5}$$

Using the Stirling formula Eq.(A.4) for $n!$ at large n, so that for f_n of the form given in Eq.(3.4), $N_{\rm opt} \sim C/|g|$. We then find that

$$\epsilon(g) \sim \exp[-C/|g|] \,. \tag{3.6}$$

Uniqueness

The fact that the asymptotic series can approximate $f(g)$ only to a finite accuracy, $\epsilon(g)$, indicates that knowledge of the asymptotic series alone does not allow us to unambiguously and uniquely determine its corresponding function $f(g)$.

Generally, if we have

$$\sum_{n=0}^{\infty} f_n g^n \approx f(g) \,, \tag{3.7}$$

where '$\approx$' means '*is asymptotic to*' [2], then it may be proved there always exists a function $f(g)$, analytic in the region $|\arg g| < \theta$ with $0 < \theta \leq \pi/2$, satisfying Eq.(3.7) for any

[2]The requirement of asymptoticity in Eq.(3.7) for a perturbation series is not a formal assumption. Its physical meaning is that there is a smooth transition in the coupling parameter between the system with interaction and the system without it.

set of coefficients $\{f_n\}$, however 'violent' the behaviour of the expansion coefficients f_n as $n \to \infty$ [59]. To a function $f(g)$ satisfying Eq.(3.7), one can add a term of the form $A\exp(-B/g^k)$, with $0 < 2k\theta < \pi$, with A real and $B > 0$, without violating Eq.(3.3) within $\mathcal{D}$ [59]

$$\sum_{n=0}^{\infty} f_n g^n \approx f(g) + A\exp[-B/g^k]\,, \tag{3.8}$$

provided that $B\cos(\theta/2) > C$ and that $|A|$ is sufficiently small. This new function is also analytic in $\mathcal{D}$ and satisfies the bound given in Eq.(3.3). Further, in contrast to Eq.(3.2), the relation (3.7) does not determine the function $f(g)$ uniquely, even when all the f_n are explicitly given and the set of rays approaching the point $g = 0$ is specified. Even then an infinite class of functions $f(g)$ is defined by Eq.(3.7). On the other hand any given function $f(g)$ can only correspond to one and only one asymptotic series. Note the ambiguity in Eq.(3.8) has the construction of a non-perturbative term. Thus the divergent nature of the perturbative series *in itself* implies that the PT cannot fully describe QFT.

However, there is one situation in which the asymptotic series defines a unique function. If $\theta \geq \pi$ then, for some g such that $|\arg g| \geq \pi/2$, $B\cos(\arg g) \leq 0$ and the only way in which the right hand side of Eq.(3.7) can be bounded by $\epsilon(g)$ is if $A \equiv 0$. Then the right hand side of Eq.(3.7) reduces to $f(g)$ over the whole domain and the asymptotic series defines $f(g)$ uniquely.

We stress that an asymptotic series need not be a divergent series. Consider a counterexample, the function $F(g) = f(g) + Ae^{-B/g}$ with A real and $B > 0$, where $f(g)$ is analytic at the origin. $F(g)$ all have, in the right half plane, the same asymptotic expansion, which is identical with the Taylor series for $f(g)$; so the asymptotic expansion of all the singular functions $F(g)$ is a convergent series because of analyticity of $f(g)$.

We emphasise that the divergence of a perturbation expansion does not signal an inconsistency in the theory. The central problem is always that of uniqueness — determining whether the asymptotic expansion uniquely determines the function $f(g)$ or not.

3.4 Borel summation

A large class of asymptotic series can be given precise meaning by means of the method of *Borel summation*, provided that certain additional conditions are imposed on $f(g)$. As a result Borel summation techniques have been widely adopted in QFT. It is important to state, however, that this procedure is only one of many possible summation methods, and

correspondingly Borel summability (Borel non-summability) cannot serve as fundamental classification criterion for the consistency (inconsistency) of a theory.

3.4.1 The Borel transform

The series

$$f(g) = \sum_{n=0}^{\infty} f_n g^n \tag{3.9}$$

is called Borel summable if [59]

- its *Borel transform* $B(z)$,

$$B(z) = \sum_{n=0}^{\infty} \frac{f_n}{n!} z^n \,, \tag{3.10}$$

  converges inside some circle, $\mid z \mid < \delta \,,\ \delta > 0$;

- $B(z)$ has the analytic continuation to the neighbourhood of an infinite strip of non-vanishing width bisected by the positive real semi-axis Re $z \geq 0$.

- the integral, called the *Borel sum*,

$$F(g) = \frac{1}{g} \int_0^{\infty} \mathrm{e}^{-z/g} B(z) \mathrm{d}z \,, \tag{3.11}$$

  converges for some $g \neq 0$.

One may regard Eq.(3.11) as the definition of the sum of the series [59], valid when it has a particular set of analytic properties. This definition, however, is far from being completely arbitrary. If $B(z)$ is replaced by its power series expansion and one integrates term by term then the series Eq.(3.9) is exactly reproduced. Strictly this procedure is not mathematically rigorous, since integration and infinite summation do not always commute and it is incorrect to write $F(g) = f(g)$. It does nonetheless suggest that $F(g) \approx f(g)$ i.e. the Borel sum of the series is asymptotic to $f(g)$.

To motivate this method of summation we use a simple example. Consider a generic quantity D, calculated in perturbation theory with the coupling a,

$$D(a) = \sum_{n=0}^{\infty} d_n a^n \,. \tag{3.12}$$

Using the definition of the factorial function this can be rewritten

$$D(a) = \sum_{n=0}^{\infty} d_n a^n \frac{1}{n!} \int_0^{\infty} \mathrm{d}t \mathrm{e}^{-t} t^n \,. \tag{3.13}$$

If the series (3.12) has a non-vanishing convergence radius δ, the integration in (3.13) can be exchanged with the sum inside the circle. If we are outside the circle or if the convergence radius is zero, $\delta = 0$, we can exchange the order of integration and summation to *define* the series by the same expression (provided that the integral converges). In either case, taking $z = at$ this gives

$$D(a) = \int_0^\infty \mathrm{d}t e^{-t} \sum_0^\infty d_n \frac{(at)^n}{n!} = \frac{1}{a} \int_0^\infty \mathrm{d}z e^{-z/a} B(z)\,, \tag{3.14}$$

where B is the Borel transform of D. The process of taking a divergent series in QFT and applying the Borel transform to extract a function which corresponds to it asymptotically is termed *Borel resummation.* This makes Borel summation a powerful tool in QFT.

Convergence properties

The convergence properties of the Borel transform (3.10) are superior to those of (3.9). To see this let us compare the convergence radius ρ_1 and ρ_2 of (3.9) and (3.10) respectively using the Cauchy root test. We have

$$1/\rho_1 = \lim_{n\to\infty} \sqrt[n]{|d_n|}\,, \qquad 1/\rho_2 = \lim_{n\to\infty} \sqrt[n]{|d_n|/n!}\,. \tag{3.15}$$

The factor $\sqrt[n]{n!}$ between ρ_1 and ρ_2 indicates that if the convergence radius of the original series is nonvanishing, that of $B(z)$ will be infinite.

Uniqueness

The Borel summability of a perturbation series is not the same as the possibility of the complete determination of the physical observable from which the perturbative expansion results. To deal with the problem of uniqueness in Borel summation we need to know more about the physical observable, and it turns out to be necessary to, a priori, prove something about the remainder function.

The necessary criterion of Borel summability is given by Watson's lemma [59], or one of the many later refinements [57]. If the full functional form of $F(g)$ may be recovered from its perturbative expansion $f(g)$ we may call such a function *Borel recoverable* [55]. Since Watson's lemma implies that the function $F(g)$ is unique, we conclude that no function of the form of Eq.(3.8) can satisfy the condition Eq.(3.3). So the limiting of the remainder function is responsible for ruling out the possibility non-perturbative effects.

In general for QCD the conditions for Borel recoverability are not satisfied, which is to be expected since non-perturbative effects are known to be present. In QCD the analyticity region is not a disc but a wedge of zero opening angle [50, 57]. To recover the full analytic form of the function in such an analyticity region the growth of the expansion coefficients cannot exceed $(\ln n)^n$, however, as we shall see in the Section 3.5 the growth is $n!$.

Universality

The Green functions of a theory are related through the Schwinger-Dyson equations and generalized Ward-Takahashi identities. Physical observables are then constructed by the means of these operations — essentially made up of multiplications and divisions — acting on the Green functions.

It is found that these operations do not result in new singularities in the Borel plane [50]. Therefore the interconnectedness, through Schwinger-Dyson equations, of all Green's functions ensures that a singularity in the Borel transform of one Green function propagates through to the Borel transform of all others. Moreover, it follows that the location of singularities in the Borel plane must be universal in all Borel transforms within each theory [60]. This implies the perturbative expansions of a theory all have the similar divergence characteristics.

3.4.2 Exploiting Borel transform technology

To give sense to Eq.(3.11) we need convergence of the integral and that $B(z)$ has no singularities in the integration range (the positive real axis).

Consider, for example, the divergent series with an alternating sign factorial behaviour of the perturbative coefficients, $d_n = (-1)^n n!$. The corresponding Borel transform and Borel sum are then given by

$$B(z) = \sum_{n=0}^{\infty} (-z)^n = \frac{1}{1+z} \longrightarrow D(a) = \int_0^{\infty} \mathrm{d}z \mathrm{e}^{-z/a} \frac{1}{1+z} . \tag{3.16}$$

where we have assumed analytic continuation along the whole real line. This integral is well-defined, and $D(a)$ has been successfully resummed.

The method can fail if we take a fixed-sign factorial behaviour, $d_n = n!$, as an example, however, we obtain

$$B(z) = \sum_{n=0}^{\infty} (z)^n = \frac{1}{1-z} \longrightarrow D(a) = \int_0^{\infty} \mathrm{d}z \mathrm{e}^{-z/a} \frac{1}{1-z} . \tag{3.17}$$

The pole at $z = 1$ on the integration range means that this integral does not exist for a positive (where $D(a)$ has a cut), nor is the Borel sum of such a series defined. For other values of a, the integral converges, selecting one of the functions having $\sum_{n=0}^{\infty} n! a^n$ as asymptotic expansion within the angle $0 < \arg a < 2\pi$. The summation can be defined in many ways; there are infinitely many functions with this asymptotic expansion. For instance, one can add any term of the form $A \exp(-1/a)$ for $0 < a < 1/2$.

More generally, we can consider

$$d_n = \left(\frac{1}{z_i}\right)^n n^\gamma n! \,. \tag{3.18}$$

with $\gamma > 0$. The Borel transform is then of the form

$$B(z) \sim \frac{1}{(1 - z/z_i)^{\gamma+1}} \,. \tag{3.19}$$

To see this we work backwards. For $|z/z_i| < 1$ we can expand binomially, and if $\gamma \geq 0$ we obtain

$$B(z) \simeq \sum_{n=0}^{\infty} \frac{(n+\gamma)!}{n!\gamma!} \left(\frac{z}{z_i}\right)^n \,. \tag{3.20}$$

Using Stirling's theorem, Eq.(A.4), one can then show that for large n

$$\frac{(n+\gamma)!}{n!\gamma!} = n^\gamma (1 + O(1/n)) \,. \tag{3.21}$$

Therefore to leading order in $1/n$ we obtain

$$B(z) \simeq \sum_{n=0}^{\infty} n^\gamma \left(\frac{z}{z_i}\right)^n \,. \tag{3.22}$$

We have seen that the Borel transform can be used to classify divergent series. The generic $n!$ divergence leads to a singularity in the Borel plane. The nature of this singularity is determined by the value of γ; if γ is a positive integer we have a pole; and for non-integer γ a branch point singularity in the z-plane at $z = z_i$. The position of the singularity in the Borel plane is determined by $(1/z_i)$. If $(1/z_i)$ is negative (positive) the singularity lies on the positive (negative) real axis of the Borel plane. Only for $(1/z_i)$ negative will the series admit Borel summation - otherwise the singularity prevents us from resumming the integral.

However, we can still give meaning to the integral such as in Eq.(3.17) by specifying a prescription to go around the pole. The result will then depend on the chosen prescription. For example if we define

$$D_{+,-}(a) = \int_0^\infty \mathrm{d}z e^{-z/a} \frac{1}{1 - z \pm i\epsilon} \,, \tag{3.23}$$

then the difference is proportional to the residue at $z = 1$

$$D_+(a) - D_-(a) \sim \exp(-1/a) \,. \tag{3.24}$$

Fortunately the resulting ambiguity is of the order $\exp(-z/a)$ so that if this quantity is small it may be neglected. For singularities more complicated than poles a similarly exponentially small ambiguity arises near $a = 0$.

3.5 The Large-N_f expansion

In strictly renormalizable theories, like ϕ_4^4, QED and QCD, there are large order divergences associated with a single class of diagrams. These *bubble chain diagrams* create a characteristic $n!$ divergence in the perturbative coefficients. Transforming to the Borel plane this behaviour induces a set of singularities called *renormalons*. This feature was first identified in QED by Lautrup [61] and 't Hooft [50] and accordingly we will begin our discussion of these singularities by looking at contributions to the QED vacuum polarization function. We will then turn to consider the analogous situation for the QCD vacuum polarization function defined in Section 1.7.1.

For a full calculation of $\Pi(Q^2)$ in QED we must take into account insertions in the photon propagator, which take the form of a vacuum polarization blob. We identify the sequence of Feynman diagrams, shown in Figure 3.1 (this is shown for QCD — for QED we replace the gluon lines with photon lines), contributions to the two-point correlator from one-loop vacuum polarization diagrams with a one-chain of fermion bubbles inserted.

There is a very natural way to separate out the perturbative contribution from one-loop vacuum polarization diagrams with a chain of n fermion bubbles inserted. We will consider variants of minimal subtraction, $\overline{\rm MS}$ with renormalization scale $\mu = \mathrm{e}^u Q$, where u is an N_f-independent number. In such cases the $1/\epsilon$ pole appearing in dimensional regularization is subtracted along with an N_f-independent finite part. The most general subtraction procedure, however, which will result in perturbative coefficients polynomial in N_f, can be regarded as $\overline{\rm MS}$ with scale $\mu = \mathrm{e}^{u+v/b} Q$, where v is again N_f-independent. We shall refer to such renormalization schemes as 'regular' schemes. Any variant of minimal subtraction with an N_f-independent renormalization scale will have v=0.

For a wide range of "quark-initiated" [62] QCD observables, the perturbative coefficients d_n can then be organized as polynomials of degree n in the number of of active quark

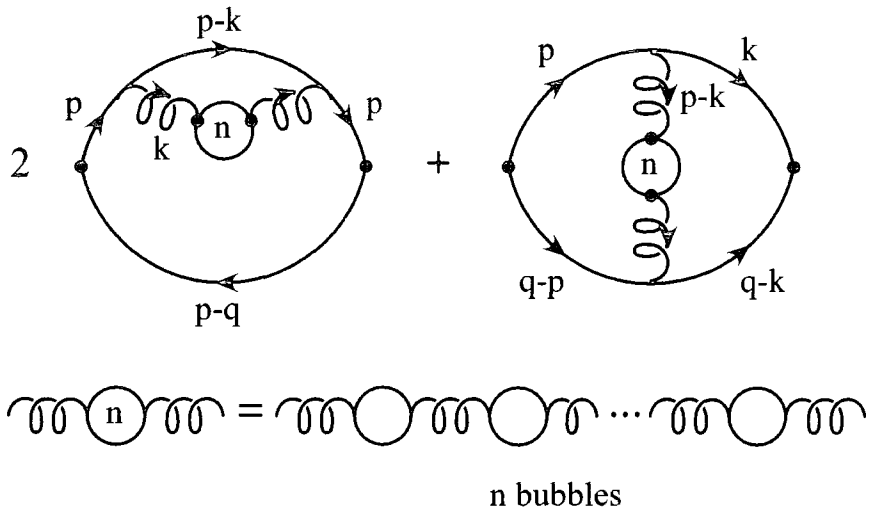

Figure 3.1: Leading large-N_f contribution at nth order in perturbation theory.

flavours, N_f – a *large* N_f *expansion*; we assume massless quarks.

$$d_n = d_n^{[n]} N_f^n + d_n^{[n-1]} N_f^{n-1} + \cdots + d_n^{[0]} \,. \tag{3.25}$$

The N_f-expansion coefficients, $d_n^{[n-r]}$, will consist of sums of multinomials in $C_A = N$ and $C_F = (N^2-1)/2N$, of SU(N) QCD; and will have the structure $C_A^{n-r-s} C_F^s$ (note the prefactor of C_F in Eq.(1.61) so that each term is of degree n.

The terms in the large-N_f-expansion correspond to Feynman diagrams with differing numbers of vacuum polarization loops. In general, when the nth coefficient is considered, the leading contribution $d_n^{[n]} N_f^n$ from the large-N_f expansion will come from the diagrams in Figure 3.1, since these diagrams contribute $\sim g^{2n+2} N_f^n \sim a^{n+1} N_f^n$. As we shall demonstrate in the next section this contribution to the perturbative series at nth order from leading coefficient $d_n^{[n]} N_f^n$ is found to behave like $n!$ for large n. This divergent behaviour of the expansion coefficients cannot be cancelled since the bubble diagrams have the highest power of N_f for any given power of the coupling a.

We should note that these single bubble chains alone contribute the leading large-N_f behaviour. For example, if we consider the behaviour of a generic two chain diagram, see Figure 3.2, then this will contribute $g^{2k+2} g^{2\ell+2} N_f^{k+\ell} \sim a^{k+\ell+2} N_f^{k+\ell}$ We find this is $O(1/N_f)$ in the large-N_f expansion and hence subleading. Some doubts have been raised as to the validity of the assumption that the subleading terms make a negligible contribution to the asymptotics [63]. This point will be discussed in more detail in Chapter 4.

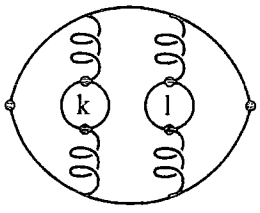

Figure 3.2: A generic two-chain diagram

Having identified the diagrams which will be of interest, we now proceed to sketch the calculation of these diagrams in this and the following section. Applying the Feynman rules to the diagrams in Figure 3.1, one finds that the leading coefficient in the large-N_f expansion, $d_n^{[n]}$, is of the form [64]

$$d_n^{[n]} \sim \int \frac{d^4k}{(2\pi)^4} \int \frac{d^4p}{(2\pi)^4} \left\{ B_{\rho\sigma}^{(n)}(p-k) \mathrm{Tr} \left[\gamma_\mu \frac{1}{\not k} \gamma_\rho \frac{1}{\not p} \gamma_\mu \frac{1}{\not p - \not q} \gamma_\sigma \frac{1}{\not k - \not q} \right] \right.$$
$$\left. + 2 B_{\rho\sigma}^{(n)}(k) \mathrm{Tr} \left[\gamma_\mu \frac{1}{\not p} \gamma_\rho \frac{1}{\not p - \not k} \gamma_\sigma \frac{1}{\not p} \gamma_\mu \frac{1}{\not p - \not q} \right] \right\} . \tag{3.26}$$

Here $B_{\rho\sigma}^{(n)}$ is the renormalized sum of n bubbles:

$$B_{\rho\sigma}^{(n)}(k) = \frac{(k_\rho k_\sigma - k^2 g_{\rho\sigma})}{(k^2)^2} \left[-\Pi_2(k^2) \right]^n , \tag{3.27}$$

where $\Pi_2(k^2)$ is the contribution of one bubble,

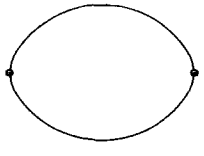

$$= \quad \frac{b}{2} \left[\ln \frac{k^2}{\mu^2} + C \right] . \tag{3.28}$$

where b is the first beta-function coefficient and C depends on the renormalization scheme. So, for $\overline{\mathrm{MS}}$ $C = -5/3$; and for the V-scheme ($\overline{\mathrm{MS}}$ with $\mu = \exp[-5/6]Q$) $C = 0$.

Summing over the large-N_f, $d_n^{[n]} N_f^n$, terms is equivalent, in the case of vacuum polarization, to performing a Dyson summation correcting the photon propagator in QED. Expanding $(1 + \Pi(k^2))^{-1}$ as a geometrical progression, and integrating over the momentum k, one can extract the coefficient $d_n^{[n]}$ to all-orders.

Large-N_f expansions have been widely used in the past in the investigation of large-order behaviour and renormalons [64]. Techniques such as the Gegenbauer polynomial x-space method [64] for evaluating the loop integrals in such diagrams exactly in all-orders have been developed and rather compact results for QCD vacuum polarization [64, 65] (and hence its Minkowski continuations, the e^+e^- QCD R-ratio and the τ-decay ratio, R_τ);

Deep Inelastic Scattering (DIS) sum rules [66]; and heavy quark decay widths and pole masses [67, 68] obtained. A general procedure enabling $d_k^{[k]}$ to be obtained from knowledge of the one-loop correction with a fictitious gluon mass has been developed [62, 69].

Progress in applying the N_f expansion in QED [70] has led Broadhurst to a generating function for the leading order (large-N_f) coefficients of the QED Gell-Mann-Low function (MOM scheme beta-function) [65]:

$$\Psi_n^{[n]} = \frac{3^{2-n}}{2}\left(\frac{\mathrm{d}}{\mathrm{d}x}\right)^{n-2} P(x)\Big|_{x=1} , \tag{3.29}$$

where

$$P(x) = \frac{32}{3(1+x)}\sum_{k=2}^{\infty}\frac{(-1)^k k}{(k^2-x^2)^2} . \tag{3.30}$$

$\Psi_n^{[n]}$ can be explicitly evaluated in closed form [65]:

$$\begin{aligned}\frac{\Psi_n^{[n]}}{(n-2)!} &= \frac{(n-1)}{(-3)^{n-1}}\Big[-2n+4-\frac{n+4}{2^n} \\ &\quad +\frac{16}{n-1}\sum_{\frac{n}{2}>s>0} s(1-2^{-2s})(1-2^{2s-n})\zeta_{2s+1}\Big] .\end{aligned} \tag{3.31}$$

Using this result one can then obtain the leading-order large-N_f result for the QCD Adler D-function. In the $\overline{\mathrm{MS}}$ scheme with $\mu^2 = Q^2$ one has [66]

$$d_n^{[n]} = 2T_F^n n!\sum_{m=0}^{n}\frac{(-\frac{5}{9})^m}{m!}\frac{\Psi_{n+2-m}^{[n+2-m]}}{(n-m)!} , \tag{3.32}$$

where the group theory factor $T_F = 1/2$ in the standard fermion representation. The $(-5/9)^m$ factors enter since one is converting from the MOM scheme Adler function to that in the $\overline{\mathrm{MS}}$ scheme. The results of Eq.(3.31) and (3.32) are in agreement with the exactly known coefficients $d_1^{[1]}$ and $d_2^{[2]}$ in Eq.(1.64) and Eq.(1.65) .

Rather than using the $\overline{\mathrm{MS}}$ scheme with $\mu = Q$ we find that considerable simplification in the form of the asymptotic behaviour results from choosing the so-called V scheme [51], $\overline{\mathrm{MS}}$ with $\mu = \mathrm{e}^{-5/6}Q$, which is directly related to the QED MOM scheme. With this choice Π_2 is a simple logarithm with no finite part. Eq.(3.32) then becomes

$$d_n^{[n]} = 2T_f^n\Psi_{n+2}^{[n+2]} . \tag{3.33}$$

We will discuss DIS sum rules and the experimentally relevant Minkowski continuations of D, the R-ratio and tau-decay ratio R_τ, in much greater detail in the Chapter 4 where we explore the possibilities of constructing all-orders resummations from our knowledge of the Borel transforms of these quantities.

3.6 Renormalons

We have identified that the contribution of the required bubble-chain diagrams is given by the highest power of N_f, the leading coefficient $d_n^{[n]}N_f^n$. We now apply our knowledge of the Borel transform to investigate the large-order behaviour of the perturbative coefficients in QED and QCD. The factorial growth of the expansion coefficients will lead to singularities in the Borel transform. We wish now to obtain information on how these z-plane singularities of the vacuum polarization function in the Borel plane encode the large-order behaviour of the perturbative coefficients.

3.6.1 Renormalons in QED

We begin again with QED. Returning to Eq.(3.26), the contribution to the order n term from insertions of chains of one-fermion bubble graphs in the expansion of the vacuum polarization function can be cast in the form

$$d_n a^{n+1} \simeq \int \frac{d^4k}{(2\pi)^4} F(k^2, k\cdot q, Q^2)\frac{a}{k^2}\Pi(k^2)\ . \tag{3.34}$$

where $\Pi(k^2) = (-\Pi_2(k^2))^n$ and $\Pi_2(k^2)$ is the second order vacuum polarization. After renormalization, and performing the d^4p and angular integrations on Eq.(3.26) we have

$$d_n a^{n+1} \simeq \int k^2 dk^2 \Phi\left(\frac{k^2}{Q^2}\right)\frac{a}{k^2}\left[-\frac{ba}{2}\ln\left(\frac{k^2}{Q^2}\right)\right]^n\ . \tag{3.35}$$

where we have inserted the leading logarithmic term only. Summing over n-bubble contributions we then obtain

$$\begin{aligned}\hat{D} &\simeq \sum_{n=0}^{\infty} d_n a^{n+1} \\ &\simeq \int k^2 dk^2 \Phi\left(\frac{k^2}{Q^2}\right)\frac{1}{k^2}\frac{a}{1+\frac{ba}{2}\ln\left(\frac{k^2}{Q^2}\right)}\ .\end{aligned} \tag{3.36}$$

We now split the integration range into small and large k^2. For the infra-red (IR) region, from $0 < k^2 < Q^2$, we can expand the kernel $\Phi(k^2/Q^2)$ in powers of its argument, leading to a generic term proportional to

$$\hat{D} \simeq Q^2 \int_0^{Q^2} \frac{dk^2}{k^2}\left(\frac{k^2}{Q^2}\right)^{j+1}\frac{a}{1+\frac{ba}{2}\ln\left(\frac{k^2}{Q^2}\right)}\ . \tag{3.37}$$

Changing variable to $t = \ln Q^2/k^2$ and further rescaling by $z = at(j+1)$ we obtain

$$\hat{D} \simeq \frac{Q^2}{j+1}\int_0^{\infty} dz e^{-z/a}\frac{1}{1-\frac{b}{2}\frac{z}{j+1}}\ . \tag{3.38}$$

This is directly in the form of a Borel transform. We see that the IR region leads to poles in the Borel plane at $z = 2(j+1)/b$, $j = 1, 2, \ldots$.

A similar procedure can be repeated for the ultraviolet region $Q^2 < k^2 < \infty$. In this case $\Phi(k^2/Q^2)$ is expanded at large k^2 in powers of Q^2/k^2 so that the generic power $(Q^2/k^2)^j$ contributes

$$\tilde{D} \simeq Q^2 \int_{Q^2}^{\infty} \frac{dk^2}{k^2} \left(\frac{Q^2}{k^2}\right)^{j-1} \frac{a}{1 + \frac{ba}{2} \ln\left(\frac{k^2}{Q^2}\right)} . \tag{3.39}$$

After changing variable to $t = \ln k^2/Q^2$, and rescaling according to $z = (j-1)at$ this becomes

$$\tilde{D} \simeq \frac{Q^2}{j-1} \int_0^{\infty} dz e^{-z/a} \frac{1}{1 + \frac{b}{2} \frac{z}{j-1}} . \tag{3.40}$$

We see that the UV region leads to poles in the Borel plane at $z = -2(j-1)/b$ ($j = 2, 3, \ldots$).

These poles are termed *renormalons* and explicit calculation shows that they are located at $z = 2l/b$, $l = -1, \pm 2, \pm 3, \ldots$. For QED we have $b = -2/3N_f$, so we find that the *infrared renormalons*, which are associated with an alternating sign factorial divergence of the perturbative coefficients, $d_n \sim (-1)^n n!$, reside on the negative real axis. They are not on the integration range, and hence do not represent an ambiguity in the reconstruction of $D(a)$ from its perturbative expansion. IR renormalons essentially arise from infrared divergences of bubble diagrams similar to that in Figure 3.1.

The *UV renormalons* are located on the positive real axis, and are associated with a fixed-sign factorial growth, $d_n \sim n!$, of the perturbative coefficients. Since they reside on the integration path they represent a genuine ambiguity in the reconstruction of a function from its divergent perturbative expansion. This, of course, corresponds to the non-perturbative region of the non-asymptotically free theory of QED. These poles are induced by the presence of the Landau pole of QED, where the running coupling diverges, i.e. the pole at $1 + \frac{1}{2}ba \ln(k^2/Q^2) = 0$. This occurs at very high momenta and is due to the same bubble insertions in the photon propagator.

3.6.2 Renormalons in QCD

For the QCD vacuum polarization function one can also consider one-loop diagrams with a single gluon line inserted. In the non-abelian QCD case the insertion of fermion loops is insufficient to reconstruct the complete beta-function. In fact the one-loop corrections to the gluon propagator are not gauge invariant. However it will be argued in Chapter 4

that if extra gauge-dependent parts of other diagrams are added the net result will simply be a gauge invariant reconstruction of the QCD beta-function coefficient b.

For the asymptotically free theory of QCD the first beta function coefficient is of opposite sign to that in QED. Therefore replacing the first QED beta-function by the first QCD beta-function in the analysis above we find that the UV and IR regions are swapped around.

If we include a number of refinements, such as subleading beta-function coefficients and logarithms, the positions of the singularities remain fixed but their nature changes, corresponding to the large-order behaviour of the QCD perturbative coefficients

$$\begin{aligned} \text{IR region} \quad & d_n \sim C_n n! n^\gamma \left(\frac{b}{2l}\right)^n \\ \text{UV region} \quad & d_n \sim C_n (-1)^n n! n^\gamma \left(\frac{b}{2l}\right)^n . \end{aligned} \tag{3.41}$$

In general we see that the Borel plane singularities will be not poles, but of the branch point type.

The final conclusion is that in QCD one in fact expects UV renormalon singularities, UV_ℓ, at $z = z_\ell = -2\ell/b$, $\ell = 1, 2, 3, \ldots$ corresponding to an alternating sign factorial growth of the perturbative coefficients; and IR renormalon singularities, IR_ℓ, at $z = z_\ell = 2\ell/b$, $\ell = 1, 2, 3, \ldots$ corresponding to a fixed-sign factorial growth.

Parisi [71] found that the UV divergences of the n-bubble diagrams have a very deep origin in the renormalization process. Based on the BPH theorem which states that all UV divergences can be removed by the introduction into the Lagrangian of counterterms of local operators, Parisi connected each pole with a local operator in the theory. Furthermore Parisi showed that the location of the UV renormalons is independent of the choice of beta-function, although their strengths have a weak dependence on the second beta-function coefficient.

In QCD it is the IR renormalon singularities, corresponding to the non-perturbative region of QCD, which reside on the integration path, and thus represent an ambiguity in the reconstruction of the observable. For the specific case of QCD vacuum polarization one expects IR_1 to be absent since, as will be discussed in the Section 3.8, there is no dimension two condensate in the corresponding OPE.

We have seen that QED and QCD have perturbative expansions that are neither convergent nor Borel summable. In the context of the Borel transform the non-Borel summability of the QED (QCD) perturbative series signals an ambiguity in $D(a)$ at very high (low)

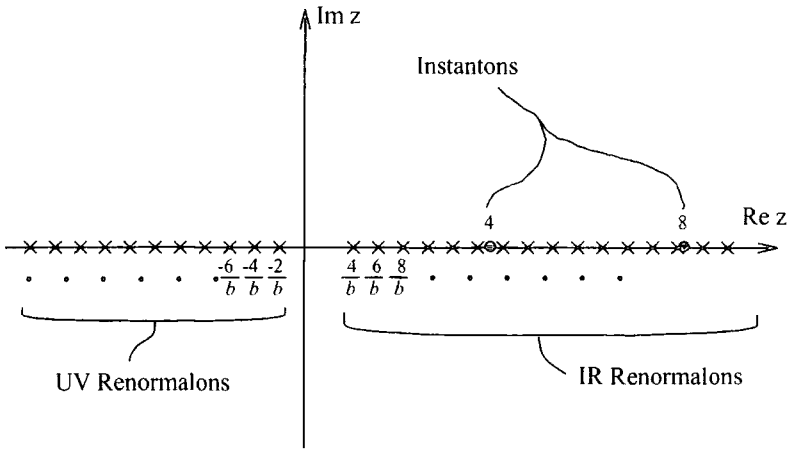

Figure 3.3: The singularity structure of the Borel transform of the QCD quantity $D(a)$, as discussed in the text. The relative positions of the singularities are based on $b = 23/6$, corresponding to SU(3) QCD with $N_f = 5$.

momenta. For QCD, however, perturbation theory is only relevant at high Q^2 where $\alpha(Q^2)$ is small due to asymptotic freedom. At large Q^2 the ambiguities in the Borel plane associated with singularities behave as $\exp(-2l/a)$. But in QCD $a = 2/b\ln(Q^2/\Lambda^2)$ so that $\exp(-2l/a) \sim (\Lambda^2/Q^2)^k$. As a result the ambiguities are power suppressed with respect to all the individual terms in the perturbative series which are only logarithmically suppressed. Similarly in QED the ambiguities are small because a is small at all realistic energies and therefore $\exp(-2l/a)$ is very small. As we noted in Section 3.4.2 it is possible to deform the contour in the Borel reconstruction integral of Eq.(3.11) around the pole by introducing a term $\sim e^{-1/a}$ which vanishes in a perturbative expansion. It is the choice of the exact method of avoiding the pole that leads to the ambiguity in $D(a)$. Terms $\sim e^{-1/a}$ correspond to non-perturbative effects and so discovering the correct method for negotiating the pole is necessarily equivalent to finding a non-perturbative solution of the theory.

3.7 Instanton singularities

There is another known source of singularities in the Borel plane from instanton contributions. Instanton singularities do not arise from a specific set of diagrams, but rather are intimately related to the proliferation of Feynman diagrams at large orders, at least for quantum mechanics and super-renormalizable field theories [72]. The reason that this relation must hold for simpler theories is that, for finite, renormalized diagrams, the di-

agrams themselves are bounded by a pure power law behaviour. Hence the only way in which factorial growth can manifest itself in the perturbative coefficients is through a combinatorical increase in the number of Feynman diagrams at large orders.

In QCD there are singularities at $z_\ell = 4\ell$, $\ell = 1, 2, 3, \ldots$ due to instanton/anti-instanton solutions of the classical equations of motion [50, 73] The known singularity structure of the D function, including instantons, is then summarised in Figure 3.3. Although instantons terms are conceptually important, since they represent a breakdown of the short-distance expansion, we shall not elaborate much further on the role of instanton singularities in QCD for two reasons. In vacuum polarization amplitudes the value of z_l corresponding to an instanton singularity is positive and large, so that the resulting ambiguities are strongly suppressed. Therefore renormalon singularities dominate the leading singularity structure in the Borel transform to the exclusion of instantons. Second, due to the universality of the location of the instanton singularities, which are independent of both N and N_f, they are invisible in the large-N and large-N_f limits. So we shall not learn about them from exact large-N_f result.

3.8 IR renormalons and the connection to the OPE

Significant progress has been made, notably by Grunberg [16] and Mueller [74], in relating IR renormalons to non-perturbative effects through the operator product expansion (OPE). The question of how we deal with poles on the positive real axis is very important. At the very least we would like to know what degree of ambiguity these poles introduce into perturbative calculations, since large ambiguities would call into question the value of continuing the programme of extending fixed order perturbative calculations of QCD observables. Less pessimistically, we might hope to obtain further insight into the non-perturbative regime of QCD. As we shall see, there is much to be learnt from studying the consequences of using a short-distance OPE to quantify some of the non-perturbative effects which we believe are intimately related to the presence of IR renormalons.

In anticipation of later calculations we assume massless QCD. From Eq.(1.66) applying a short distance OPE to $D(Q^2)$ yields the representation

$$D(Q^2) = D_{PT}(a) + \mathcal{C}_{GG}(Q/\mu, a)\frac{\langle 0|G_{\mu\nu}G^{\mu\nu}|0\rangle(\mu)}{Q^4} + \text{higher dimensional condensates}\,. \tag{3.42}$$

Here the unit operator is the usual perturbative contribution, Eq.(1.62), and for massless QCD the leading (lowest dimensional) condensate contribution is the gluon condensate

with Wilson coefficient $\mathcal{C}_{GG}(Q/\mu, a)$. We will denote the gluon condensate by $G(a)$.

Now, we expect $D_{PT}(a)$ and $G(a)$ to be separately RG invariant. If we consider a condensate with dimension $2l$ (that is, with scaling behaviour $\sim Q^{-2l}$) we can determine the a-dependence of $G(a)$ by requiring that $G(a)$ satisfies the RGE (see Eq(1.36)). Taking the NLO form for the QCD beta-function, Eq.(2.11), we find that $G(a)$ must take the form (c.f. Eq.(1.66))

$$G(a) = C\left(\mu^2/Q^2\right)^{2l/2} \exp[-z_l/a]\, a^{\delta}\,(1 + O(a)) \sim Q^{-2l}\,, \tag{3.43}$$

where

$$\delta = \frac{2\gamma_0}{b} - cz_l\,, \qquad z_l = 2l/b \tag{3.44}$$

with γ_0 the one-loop anomalous dimension of the corresponding operator. C is a scale-independent constant which contains the non-perturbative information. Eq.(3.43) can be re-expressed in the form [16]

$$G(a) = \frac{C z_\ell^{\delta-1}}{\Gamma(\delta)} \int_{z_\ell}^{\infty} \mathrm{d}z \frac{\mathrm{e}^{-z/a}}{(z/z_\ell - 1)^{1-\delta}}\,. \tag{3.45}$$

This form for $G(a)$ has an essential singularity at $a = 0$, so that the OPE motivated expression in Eq.(3.42) is only meaningful when we have a resummation prescription for $D_{PT}(a)$. This will be provided by the Borel transform, in which the IR renormalon poles will be negotiated by performing the reconstruction integral along a contour displaced above or below the real z-axis.

We assume the first IR renormalon pole is an integrable branch point of the form of Eq.(3.41) at z_0. Further we assume $\gamma < 1$ though the result will have general validity. This yields (disregarding any UV renormalons on the negative real z-axis) the large order behaviour

$$d_n \sim K\left(\frac{\mu^2}{Q^2}\right)^{bz_0/2} \left(\frac{1}{z_0}\right)^n \frac{\Gamma(n+\gamma)}{\Gamma(\gamma)} \left[1 + O\left(1 + \frac{1}{n}\right)\right]\,. \tag{3.46}$$

For $z > z_0$ the $(1 - z/z_0)^{-\gamma}$ factor implies that this contribution has an ambiguous imaginary part (for $a > 0$). We can then write the "renormalon contribution" to $D_{PT}(a)$ in terms of its Borel representation in the region of the first IR renormalon pole

$$D_{PT}(a) = \int_0^{z_0} dz\, \mathrm{e}^{-z/a} B[D_{PT,0}](z) + \int_{z_0}^{\infty} dz\, \mathrm{e}^{-z/a} B[\mathrm{Im}\, D_{PT,0}](z)\,, \tag{3.47}$$

where

$$B[D_{PT,0}](z) = K\left(\frac{\mu^2}{Q^2}\right)^{bz_0/2} \frac{1}{(1 - z/z_0)^{\gamma}} \tag{3.48}$$

$$B[\mathrm{Im}\, D_{PT,0}](z) = K\left(\frac{\mu^2}{Q^2}\right)^{bz_0/2} \frac{1}{(z/z_0 - 1)^{\gamma}} \exp(\pm i\pi\gamma)\,. \tag{3.49}$$

where K is a scale independent factor and we neglect terms of $O(1 - z/z_0)$. The resulting ambiguity in Eq.(3.49) result depends on whether the contour is taken above or below the real z-axis.

If this ambiguity is to be avoided we must obtain some compensating factor from the non-perturbative part of the theory. Due to non-logarithmic UV divergences [75] C acquires an ambiguous imaginary part. We therefore assume that the constant C in Eq.(3.45), is in fact complex. So we will have $C \to C_R \pm iC_I$, with the ambiguous imaginary part reflecting the renormalon-induced ambiguity in $D_{PT}(a)$.

The critical step is now to require cancellation of these ambiguities between the perturbative, Eq.(3.47), and non-perturbative, Eq.(3.45) parts of the theory. This leads to the following relations:

$$z_0 = z_l = 2\ell/b \tag{3.50}$$

$$\delta = 1 - \gamma \tag{3.51}$$

$$K = -\frac{C_I z_l^{\delta-1}}{\sin\pi\delta\Gamma(\delta)} \,. \tag{3.52}$$

There are a number of important points to raise about these relations. First, the renormalon residue is related to the condensate parameter, which leads us to expect that it is a process independent quantity. The implication that one can obtain, by making an all-orders perturbative calculation, a "perturbation theory determined" part of the condensate contribution is misleading in that exponentially small terms may be shifted between $D_{PT}(a)$ and $G(a)$ [16].

Secondly, Eq.(3.50) tells us the location of the IR renormalon poles on the positive real z-axis. The condensates obtained from performing a short distance OPE have dimensions $d = 4, 6, 8, \ldots$, implying that the Borel transform for the Adler D-function will have IR renormalon singularities at $z_\ell = \frac{2\ell}{b}$ $(\ell = 2, 3, 4, \ldots)$. Notice that the lowest dimension condensate in the OPE is the gluon condensate with $d = 4$. Hence we expect that there will be no IR renormalon at $z = 2/b$ since there is no dimension two condensate to compensate for it. We shall discuss this issue in more detail in Chapter 4.

The perturbative and condensate contributions can be combined in a single representation by defining a regularization, $\overline{\text{PV}}$, by averaging the integrals above and below the positive real axis

$$D(Q^2) = \overline{\text{PV}} \int_0^\infty \mathrm{d}z \frac{K\mathrm{e}^{-z/a}}{(1 - z/z_\ell)^\gamma} \left[1 + \tilde{C}\theta(z - z_\ell)\right] \,. \tag{3.53}$$

The final point to be made is that Eq.(3.51) gives the structure of the renormalon sin-

gularities. In general they will be branch point singularities; but in the case of a large-b expansion (which we shall motivate in section 4.1 of Chapter 4), $\gamma \to 1$, they reduce to simple or double poles. The regularization $\overline{\text{PV}}$ in Eq.(3.53) then reduces to an ordinary Cauchy principal value.

3.9 Summary and conclusions

We have demonstrated in this chapter that QCD perturbation theory may be re-interpreted as an asymptotic series, which may be summed by the application of the Borel transform. Applying the large-N_f expansion, we went on to identify a sequence of Feynman diagrams which contribute factorial growth to the expansion coefficients in QED and QCD. The UV and IR divergences of n-bubble insertions into the photon and gluon propagator enter the Borel transform as UV renormalon and IR renormalon singularities. Figure 3.3 shows the singularity structure in the Borel plane for the Borel transform of the QCD Adler D-function.

In QCD the UV renormalons are confined to the negative real z-axis and do not present problems for the reconstruction of QCD observables from their divergent perturbative expansions. Their existence and location are a product of the renormalization procedure, and may be compensated by introducing counterterms of local operators into the Lagrangian. However, the IR renormalons on the positive real z-axis result in ambiguities in the reconstruction of the observable. To relate IR renormalons to non-perturbative effects we reviewed how we can use the mechanism of the OPE. We found that the Borel integral (the regulated Borel sum) provides a satisfactory prescription for combining non-perturbative vacuum condensates in the OPE with the perturbation theory in order to arrive at a well-defined result for D.

A final purpose of this chapter was to introduce some techniques and notation. Having set up some of the formalism, in Chapters 4 and 5 we will move on to examining some of the practical applications of these techniques.

Chapter 4

RS-invariant all-orders leading-b resummations

4.1 Introduction

There has been a great deal of interest recently in the possibility of identifying and resumming to all-orders the Feynman diagrams which dominate the large-order asymptotics of perturbation theory [62, 69, 76, 77, 78, 79]. In particular, the resummation to all-orders of the perturbative corrections contributed by QCD renormalons has been pursued vigorously. Notwithstanding the theoretical importance of establishing to what extent physical observables can be formally reconstructed from their divergent perturbative expansions, there is a more phenomenological motivation; specifically, the need to assess the reliability of a growing number of NNLO perturbative calculations so that the uncertainty in the fundamental QCD parameter $\Lambda_{\overline{\rm MS}}$ may be determined.

In the last chapter we introduced a selection of ideas connected with investigating the large order behaviour of the perturbative coefficients in quantum field theory. We concluded by reviewing recent progress in the use of an expansion in $1/N_f$, with N_f the number of fermion flavours, to probe the QED and QCD renormalon singularity structure in the Borel plane.

To be more precise let us first recap on some points raised in the last chapter. Consider a generic dimensionless QCD observable $D(Q)$, dependent on the single dimensionful scale Q, with a perturbation series

$$D(Q) = a + d_1 a^2 + d_2 a^3 + \cdots + d_k a^{k+1} + \cdots , \tag{4.1}$$

where $a \equiv \alpha_s/\pi$ is the renormalization group (RG) improved coupling. The perturbative

coefficients d_n can be organized as polynomials of degree n in the number of of active quark flavours, N_f. In general, as discussed in Section 3.5 the leading $d_n^{[n]}$ coefficient corresponds to the evaluation in each order of perturbation theory of a gauge-invariant set of Feynman diagrams containing chains of n fermion bubbles.

Whilst the resummation of such diagrams provides a gauge-invariant effective charge in QED, it is a poor approximation in QCD. In particular in the large-N_f limit asymptotic freedom is lost, and so such a resummation will give no useful information for comparisons of $D(Q)$ with fixed-order $N = 3$ QCD results with experimentally-relevant values of N_f. To perform an analogous Dyson summation in QCD one would need to include chains of gluon self-energy loops and ghost loops. The resulting corrected gluon propagator is then hopelessly gauge-dependent. In fact the isolation of a gauge-invariant subset of diagrams providing an analogous QCD effective charge is problematic [80].

To overcome this one needs a method of assembling pieces of Feynman diagrams to arrive at a gauge-invariant result. In the background field method one arrives at an effective vacuum polarization piece [81]

$$\Pi(k^2, \xi_q) = a(\mu)\frac{b}{2}\left[\ln\left(\frac{\mu^2}{k^2}\right) + \frac{5}{3} + F(\xi_q)\right] , \tag{4.2}$$

where

$$F(\xi_q) \equiv \frac{2}{3b}C_A[1 - \frac{3}{16}(1 - \xi_q)(7 + \xi_q)] . \tag{4.3}$$

$\overline{\rm MS}$ renormalization has been used. ξ_q denotes the quantum gauge parameter. Crucially the $\ln(\mu^2/k^2)$ piece arising from renormalization has a gauge-independent coefficient proportional to b, the first beta-function coefficient of QCD. As expected on the grounds of gauge invariance, however, part of the result is proportional to b^k, where b is the first beta-function coefficient, $b{=}\frac{1}{6}(11N{-}2N_f)$, for SU($N$) QCD.

As we shall emphasize, it therefore is actually more useful for our purposes to consider an expansion in powers of b [1]. Since for large-N_f one must reproduce the QED bubble-sum result one can replace $N_f \to \frac{11}{2}N - 3b$ in the 'N_f-expansion' of Eq.(3.25) to recast it in powers of b and arrive at a *large-b expansion*

$$d_n = d_n^{(n)}b^n + d_n^{(n-1)}b^{n-1} + \cdots + d_n^{(0)} , \tag{4.4}$$

where

$$d_n^{(n)} = (-3)^n d_n^{[n]} , \tag{4.5}$$

[1] Although this expansion in b is convenient, we should emphasize that it does not have such an obvious interpretation in terms of a class of Feynman diagrams as does the large-N_f expansion.

so that exact knowledge of the leading-N_f $d_n^{[n]}$ to all-orders implies exact knowledge of the leading-b $d_n^{(n)}$ to all-orders as well. Hence from Eq.(4.5) and Eq.(3.33) we obtain

$$d_n^{(n)} = 2\left(-\frac{3}{2}\right)^n \Psi_{n+2}^{[n+2]} . \tag{4.6}$$

Expanding $(1 + \Pi(k^2, \xi_q))^{-1}$ in a geometrical progression and integrating over k, as in Section 3.5, one then obtains the QCD Dyson summation coefficients,

$$\widehat{d}_n(\xi_q) = d_n^{(n)} b^n + (\xi_q\text{-dependent pieces}) . \tag{4.7}$$

The existence of so-called infra-red (IR) and ultra-violet (UV) renormalon singularities in the Borel plane at positions $z{=}2l/b$ with l a positive or negative integer, respectively, means that in large-orders the perturbative coefficients are expected to grow as $d_n \sim b^n n!$. As shown in references [82, 83] this singularity structure leads to the expectation that the 'leading-b' term when expanded in powers of N_f should, asymptotically, reproduce the sub-leading coefficients. That is, expressing $d_n^{(n)} b^n$ as

$$d_n^{(n)} b^n = d_n^{[n]} N_f^n + \tilde{d}_n^{[n-1]} N_f^{n-1} + \cdots + \tilde{d}_n^{[n-r]} N_f^{n-r} + \cdots + \tilde{d}_n^{[0]} , \tag{4.8}$$

one can show that,

$$\tilde{d}_n^{[n-r]} \sim d_n^{[n-r]} \left[1 + O(\frac{1}{n})\right] , \tag{4.9}$$

so that for fixed r and large n the sub-leading 'N_f-expansion' coefficients are reproduced. The leading-b expansion encodes the divergent behaviour of the perturbative coefficients at large orders.

As we shall demonstrate in Section 4.2.1 for both the e^+e^- Adler D-function and DIS sum rules this asymptotic dominance of the leading-b term is already apparent in comparisons with the exact next-to-leading order (NLO) and next-to-NLO (NNLO) perturbative coefficients, d_1 and d_2.

The above observations suggest that there should be some merit in resumming to all-orders the 'leading-b' terms, In a number of recent papers [62, 69, 76, 77, 78, 79] such a programme has been carried out.

Whilst such a summation can be performed many features of the approximation remain to be clarified. To fully justify it one needs to understand how it operates at the level of Feynman diagrams. Even without this deeper motivation, one can anticipate that the resummation will have a number of defects.

- The resulting expressions are dependent on the chosen renormalization scheme (RS). Changing the RS changes the definition of the renormalization group (RG)-improved

coupling and hence the coupling 'a' appearing in the summation changes. In the full sum this change is precisely compensated by the RG transformations of the coefficient d_k under the change in RS. However, by restricting oneself to the 'leading-b' piece of the coefficients this exact compensation is destroyed and the resulting sum is fatally RS-dependent [76, 84].

- For several QCD observables one has exact results for the first two perturbative coefficients d_1 and d_2, usually in the modified minimal subtraction ($\overline{\rm MS}$) scheme with renormalization scale μ=Q [17, 18, 28, 29]. One would like to include the exact NLO and NNLO coefficients without introducing a matching ambiguity.

- The full QCD Dyson sum involves the ξ_q-dependent coefficients, and depends on which basic ingredient is chosen for the one-loop correction to the gluon propagator. The leading-b resummation simply discards these ξ_q-dependent terms.

What is clearly needed is a resummation in which the exact NLO and NNLO contributions are included, and an approximate resummation of the higher orders performed, in such a way that the full sum is explicitly RS (and ξ_q) invariant under the full QCD RG transformations.

The plan of the chapter is as follows: In Section 4.2 we demonstrate the asymptotic dominance of the leading-b term at NLO and NNLO, review the 'naive' all-orders leading-b resummation and exhibit its RS dependence. In Section 4.3 we propose an improved RS-invariant leading-b resummation, which includes the exact NLO and NNLO contributions. To achieve explicit RS-invariance under the full QCD RG we invoke the effective charge formalism. In Section 4.4 we apply this RS-invariant resummation to assess the reliability of fixed-order perturbation theory and determine the uncertainty in the fundamental QCD parameter $\Lambda_{\overline{\rm MS}}$. Section 4.5 contains discussion of some technical issues and Section 4.6 a summary of our conclusions.

Parts of Section 4.2 and Sections 4.3–4.6 have been previously summarised in reference [85].

4.2 "Naive" leading-b resummations

4.2.1 Leading-b expansions

To compare the leading-b coefficients with exact perturbative calculations we presented in Section 1.7.1 we re-expand the NLO and NNLO coefficients using $N_f \to (\frac{11}{2}N - 3b)$ to obtain a b-expansion.

For the D-function expanding d_1 and d_2 in b as in Eq.(4.4) gives

$$d_1 = \left(\frac{11}{4} - 2\zeta_3\right) b + \frac{C_A}{12} - \frac{C_F}{8}, \tag{4.10}$$

$$\begin{aligned} d_2 = {} & \left(\frac{151}{18} - \frac{19}{3}\zeta_3\right) b^2 + C_A \left(\frac{31}{6} - \frac{5}{3}\zeta_3 - \frac{5}{3}\zeta_5\right) b \\ & + C_F \left(\frac{29}{32} - \frac{19}{2}\zeta_3 + 10\zeta_5\right) b + C_A^2 \left(-\frac{799}{288} - \zeta_3\right) \\ & + C_A C_F \left(-\frac{827}{192} + \frac{11}{2}\zeta_3\right) + C_F^2 \left(-\frac{23}{32}\right) . \end{aligned} \tag{4.11}$$

Expanding in powers of b for K, we obtain

$$K_1 = b + \left(\frac{C_A}{12} - \frac{7}{8}C_F\right), \tag{4.12}$$

$$\begin{aligned} K_2 = {} & \left(\frac{115}{72}\right) b^2 + C_A \left(\frac{335}{144} + \frac{3}{2}\zeta_3 - \frac{15}{9}\zeta_5\right) b + C_F \left(-\frac{133}{288} - \frac{5}{6}\zeta_3\right) b \\ & + C_A^2 \left(-\frac{179}{144} - \frac{11}{4}\zeta_3\right) + C_A C_F \left(-\frac{389}{192} + \frac{11}{4}\zeta_3\right) + C_F^2 \left(\frac{1}{32}\right) . \end{aligned} \tag{4.13}$$

Finally for $\tilde{U}$ we have

$$U_1 = \frac{4}{3}b + \left(\frac{C_A}{12} - \frac{11}{8}C_F\right), \tag{4.14}$$

$$\begin{aligned} U_2 = {} & \left(\frac{155}{72}\right) b^2 + C_A \left(\frac{275}{144} - \frac{7}{2}\zeta_3 + 5\zeta_5\right) b + C_F \left(-\frac{335}{96} + \frac{1}{2}\zeta_3\right) b \\ & + C_A^2 \left(+\frac{295}{144} + \frac{137}{12}\zeta_3 - \frac{115}{6}\zeta_5\right) + C_A C_F \left(-\frac{2413}{192} - \frac{125}{4}\zeta_3 + \frac{95}{2}\zeta_5\right) \\ & + C_F^2 \left(\frac{313}{32} + \frac{47}{2}\zeta_3 - 35\zeta_5\right) . \end{aligned} \tag{4.15}$$

We now demonstrate that the leading term in the b-expansion, when expanded in N_f, approximates the N_f-expansion coefficients well even in rather low orders. For instance, for SU(N) QCD the exact perturbative coefficients for D in numerical form are given by

$$d_1 = -.115N_f + \left(.655N + \frac{.063}{N}\right) \tag{4.16}$$

$$d_2 = .086N_f^2 + N_f \left(-1.40N - \frac{.024}{N}\right) + \left(2.10N^2 - .661 - \frac{.180}{N^2}\right) . \tag{4.17}$$

These are to be compared with the the leading-b terms

$$d_1^{(1)}b = .345b = -.115N_f + .634N \ , \tag{4.18}$$

$$d_2^{(2)}b^2 = .776b^2 = .086N_f^2 - .948N_fN + 2.61N^2 \ . \tag{4.19}$$

The subleading N, N_fN and N^2 coefficients approximate well in sign and magnitude those in the exact expressions in Eq.(4.16) and Eq.(4.17). The leading N_f and N_f^2 coefficients of course agree exactly.

For K_1 and K_2 we have from Section 1.8.3

$$K_1 = -.333N_f + \left(1.48N + \frac{.438}{N}\right) \ , \tag{4.20}$$

$$K_2 = .177N_f^2 + N_f\left(-2.51N - \frac{.244}{N}\right) + \left(4.53N^2 + .686 + \frac{.008}{N^2}\right) \ . \tag{4.21}$$

compared with

$$K_1^{(1)}b = b = -.333N_f + 1.83N \ , \tag{4.22}$$

$$K_2^{(2)}b^2 = 1.59b^2 = .177N_f^2 - 1.95N_fN + 5.37N^2 \ . \tag{4.23}$$

The agreement with the exact N, N_fN and N^2 coefficients in Eq.(4.20) and Eq.(4.21) is again rather good.

Finally for $\check{U}$ we have

$$U_1 = -.444N_f + \left(1.84N + \frac{.687}{N}\right) \ , \tag{4.24}$$

$$U_2 = .239N_f^2 + N_f\left(-3.11N - \frac{.481}{N}\right) + \left(5.77N^2 + 2.22 + \frac{.434}{N^2}\right) \ . \tag{4.25}$$

compared with

$$U_1^{(1)}b = 1.33b = -.444N_f + 2.44N \ , \tag{4.26}$$

$$U_2^{(2)}b^2 = 2.15b^2 = .239N_f^2 - 2.63N_fN + 7.24N^2 \ . \tag{4.27}$$

Again the agreement with the exact coefficients in Eq.(4.24) and Eq.(4.25) is quite good.

As reference [76] notes, whilst the leading-b term reproduces the sub-leading coefficients in the N_f-expansion at the $\sim 20\%$ level, there are significant cancellations between large terms and as a result the overall NNLO perturbative coefficients for the Euclidean observables $\check{D}$, $\check{K}$, $\check{U}$ are significantly overestimated by the leading-b term. For example, for $N_f = 3$ and SU(3) QCD one has the exact ($\overline{\rm MS}$, $\mu = Q$) coefficient $d_2 = 6.37$, to be compared with the leading-b term $d_2^{(2)}b^2 = 15.7$. In every case the leading-b piece is a factor ~ 2 larger than the exact coefficient.

Notice that the level of accuracy with which the sub-leading coefficients $d_k^{[k-r]}$ are reproduced is far in excess of that to be anticipated from the asymptotic expectation of Eq.(4.9). This is a rather weak statement which implies only that $d_k^{[k-r]}$ should be reproduced to $O(1/k)$ accuracy for fixed r and large k on expanding $d_k^{(k)}b^k$, whereas the $d_k^{[0]}$ (r=k) coefficient, which is leading in the $1/N$ expansion for a large number of colours, is reproduced accurately for k=1 and k=2.

4.2.2 Borel resummation of the leading-b expansion

Given the observed dominance of the leading-b terms, an obvious proposal is to perform all-orders resummations for some phenomenologically interesting QCD observables. We shall refer mainly to the results of reference [76].

Since $d_k^{(k)}$=$(-3)^k d_k^{[k]}$ exact all-orders large-N_f results can be used to perform a "leading-b" resummation. Following [76] we define

$$D^{(L)} \equiv \sum_{k=0}^{\infty} d_k^{(L)} a^{k+1} \tag{4.28}$$

where $d_k^{(L)} \equiv d_k^{(k)} b^k$ ($d_0^{(L)} \equiv 1$). We can also consider the complementary sum over the sub-leading b terms

$$D^{(NL)} \equiv \sum_{k=1}^{\infty} d_k^{(NL)} a^{k+1} \tag{4.29}$$

where $d_k^{(NL)} \equiv d_k - d_k^{(L)}$. Hence

$$D = D^{(L)} + D^{(NL)} \, . \tag{4.30}$$

In reference [76] the summation in Eq.(4.28) was defined using Borel summation. The Borel integral can be split into two components corresponding to UV_ℓ and IR_ℓ renormalon singularities, respectively. The integral is well defined for the UV_ℓ singularities on the negative axis, which contribute poles to the Borel transform of $D^{(L)}$. The piece of the Borel integral for $D^{(L)}$ involving the IR_ℓ singularities on the positive real axis is formally divergent; a principal value or other regulation can be used to go around the poles. As we saw in Section 3.8 the IR_ℓ singularities are intimately connected with OPE for the observable in question, and the chosen regulation of the IR singularities determines the definition of non-perturbative condensates [16]. In reference [76] the integral was performed explicitly in terms of exponential integral functions and other elementary functions with the IR renormalon singularities principal value (PV) regulated.

For the Euclidean quantity $\hat{D}$ defined in Section 1.7.1 it can be deduced from the exact large-N_f results that, in the 'V-scheme' ($\overline{\rm MS}$ scheme with $\mu{=}{\rm e}^{-5/6}Q$), the Borel transform, $B[D](z)$, is of the form [82]

$$\begin{aligned} B[\hat{D}](z) &= \sum_{\ell=1}^{\infty} \frac{A_0(\ell) + A_1(\ell)z + \overline{A}_1(\ell)z + \overline{A}_2(\ell)z^2 + \cdots}{\left(1+\frac{z}{z_\ell}\right)^{\alpha_\ell+\overline{\alpha}_\ell}} \\ &\quad + \sum_{\ell=1}^{\infty} \frac{B_0(\ell) + B_1(\ell)z + \overline{B}_1(\ell)z + \overline{B}_2(\ell)z^2 + \cdots}{\left(1-\frac{z}{z_\ell}\right)^{\beta_\ell+\overline{\beta}_\ell}} + \cdots , \end{aligned} \tag{4.31}$$

where $z_\ell{=}2\ell/b$. The two terms correspond to a infinite summation over the ultraviolet renormalon singularities, ${\rm UV}_\ell$ at $z{=}{-}z_l$, and infrared renormalon singularities, ${\rm IR}_\ell$ at $z{=}z_l$, respectively. $A_0(\ell)$, $A_1(\ell)$, α_ℓ and $B_0(\ell)$, $B_1(\ell)$, β_ℓ will be obtained from the large-N_f results.

The barred terms are sub-leading in N_f and remain unknown. The use of the 'V-scheme' [51] means that only the constant and $O(z)$ terms in the numerator polynomials are leading in N_f. For a general $\overline{\rm MS}$ scale, $\mu{=}{\rm e}^u Q$, an overall factor ${\rm e}^{bz(u+5/6)}$ should multiply the unbarred leading-N_f terms in the numerator. The presence of this exponential factor, when it is expanded in powers of z, can mask the presence of the UV and IR renormalons in low orders of perturbation theory.

For the full branch point structure of the renormalon singularities one needs to incorporate the subleading in N_f, $\overline{\alpha}_\ell$ and $\overline{\beta}_\ell$, pieces of the exponents. One expects

$$\begin{aligned} \overline{\alpha}_\ell &= -cz_\ell + \gamma_\ell \, , \\ \overline{\beta}_\ell &= cz_\ell + \gamma'_\ell \, . \end{aligned} \tag{4.32}$$

As we have already noted in Chapter 3, the first term can be deduced from RG considerations and (see Section 3.8) the γ_ℓ and γ'_ℓ are the one-loop anomalous dimensions of the relevant operators [16, 63]. For $\hat{D}$ it is known that ${\rm IR}_2$ has a corresponding OPE operator with vanishing one-loop anomalous dimension, $\gamma'_2{=}0$ [74], so $\overline{\beta}_2{=}cz_2$ is known. The remaining γ_ℓ and γ'_ℓ's are unknown.

The Adler D-function

We now turn to the explicit determination of the coefficients and exponents for $\hat{D}$. While the general expectations for the Borel plane singularity structure were discussed in Section 3.6, the exact large-N_f result of Eq.(3.32) can now be used to exhibit what its singularity

structure actually is. Using Eq.(3.33) it can be deduced that the that the coefficients and exponents in Eq.(4.31) for $B[\tilde{D}](z)$ are [82]

$$\begin{aligned} A_0(\ell) &= \frac{8}{3}\frac{(-1)^{\ell+1}(3\ell^2+6\ell+2)}{\ell^2(\ell+1)^2(\ell+2)^2}, \quad A_1(\ell) = \frac{8}{3}\frac{b(-1)^{\ell+1}(\ell+\frac{3}{2})}{\ell^2(\ell+1)^2(\ell+2)^2} \\ \ell &= 1,2,3,\ldots \\ & B_0(1)=0, \quad B_0(2)=1, \quad B_0(\ell) = -A_0(-\ell) \quad \ell \geq 3 \\ & B_1(1)=0, \quad B_1(2)=0, \quad B_1(\ell) = -A_1(-\ell) \quad \ell \geq 3 \\ & \alpha_\ell = 2 \;\; \ell = 1,2,3,\ldots, \quad \beta_2 = 1, \; \beta_\ell = 2 \quad \ell \geq 3\,. \end{aligned} \tag{4.33}$$

In the specific case of the Adler D-function, one observes that IR_1 is absent, reflecting the absence of a relevant operator of dimension two in the OPE for vacuum polarization (as mentioned in Section 3.8) [82, 64]. IR_2 is a single pole and the remaining singularities are double poles. Notice that the branch point exponent cz_ℓ is sub-leading in the N_f, b expansion and so one sees poles and not branch points in the large-N_f limit. The coefficients for the UV_ℓ and IR_ℓ singularities are related by the symmetry $B_{0,1}(\ell)=-A_{0,1}(-\ell)$, and an additional relation $A_0(\ell)=-B_0(\ell+2)$ resulting from the form of $A_0(\ell)$. This second relation results in the constant term in the numerator polynomial for UV_ℓ exactly cancelling that for $\mathrm{IR}_{\ell+2}$. This ensures that

$$\sum_{\ell=1}^{\infty}(A_0(\ell)+B_0(\ell)) = B_0(2) = 1\,,$$

which is required to reproduce the unit coefficient of the $O(a)$ term in the perturbative expansion.

For the Adler D-function the singularity nearest the origin is UV_1. From $A_0(1)$, $A_1(1)$ in Eq.(4.33) this will correspond to

$$d_n^{(n)}|_{UV_1} = \left(-\frac{1}{2}\right)^n \frac{12n+22}{27} n!\,. \tag{4.34}$$

In the V-scheme the UV_1 renormalon dominates the contribution to the exact leading-b coefficients, $d_n^{(n)}$, even in low orders and the expected alternating sign factorial behaviour is a observed [76].

To perform the leading-b resummation defined in Eq.(4.28) one can use the Borel integral of Eq.(3.11). For the Adler D-function we then have [76]

$$\begin{aligned} \tilde{D}^{(L)}(a) &= \int_0^\infty \mathrm{d}z\, \mathrm{e}^{-z/a}\mathrm{e}^{bz(u+5/6)} \sum_{\ell=1}^{\infty} \frac{A_0(\ell)+A_1(\ell)z}{(1+\frac{z}{z_\ell})^2} \\ &+ \int_0^\infty \mathrm{d}z\, \mathrm{e}^{-z/a}\mathrm{e}^{bz(u+5/6)} \left(\frac{B_0(2)}{(1-\frac{z}{z_2})} + \sum_{\ell=3}^{\infty} \frac{B_0(\ell)+B_1(\ell)z}{(1-\frac{z}{z_\ell})^2} \right)\,, \end{aligned} \tag{4.35}$$

where $\overline{\rm MS}$ subtraction with $\mu = {\rm e}^{u+v/b}Q$ is assumed (this subsumes MOM, see 2.3.2). Notice that v does not appear in the expression for $\tilde{D}^{(L)}(a)$ since the leading-b terms are v-independent. Assuming that a finite RS (say the 't Hooft scheme introduced in Section 2.2.3) with beta-function $B(x)$ has been used, then the coupling, a, is defined by the integrated beta-function equation

$$\frac{1}{a} = b\ln\left(\frac{{\rm e}^{u+v/b}Q}{\Lambda_{\overline{\rm MS}}}\right) - c\ln\frac{ca}{1+ca} - \int_0^a {\rm d}x\left[-\frac{1}{x^2B(x)} + \frac{1}{x^2(1+cx)}\right] . \tag{4.36}$$

In such finite schemes, where c_2, c_3, ... are N_f-independent, the leading-b expansion of Eq.(4.4) contains additional inverse powers of b so that the d_n are no longer polynomials in N_f. In 'regular' schemes the leading-b coefficients, $d_k^{(k)}$, are independent of c_2, c_3, ..., since these beta-function coefficients, c_k, are $O(1/N_f)$ relative to d_k.

Substituting from Eq.(4.36) for $1/a$ in Eq.(4.35) one then obtains

$$\begin{aligned}\tilde{D}^{(L)}(F(a)) \;=\; & \int_0^\infty {\rm d}z\,{\rm e}^{-F(a)z}\sum_{\ell=1}^{\infty}\frac{A_0(\ell)+A_1(\ell)z}{(1+\frac{z}{z_\ell})^2} \\ & + \int_0^\infty {\rm d}z\,{\rm e}^{-F(a)z}\left(\frac{B_0(2)}{(1-\frac{z}{z_2})} + \sum_{\ell=3}^{\infty}\frac{B_0(\ell)+B_1(\ell)z}{(1-\frac{z}{z_\ell})^2}\right) ,\end{aligned} \tag{4.37}$$

where

$$F(a) = b\ln\frac{Q}{\Lambda_{\overline{\rm MS}}} - \frac{5}{6}b - c\ln\frac{ca}{1+ca} + v - \int_0^a {\rm d}x\left[-\frac{1}{x^2B(x)} + \frac{1}{x^2(1+cx)}\right] . \tag{4.38}$$

The u-dependence in Eq.(4.35) has cancelled exactly, since it is compensated by the leading-b scale dependence of a. The scale dependence subleading in b is not compensated. This makes the partial resummation RS dependent, a subject we return to in Section 4.2.3.

The integral in Eq.(4.37) may now be evaluated in terms exponential integral functions, ${\rm Ei}(x)$; see Appendix A.4 for their definition. The UV renormalon terms are performed in terms of ${\rm Ei}(x)$ (with negative argument) — see Eq.(A.6); and the principal value regulated IR renormalons in terms of ${\rm Ei}(x)$, which are defined for positive argument as a Cauchy principal value — see Eq.(A.7). Defining

$$\tilde{D}^{(L)}(F(a)) = \tilde{D}^{(L)}(a)|_{UV} + \tilde{D}^{(L)}(F(a))|_{IR} , \tag{4.39}$$

one then obtains the closed form expressions [76]

$$\begin{aligned}\tilde{D}^{(L)}(F(a))|_{UV} \;=\; & \sum_{\ell=1}^{\infty} z_\ell\{{\rm e}^{F(a)z_\ell}{\rm Ei}(-F(a)z_\ell)\,[F(a)z_\ell(A_0(\ell)-z_\ell A_1(\ell)) - z_\ell A_1(\ell)] \\ & +(A_0(\ell)-z_\ell A_1(\ell))\}\end{aligned} \tag{4.40}$$

$$\begin{aligned}\tilde{D}^{(L)}(F(a))|_{IR} &= \mathrm{e}^{-F(a)z_2} z_2 B_0(2)\mathrm{Ei}(F(a)z_2) \\ &+\sum_{\ell=3}^{\infty} z_\ell \{\mathrm{e}^{-F(a)z_\ell}\mathrm{Ei}(F(a)z_\ell)\,[F(a)z_\ell(B_0(\ell)+z_\ell B_1(\ell)) - z_\ell B_1(\ell)] \\ &-(B_0(\ell)+z_\ell B_1(\ell))\}\,. \end{aligned} \tag{4.41}$$

R-Ratio

Analogous resummations have been derived for the Minkowski continuations of the D-function, the e^+e^- annihilation R-ratio and the analogous quantity in τ-decay, R_τ [76]. Inserting the Borel representation of D into Eq.(1.72) one can directly obtain in the large-N_f limit [76]

$$B[\tilde{R}](z) = \frac{\sin(\pi b z/2)}{\pi b z/2} B[\tilde{D}](z)\,. \tag{4.42}$$

The leading-b resummation is then obtained from Eq.(4.37) simply by adding an extra $\frac{\sin(\pi bz/2)}{\pi bz/2}$ factor in the integrand.

The integrals are then evaluated in terms of generalized exponential integral functions; see Appendix A.4 for details. The UV renormalons are performed in terms of $\mathrm{Ei}(n,w)$, with complex argument w, defined for $\mathrm{Re}\,w > 0$ — see Eq.(A.8). The principal value regulated IR renormalons are performed in terms of $\mathrm{Ei}(n,w)$, for $\mathrm{Re}\,w < 0$ — see Eq.(A.9). To evaluate this contribution correctly one needs to continue $\mathrm{Ei}(n,w)$ as a real function, the method for which is explained in Appendix A.4. Defining

$$\tilde{R}^{(L)}(F(a)) = \tilde{R}^{(L)}(F(a))|_{UV} + \tilde{R}^{(L)}(F(a))|_{IR}\,. \tag{4.43}$$

One then obtains the closed form expressions [76]

$$\begin{aligned}\tilde{R}^{(L)}(F(a))|_{UV} &= \frac{2}{\pi b}\left(\frac{8\zeta_2}{3}-\frac{11}{3}\right)\arctan\left(\frac{\pi b}{2F(a)}\right) \\ &+\frac{2}{\pi b}\sum_{\ell=1}^{\infty}\Big\{A_0(\ell)\phi_+(1,\ell)+(A_0(\ell)-A_1(\ell)z_\ell)\phi_+(2,\ell)\Big\}\end{aligned} \tag{4.44}$$

$$\begin{aligned}\tilde{R}^{(L)}(F(a))|_{IR} &= \frac{2}{\pi b}\left(\frac{14}{3}-\frac{8\zeta_2}{3}\right)\arctan\left(\frac{\pi b}{2F(a)}\right)+\frac{2B_0(2)}{\pi b}\phi_-(1,2) \\ &+\frac{2}{\pi b}\sum_{\ell=3}^{\infty}\Big\{B_0(\ell)\phi_-(1,\ell)+(B_0(\ell)+B_1(\ell)z_\ell)\phi_-(2,\ell)\Big\}.\end{aligned} \tag{4.45}$$

where, defining $F_\pm = F(a) \pm \frac{i\pi b}{2}$, we have

$$\begin{aligned}\phi_+(p,q) &= \mathrm{e}^{F(a)z_q}(-1)^q\mathrm{Im}[\mathrm{Ei}(p,F_+z_q)] \\ \phi_-(p,q) &= \mathrm{e}^{-F(a)z_q}(-1)^q\mathrm{Im}[\mathrm{Ei}(p,-F_+z_q)] - \frac{\mathrm{e}^{-F(a)z_q}(-1)^q z_q^{p-1}}{(p-1)!}\pi\mathrm{Re}[(F_+)^{p-1}]\,,\end{aligned}$$

and we have used

$$\int_0^\infty \mathrm{d}z\, \mathrm{e}^{-F(a)z}\, \frac{\sin(\pi bz/2)}{z} = \arctan\left(\frac{\pi b}{2F(a)}\right) . \tag{4.46}$$

Hadronic tau-decay ratio R_τ

For R_τ we have

$$B[\tilde{R}_\tau](z) = \frac{\sin(\pi bz/2)}{\pi bz/2}\left[\frac{2}{(1-\frac{bz}{2})} - \frac{2}{(1-\frac{bz}{6})} + \frac{1}{(1-\frac{bz}{8})}\right] B[\tilde{D}](z) . \tag{4.47}$$

Proceeding in a manner analogous to that for the R-ratio, we define

$$\tilde{R}_\tau^{(L)}(F(a)) = \tilde{R}_\tau^{(L)}(F(a))|_{UV} + \tilde{R}_\tau^{(L)}(F(a))|_{IR} . \tag{4.48}$$

The UV and IR contributions are then [76]

$$\begin{aligned}
\tilde{R}_\tau^{(L)}(F(a))|_{UV} &= \frac{2}{\pi b}\left(\frac{8\zeta_2}{3} - \frac{11}{3}\right)\arctan\left(\frac{\pi b}{2F(a)}\right) \\
&\quad + \frac{4}{\pi b}\sum_{\ell=1}^{\infty}[(A_0(\ell)(G(\ell)+H(\ell)) - z_\ell A_1(\ell)G(\ell))\phi_+(1,\ell) \\
&\quad + H(\ell)(A_0(\ell) - z_\ell A_1(\ell))\phi_+(2,\ell)] \qquad (4.49) \\
\tilde{R}_\tau^{(L)}(F(a))|_{IR} &= \frac{2}{\pi b}\left(\frac{14}{3} - \frac{8\zeta_2}{3}\right)\arctan\left(\frac{\pi b}{2F(a)}\right) \\
&\quad + \frac{4}{\pi b}\left(-\frac{14}{3} + \frac{64}{3}\ln 2 - 8\zeta_3 + bz_1\left(\frac{23}{3} - \frac{32}{3}\ln 2\right)\right)\phi_-(1,1) \\
&\quad - \frac{12}{\pi b}\phi_-(1,2) + \frac{4}{\pi b}\left(-\frac{703}{18} + 64\ln 2 + bz_3\left(\frac{245}{36} - \frac{32}{3}\ln 2\right)\right)\phi_-(1,3) \\
&\quad + \frac{4}{\pi b}\left(-\frac{1627}{972} - \frac{128}{81}\ln 2 + bz_4\left(\frac{2035}{7776} + \frac{16}{81}\ln 2\right)\right)\phi_-(1,4) \\
&\quad + \frac{4}{\pi b}\left(-\frac{11}{27} + \frac{bz_3}{6}\right)\phi_-(2,3) + \frac{4}{\pi b}\left(\frac{247}{648} - \frac{5bz_4}{162}\right)\phi_-(2,4) \\
&\quad - \frac{8}{\pi b}\left(-\frac{11}{27} + \frac{bz_3}{18}\right)\phi_-(3,3) + \frac{8}{\pi b}\left(\frac{13}{432} - \frac{5bz_4}{1728}\right)\phi_-(3,4) \\
&\quad + \frac{4}{\pi b}\sum_{\ell=5}^{\infty}[(B_0(\ell)(G(-\ell)+H(-\ell)) + z_\ell B_1(\ell)G(-\ell))\phi_-(1,\ell) \\
&\quad + H(-\ell)(B_0(\ell) + z_\ell B_1(\ell))\phi_-(2,\ell)] , \qquad (4.50)
\end{aligned}$$

where

$$G(\ell) = \frac{6\ell(3\ell^2+16\ell+19)}{(\ell+1)^2(\ell+3)^2(\ell+4)^2}, \quad H(\ell) = \frac{6}{(\ell+1)(\ell+3)(\ell+4)} .$$

PBjSR and GLSSR

For the PBjSR and GLSSR the generating function for the leading-b coefficient in the V-scheme is [66]

$$K_n^{(n)} = \frac{1}{3}\left(\frac{1}{2}\right)^n \frac{\mathrm{d}^n}{\mathrm{d}x^n} \frac{(3+x)}{(1-x^2)(1-\frac{x^2}{4})}\bigg|_{x=0} . \tag{4.51}$$

This gives the Borel transform [76]

$$B[\tilde{K}](z) = \frac{\frac{4}{9}}{(1+\frac{bz}{2})} - \frac{\frac{1}{18}}{(1+\frac{bz}{4})} + \frac{\frac{8}{9}}{(1-\frac{bz}{2})} - \frac{\frac{5}{18}}{(1-\frac{bz}{4})} . \tag{4.52}$$

The terms correspond to UV_1, UV_2, IR_1, IR_2 respectively.

$K_n^{(n)}$ is then given by (we assume the V-scheme)

$$K_n^{(n)} = \frac{8}{9}n!\left(\frac{1}{2}\right)^n + \frac{4}{9}n!\left(-\frac{1}{2}\right)^n - \frac{5}{18}n!\left(\frac{1}{4}\right)^n - \frac{1}{18}n!\left(-\frac{1}{4}\right)^n . \tag{4.53}$$

$K_n^{(n)}$ is dominated, even in low orders, by the combined UV_1+IR_1 contributions of the two singularities nearest the origin, the first two terms of Eq.(4.53) [76].

Analogously to the Adler D-function, we can evaluate the Borel integral in terms of $\mathrm{Ei}(x)$ functions using Eq.(4.52). Defining

$$\tilde{K}^{(L)}(F(a)) = \tilde{K}^{(L)}(F(a))|_{UV} + \tilde{K}^{(L)}(F(a))|_{IR} , \tag{4.54}$$

one then obtains the closed form expressions

$$\tilde{K}^{(L)}(F(a))|_{UV} = \left[-\frac{4}{9}\mathrm{e}^{F(a)z_1} z_1 \mathrm{Ei}(-F(a)z_1) + \frac{1}{18}\mathrm{e}^{F(a)z_2} z_2 \mathrm{Ei}(-F(a)z_2)\right] \tag{4.55}$$

$$\tilde{K}^{(L)}(F(a))|_{IR} = \left[\frac{8}{9}\mathrm{e}^{-F(a)z_1} z_1 \mathrm{Ei}(F(a)z_1) - \frac{5}{18}\mathrm{e}^{-F(a)z_2} z_2 \mathrm{Ei}(F(a)z_2)\right] . \tag{4.56}$$

BjSR

In addition to those observables considered in [76] we can use the large-N_f result for the BjSR to evaluate the corresponding large-b resummation. The generating function for the leading-b coefficient in the V-scheme is [87]

$$U_n^{(n)} = \left(\frac{1}{2}\right)^n \frac{\mathrm{d}^n}{\mathrm{d}x^n} \frac{1}{(1-x)(1-\frac{x^2}{4})}\bigg|_{x=0} . \tag{4.57}$$

The Borel transform is then found to be

$$B[\tilde{U}](z) = \frac{\frac{4}{3}}{(1-\frac{bz}{2})} - \frac{\frac{1}{2}}{(1-\frac{bz}{4})} + \frac{\frac{1}{6}}{(1+\frac{bz}{4})} . \tag{4.58}$$

The terms correspond to IR_1, IR_2 and UV_2 respectively. Note the absence of the UV_1 singularity. As before each numerator and exponent will contain in addition $O(1/N_f)$ corrections corresponding to the barred terms in Eq.(4.31). The constant terms in the numerators sum to 1 ensuring a unit $O(a)$ coefficient in $\tilde{U}$.

$U_n^{(n)}$ is then given in the V-scheme by

$$U_n^{(n)} = \frac{4}{3}n!\left(\frac{1}{2}\right)^n - \frac{1}{2}n!\left(\frac{1}{4}\right)^n + \frac{1}{6}n!\left(-\frac{1}{4}\right)^n \ . \tag{4.59}$$

As one might expect the leading-b perturbative coefficients $U_n^{(n)}$ are dominated by the contribution from the IR_1 singularity nearest the origin, the first term in Eq.(4.59).

Analogously to $\tilde{D}$ we will then have, using Eq.(4.58),

$$\begin{aligned}\tilde{U}^{(L)}(F(a)) &= \int_0^\infty \mathrm{d}z\, \mathrm{e}^{-F(a)z}\left(\frac{\frac{1}{6}}{(1+\frac{z}{z_2})}\right) \\ &\quad + \int_0^\infty \mathrm{d}z\, \mathrm{e}^{-F(a)z}\left(\frac{\frac{4}{3}}{(1-\frac{z}{z_1})} - \frac{\frac{1}{2}}{(1-\frac{z}{z_2})}\right) \ .\end{aligned} \tag{4.60}$$

These integrals may be expressed once again in terms of $\mathrm{Ei}(x)$. Defining

$$\tilde{U}^{(L)}(F(a)) = \tilde{U}^{(L)}(F(a))|_{UV} + \tilde{U}^{(L)}(F(a))|_{IR} \ , \tag{4.61}$$

we obtain the UV and IR contributions

$$\tilde{U}^{(L)}(F(a))|_{UV} = \frac{1}{6}\mathrm{e}^{F(a)z_2} z_2 \mathrm{Ei}(-F(a)z_2) \tag{4.62}$$

$$\tilde{U}^{(L)}(F(a))|_{IR} = \frac{4}{3}\mathrm{e}^{-F(a)z_1} z_1 \mathrm{Ei}(F(a)z_1) - \frac{1}{2}\mathrm{e}^{-F(a)z_2} z_2 \mathrm{Ei}(F(a)z_2) \ . \tag{4.63}$$

4.2.3 RS-dependence of the "naive" resummation

In this section we focus on the question of the RS dependence of $D^{(L)}(a)$. For a generic quantity we can write

$$D = D^{(L)}(a) + D^{(NL)}(a) \ . \tag{4.64}$$

Here D denotes the full Borel sum in Eq.(4.31) with barred and unbarred terms included and the IR singularities PV regulated; we assume that this exists. The full Borel sum is formally RS-invariant and so will not depend on 'a'. The $D^{(L)}$ and $D^{(NL)}$ components do depend on 'a', however, and so are separately dependent on the chosen RS. As discussed in Chapter 2, changing the RS changes the definition of the renormalization group (RG)-improved coupling so that the 'a' appearing in the summation changes. In the full sum

this change is precisely compensated by the RG transformations of the coefficient d_k under the change in RS. By restricting oneself to the 'leading-b' piece, however, of the coefficients this exact compensation is destroyed and the resulting sum $D^{(L)}$ is strongly RS-dependent [76, 84].

Even at NLO the RS dependence is quite destructive. Let us denote the perturbative coefficients in the $\overline{\rm MS}$ scheme with $\mu = Q$ (u=v=0) by d_k; and those with general u and v by d'_k. Then

$$\begin{aligned} d'_1 &= (d_1^{(1)} + u)b + (d_1^{(0)} + v) \\ &= d_1 + bu + v \,. \end{aligned} \tag{4.65}$$

Changing v, one can make the $d_1^{(0)}$ coefficient as large as one pleases and hence destroy the dominance of the leading-b term noted in Section 4.2.1 for the observables in low orders. Similar remarks will apply at higher orders in perturbation theory. Of course the leading-b term should still reproduce asymptotically the $d_k^{[k-r]}$ coefficients to $O(1/k)$ accuracy.

To exhibit the RS dependence more explicitly one can consider 'a' varying between a=0 and a=+∞, labelling possible RS's. From Eq.(4.38), as $a \to 0$ so $F(a) \to +\infty$, resulting from the $-c \ln \frac{ca}{1+ca}$ term (we assume $c > 0$ which is true for $N_f \leq 8$ in SU(3) QCD). One then has $D^{(L)}(0)$=0. Correspondingly, from Eq.(4.64), $D^{(NL)}(0)$=D and so, as $a \to 0$, the NL component contributes the whole resummed D. As 'a' increases the $-c \ln \frac{ca}{1+ca}$ term in Eq.(4.38) decreases and as $a \to \infty$ it vanishes, resulting in a finite limit $F(\infty)$

$$F(\infty) = b \ln \frac{Q}{\Lambda_{\overline{\rm MS}}} - \frac{5}{6} b + v - \int_0^\infty {\rm d}x \left[-\frac{1}{x^2 B(x)} + \frac{1}{x^2(1+cx)} \right] . \tag{4.66}$$

We assume that $B(x)$ is such that the integral exists.

In Figures 4.1(a) to 4.1(e) we plot the observables versus a, where $a = 1/F(a)$, and $F(a)$ is given in Eq.(4.38). So as to fit the full variation of $a = 0 \ldots \infty$ ($F = \infty \ldots 0$) we plot versus $\hat{a} = 1 - {\rm e}^{-a}$. The range then corresponds to the unit interval $\hat{a} = 0 \ldots 1$. For each observable we choose an appropriate value of N_f, though it should be emphasised that the form of the plots does not significantly alter with flavour thresholds. In addition to the overall resummation, $\tilde{D}(F(a))$, denoted by a solid curve, we have plotted curves for the $\tilde{D}^{(L)}(F(a))|_{UV}$ (dashed) and $\tilde{D}^{(L)}(F(a))|_{IR}$ (dashed-dotted) contributions. The relative sizes of the UV and IR contributions reflect the disposition of the UV and IR renormalon singularities.

Turning first to the Adler D-function, Figure 4.1(a), we observe that $\tilde{D}(F(a))$, initially

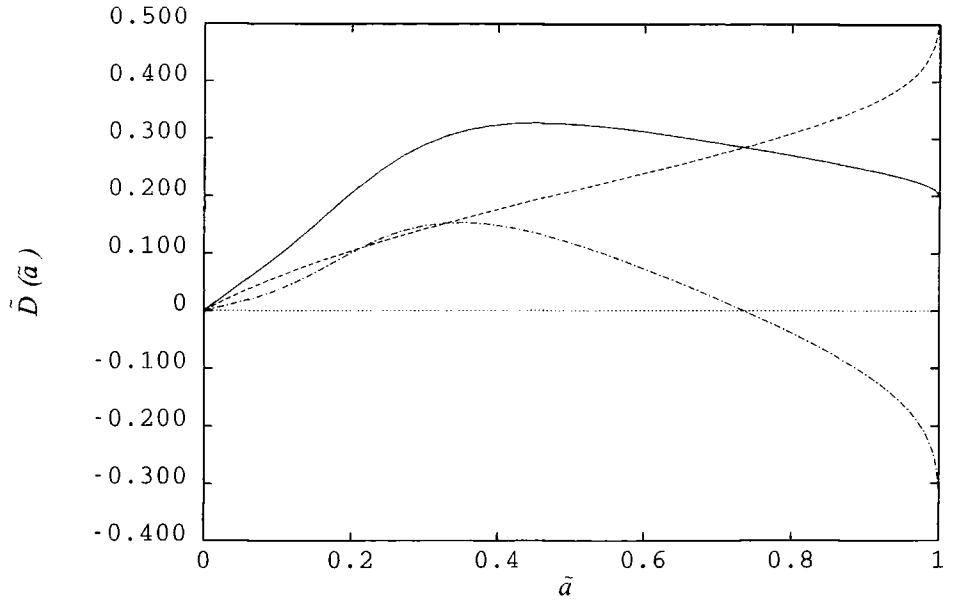

Figure 4.1(a): The leading-b resummation, $\tilde{D}(F(a))$, plotted versus $\tilde{a} = 1 - e^{-a}$ and assuming $N_f = 5$. The solid curve denotes the overall resummation split into $\tilde{D}^{(L)}(F(a))|_{UV}$ (dashed) and $\tilde{D}^{(L)}(F(a))|_{IR}$ (dashed-dotted).

zero for $a = 0$, monotonically rises with increasing a to a maximum, followed by a monotonic decrease to a finite value for $a = \infty$. For most phenomenologically relevant energy scales ($Q \gg \Lambda$) and renormalization schemes, we are only interested in the portion of the plot to the left hand side of the maximum. This corresponds to asymptotic freedom, with $\lim_{Q \to \infty} \tilde{D}(a(Q)) = 0$. The interpretation of the right hand portion of the plot is somewhat ambiguous, and we will return to this question later in Section 4.5.3. The presence of a maximum value for $\tilde{D}(F(a))$ will have an important consequence when we turn to construct RS-invariant resummations in section 4.4.2, and the implications are discussed further in Section 4.5.3.

The individual contributions from the UV and IR singularities are, as would be expected, somewhat discordant in behaviour. $\tilde{D}^{(L)}(F(a))|_{UV}$ (dashed) is a monotonically increasing function, such that $\tilde{D}^{(L)}(F(a))|_{UV} \to \infty$ as $a \to \infty$ ($F \to 0$). $\tilde{D}^{(L)}(F(a))|_{IR}$ (dashed-dotted) initially increases, but unlike $\tilde{D}^{(L)}(F(a))|_{UV}$, eventually reaches a maximum. Following this $\tilde{D}^{(L)}(F(a))|_{IR}$ decreases, such that $\tilde{D}^{(L)}(F(a))|_{IR} \to -\infty$ as $a \to \infty$. The IR contribution is therefore directly responsible for the maximum in $\tilde{D}(F(a))$. As expected the dominance of the UV_1 singularity results in the contribution from the UV singularities being dominant for most scenarios. We note, however, that the IR singularities exert

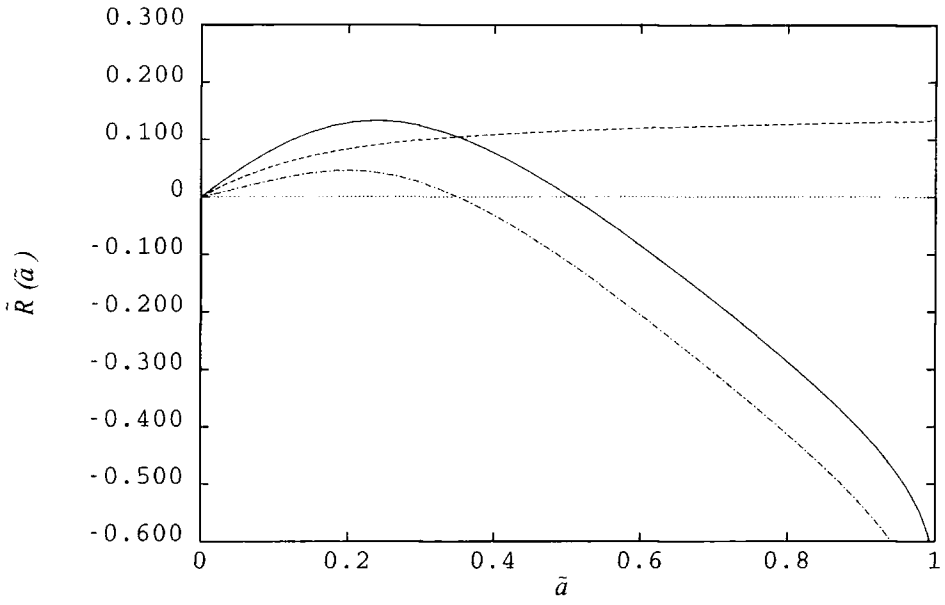

Figure 4.1(b): As for Figure 4.1 but for $\tilde{R}(F(a))$ (assuming $N_f = 5$).

increasing influence on the overall contribution as a increases, most particularly in the region to the right-hand side of the maximum.

For $\tilde{R}^{(L)}(F(a))$, Figure 4.1(b), the behaviour for $\tilde{a} < 0.3$ is qualitatively similar to that of $\tilde{D}^{(L)}(F(a))$, with the $\tilde{R}^{(L)}(F(a))|_{UV}$ the dominant contributory source. Quantitatively the maximum value of $\tilde{R}^{(L)}(F(a))$ is somewhat smaller. For $\tilde{a} > 0.3$, however, the IR contribution becomes almost totally dominant, since $\tilde{R}^{(L)}(F(a))|_{IR}$ decreases rapidly, while the monotonic increase of $\tilde{R}^{(L)}(F(a))|_{UV}$ slows. Note that for $a = \infty$ both $\tilde{R}^{(L)}(F(a))|_{UV}$ and $\tilde{R}^{(L)}(F(a))|_{IR}$ are finite.

The behaviour of $\tilde{R}_\tau^{(L)}(F(a))$, Figure 4.1(c) reflects the additional strength of the IR singularities relative to $\tilde{R}$. For $\tilde{R}_\tau$ we can see from Eq.(4.47) that we will have double poles at IR_3 and IR_4, rather than single poles as is the case for $\tilde{R}$. Initially, the UV contribution is greater, but it is quickly overwhelmed by the IR contribution which rises rapidly. Unlike $\tilde{D}^{(L)}(F(a))|_{IR}$ and $\tilde{R}^{(L)}(F(a))|_{IR}$, $\tilde{R}_\tau^{(L)}(F(a))|_{IR}$ is positive for all a. As a direct result the value of the maximum is very much larger than that for $\tilde{D}^{(L)}(F(a))$ or $\tilde{R}^{(L)}(F(a))$. Again for $a = \infty$ both $\tilde{R}_\tau^{(L)}(F(a))|_{UV}$ and $\tilde{R}_\tau^{(L)}(F(a))|_{IR}$ are finite.

Lastly, we turn to the DIS sum rules $\tilde{K}^{(L)}(F(a))$ and $\tilde{U}^{(L)}(F(a))$, Figure 4.1(d) and Figure 4.1(e), respectively. As expected the IR contribution dominates for both these

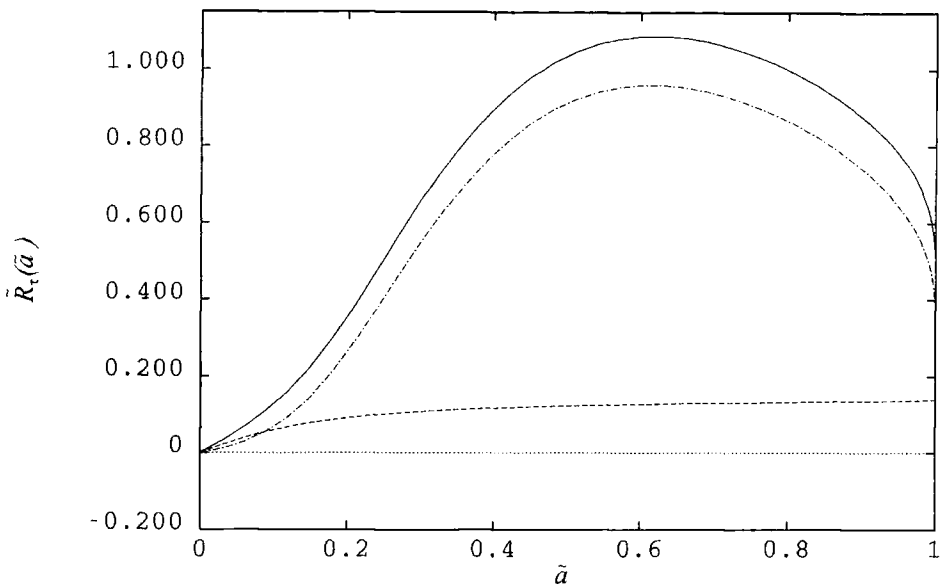

Figure 4.1(c): As for Figure 4.1 but for $\tilde{R}_\tau(F(a))$ (assuming $N_f = 3$).

observables. This effect is more visible for $\tilde{U}^{(L)}(F(a))$ which is totally dominated by the IR_1 singularity. As was the case for the other Euclidean observable, for $a = \infty$ we find $\tilde{K}^{(L)}(F(\infty))|_{UV} = \infty$ $\tilde{K}^{(L)}(F(\infty))|_{IR} = \infty$, and similarly for $\tilde{U}^{(L)}(F(\infty))$.

Except at low energy scales, the RS dependence of $D^{(L)}(a)$ is monotonic. This is problematic since there is no basis for choosing a particular scheme. There is also a dependence on the particular finite scheme, characterised by the choice of $B(x)$, and on the parameter v. The maximum value, $D^{(L)}(\infty)$, does perhaps minimize the relative contribution of the unknown $D^{(NL)}$ component but there is no guarantee that $D^{(NL)}(\infty)$ is positive; and it is entirely possible that $D^{(L)}(\infty)$ overestimates D. Since both fixed order perturbation theory and the leading-b resummed results exhibit RS-dependence it is not at all obvious which procedure gives the closest approximation to the all-orders sum.

In the recent papers [62, 69, 77, 78, 79] resummation of the leading-b terms has also been considered. In these papers it has been motivated as a generalization of the BLM scale fixing prescription [51], discussed in Section 2.4.2, and termed "naïve non-abelianization" [88]. In response to the RS dependence problem they artificially restrict the RG-transformation of 'a' to that contributed by the first term in the beta-function only. With this restriction the summation $D^{(L)}$ is then RS-invariant since RS changes are exactly compensated for at

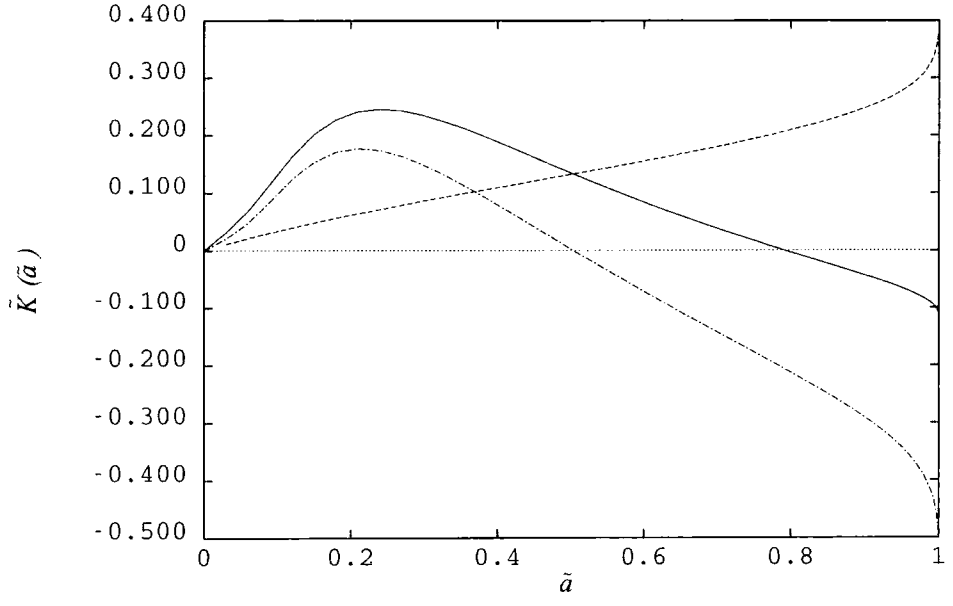

Figure 4.1(d): As for Figure 4.1 but for $\tilde{K}(F(a))$ (assuming $N_f = 3$).

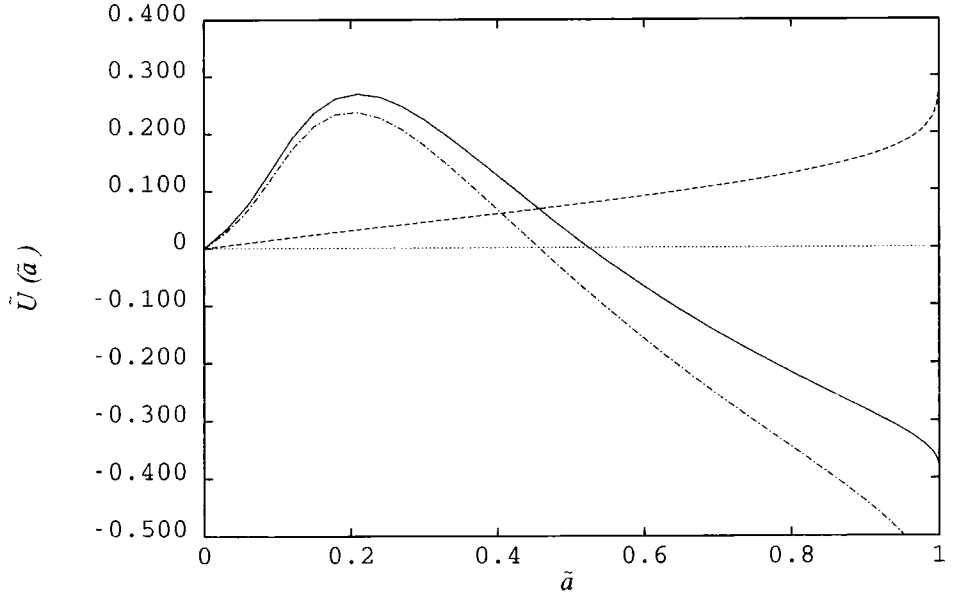

Figure 4.1(e): As for Figure 4.1 but for $\tilde{U}(F(a))$ (assuming $N_f = 3$).

the 'leading-b' level. References [62, 69, 77, 78, 79] all define a to be the one-loop coupling in the V-scheme ($\overline{\rm MS}$ scheme with μ=e$^{-5/6}Q$)

$$a_{\text{1-loop}} = \frac{1}{b \ln \frac{Q}{\Lambda_V}} , \tag{4.67}$$

where Λ_V=e$^{5/6}\Lambda_{\overline{\rm MS}}$. Using the one-loop form for $a(\mu)$ makes the leading-b summation μ-independent. With this choice one has

$$F(\infty) = b \ln \frac{Q}{\Lambda_{\overline{\rm MS}}} - \frac{5}{6} b \, ; \tag{4.68}$$

One can observe that this corresponds a variant of minimal subtraction with $v = 0$ and $B(x)$=$1 + cx$, the 't Hooft scheme.

In our view, however, one can and should do much better than this. For several QCD observables one has exact results for the first two perturbative coefficients d_1 and d_2, usually in the modified minimal subtraction ($\overline{\rm MS}$) scheme with renormalization scale μ=Q [17, 18, 28, 29]. Only the leading-b pieces of these exacts calculations included in a 'naive' leading-b resummation. In particular if the exact NLO and NNLO coefficients are available it would seem sensible to include them and approximate only the unknown $d_3, d_4, \cdots$, higher coefficients by $d_3^{(L)}, d_4^{(L)}$. Unfortunately, however, the resummed result explicitly depends on the RS chosen for evaluating the exact d_1, d_2 coefficients. Any attempt to additively include the non-leading pieces of the NLO and NNLO perturbative coefficients, as in reference [77], will destroy the RG invariance, leading to a matching ambiguity due to the RS dependence of the resummation. In Section 5.5.4 we will explicitly exhibit the effect of this RS dependence on the determination of $\alpha_s(m_\tau)$ from $\tilde{R}_\tau^{(L)}$.

These difficulties greatly limit the phenomenological application of such resummations. There is clearly a requirement for a resummation in which the NLO and NNLO coefficients are included exactly, and an approximate resummation of the higher orders coefficients performed; in such a way that the full sum is explicitly RS-invariant under the full QCD RG transformations. In this way one would have a test bed for assessing the reliability of fixed-order perturbation theory in any RS by seeing how it differed from the RS-invariant resummed result. As one reduced the energy scale Q (e.g. the centre of mass-energy in e^+e^- annihilation) one could also assess how the reliability of fixed-order perturbation theory deteriorates.

4.3 RS-invariant leading-b Resummations

The problematic RS-dependence may be avoided by performing a resummation of the EC beta-function which is explicitly RG-invariant.

4.3.1 The leading-b expansion of the EC beta-function

To construct RS-invariant resummations the strategy will be to approximate the RS-invariants ρ_k, and then use Eq.(2.30), to obtain the approximate perturbative coefficients in any arbitrary RS. In this way invariance under the full RG transformations of QCD is guaranteed.

For later convenience we recall from Eq.(2.76) that $\rho_0{=}\tau - d_1$ is RS-invariant. Therefore we can use d_1 itself, rather than τ, as was used in Eq.(2.30), to label the RS. Eq.(2.30) then becomes

$$\begin{aligned} d_2(d_1,c_2) &= d_1^2 + cd_1 + (\rho_2 - c_2) \\ d_3(d_1,c_2,c_3) &= d_1^3 + \frac{5}{2}cd_1^2 + (3\rho_2 - 2c_2)d_1 + \frac{1}{2}(\rho_3 - c_3) \\ &\vdots \qquad\quad \vdots \end{aligned} \tag{4.69}$$

The result for $d_n(d_1,c_2,\cdots,c_n)$ is a polynomial of degree n in d_1 with coefficients involving ρ_n,ρ_{n-1},$\cdots$,c and c_2,c_3,$\cdots$,c_n; such that $d_n(0,\rho_2,\rho_3,\cdots,\rho_n){=}0$. Given just these numbers the perturbative coefficients in any RS can be obtained from Eq.(4.69).

The ρ_k invariants can be organized as an expansion in b, with

$$\rho_k = \rho_k^{(k)} b^k + \rho_k^{(k-1)} b^{k-1} + \cdots + \rho_k^{(0)} + \rho_k^{(-1)} b^{-1} \; . \tag{4.70}$$

The $\rho_k^{(k)}$ can be obtained to all-orders from the large-N_f result for $d_k^{(k)}$. The b^{-1} term arises from the fact that in a 'regular' RS such as minimal subtraction the d_k are polynomials in b of degree k [86], whereas the corresponding beta-function coefficients c_k are polynomials in b of degree k-1 with additional b^{-1} terms (c.f. the expression for $c{=}c_1$ in Eq.(2.5)). The RS-invariant combinations in Eq.(4.70) in principle could contain arbitrary inverse powers of b, but RG considerations guarantee that only b^{-1} terms remain [86]. Thus $b\rho_k$ is a polynomial of degree $k{+}1$ in b.

The effective charge beta-function $\rho(D)$, Eq.(2.60), will contain Borel plane singularities at the same positions as those in $D(a)$ [54] and hence one should expect a weak asymptotic

result analogous to Eq.(4.9), with the $\rho_k^{(k)} b^{k+1}$ term asymptotically reproducing the N_f-expansion coefficients of $b\rho_k$. For the Adler D-function and DIS sum rules the level at which this works is again far in excess of that to be anticipated from the asymptotic result. The $\rho_k^{(k)}$ term involves only combinations of the $d_k^{(k)}$, with for instance $\rho_2^{(2)}=d_2^{(2)} - (d_1^{(1)})^2$, and so the $\rho_k^{(k)}$ can be obtained to all-orders given the exact leading-N_f all-orders results.

For the Adler D-function ($\tilde{D}$) one has the exact result for SU(N) QCD (where the "light-by-light" contribution $\hat{\tilde{D}}$ is excluded, see [76])

$$\begin{aligned} b\rho_2(\tilde{D}) &= -0.0243N_f^3 + (0.553N - 0.00151\frac{1}{N})N_f^2 \\ &\quad +(-3.32N^2 + 0.344 + 0.0612\frac{1}{N^2})N_f \\ &\quad +(3.79N^3 - 1.45N - 0.337\frac{1}{N}) . \end{aligned} \tag{4.71}$$

This is to be compared with the 'leading-b' piece

$$\begin{aligned} b^3\rho_2^{(2)}(\tilde{D}) &= b^3(d_2^{(2)} - (d_1^{(1)})^2) = 0.656b^3 \\ &= -0.0243N_f^3 + 0.401NN_f^2 - 2.21N^2N_f + 4.04N^3 . \end{aligned} \tag{4.72}$$

Notice the good agreement of the sub-leading NN_f^2, N^2N_f, and N^3 coefficients. This gives us some confidence that the remarkable accuracy with which the sub-leading coefficients $d_k^{[k-r]}$ are reproduced is not just an artefact of the particular RS choice of $\overline{\rm MS}$ with $\mu = Q$.

In order to further extend this conviction we can consider K and U. For polarized Bjorken or GLS sum rule, $\tilde{K}$ [76]) one has the exact result

$$\begin{aligned} b\rho_2(\tilde{K}) &= -0.0221N_f^3 + (0.513N + 0.00665\frac{1}{N})N_f^2 \\ &\quad +(-3.29N^2 + 0.505 + 0.0143\frac{1}{N^2})N_f \\ &\quad +(3.85N^3 - 1.73N - 0.337\frac{1}{N}) , \end{aligned} \tag{4.73}$$

which is to be compared with

$$\begin{aligned} b^3\rho_2^{(2)}(\tilde{K}) &= 0.597b^3 \\ &= -0.0221N_f^3 + 0.365NN_f^2 - 2.01N^2N_f + 3.68N^3 , \end{aligned} \tag{4.74}$$

The NN_f^2, N^2N_f, and N^3 coefficients are well reproduced.

Finally, for the (unpolarized) Bjorken sum rule the exact result is

$$b\rho_2(\tilde{U}) = -0.0139N_f^3 + (0.568N + 0.0432\frac{1}{N})N_f^2$$

$$+(-3.50N^2 + 0.342 + 0.0128\frac{1}{N^2})N_f \qquad (4.75)$$
$$+(4.38N^3 - .572N - 0.0704\frac{1}{N}) \ ,$$

which is to be compared with

$$\begin{aligned} b^3\rho_2^{(2)}(\check{U}) &= 0.375b^3 \\ &= -0.0139N_f^3 + 0.229NN_f^2 - 1.26N^2N_f + 2.31N^3 \ , \end{aligned} \qquad (4.76)$$

In this case we find that the the NN_f^2, N^2N_f, and N^3 coefficients are not well reproduced by the leading-b expansion.

For two of the three cases in the large-N limit (N_f=0) the RS-invariant ρ_2 is approximated to better than 10% accuracy. The 20% level agreement of the sub-leading coefficients does not, unfortunately, guarantee that the overall RS-invariant is reproduced to the same accuracy for all N, N_f since there are large numerical cancellations. For instance for N=3 and N_f=5 one has $\rho_2(\hat{D})$=-2.98 (exact), whereas $b^2\rho_2^{(2)}(\hat{D})$=9.64.

4.3.2 The Borel resummation of the EC beta-function

Approximating the unknown RS-invariant EC beta-function coefficients ρ_k ($k = 2, 3, \ldots$) by retaining only the portion involving the highest power of b, $\rho_k^{(L)} \equiv \rho_k^{(k)}b^k$, one can now define the RS-invariant resummation $D^{(L*)}(Q)$. Expanding $D^{(L*)}(Q)$ in the coupling a appropriate to some RS one then obtains

$$D^{(L*)}(Q) \equiv \sum_{k=0}^{\infty} d_k^{(L*)}a^{k+1} \ , \qquad (4.77)$$

where in a general RS $d_k^{(L*)}(d_1, c_2, c_3, \cdots, c_k)$ is obtained by replacing ρ_k in Eq.(4.69) by $\rho_k^{(L)}$, so that

$$\begin{aligned} d_0^{(L*)} &= 1 \\ d_1^{(L*)} &= d_1 \\ d_2^{(L*)}(d_1, c_2) &= d_1^2 + cd_1 + (\rho_2^{(L)} - c_2) \\ d_3^{(L*)}(d_1, c_2, c_3) &= d_1^3 + \frac{5}{2}cd_1^2 + (3\rho_2^{(L)} - 2c_2)d_1 + \frac{1}{2}(\rho_3^{(L)} - c_3) \\ &\vdots \qquad \vdots \end{aligned} \qquad (4.78)$$

Notice that, unlike the strict 'leading-b' approximation of Eq.(4.28), the NLO coefficient d_1 is now included exactly. If an exact NNLO calculation exists then the exact ρ_2 can

be used and ρ_3,ρ_4,$\cdots$ approximated by $\rho_3^{(L)}$,$\rho_4^{(L)}$,$\cdots$, so that d_2 (in any RS) is included exactly. The approximated $d_3^{(L*)}$ and higher coefficients may be obtained in any RS from the approximated $\rho_k^{(L)}$ invariants using the exact QCD RG. In this approach the maximum available exact information is included in the all-orders sum, Eq.(4.77), in a formally RS-invariant manner.

It can further be seen that the dependence of the gauge ξ_q is also avoided. The RS-invariants constructed from the $\hat{d}_n(\xi_q)$ of Eq.(4.7) are ξ_q-independent. For instance,

$$\begin{aligned} \rho_2^{(L)} &= d_2^{(L)} - (d_1^{(L)})^2 \\ &= \hat{d}_2(\xi_q) - (\hat{d}_1(\xi_q))^2 \, . \end{aligned} \tag{4.79}$$

This follows because the ξ_q dependence can be absorbed into the choice of renormalization scale, since the $\ln(\mu^2/k^2)$ term in Eq.(4.2) is ξ_q-independent.

The next task is to define the all-orders resummation in Eq.(4.77). The improved resummation $D^{(L*)}$ of Eq.(4.77) will correspond to the solution of the EC integrated beta-function equation (2.25)

$$\begin{aligned} \frac{1}{D^{(L*)}} + c \ln \frac{cD^{(L*)}}{1+cD^{(L*)}} &= b \ln \frac{Q}{\Lambda_{\overline{\rm MS}}} - d_1^{\overline{\rm MS}}(\mu = Q) \\ &\quad - \int_0^{D^{(L*)}} {\rm d}x \left[-\frac{1}{\rho^{(L*)}(x)} + \frac{1}{x^2(1+cx)} \right] \end{aligned} \tag{4.80}$$

with $x^2B(x)$=$\rho(x)$ replaced by $\rho^{(L*)}(x)$, where

$$\rho^{(L*)}(x) \equiv x^2(1 + cx + \rho_2 x^2 + \sum_{k=3}^{\infty} \rho_k^{(L)} x^k) \, . \tag{4.81}$$

One has arrived at the definition of the resummed EC beta-function. For the observables to which we shall apply the resummation exact NNLO results exist and so we have included the exact ρ_2, rather than $\rho_2^{(L)}$, so that $d_2^{(L*)} = d_2$. Taking $d_3^{(L*)}$, for example, we find this differs from the exact d_3 only in the unknown ρ_3 term (we remind the reader that $c_3^{\overline{\rm MS}}$ has now been computed [49]), the known ρ_2 has been exactly included.

We can define $\rho^{(L*)}$ using the principal value (PV) regulated Borel sum results for $D^{(L)}(a)$ of Eq.(4.37) [76]

$$D^{(L)}(a) = {\rm PV} \int_0^{\infty} {\rm d}z \, {\rm e}^{-z/a} B[D^{(L)}](z) \, , \tag{4.82}$$

where $B[D^{(L)}](z)$ denotes the Borel transform which as discussed in Section 4.2.2 contains an infinite set of poles at z=z_l=$\frac{2l}{b}$ (l=$1,2,3,\cdots$) corresponding to infra-red renormalons (IR$_l$), and at z=$-z_l$ corresponding to ultra-violet renormalons (UV$_l$).

It finally remains to perform the resummation $\rho^{(L*)}$ by utilizing the explicit expressions for five observables $\tilde{D}^{(L)}(F)$, $\tilde{R}_\tau^{(L)}(F)$, $\tilde{R}_\tau^{(L)}(F)$ $\tilde{K}^{(L)}(F)$, and $\tilde{U}^{(L)}(F)$ which were given in closed form in terms of exponential integral functions in Section 4.2.2. Defining

$$\rho^{(L)}(x) \equiv x^2(1 + \sum_{k=2}^{\infty} \rho_k^{(L)} x^k) \,, \tag{4.83}$$

and using the chain rule, Eq.(2.28), to relate beta-function in the EC scheme to that in a general RS, one has at the leading-b level, $\beta(a)=a^2$,

$$\rho^{(L)}(x) = \left(a^{(L)}(x)\right)^2 \frac{\mathrm{d}D^{(L)}(a)}{\mathrm{d}a}\bigg|_{a=a^{(L)}(x)} \tag{4.84}$$

where $a^{(L)}(x)$ is the inverse function to $D^{(L)}(a)$, i.e. $D^{(L)}(a^{(L)}(x))=x$. $\rho^{(L)}(x)$ can then be straightforwardly obtained from the corresponding $D^{(L)}(F)$ expressions of [76] for the various observables. The first step is to numerically solve for a given x

$$D^{(L)}(F(x)) = x \,, \tag{4.85}$$

to obtain $F(x)$. Recalling that $F \equiv \frac{1}{a}$ one can then determine from Eq.(4.84)

$$\rho^{(L)}(x) = -\frac{\mathrm{d}}{\mathrm{d}F} D^{(L)}(F)\bigg|_{F=F(x)} \tag{4.86}$$

by differentiating the explicit $D^{(L)}(F)$ expressions in terms of Ei functions. Finally on comparing Eq.(4.81) and Eq.(4.83) one has

$$\rho^{(L*)}(x) = \rho^{(L)}(x) + cx^3 + \rho_2^{(NL)} x^4 \,, \tag{4.87}$$

where $\rho_2^{(NL)} \equiv \rho_2 - \rho_2^{(L)}$. The improved RS-invariant resummation $D^{(L*)}(Q)$ can then be obtained as the solution of the integrated beta-function equation (4.80).

Given the known exact NLO perturbative coefficient $d_1^{\overline{\mathrm{MS}}}(\mu = Q)$ and a value for $\Lambda_{\overline{\mathrm{MS}}}$, $\rho^{(L*)}(x)$ can then be inserted in Eq.(4.80) and the integral performed numerically. On solving the transcendental equation the RS-invariant resummation $D = D^{(L*)}(Q)$ can be evaluated. Conversely given $D=D^{(L*)}=D_{data}$, from the experimental measurement of the observable, one can solve Eq.(4.80) for $\Lambda_{\overline{\mathrm{MS}}}$. By varying Q, with $\Lambda_{\overline{\mathrm{MS}}}^{(N_f)}$ and $d_1^{\overline{\mathrm{MS}}}(\mu = Q)$ evaluated with the number of active quark flavours, N_f, changing across quark thresholds, one can study the Q-dependence of $D^{(L*)}(Q)$. The resummed result $D^{(L*)}$ can also be compared with N$^{\mathrm{n}}$LO fixed-order perturbative results. We return to discuss the method we will use to do this in Section 4.3.4.

4.3.3 Numerical evaluation of the resummation $D^{(L*)}$

Before proceeding to consider the the results of evaluating these RS-invariant leading-b resummations, we would like to remark on their ease of evaluation.

The expressions for $\tilde{D}^{(L)}$ (Eq.(4.40,4.41), $\tilde{R}^{(L)}$ Eq.(4.44,4.45), and $\tilde{R}_\tau^{(L)}$ Eq.(4.49,4.50), respectively, contain infinite summations over the contributions for the UV_ℓ and IR_ℓ singularities. However, successive terms in the sums are strongly damped, with the result that, in order to obtain the four significant figure accuracy of the resummed results, it is only necessary to retain terms up to and including $\ell \simeq 10$ in each sum. Note that to ensure the constant term in the numerator polynomial for UV_ℓ exactly cancels that for $\mathrm{IR}_{\ell+2}$, we must make use of the relation $A_0(\ell)=-B_0(\ell+2)$. Hence if we truncate the summation over the contributions for the UV_ℓ singularities at order ℓ, we, correspondingly, truncate the summation over the contributions for the IR_ℓ singularities at order $\ell+2$. For all observables the computing time is then dominated by that required for the solution of Eq.(4.85). We used the symbolic algebra software MAPLE to numerically solve the transcendental integral equation Eq.(4.85).

There is a further complication to the solution of Eq.(4.85). It was noted in Section 4.2.3 that all five observables have a maximum value, D_{max} say, when plotted versus F (or a). As a result for some values of $D^{(L)}(F)$ there are two corresponding values of F. When solving Eq.(4.85) it is therefore necessary to select one of the two possible values. Imposing asymptotic freedom, $D(F(Q)) \to 0$ for $Q \to \infty$, we choose that solution which is connected to $F = \infty$ ($a = 0$) as $Q \to \infty$. It is therefore necessary to constrain the domain of F over which one solves Eq.(4.85). An immediate consequence of a maximum value for $\tilde{D}^{(L)}(F)$ is that we cannot reconstruct our observable $D^{(L*)}$ for $D > D_{max}$. We consider the consequences of this problem further in Section 4.5.3.

To numerically reconstruct the function $\rho^{(L)}(x)$ by inversion of $D^{(L)}$ we use Eq.(4.86). The closed form expressions for the five observables $\tilde{D}^{(L)}(F)$, $\tilde{K}^{(L)}(F)$, $\tilde{U}^{(L)}(F)$, $\tilde{R}^{(L)}(F)$ and $\tilde{R}_\tau^{(L)}(F)$ allow one to exactly perform the differentiation. Performing the resummation to obtain $\rho^{(L*)}(x)$ to 4 significant figures using the symbolic algebra software MAPLE on a HEWLETT-PACKARD 712/80 took between 1/2 hour, for $\tilde{U}^{(L)}$, and 6 hours, for $\tilde{R}_\tau^{(L)}$.

Once $\rho^{(L*)}(x)$ has been numerically determined over the full range, one can insert each $\rho^{(L*)}(x_i)$ ($i = 1 \ldots n$) data point into the the integrand of in Eq.(4.80), denoted $\Delta\rho_0(x)$ in Eq.(2.66). A polynomial interpolation algorithm is used to fit the resulting data points.

Integrating the fit polynomial we obtain a polynomial expression for $\Delta\rho_0(D^{(L*)})$.

We may compare our numerical reconstruction of $\Delta\rho_0(D^{(L*)})$ with the asymptotic ($Q \to \infty$) form of $\Delta\rho_0$. This may be found by expanding the integrand in Eq.(2.66) as a power series in x and integrating term-by-term. We obtain

$$\Delta\rho_0(Q) = \rho_2 D + (\rho_3 - 2\rho_2 c)\frac{D^2}{2} + (\rho_4 - 2c\rho_3 + 2c^2\rho_2 + 2c^2 - {\rho_2}^2)\frac{D^3}{3} + \dots . \quad (4.88)$$

For $D^{(L*)} \to 0$ corresponding to $Q \to \infty$ our numerical reconstruction of $\Delta\rho_0(D^{(L*)})$ agrees with the asymptotic form in Eq.(4.88). Given a NLO coefficient $d_1^{\overline{\rm MS}}$, a value for $\Lambda_{\overline{\rm MS}}$, and an initial trial value for D, an iterative procedure evaluates the RS-invariant resummation $D^{(L*)}$.

4.3.4 Evaluating the fixed-order approximants $D^{(L*)(n)}$

The resummed result $D^{(L*)}$ can be compared with the NLO, NNLO, N^{3}LO,...,N^{n}LO,... fixed-order perturbative approximations to assess the accuracy of the fixed-order results. We define the n^{th} order truncations of Eq.(4.77)

$$D^{(L*)(n)} \equiv \sum_{k=0}^{n} d_k^{(L*)} a^{k+1} . \quad (4.89)$$

Since d_1 and d_2 are exactly included in any RS one has $D^{(L*)(1)}=D^{(1)}$, $D^{(L*)(2)}=D^{(2)}$, with $D^{(1)}$, $D^{(2)}$ denoting the exact NLO and NNLO results.

We shall choose to consider fixed-order approximants in the EC scheme. Correspondingly we need to define the truncations of $\rho^{(L*)(n)}(x)$; we define

$$\rho^{(L*)(n)}(x) \equiv x^2(1 + cx + \rho_2 x^2 + \sum_{k=3}^{n} \rho_k^{(L)} x^k) . \quad (4.90)$$

The N^{n}LO fixed-order perturbative result $D^{(L*)(n)}(EC)$ of Eq.(4.89) will correspond to solution of Eq.(4.80) with $\rho^{(L*)}(x)$ replaced by $\rho^{(L*)(n)}(x)$.

To evaluate Eq.(4.90) at order n we need to calculate $\rho_k^{(L)}$ for $k = 3 \cdots n$. In Section 2.2.3 we expanded out Eq.(2.28) and compared coefficients of a to calculate the first few ρ_k. This method, however, proves to be rather cumbersome for higher order ρ_k. A more efficient method by which to obtain ρ_k is by reversion of power series.

Consider a power series, $D(a)$, which starts at $O(a)$

$$D(a) = d_0 a + d_1 a^2 + \cdots + d_k a^{k+1} + \cdots , \tag{4.91}$$

then its inverse or reversed series, $a(D)$, is defined by

$$a(D) = K_1 D + K_2 D^2 + K_3 D^3 + \cdots + K_k D^k + \cdots \tag{4.92}$$

The reversion coefficients, K_i, are multinomials in the d_i. A brute force approach to determine K_i is to simply substitute Eq.(4.91) into Eq.(4.92) and equate coefficients. However, there is a more elegant and powerful method; using the calculus of residues it is possible to show that [89]

$$K_n = \frac{1}{n!}\left[\frac{\mathrm{d}^{n-1}}{\mathrm{d}t^{n-1}}\left(\frac{t}{D(t)}\right)\right]_{t=0} . \tag{4.93}$$

For a derivation of Eq.(4.93) and the explicit form of the first six coefficients, K_n, see Appendix B.1.

We now rewrite Eq.(2.28) in the form

$$\rho(D) = \frac{\beta(a(D))}{\mathrm{d}a(D)/\mathrm{d}D} , \tag{4.94}$$

This may now be expanded as a power series in D. Equating powers of D one can express ρ_i in terms of the reversion coefficients K_i. Note the K_i are scheme dependent. Using Eq.(4.93) with $d_0 = K_1 \equiv 1$ we can evaluate ρ_i in terms of c and d_k $(k = 1 \cdots i)$. Substituting the complete beta-function in Eq.(4.94) one can calculate the exact expressions for ρ_k. The first six are listed in Appendix B.2.

For Eq.(4.90), however, we only require $\rho_i^{(i)}$, so one truncates the beta-function at leading-b level, $\beta(a) = -a^2$. To numerically evaluate the resulting expressions for $\rho_i^{(i)}$ we use our knowledge of $d_k^{(k)}$ the leading-b part of the perturbative coefficients. For the Euclidean observables, $\tilde{D}$, $\tilde{K}$ and $\tilde{U}$, we use Eq.(4.6), Eq.(4.53) and Eq.(4.59), respectively. For the Minkowski quantities R and $\check{R}_\tau$ we express $r_n^{(n)}$ and $r_{\tau\, n}^{(n)}$ in terms of $d_n^{(n)}$ by using Eq.(4.42) and Eq.(4.47), respectively. It is then straightforward to show (assuming the V-scheme)

$$r_n^{(n)} = n! \sum_{k=0}^{Int(\frac{n}{2})} (-1)^k \frac{(\pi/2)^{2k}}{(2k+1)!} \frac{d_{n-2k}^{(n-2k)}}{(n-2k)!} \tag{4.95}$$

and

$$r_{\tau\, n}^{(n)} = n! \sum_{i=0}^{n} \left(2\left(\frac{1}{2}\right)^{n-i} - 2\left(\frac{1}{6}\right)^{n-i} + \left(\frac{1}{8}\right)^{n-i}\right) \sum_{k=0}^{Int(\frac{i}{2})} (-1)^k \frac{(\pi/2)^{2k}}{(2k+1)!} \frac{d_{i-2k}^{(i-2k)}}{(i-2k)!} , \tag{4.96}$$

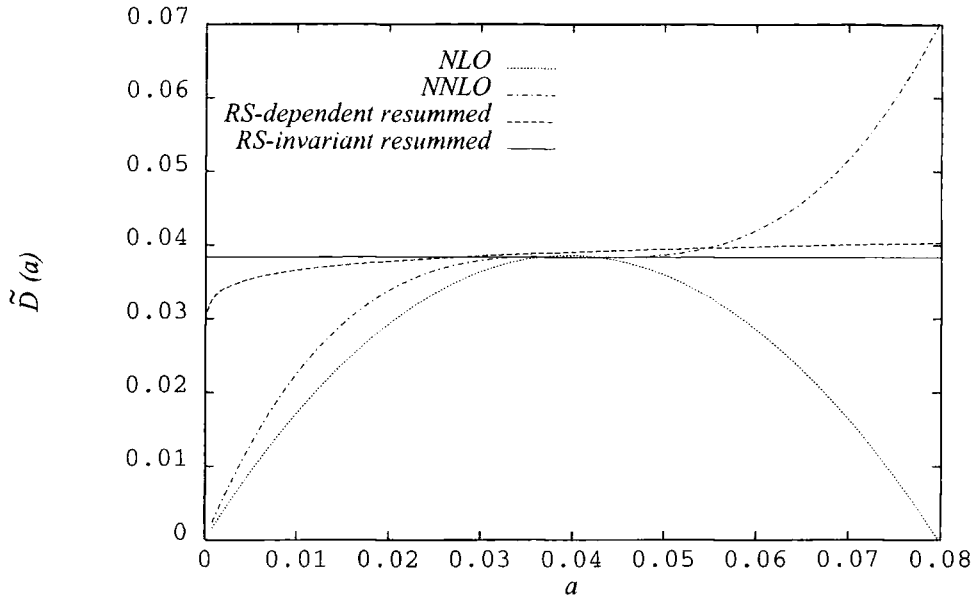

Figure 4.2(a): NLO and NNLO fixed-order perturbation theory, the naive RS-dependent leading-b resummation, and RS-invariant leading-b resummation, for $\tilde{D}$ at $Q = 91$ GeV plotted against 'a'; $c_2 = 0$ has been assumed.

where $d_k^{(k)}$ was defined in Eq.(4.6). On substituting these leading-b perturbative approximations into the expressions derived from Eq.(4.94), with one-loop beta-function, we can evaluate ρ_k^k. Implementing this procedure using MAPLE on a Hewlett-Packard 712/80 it took 3 hours to calculate $\rho_{24}^{(L)}$. The numerical values of $\rho_n^{(L)}$ $(n = 2 \cdots 12)$ for each observable are tabulated in Appendix B.3.

It should be noted that both MAPLE and MATHEMATICA have library functions to obtain the reversed series (and hence reversion coefficients) to arbitrary order. It was found, however, that while this was effective at lower orders ($n < 10$), the procedure detailed above was more computationally efficient to obtain higher-order ρ_k.

4.4 Numerical results

4.4.1 Comparison of FOPT with leading-b resummations

In Figure 4.2(a) we have plotted as the dashed curve the leading-b resummation $\check{D}^{(L)}(a)$ versus the coupling 'a' for the Adler D-function with Q=91 GeV, the t'Hooft scheme corresponding to $B(x)$=1+cx, and minimal subtraction have been assumed with $\Lambda_{\overline{\rm MS}}^{(5)}$=200

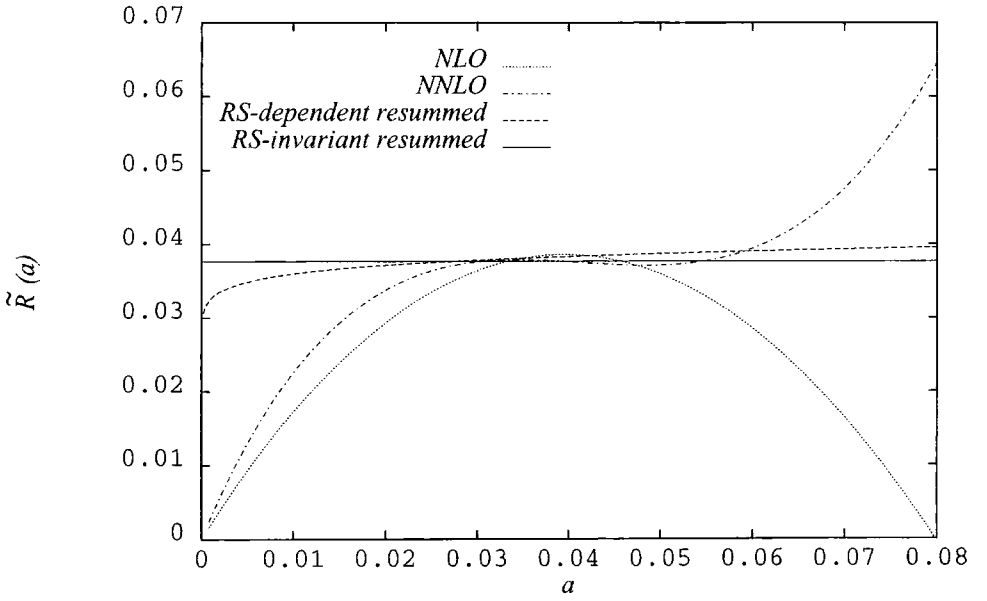

Figure 4.2(b): As for Figure 4.2(a) but for $\tilde{R}$ at $Q = 91$ GeV.

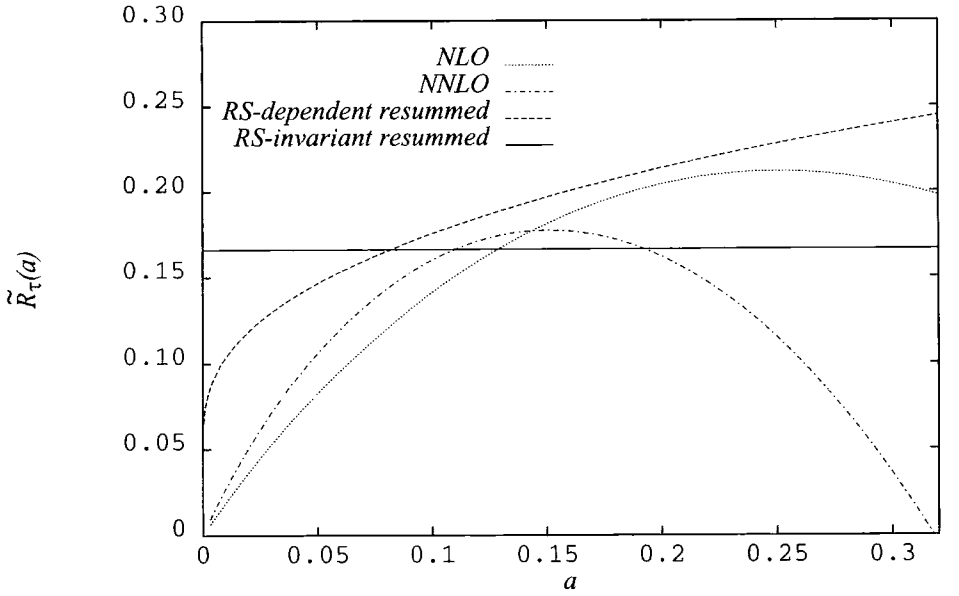

Figure 4.2(c): As for Figure 4.2(a) but for $\tilde{R}_\tau$ at $Q = 1.78$ GeV.

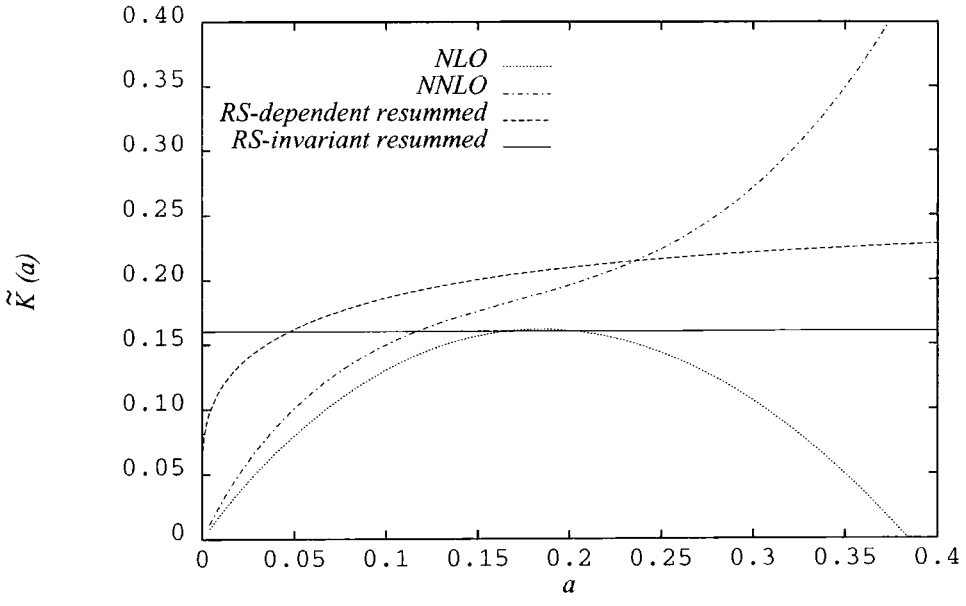

Figure 4.2(d): As for Figure 4.2(a) but for $\tilde{K}$ at $Q = 1.5$ GeV.

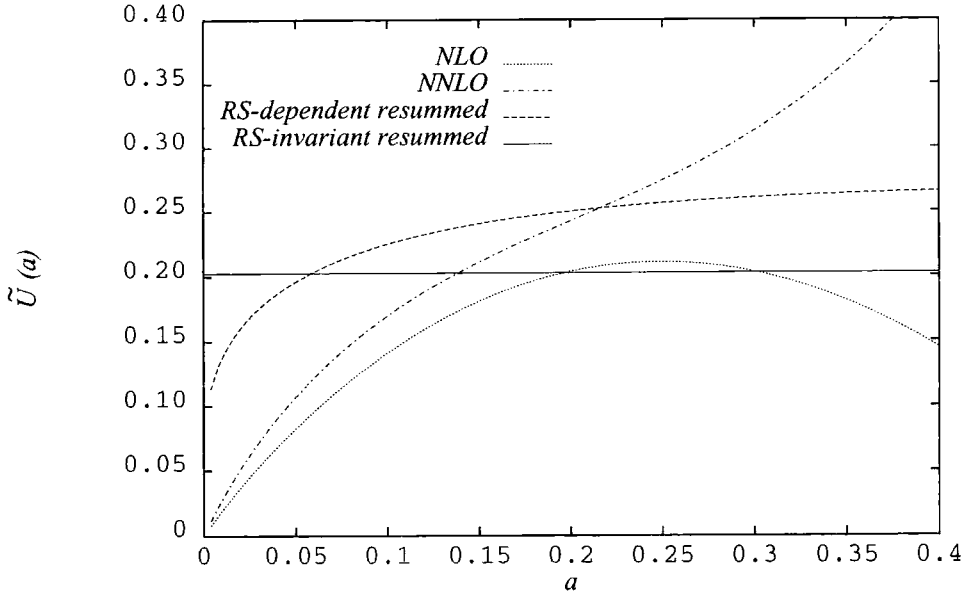

Figure 4.2(e): As for Figure 4.2(a) but for $\tilde{U}$ at $Q = 1.5$ GeV.

MeV. There is a monotonic RS-dependence as discussed in Section 5.3.3 and reference [76]. Noting that τ is related to 'a' using Eq.(2.25) one can use 'a' to label the exact NLO and NNLO approximants, $\tilde{D}^{(1)}(a)$, $\tilde{D}^{(2)}(a, c_2)$. The dotted line shows $\tilde{D}^{(1)}(a)$, and the dashed-dotted line gives $\tilde{D}^{(2)}(a, 0)$. We have chosen c_2=0 to avoid adding an extra axis to the plot. The solid line gives the RS-invariant resummation $\tilde{D}^{(L*)}$. Figure 4.2(b) gives the analogous plot for the e^+e^- R-ratio with Q=91 GeV.

We note that the fixed-order results agree best with the $\tilde{D}^{(L*)}$ and $\tilde{R}^{(L*)}$ resummations in the vicinity of the stationary points with respect to variation of the RS. This is to be anticipated since the Principal of Minimum Sensitivity (PMS) [37] choice of RS avoids the inclusion of potentially large UV logarithms connected with the choice of renormalization scale [38]. A similar statement holds for the NLO and NNLO results in the EC scheme [38], $\tilde{R}^{(1)}(EC)$ and $\tilde{R}^{(2)}(EC)$, corresponding to solutions of Eq.(4.80) with $\rho^{(L*)(n)}$ as in Eq.(4.90). These are numerically very close to the PMS approximants. The 'optimized' PMS/EC fixed-order NNLO approximant is thus seen to be very close to to the RS-invariant resummed result for the R-ratio at LEP energy, indicating that the approximated effect of including N^{3}LO and higher corrections is small, and thus suggesting that one can in principle accurately determine $\Lambda^{(5)}_{\overline{\rm MS}}$ given ideal data.

In Figures 4.2(c), 4.2(d) and 4.2(e) the analogous plots for the $\tilde{R}_\tau$, (Q=m_τ=1.777 GeV) and DIS sum rules $\tilde{K}, \tilde{U}$ (Q=1.5 GeV), have been given. $\Lambda^{(3)}_{\overline{\rm MS}}$=320 MeV has been assumed. In contrast to Figure 4.2(a) and 4.2(b) the differences between the fixed-order results and the RS-invariant resummations are clearly much larger. Thus at these lower values of Q the significance of N^{3}LO and higher effects is apparently much greater, and the reliability with which $\Lambda^{(3)}_{\overline{\rm MS}}$ can be determined correspondingly less. We shall quantify this more carefully in just a moment.

4.4.2 The reliability of FOPT

Adler D-function

In Figure 4.3(a) we plot, for the Adler D-function at Q=91 GeV, the fixed-order perturbative results $\tilde{D}^{(L*)(n)}(EC)$ (Eq.(4.89)) for n=2 (NNLO) and higher orders (crosses) compared with the RS-invariant resummed result $\tilde{D}^{(L*)}$ (dashed line). $\Lambda^{(5)}_{\overline{\rm MS}}$=200 MeV has again been assumed. We could of course have chosen to plot the fixed-order approximants in any RS, for instance $\overline{\rm MS}$ with μ=Q, but as discussed in connection with Figure 4.1(a), we expect the 'optimized', EC or PMS, choice of RS to approach the resummed

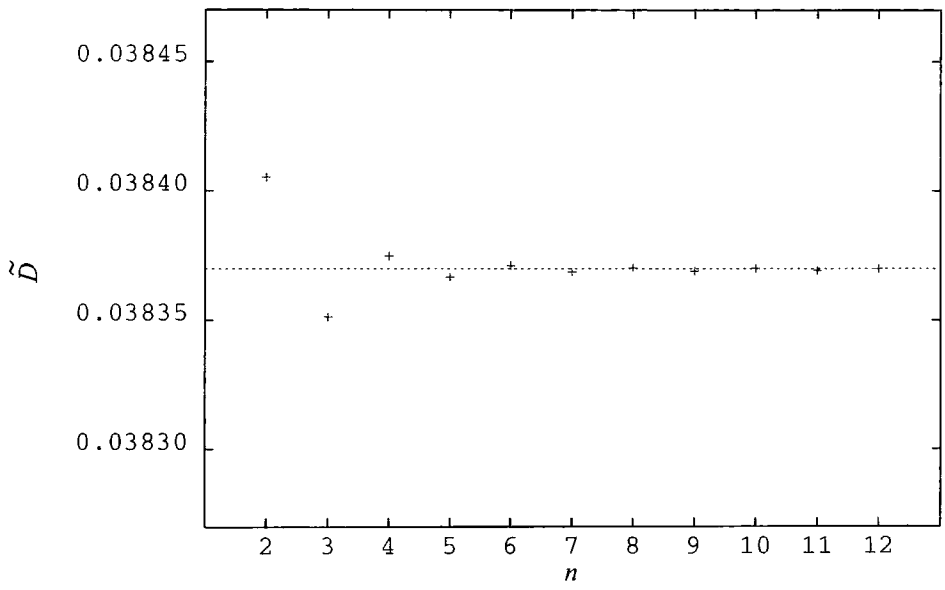

Figure 4.3(a): Comparison of fixed-order EC perturbation theory (denoted "+") with the RS-invariant resummation (dashed line) for $\tilde{D}$ at $Q = 91$ GeV.

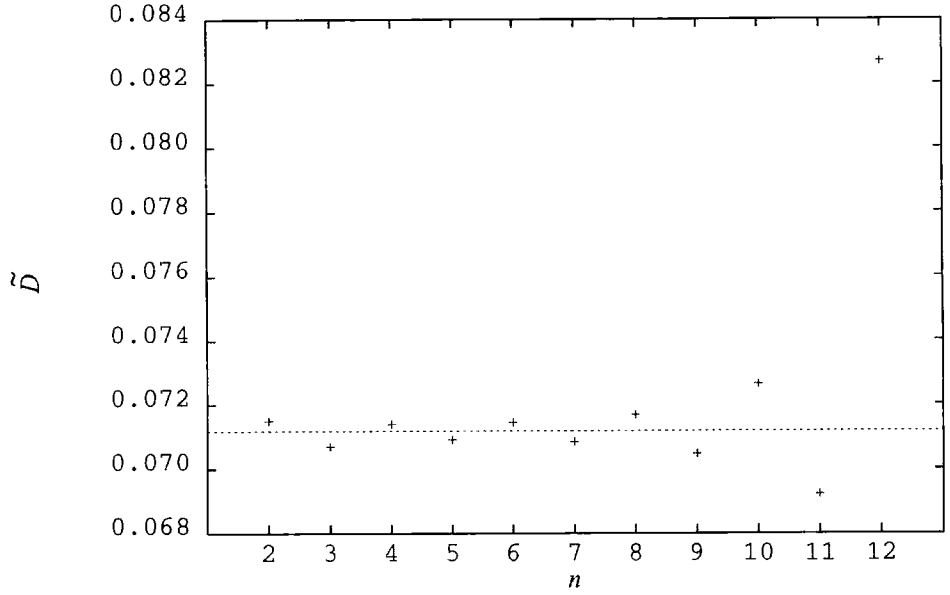

Figure 4.3(b): As for Figure 4.3(a) except at $Q = 5$ GeV.

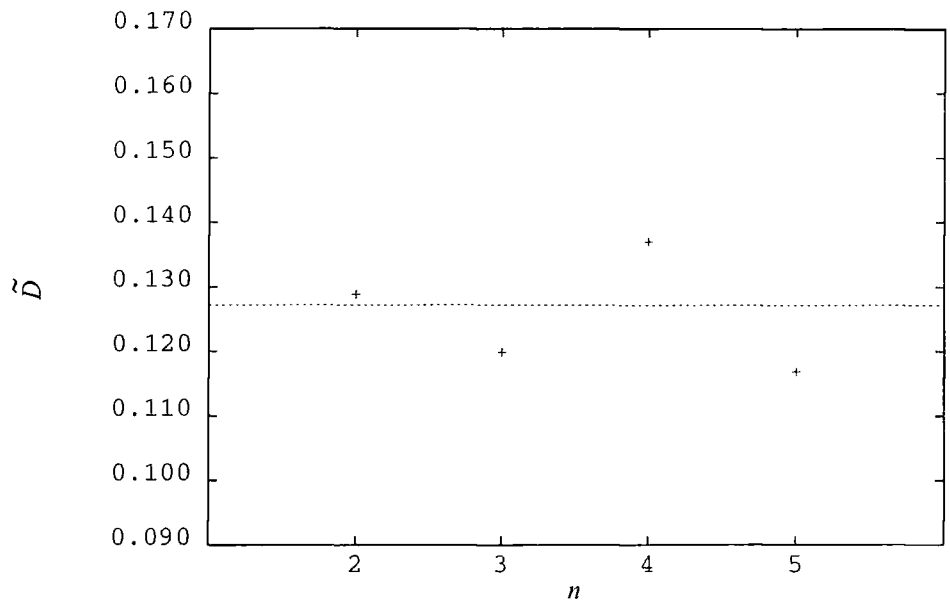

Figure 4.3(c): As for Figure 4.3(a) except at $Q = 1.5$ GeV.

result more rapidly. We stress that the fixed-order $\tilde{D}^{(L*)(n)}(EC)$ approximants correspond to the solutions of Eq.(4.80) with $\rho(x) = \rho^{(L*)(n)}(x)$. Since ρ_2 is included exactly $\tilde{D}^{(L*)(2)}(EC)$=$\tilde{D}^{(2)}(EC)$. As can be seen from Figure 4.2(a) the N^{7}LO and higher results are indistinguishable from the resummed result with the chosen scale.

In Figure 4.3(b) we show a similar plot for $\tilde{D}$ at Q=5 GeV. $\Lambda^{(4)}_{\overline{\rm MS}}$=279 MeV has been assumed. We see that the fixed-order approximants are always distinguishable from the resummed result and the approach is less rapid. The oscillation of successive fixed-order approximants above and below the resummed result is explained by the dominance of the UV$_1$ singularity at z=$-\frac{2}{b}$ in the Borel plane, which is the closest to the origin for the D-function. As mentioned in Section 4.2.2 this is a double pole in the leading-b approximation. This singularity is responsible for alternating sign factorial growth of the perturbative coefficients. In Table B.2 of Appendix B we tabulate the numerical values of $\rho_k^{(L)}$. The alternating sign factorial growth in the $\rho_k^{(L)}$ is immediately apparent, and is responsible for the pattern shown in the Figures 4.2(a)-(c). Beyond order n=9 the amplitude of the oscillations increases dramatically, and the fixed-order approximants diverge increasingly from the resummation; full breakdown occurs for $n \geq 12$. This is precisely what one would expect to see on comparing the Borel sum of an alternating sign asymptotic series with its truncations. We note that a similar oscillating behaviour with

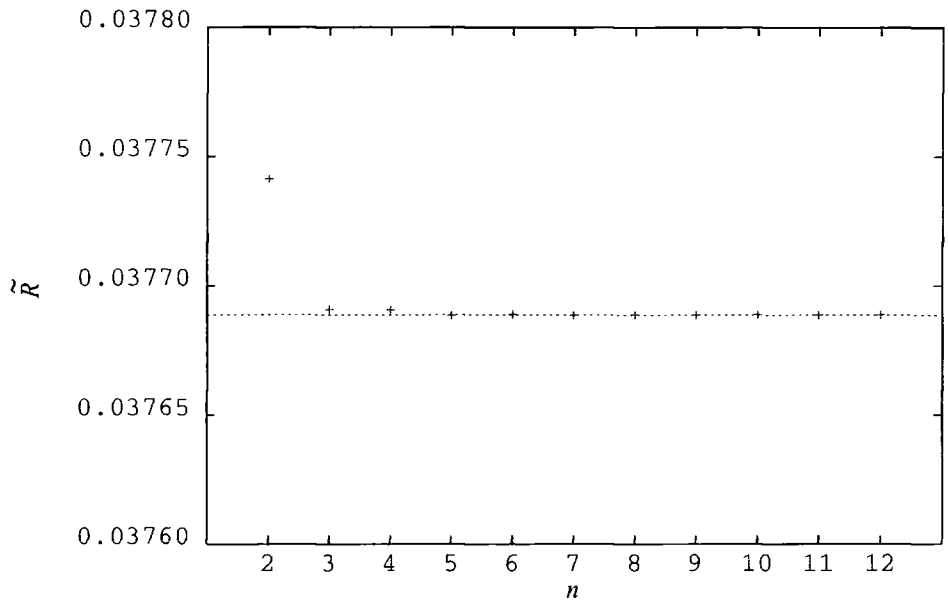

Figure 4.4(a): Comparison of fixed-order EC perturbation theory (denoted "+") with the RS-invariant resummation (dashed line) for $\tilde{R}$ at $Q = 91$ GeV.

eventual wild oscillations setting in would also have been apparent in Figure 4.2(a) had we used a finer vertical scale. Naively from the large-order behaviour in Eq.(4.34) one would not expect the wild oscillations to set in until $n > 50$.

Figure 4.3(c) finally shows the corresponding plot for $\tilde{D}$ at Q=1.5 GeV, with $\Lambda^{(3)}_{\overline{\rm MS}}$ as above. The fixed-order start to diverge away from resummed result immediately with wild oscillations for $n > 5$. Nonetheless even at this low energy fixed-order perturbation theory (in particular NNLO) is approximating the resummed results, though not particularly well.

e^+e^- R-ratio

In Figures 4.4(a)-4.4(c) we give the analogous plots for the e^+e^- R-ratio, plotted on the same vertical scales for direct comparison. As can be seen from Figure 4.4(a) at $Q = 91$ GeV the N^{4}LO and higher fixed-order results are indistinguishable from the resummed result with the chosen vertical scale, and there is only a small shift between the NNLO and resummed results. Evidently fixed-order perturbation theory in the EC scheme seems to be working very well for the R-ratio at LEP/SLD energies.

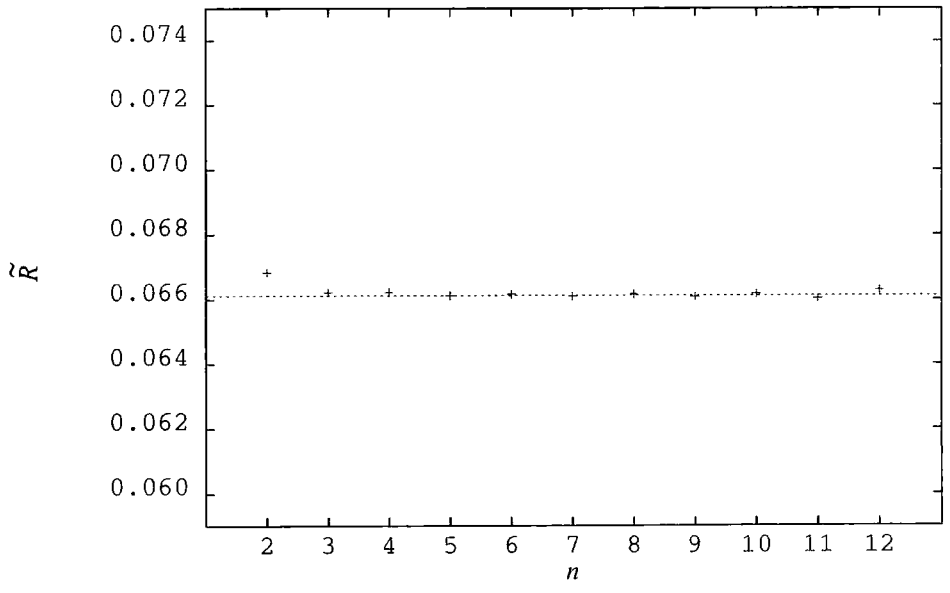

Figure 4.4(b): As for Figure 4.4(a) except at $Q = 5$ GeV.

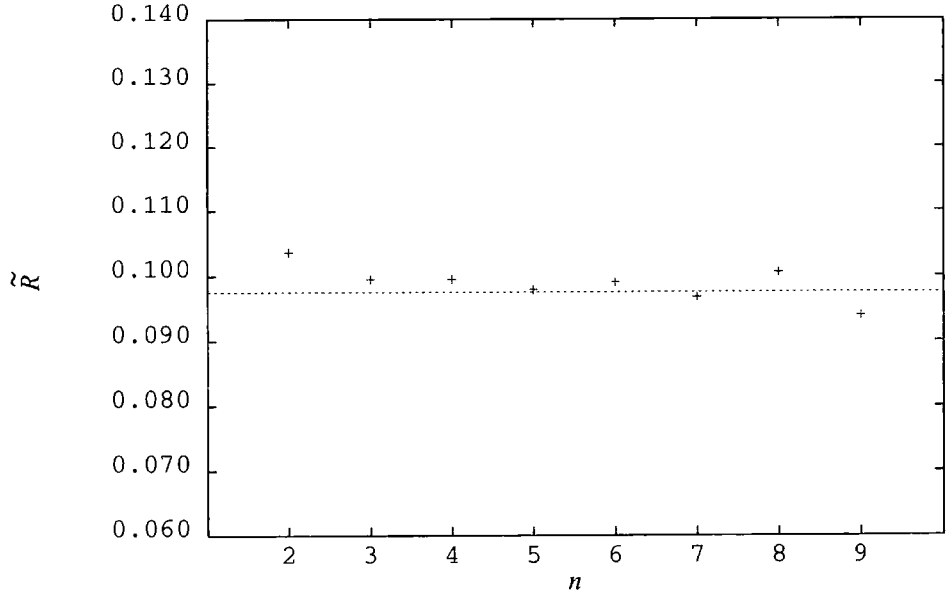

Figure 4.4(c): As for Figure 4.4(a) except at $Q = 1.5$ GeV.

Clearly in Figure 4.4(b), at $Q = 5$ GeV, the approach to the resummed result is somewhat more rapid than for Figure 4.3(b). A similar oscillatory behaviour is also evident for the conventional fixed-order perturbative approximants for $\tilde{R}$, but with much smaller amplitude. Beyond order n=12, however, the amplitude of the oscillations increases dramatically, and the fixed-order approximants diverge increasingly from the resummation.

Figure 4.4(c) shows the plot for $\tilde{R}$ at Q=1.5 GeV. The approach to the resummed result is still slower, and the oscillations have only just become established when they increase wildly beyond n=9. Nonetheless even at this low energy fixed-order perturbation theory is approximating the resummed results, albeit much less well.

The difference in behaviour of $\tilde{R}$ from $\tilde{D}$ derives from the fact that for $\tilde{R}$ the UV_1 singularity is softened to a single pole, again in the leading-b approximation. To see this we note from Eq.(4.42) that since $\sin(\pi bz/2)$ has single zeros $\sim (z - z_\ell)$ at the same positions as the renormalon singularities one finds that renormalon poles of order p in $B[\tilde{D}]$ are converted to poles of order $p-1$ in $B[\tilde{R}]$. This implies that the poles in $B[\tilde{R}]$ are simple poles except for IR_2 which was a simple pole in $B[\tilde{D}]$ and hence apparently vanishes [64]. The absence of the IR_1 singularity at $z = 2/b$ in the exact large-N_f for $B[\tilde{D}](z)$ implies from Eq.(4.42) that $B[\tilde{R}](z)$ must have a compensating zero at this position.

The leading asymptotics of the coefficients r_n will be given by UV_1 for $B[\tilde{R}](z)$. Expanding around $z = -2/b$ we have

$$\frac{\sin(\pi bz/2)}{\pi bz/2} = \left(1 + \frac{bz}{2}\right) + O\left(\left(1 + \frac{bz}{2}\right)^2\right) \tag{4.97}$$

Since the leading-N_f asymptotics are given by [82]

$$d_n^{[n-r]} \sim \frac{n^{p+r-1}}{r!} n! \tag{4.98}$$

where p is the order of the pole in the Borel transform and $r = 0, 1, 2, \ldots$. Hence from Eq.(4.42) we find that the asymptotic behaviour of r_n is given by changing the $p \to p-1$ in the results for Eq.(4.98). This implies that on very general grounds one expects [82, 64].

$$\frac{r_n}{d_n} \approx \frac{1}{n}(1 + O(1/n)) \tag{4.99}$$

so that the r_k coefficients grow more slowly asymptotically. Correspondingly for the RS-invariants quantities ρ_k we have, asymptotically,

$$\rho_n \simeq (n-1) d_n(d_1 = 0) \,, \tag{4.100}$$

where $d_n(d_1 = 0)$ denotes d_n in an RS where $d_1 = 0$. So that one expects

$$\frac{\rho_n^R}{\rho_n^D} \simeq \frac{1}{n} \,. \tag{4.101}$$

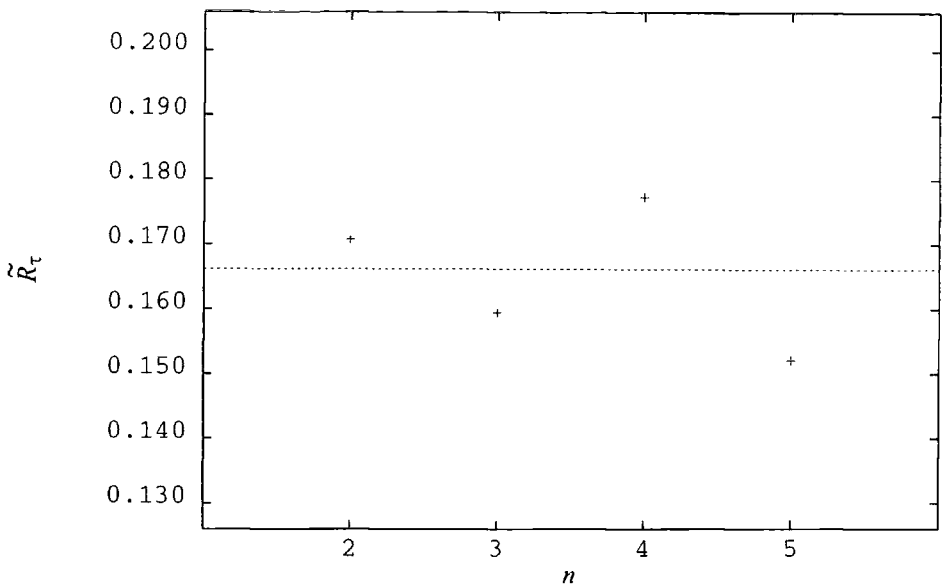

Figure 4.5: Comparison of fixed-order EC perturbation theory (denoted "+") with the RS-invariant resummation (dashed line) for $\tilde{R}_\tau$.

Turning to Table B.3 in Appendix B we tabulate $\rho_n^{(L)R}$. The factorial growth of the ρ_n is seen to be slower than that in Table B.1 for the Adler D function. In fact Eq.(4.101) is predicting the relative sizes at quite low orders ($n \geq 5$). Table B.2 also explains why for $\grave{R}$ the alternating sign behaviour, above and below the resummed result, does not set in immediately as was the case of $\tilde{D}$. The first four ρ_n are all negative.

Hadronic tau-decay ratio R_τ

In Figure 4.5 we show the analogous plot for the hadronic τ-decay ratio, R_τ, plotted on the same vertical scale as Figure 4.3(c). Here evidently $Q = m_\tau = 1.78$ GeV, and the same $\Lambda^{(3)}_{\overline{\rm MS}}$ as above has been assumed. Fixed-order EC perturbation theory is seen to be working reasonably well with oscillating behaviour around the resummed result which becomes wild for $n \geq 5$. Notice, however, that the performance is much worse than that of $\grave{R}$ at the comparable $Q = 1.5$ GeV in Figure 4.4(c). In Table B.4 of Appendix B the tabulated values of $\rho_n^{(L)}$ for $\grave{R}_\tau$ are somewhat larger than for $\tilde{R}$. This inferior performance can be attributed to the presence of double poles at IR_3 and IR_4 in the Borel plane.

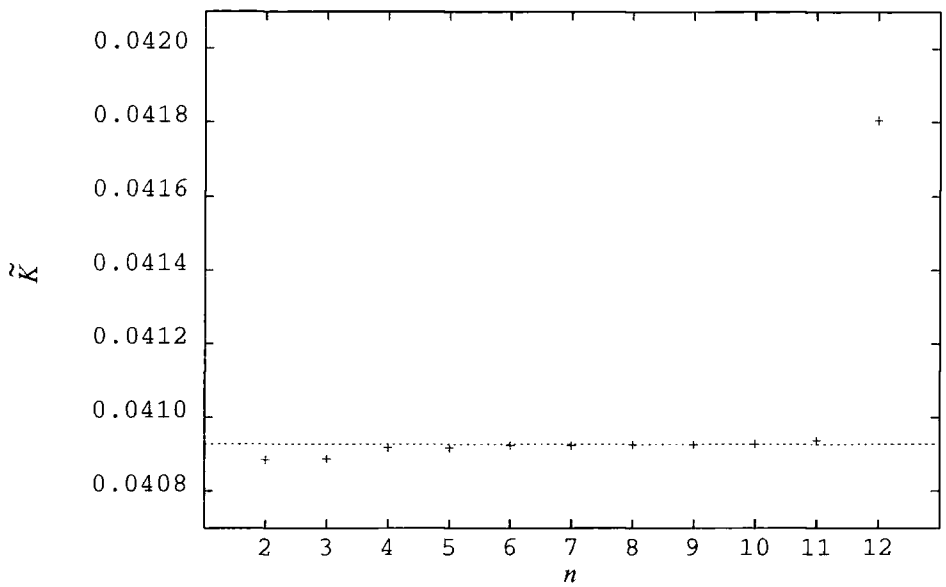

Figure 4.6(a): Comparison of fixed-order EC perturbation theory (denoted "+") with the RS-invariant resummation (dashed line) for $\tilde{K}$ at $Q = 91$ GeV.

The PBjSR and GLSSR

This reasonable performance of fixed-order perturbation theory for $\tilde{D}$ and $\tilde{R}$ is to be contrasted with the situation for the DIS sum rules $\tilde{K}$. Figures 4.6(a), 4.6(b), and 4.6(c) are plotted at the same values of Q as the corresponding Figures for $\tilde{D}$. The vertical scales for Figures 4.6(a) and 4.6(b) are seven and two times coarser than for Figures 4.3(a) and 4.3(b), respectively. In Figure 4.6(a) at Q=91 GeV we see a much slower approach to the resummed result. The fixed-order EC approximations then track the resummed result between sixth and tenth order and then for n=12 there is a dramatic breakdown. The Borel plane singularities nearest the origin for $\tilde{K}$ are now [76] IR_1 at $z=\frac{2}{b}$, and UV_1 at $z=-\frac{2}{b}$. It is the presence of the IR_1 singularity which leads to fixed-sign factorial growth of the perturbative coefficients and a consequent deterioration in the performance of fixed-order perturbation theory. The relative deterioration compared to the R-ratio can be seen even more clearly in Figure 4.6(b) at Q=5 GeV. There is a monotonic increase in successive orders with no tendency to track the resummed result.

The stair-like pattern, with neighbouring odd and even orders roughly similar in low orders, follows from directly from the values of $\rho_n^{(L)}$ tabulated for $\tilde{K}$ in Table B.5. of Appendix B. These values can be attributed to the Borel structure of $\tilde{K}$. In even orders

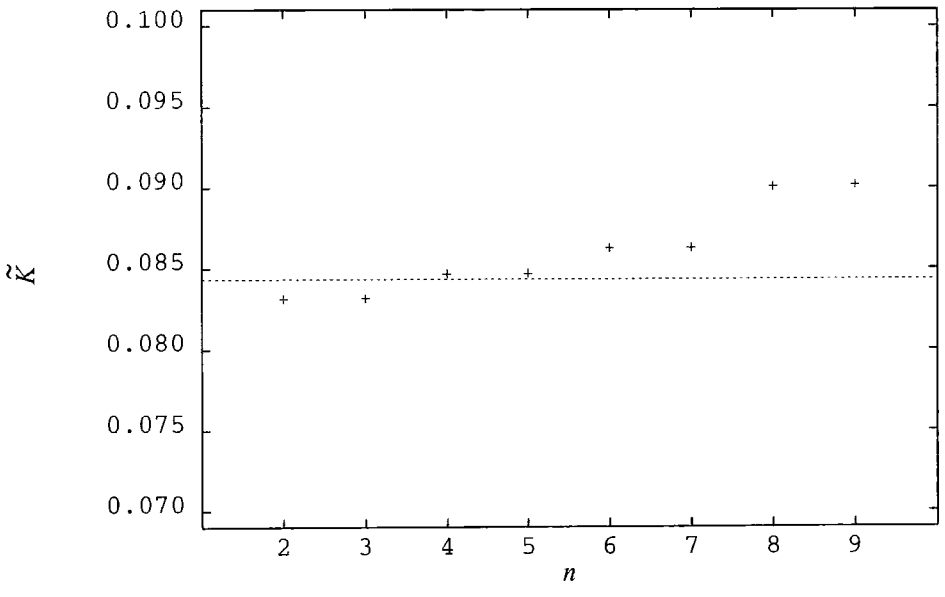

Figure 4.6(b): As for Figure 4.6(a) except at $Q = 5$ GeV.

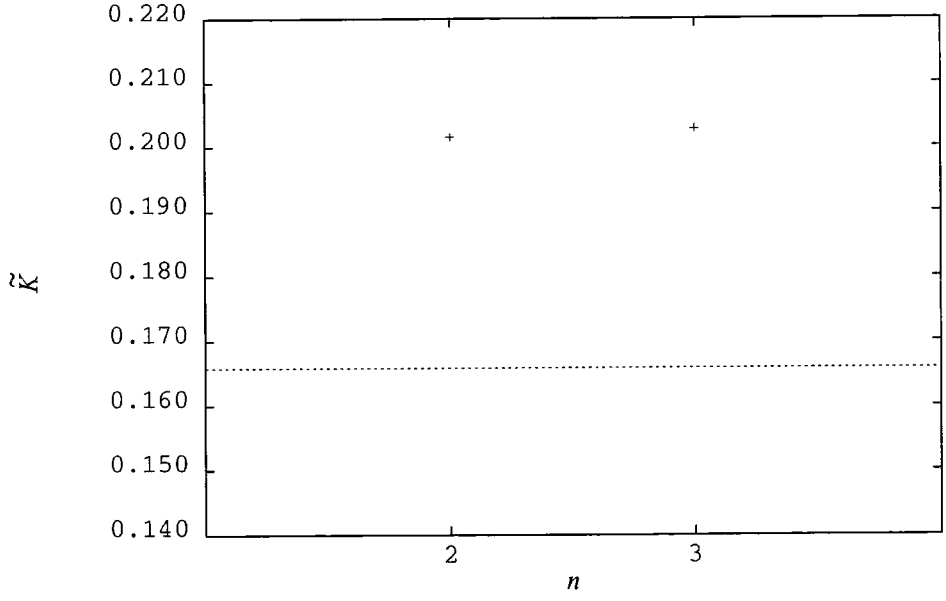

Figure 4.6(c): As for Figure 4.6(a) except at $Q = 1.5$ GeV.

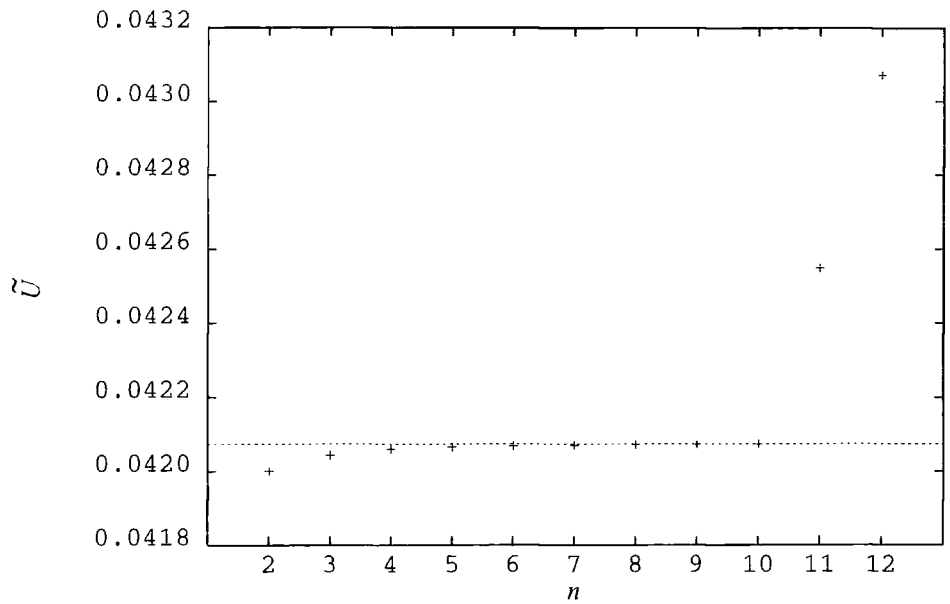

Figure 4.7(a): Comparison of fixed-order EC perturbation theory (denoted "+") with the RS-invariant resummation (dashed line) for $\tilde{U}$ at $Q = 91$ GeV.

the fixed-sign (IR_1) and alternating-sign (UV_1) behaviour constructively add to give a large $\rho_n^{(L)}$. In odd orders there is a partial cancellation between the fixed-sign (IR_1) and alternating-sign (UV_1) behaviour, resulting in a small value for $\rho_n^{(L)}$.

In Figure 4.6(c) we see that at Q=1.5 GeV fixed-order EC perturbation theory is a poor approximation to the resummed result for the DIS sum rules. Only n=2 and n=3 are shown since for $n \geq 4$ fixed-order perturbation theory is not defined in the EC scheme. If $\rho(x)$ has a zero at x=x^* (where $x^* > 0$ is the closest zero to the origin) then Eq. (4.80) has a solution $D = D^*$, with $D^* < x^*$. This will be the case if the expansion coefficients of $\rho(x)$ have alternating factorial behaviour, at least in either odd or even orders. If, however, the coefficients have fixed-sign factorial growth, as is the case for the DIS sum rules, then $\rho(x)$ will have no positive zeros. In this case Eq.(4.80) may fail to have a solution, the condition for this being that in the limit as $D \to +\infty$ the right-hand side of Eq.(4.80) is negative.

BjSR

Finally, in Figures 4.7(a), 4.7(b) and 4.7(c) the unpolarized Bjorken sum rule is plotted at the same values of Q as the corresponding figures for $\tilde{K}$, and on the same vertical scale

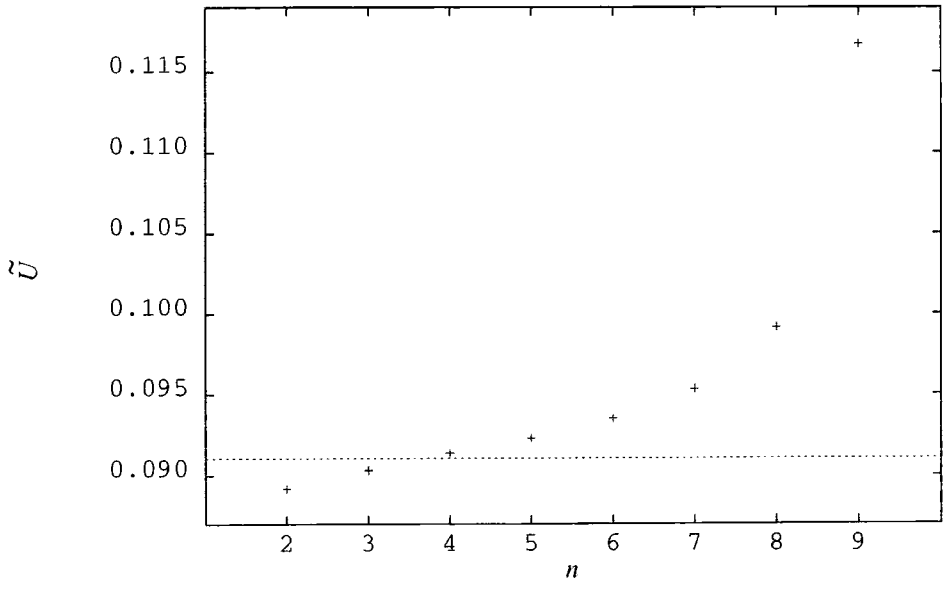

Figure 4.7(b): As for Figure 4.7(a) except at $Q = 5$ GeV.

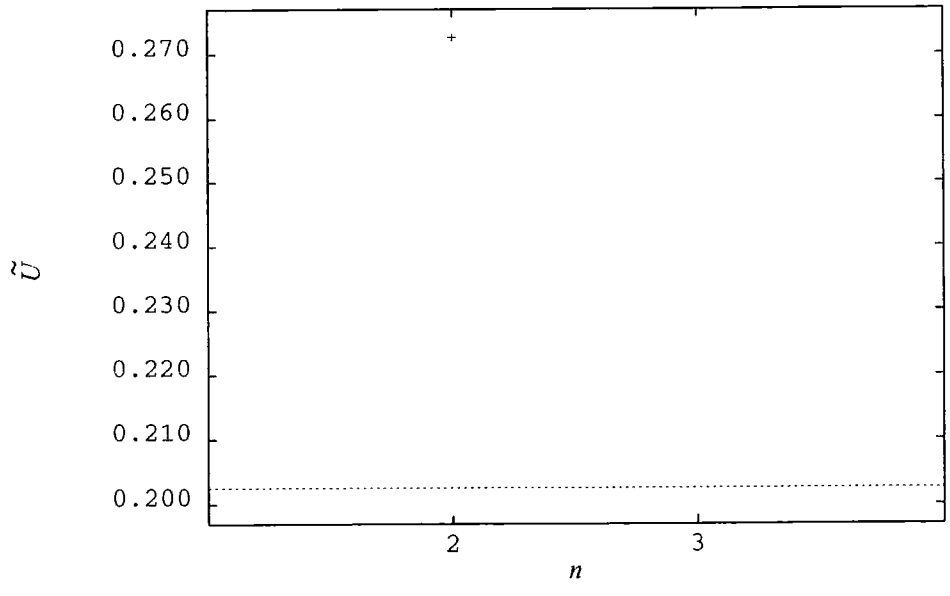

Figure 4.7(c): As for Figure 4.7(a) except at $Q = 1.5$ GeV.

to enable direct comparison. For all three energy scales the performance is inferior to the PBjSR/GLSSR. In particular, we note that at 1.5 GeV the NNLO result is a very poor approximation to the resummed value. This is expected since there is no UV_1 renormalon singularity, resulting in the BjSR being totally dominated by the IR_1 singularity. The absence of a UV_1 singularity also explains the absence of the stair-like pattern observed for the PBjSR/GLSSR. In Table B.6 the tabulated values of $\rho_n^{(L)}$ are given for $\check{U}$. We note that, compared to $\check{K}$, there is only a small cancellation in odd orders — this is due to the UV_2 singularity.

4.4.3 Energy dependence of the resummation and FOPT

We can summarize the behaviour exhibited in the foregoing figures by plotting the energy dependence of $\check{D}$, $\check{R}$, $\check{K}$ and $\check{U}$. Figure 4.8(a) shows $\check{D}^{(L*)}$ (solid line), $\check{D}^{(1)}(EC)$ (dotted line), and $\check{D}^{(2)}(EC)$ (dashed-dotted line), plotted versus $\ln Q/GeV$ over a range equivalent to $Q = 1 - 91$ GeV. Flavour thresholds in Q at $m_b = 4.5$ GeV, $m_c = 1.25$ GeV, have been assumed and values of $\Lambda_{\overline{\rm MS}}^{(N_f)}$ chosen as above. Figure 4.8(b) gives a similar plot for $\check{R}$. We note the reasonably satisfactory behaviour for $\check{D}$ and $\check{R}$; in particular at all energies the NNLO EC approximation is closer to the resummed result than the NLO, as one would hope.

In contrast for $\check{K}$ and $\check{U}$ below $Q \sim 3$ GeV the NLO becomes closer than NNLO to the resummed result, making the use of fixed-order perturbation theory dubious. Notice in addition that the vertical scale in Figures 4.8(c) and 4.8(d) is four times as coarse as that in Figure 4.8(a) and 4.8(b).

4.4.4 Determining the uncertainty in $\Lambda_{\overline{\rm MS}}^{(N_f)}$ and $\alpha_s(M_Z)$

We would finally like to use the RS-invariant all-orders resummation to assess the likely accuracy to which $\Lambda_{\overline{\rm MS}}^{(N_f)}$, or $\alpha_s(M_Z)$, can be determined for various observables at various energies. We focus on the three most phenomenologically relevant observables $\hat{R}$, $\hat{R}_\tau$ and $\hat{K}$.

In Table 1 we have given the $\Lambda_{\overline{\rm MS}}^{(N_f)}$ values obtained by fitting the NLO, NNLO EC fixed-order perturbative and the RS-invariant resummed results to the central values of the data for $\hat{R}(Q{=}91$ GeV) [90], $\hat{R}(Q{=}9$ GeV) [91], $\hat{R}_\tau$ [25], and $\hat{K}(Q^2{=}5$ GeV^2). For $\hat{K}(Q^2 = 5\text{GeV}^2)$ we have taken the GLS sum rule result of the CCFR collaboration [92] corrected

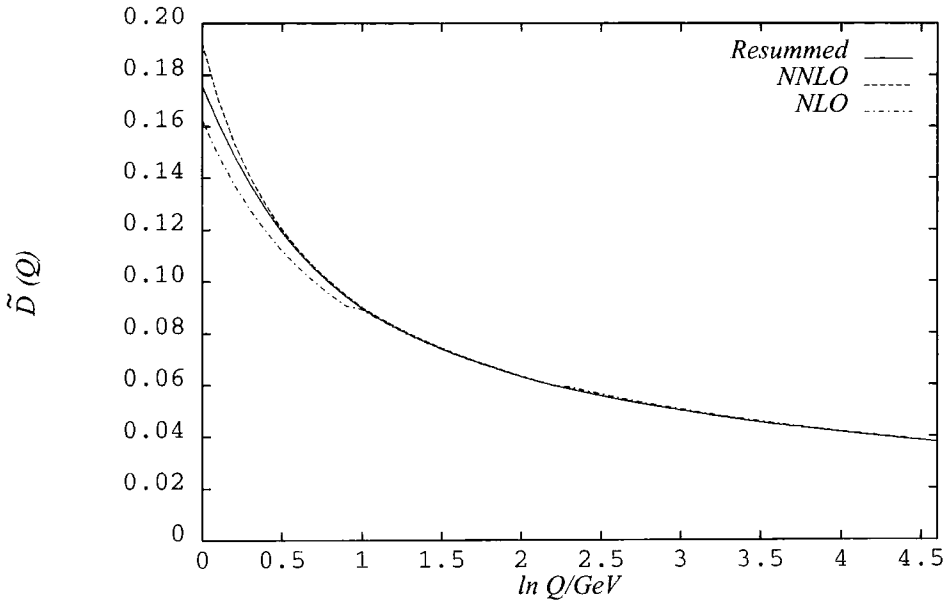

Figure 4.8(a): NLO, NNLO fixed-order results in the EC scheme, and RS-invariant resummation, for $\tilde{D}$ plotted versus $\ln Q/\text{GeV}$ over the range $1 \leq Q \leq 91$ GeV.

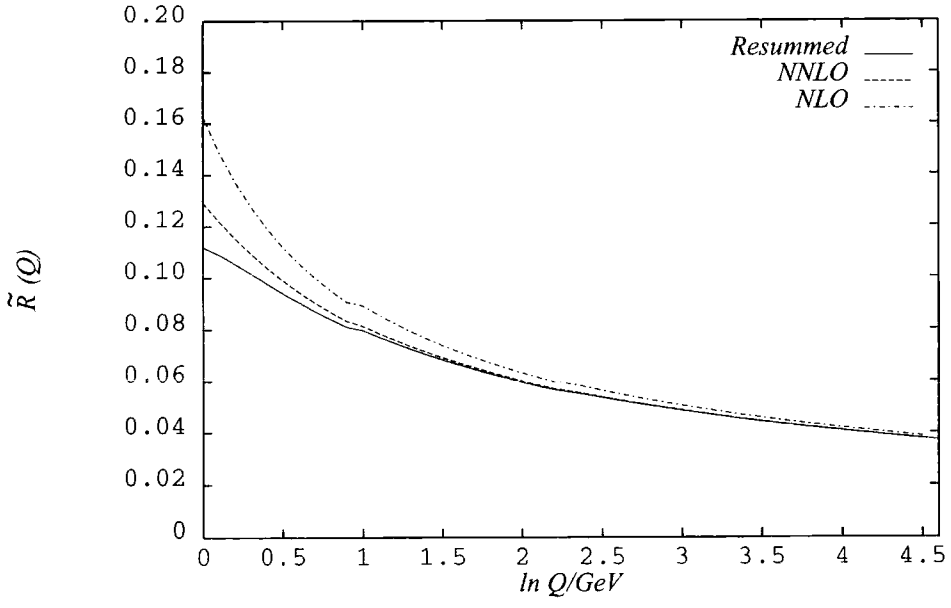

Figure 4.8(b): As for Figure 4.8(a) except for $\tilde{R}$.

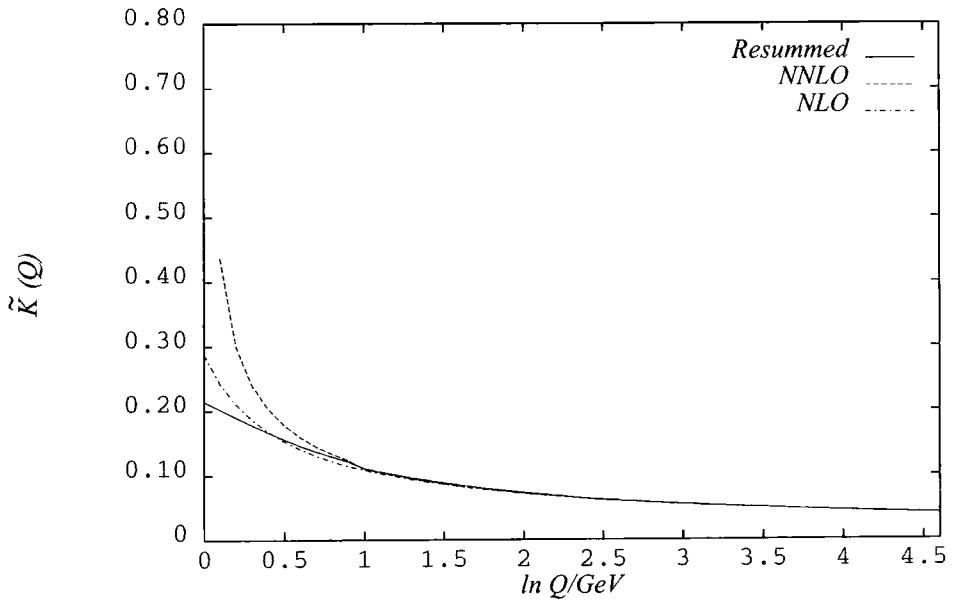

Figure 4.8(c): As for Figure 4.8(a) except for $\tilde{K}$.

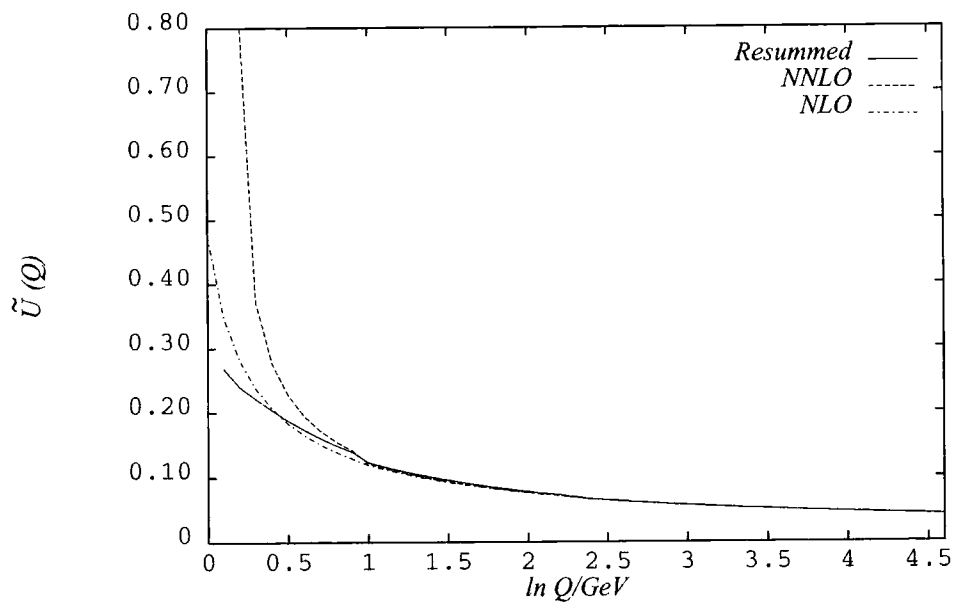

Figure 4.8(d): As for Figure 4.8(a) except for $\tilde{U}$.

Observable	Energy Q/GeV	N_f	Data	$\Lambda_{\overline{\rm MS}}^{(N_f)}$/MeV fitted to experiment		
				NLO	NNLO	Resummed
$\tilde{R}$	91	5	0.040 ± 0.004	252^{+190}_{-126}	293^{+228}_{-149}	296^{+232}_{-150}
	9	5	0.073 ± 0.024	399^{+478}_{-322}	516^{+735}_{-423}	537^{+823}_{-443}
$\tilde{R}_\tau$	1.777	3	0.205 ± 0.006	319^{+7}_{-7}	387^{+11}_{-11}	404^{+12}_{-12}
$\tilde{K}$	2.24	3	0.154 ± 0.075	437^{+187}_{-299}	379^{+138}_{-252}	426^{+386}_{-303}

Table 4.1: Values of $\Lambda_{\overline{\rm MS}}^{(N_f)}$ adjusted to fit the predictions of NLO, NNLO fixed-order results in the EC scheme, and the RS-invariant resummation to the experimental data for $\tilde{R}$, $\tilde{R}_\tau$ and $\tilde{K}$.

by subtracting off the Q^{-2} higher-twist corrections suggested by reference [93], so that

$$\tilde{K}(Q) = \tilde{K}_{CCFR}(Q) + \frac{(0.27 \pm 0.14)}{Q^2} . \tag{4.102}$$

The errors have been combined in quadrature.

The results in Table 1 are encouraging in that they indicate rather small differences between the NNLO EC and resummed fits. From these differences one would estimate that one could determine $\Lambda_{\overline{\rm MS}}^{(5)}$ to an accuracy of $\sim \pm 3$ MeV at LEP/SLD energies given ideal data for $\tilde{R}$, corresponding to determining $\alpha_s(M_Z)$ to three significant figures. Needless to say even with ideal data undetermined finite quark mass effects would in fact introduce far larger uncertainties.

At $Q = 9$ GeV $\Lambda_{\overline{\rm MS}}^{(5)}$ would apparently be determined to an accuracy of $\sim \pm 20$ MeV. The data for $\tilde{R}(Q = 91$ GeV) imply NNLO $\alpha_s(M_Z)$ ($\overline{\rm MS}$) values of $\alpha_s(M_Z)$=0.122 $\pm$ 0.012; NNLO EC and resummed are the same to the quoted number of significant figures.

For $\tilde{R}_\tau$ a comparison of the NNLO EC and resummed fits would suggest that $\Lambda_{\overline{\rm MS}}^{(3)}$ could be determined with a precision of $\sim \pm 15$ MeV. One finds $\alpha_s(m_\tau)$=0.320 $\pm$ 0.005 (NNLO EC) and $\alpha_s(m_\tau)$=0.328 $\pm$ 0.005 (resummed). To obtain $\alpha_s(M_Z^2)$ we evolved the three-loop (NNLO) coupling $\alpha_s^{\overline{\rm MS}}$ from $N_f = 3$ to $N_f = 5$ using Bernreuther-Wetzel matching [36], with flavour thresholds at $m_c = 1.25$ GeV and $m_b = 4.5$ GeV. Choosing the matching

scale $\mu_M = m_q$ in Eq.(1.101) the three-loop matching condition becomes

$$a_{f-1}(m) = a_f(m) + \frac{11}{72}a_f(m)^3 \,. \tag{4.103}$$

This choice of matching condition leads to an approximate continuity of the running coupling. This then yields $\Lambda^{(5)}_{\overline{\rm MS}}$=$253^{+9}_{-9}$ MeV (NNLO EC) and $\Lambda^{(5)}_{\overline{\rm MS}}$=$267^{+10}_{-10}$ MeV (resummed), corresponding to $\alpha_s(M_Z)$=0.1190 ± 0.0006 (NNLO EC) and $\alpha_s(M_Z)$=0.1202 ± 0.0007 (resummed). A conservative estimate of the theoretical uncertainty due to higher order perturbative corrections is then $\delta\alpha_s(M_Z)$=0.001. We will consider the possible effect of varying the matching scale on the evolution $\alpha_s(m_\tau) \to \alpha_s(M_Z)$ in Section 5.4 of Chapter 5.

If taken seriously the above estimate of the accuracy with which $\Lambda^{(5)}_{\overline{\rm MS}}$ ($\alpha_s(M_Z)$) can be determined from R_τ measurements is very reassuring, and clearly indicates that this is indeed potentially the most reliable determination. The uncertainty is somewhat smaller than has been assumed based on more naive estimates of the size of the $O(a^4)$ perturbative coefficient [94]. It is much smaller than $\delta\alpha_s(m_\tau) = 0.05$ inferred by Neubert in reference [78] based on comparison of the exact $O(\alpha_s^3)$ NNLO perturbative result in the $\overline{\rm MS}$ scheme with μ=m_τ, and a straightforward resummation of the leading-b terms, which is essentially our $\tilde{R}^{(L)}_\tau$ (c.f. Eq.(4.28)), with a=$\frac{\alpha_s(m_\tau)}{\pi}$. As can be seen from Figure 4.2(c) the dashed curve $\tilde{R}^{(L)}_\tau(a)$ lies above the RS-invariant resummation (solid line) for a=$\frac{\alpha_s(m_\tau)}{\pi} \simeq 0.12$, and there is a strong 'a' dependence in this region. The NNLO EC result, and indeed the $\overline{\rm MS}$ $\mu = m_\tau$ NNLO result, are both much closer to the RS-invariant resummation. The implication then is that the rather large difference between the exact fixed-order and naive resummed leading-b results found in [78] is just a reflection of the inadequacy of the naive resummation, which was our original motivation for improving it.

We finally turn to the GLS sum rule results in Table 4.1. Whilst the $\Lambda^{(3)}_{\overline{\rm MS}}$ values for NLO, NNLO, and resummed are in reasonable agreement with that obtained for $\tilde{R}_\tau$, we note once again the worrying feature that the NLO result is closer to the resummed than the NNLO. We have also had to assume and correct for sizeable power corrections, based on the modelled suggestion of reference [93]. Also note the very large errors which reflect the difficulty in reconstructing the sum rule by combining data from various DIS experiments [92]. One finds $\alpha_s(Q^2 = 5{\rm GeV}^2)$=$0.316^{+0.068}_{-0.116}$ (NNLO EC) and $\alpha_s(Q^2 = 5{\rm GeV}^2)$=$0.332^{+0.248}_{-0.134}$ (resummed). Evolving the three-loop coupling $\alpha_s^{\overline{\rm MS}}$ from $N_f = 3$ to $N_f = 5$, using Bernreuther-Wetzel matching [36], with the quark mass thresholds noted above yields $\Lambda^{(5)}_{\overline{\rm MS}}$=$247^{+118}_{-183}$ MeV (NNLO EC) and $\Lambda^{(5)}_{\overline{\rm MS}}$=$286^{+374}_{-224}$ MeV (resummed), corresponding to $\alpha_s(M_Z)$=$0.118^{+0.008}_{-0.019}$ (NNLO EC) and $\alpha_s(M_Z)$=$0.121^{+0.018}_{-0.023}$ (resummed). Clearly $\tilde{K}$ will not be competitive with $\tilde{R}_\tau$ as a way of determining $\Lambda_{\overline{\rm MS}}$.

4.5 Technical issues related to the resummations

Before concluding this chapter it is appropriate to discuss several possibilities which could improve or extend the RS-invariant resummations, and mention some technical issues related to them.

4.5.1 Analytical continuation between the ρ_k^D and ρ_k^R, $\rho_k^{R_\tau}$

The first concerns the analytical continuation between the Euclidean Adler D-function and the Minkowski quantities $\check{R}$ and $\check{R}_\tau$. This will imply definite relations between the corresponding RS-invariants ρ_k^D, ρ_k^R, $\rho_k^{R_\tau}$. For instance for $\check{R}$ one has [95]

$$\begin{aligned} \rho_2^R &= \rho_2^D - \frac{1}{12}b^2\pi^2 \\ \rho_3^R &= \rho_3^D - \frac{5}{12}cb^2\pi^2 \\ \rho_4^R &= \rho_4^D - \frac{1}{12}(8\rho_2^D + 7c^2)b^2\pi^2 + \frac{1}{360}b^4\pi^4 \\ &\vdots \quad\quad \vdots \end{aligned} \tag{4.104}$$

The procedure we have used to construct $\tilde{R}^{(L*)}$ involves resumming the effective charge beta-function using the exact ρ_2^R and the leading-b approximations to ρ_k^R, $k > 2$. This means the $-\frac{5}{12}cb^2\pi^2$ analytical continuation term in ρ_3^R, or the $-\frac{7}{12}c^2b^2\pi^2$ in ρ_4^R, have been omitted since they are sub-leading in b. Since ρ_2^D is known exactly we could also improve the resummation by using the exact ρ_2^D in evaluating the $-\frac{2}{3}\rho_2^D b^2\pi^2$ term in ρ_4^R. One could envisage an improved resummation $\rho_R^{(L**)}(x)$ incorporating these extra terms.

$$\rho_R^{(L**)}(x) = \rho_R^{(L*)}(x) + \tilde{\rho}_R(x)\ , \tag{4.105}$$

where the extra terms to $O(x^7)$ are explicitly

$$\tilde{\rho}_R(x) = -\frac{5}{12}cb^2\pi^2x^5 - (\frac{2}{3}\rho_2^{D(NL)} + \frac{7}{12}c^2)b^2\pi^2x^6 + O(x^7) + \cdots\ . \tag{4.106}$$

This resummation to all-orders can be accomplished in principle by representing $\tilde{R}$ as a contour integral involving $\tilde{D}$ as in Eq.(1.74) [95]. Using $\tilde{D}^{(L*)}$ in the integrand would formally produce $\tilde{R}^{(L**)}$ corresponding to the above effective charge beta-function $\rho_R^{(L**)}$, but one would have to evaluate $\tilde{D}^{(L*)}$ at complex values of Q. Similar remarks apply to $\check{R}_\tau$ [95]. One might note that in the NNLO case, where we can compare with the exact result, $\rho_2^{D(L)}$ is only a good approximation to the exact ρ_2 for $N_f \approx 0$ or for large N_f.

Hence one could conclude that the uncertainties in the basic approximation are such that the attempted improvement is not warranted. Nonetheless it would be very worrying if any of our conclusions for R, R_τ changed on including these extra terms. This subject will form part of the motivation for Chapter 5.

4.5.2 Analytic inversion of $D^{(L)}(a)$ to obtain $\rho^{(L*)}$

Another aspect of the resummations which requires elucidation is the way the resummed $\rho^{(L*)}$ effective charge beta-function is obtained by numerically inverting the P.V. regulated Borel integral representation of $D^{(L)}(a)$, as detailed in Eq.(4.82) to Eq.(4.87). From Eq.(2.60) we see that $\rho(D(Q))$ is directly related to the Q-evolution of the observable $D(Q)$, and is therefore of central physical importance in studying power corrections. One might then imagine defining

$$\rho(D) = Reg \int_0^\infty \mathrm{d}z\, \mathrm{e}^{-z/D} B[\rho](z) + \rho_{NP}^{Reg}(D)\ , \tag{4.107}$$

where $B[\rho]$ denotes the perturbatively defined Borel transform of ρ. This will contain singularities at the same positions in the Borel plane as $D(a)$ [54], and to control the IR_l infra-red renormalon singularities on the positive-z axis the integral will have to be regulated, denoted Reg. There will be an additional $\rho_{NP}^{Reg}(D)$ incorporating the power corrections ($e^{-1/D}$ terms) whose precise definition will depend on the chosen method of regulation [16].

If $B[\rho]$ is defined in the leading-b approximation we can then ask if the first term in Eq.(4.107) with P.V. regulation exactly reproduces the $\rho^{(L*)}$ defined by numerically inverting the P.V. regulated $D^{(L)}(a)$.

This can be reduced to a simpler problem. Consider

$$\begin{aligned} D(x) &\equiv P.V. \int_0^\infty \mathrm{d}z\, \mathrm{e}^{-z/x} B[D](z) \\ a(x) &\equiv P.V. \int_0^\infty \mathrm{d}z\, \mathrm{e}^{-z/x} B[a](z) \end{aligned} \tag{4.108}$$

where $B[D]$ denotes the perturbatively defined Borel transform of $D(a)$, and $B[a]$ denotes the perturbatively defined Borel transform of the inverse function of $D(a)$, which can unambiguously be defined by formally transforming the coefficients of the power series $D(a)$. With these definitions one can then ask whether $D(a(x)) = x$ exactly or whether there are additional $e^{-1/x}$ terms. Existing results on such problems are in short supply [96], but work in progress [60] strongly suggests that the relation $D(a(x)) = x$ does hold

exactly. Unfortunately the result probably only holds for P.V. regulation. The pragmatic reason for studying this question is that $B[\tilde{D}^{(L)}](z)$ is given by rather simple expressions as a sum of poles [76], whereas $B[\rho](z)$ will have an extremely complicated form. Hence it is impractical to construct $B[\rho](z)$ directly, and the numerical inversion route is the only possibility.

4.5.3 Infra-red properties of $\rho(x)$

The properties of the function $\rho(x)$ fix the infra-red properties of the observable. For instance if $\rho(D^*) = 0$ then $D \to D^*$ as $Q \to 0$. It has been suggested [97, 98] that such infra-red freezing is supported by a wide body of indirect phenomenological evidence. In reference [99] the assumption of universal infra-red behaviour of an effective coupling $\alpha_{eff}(k)$ has been used to interrelate power corrections for different observables. It is interesting that for all the observables we have studied in this chapter $D^{(L)}(a)$ has a maximum value, D_{max}, say. This means that $\rho^{(L)}(x)$ is undefined for $x > D_{max}$. If ρ is to be defined in the infra-red this is presumably a signal that power corrections have to be included beyond a certain point. An interesting consistency check on this interpretation is that if only ultra-violet renormalon singularities are present then $\tilde{D}^{(L)}(a)$ does not have a maximum, $D^{(L)}(a)|_{UV}$ increases monotonically and $\rho^{(L)}(x)$ will be defined for all x. This is also true for $\tilde{K}^{(L)}(a)$ and $\tilde{U}^{(L)}(a)$. The absence of IR renormalons is consistent with there being no power corrections, or at least they are not constrained by the large-order perturbative behaviour. However, for the two Minkowski quantities the absence of IR renormalons does not guarantee our ability to reconstruct $\rho(x)$ for all x.

To look at this more quantitatively we consider the infra-red behaviour of the EC beta-function $\rho(x)$ for $\tilde{D}$ and $\tilde{R}$, with $N_f = 2$. In Figure 4.9(a) and 4.9(b) we plot the behaviour of $\rho(x)$ for $x = \tilde{D}$ and $x = \tilde{R}$, respectively. We consider three possible definitions of $\rho(x)$: $\rho^{(L*)}(x)$, defined in Eq.(4.81); $\rho^{(L)}(x)$, defined in Eq.(4.83); and $\rho^{(2)}(x)$ defined in Eq.(4.90) for $n = 2$.

For an infra-red fixed-point, $\beta(a_*) = 0$ ($a_* > 0$), we require at NNLO the condition that

$$1 + ca_* + c_2 a_*^2 = 0 \; . \tag{4.109}$$

In the effective charge scheme, $a = \tilde{D}$ (or $\tilde{R}$) and $c_2^{EC} = \rho_2$. Therefore for $\tilde{D}$ the NNLO EC approximant $\rho^{(2)}(x)$ has no infra-red fixed point since $\rho_2^D = 9.37140$ for $N_f = 2$, and Eq.(4.109) has no positive root. For $\tilde{R}$, however, $\rho_2^R = -9.842342$ for $N_f = 2$, so $\rho^{(2)}(\tilde{R})$ has a positive root for $\tilde{R} = 0.435$.

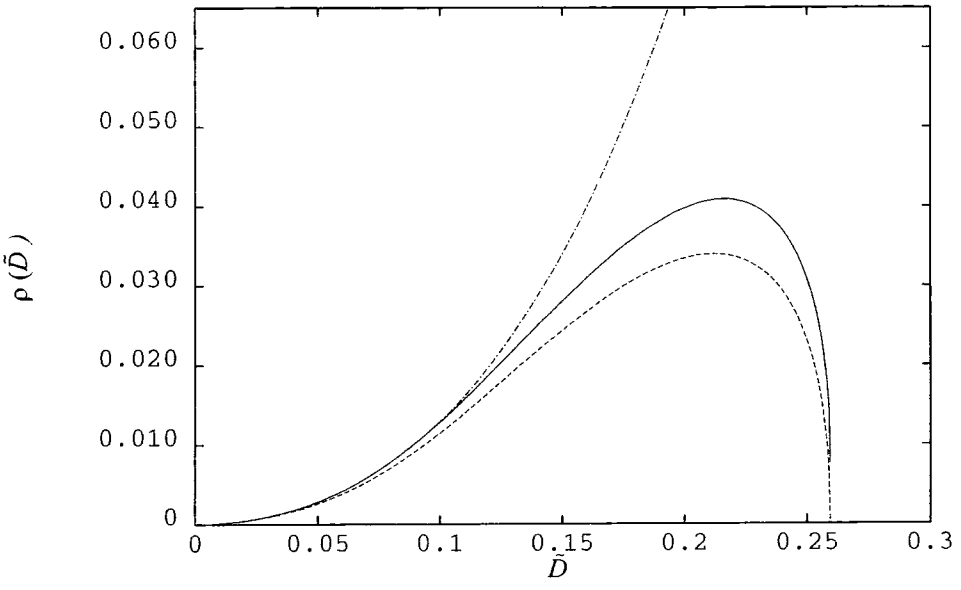

Figure 4.9(a): The effective charge beta function $\rho(\tilde{D})$ for $\tilde{D}$ for $N_f = 2$. Plotted are $\rho^{(L*)}(\tilde{D})$ (solid curve), $\rho^{(L)}(\tilde{D})$ (dashed curve) and $\rho^{(L*)(2)}(\tilde{D})$ (dashed-dotted curve).

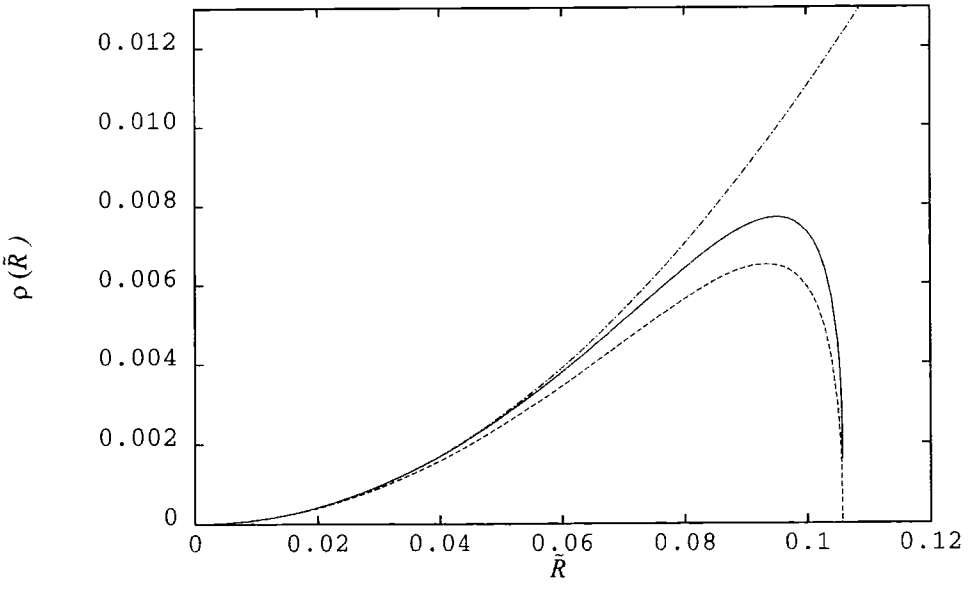

Figure 4.9(b): As for Figure 4.9(a) except for $\tilde{R}$.

For the RS-invariant leading-b resummation, $\rho^{(L)}(x)$, there is an IR fixed point for both $\tilde{D}$ and $\tilde{R}$. This is also true for the other observables. This follows from the observation that, from Eq.4.86), $\rho^{(L)}(x)$ is zero for $\mathrm{d}D^{(L)}(F)/\mathrm{d}F = 0$. The condition for an IR fixed-point is therefore that $\tilde{D}^{(L)}(F)$ has a stationary point. Since all five quantities considered have a maximum value, D_{max}, it follows that the IR fixed point is given by D_{max}. For the $\tilde{D}$ the IR fixed-point is at $\tilde{D} = 0.260$ ($F = 2.07$) for $N_f = 2$. This varies with N_f: for $N_f = 5$ we obtain an IR fixed-point at $\tilde{D} = 0.327$ ($F = 1.65$). For $\tilde{R}$ the IR fixed-point is at $\tilde{D} = 0.106$ ($F = 4.62$) for $N_f = 2$.

We see that, unlike the pure leading-b resummation, $\rho^{(L*)}(x)$ is not zero for any $x \neq 0$. As a result neither $\tilde{D}^{(L*)}$ nor $\tilde{R}^{(L*)}$ has a IR fixed-point. At R_{max} the value of $\rho^{(L*)}(\tilde{R}_{max}) = 0.00159$, which is small but non-zero.

4.5.4 Approximation of the large-N limit by the large- b expansion

A final underlying issue which needs further clarification is the explanation for the excellent performance of the leading-b approximation itself. For all the cases where exact NNLO QCD calculations exist the leading-b approximation not only gives exact results for perturbative coefficients and ρ_k RS-invariants in the large-N_f limit, but remarkably is also an excellent ($\sim 5\%$ level) approximation in the large-N limit of a large number of colours. As pointed out unfortunately it may be a rather poor approximation in-between these extremes, for N_f=5, N=3, for instance. Although the sub-leading N_f-expansion coefficients are reproduced remarkably well ($\sim 20\%$ level).

This clearly suggests that there is some far more powerful effect at work which guarantees that the leading-b term reproduces large-N_f and large-N coefficients simultaneously. An idea as to how this might operate comes from noting that we could formulate a second version of the b-expansion based on the large-N expansion of the coefficients by making the replacement $N \to \frac{2}{11}(3b + N_f)$. For simplicity we replace C_F by $N/2$, throwing away some $1/N$ terms; this yields an expansion

$$d_k = d_k^{<k>} b^k + d_k^{<k-1>} b^{k-1} + \cdots + d_k^{<0>} \ , \tag{4.110}$$

where $d_k^{<k>}$ is a pure number and $d_k^{<k-r>} \sim N_f^r$. We would then hope to be able to explain why $d_k^{(k)} \simeq d_k^{<k>}$. This "large-$N_f$–large-$N$ duality", which is found empirically from comparison with exact calculations is clearly an intriguing feature of QCD; and it provides a motivation for resumming the leading-b terms to all orders. A clearer understanding of

its origins will be crucial in assessing the value of such resummations.

A possible Feynman-diagrammatic explanation runs as follows. In the large-N limit of QCD only planar diagrams contribute. 't Hooft has shown that if one restricts oneself to UV-finite planar diagrams perturbation theory converges [100]. As far as perturbative estimates are concerned these diagrams can be discarded, therefore, since they do not contribute to $n!$ growth of the coefficients. The remaining UV-divergent planar diagrams will contain among them diagrams containing chains of gluon self-energy insertions and other structures which must be combined with renormalon diagrams with chains of internal fermion bubbles and other structures to produce a gauge-invariant contribution proportional to a power of b, using the pinch technique or background field method [80]. The planar diagrams of interest are those *not* involved in the construction of a gauge-invariant effective charge, therefore. The hope would be to understand why their contribution is 'small'.

The purely Feynman-diagrammatic approach to this problem is potentially horrendously complicated. A more tractable method may be to consider the approach of Parisi [71], in which the structure of the leading UV renormalon singularity can be inferred by computing the insertion of dimension-six operators into the Green functions corresponding to, for instance, the vector correlator. Consideration of this approach in planar approximation has revealed considerable simplification in the case of the Adler D-function, with three of the four potential four-fermion operators not contributing. One can then establish exact results for the contribution of Feynman diagrams proportional to $N_f^{n-r}N^r$ as $n \to \infty$, and these confirm that the weak dominance of the leading-b term which holds for the exchange of one-renormalon chain survives the inclusion of any number of chains [83].

4.6 Summary and conclusions

In this chapter we have proposed an improvement of the renormalon-inspired 'leading-b' resummations of QCD perturbation theory which have been previously used by various authors [62, 69, 76, 77, 78, 79] to assess the reliability of fixed-order perturbative predictions. Such resummations are RS-dependent under the full QCD RG transformations. To avoid this difficulty the strategy is to approximate the RS-invariant effective charge beta-function coefficients by retaining their 'leading-b' part, which is completely determined by exact all-orders large-N_f results. Fixed-order perturbative approximations in any RS can then be obtained from the approximated RS-invariants by using the exact QCD RG. If the exact NNLO invariant is known it can be included. In this way the resummation

includes the exact NLO and NNLO perturbative coefficients in any RS.

The RS-invariant resummation was performed for the Adler D-function, e^+e^- R-ratio, R_τ the analogous decay ratio for the tau-lepton, and DIS sum rules. Comparison with fixed-order perturbation theory in the effective charge RS revealed impressive convergence to the resummed result for the e^+e^- R-ratio at LEP/SLD energies, $Q = 91$ GeV. As the value of Q was reduced oscillatory behaviour of the fixed-order results above and below the resummed value was increasingly evident, reflecting the alternating-sign factorial growth of the perturbative coefficients resulting from the dominant UV_1 renormalon singularity. Even at $Q = 1.5$ GeV the resummed value was reasonably approximated until ninth order perturbation theory.

For $R_\tau(Q = m_\tau)$, which is also UV_1 dominated, there was also a satisfactory approximation to the resummed value, although with much larger oscillations than for $\tilde{R}$ at a comparable value of Q, and with an earlier breakdown of perturbation theory beyond fifth-order. This is attributed to the IR_3 and IR_4 double poles.

In contrast DIS sum rules which have an leading IR_1 infra-red singularity exhibited much less satisfactory behaviour with successive orders moving steadily away from the resummed result, reflecting the fixed-sign factorial growth of the coefficients.

Using the difference between the exact NNLO EC approximation and the resummation to estimate the uncertainty with which $\Lambda_{\overline{\mathrm{MS}}}$ could be determined indicates that for $\tilde{R}$ at $Q = 91\mathrm{GeV}$ $\alpha_s(M_Z)$ could be determined to three significant figures with ideal data.

For $\tilde{R}_\tau$ one concludes that $\delta\alpha_s(M_Z) = 0.001$ in the $\overline{\mathrm{MS}}$ scheme from the NNLO-resummed difference. This is a much smaller uncertainty than deduced by Neubert [78] from a comparison with the naive RS-dependent leading-b resummation. The RS-dependence means that the naive resummation is sensitive to the $\overline{\mathrm{MS}}$ scheme $\alpha_s(m_\tau)$ being assumed for the coupling. Other *a priori* reasonable choices would dramatically change the resummed result, and hence we would argue that this estimate of the uncertainty is too pessimistic.

We regard the impressive performance of fixed-order QCD perturbation theory for the UV-renormalon dominated quantities as the key result of this analysis.

Various technical issues related to the resummation and possibilities for future developments were also discussed. In the next chapter we shall pursue one of these, the inclusion of analytical continuation terms as discussed in Section 4.5.1

Chapter 5

Contour-improved RS-invariant resummations

5.1 Introduction

There has been extensive recent interest [94, 101, 102] in the possibility of using measurements of R_τ, the total hadronic decay width of the τ lepton normalized to the leptonic decay width, for precise determination of the renormalized strong coupling $\alpha_s(M_z^2)$ (or more fundamentally $\Lambda_{\overline{\rm MS}}$). For this purpose R_τ apparently possesses a number of advantages compared with other QCD observables.

- It is an inclusive quantity which can be computed in QCD using the operator product expansion (OPE) supplemented by analyticity [20, 21, 22].
- It has been calculated in QCD perturbation theory to next-to-next-to-leading order (NNLO) $O(\alpha_s^3)$ [17, 18].
- Power corrections are expected to be small [21, 22].
- The τ mass is below the threshold for charmed hadron production only the light quarks u, d, s are active, so QCD with $N_f = 3$ massless quark flavours should be applicable.
- R_τ can be rather accurately determined from the measured electronic branching ratio of the τ or from the τ lifetime [25].
- In evolving up in energy scale from $\alpha_s(m_\tau^2)$ to $\alpha_s(M_Z^2)$, which is customarily quoted in global comparisons, the fractional error in $\alpha_s(\Lambda_{\overline{\rm MS}})$ is reduced by a factor equal to the ratio of $\alpha_s(M_Z^2)$ to $\alpha_s(m_\tau^2)$.

Measurement of the hadronic width of the Z^0 to directly determine $\alpha_s(M_z^2)$ shares the same advantages of being inclusive, calculated to NNLO in perturbation theory and having small power corrections, but suffers significant corrections from heavy quark masses, and much larger systematic experimental errors.

Despite these undoubted advantages possessed by R_τ as a means of determining α_s, the relatively low energy scale involved, $s = m_\tau^2$, might lead one to expect sizeable corrections from uncalculated $O(\alpha_s^4)$ and higher orders in perturbation theory. To assess the effect of these terms with our present limited state of knowledge one can employ a, necessarily approximate, all-orders resummation of the QCD perturbation series. A well-motivated framework for this is provided by the leading-b approximation, discussed in Chapter 4, [76, 82], also sometimes referred to as naive non-abelianization [62, 88].

In several recent papers it has been claimed that applying the leading-b resummation to R_τ indicates rather large perturbative uncertainties [69, 78, 79]. Indeed the estimated uncertainty in $\alpha_s(M_Z^2)$ is of the same order as that normally quoted in determinations from jet observables at LEP and SLD [34].

In the last chapter we pointed out that a straightforward resummation of the leading-b terms of the kind employed in references [69, 78, 79], is renormalization scheme (RS) dependent. This occurs because the compensation mechanism between the renormalization group (RG) improved coupling and the perturbative coefficients is destroyed by retaining only the leading-b terms. As a result the 'naive' leading-b resummation is not RS-invariant under the full QCD renormalization group (RG). Whilst at large energies the resulting ambiguities are mild, at $s = m_\tau^2$ this RS dependence is serious and in our view invalidates the rather pessimistic conclusions of these references regarding the likely uncertainty in $\alpha_s(M_Z^2)$ determined from R_τ.

Following on from this observation we proposed an improved RS-invariant resummation based on approximating the unknown effective charge (EC) beta-function coefficients by the portion containing the highest power of b. Approximated perturbative coefficients in any RS can then be obtained using the exact QCD RG. The leading-b effective charge beta-function can be resummed using exact all-orders large-N_f results.

The difference between the exact NNLO result for R_τ in the effective charge RS, and the RS-invariant all-orders resummation indicates a rather small uncertainty due to the approximated higher order terms, and the estimated uncertainty in $\alpha_s(M_Z^2)$ is correspondingly small, $\delta\alpha_s(M_Z^2) \simeq 0.001$.

In this chapter we wish to explore the perturbative uncertainty in R_τ in somewhat more detail. Both R_τ and e^+e^- R-ratio can be represented by a contour integral involving $D(se^{i\theta})$, where $D(-s)$ is the Euclidean Adler D-function, around a circle, cut along the positive real axis, $\theta = -\pi$ to $\theta = \pi$, in the complex s-plane (as in Eq.(1.74)) [20]. Here $s = m_\tau^2$ for R_τ. Conventional perturbation theory involves an expansion in $\alpha_s(s)$ obtained by re-expressing $\alpha_s(se^{i\theta})$ as an expansion in $\alpha_s(s)$ which is then truncated. Alternatively one can simply numerically perform the contour integration for the $\alpha_s^k(se^{i\theta})$ terms up to a given order [94]. This procedure includes in addition to conventional fixed-order perturbation theory a resummation of analytical continuation terms. A subset of these terms involve powers of the first beta-function coefficient, b, together with π^2 factors, and are resummed to all-orders in the leading-b approach. In addition, however, there are potentially large contributions involving higher beta-function coefficients [104]. It would seem sensible, therefore to perform the improved RS-invariant resummation for $D(se^{i\theta})$, and numerically evaluate the contour integral. In this way additional analytical continuation terms not captured in the leading-b resummation are included exactly. This can then be compared with the exact NNLO result for $D(se^{i\theta})$ in the EC scheme, with the contour integral again numerically evaluated. Since in both cases the analytical continuation terms are resummed the difference should be indicative of the effect of the approximated higher effective charge RS invariants for D beyond NNLO.

The plan of the chapter is as follows. In Section 5.2 we shall introduce the contour integral representations of the e^+e^- R-ratio and R_τ in terms of the Adler D-function. Using Taylor's theorem we can then expand R and R_τ in terms of $D(s)$ and its energy derivatives, which in turn can be expressed in terms of the effective charge beta-function for D and its derivatives. These results can be easily used to express the perturbative coefficients of the Minkowski quantities R and R_τ in terms of those of the Euclidean Adler D-function and its effective charge RS invariants. We have compared these with existing expressions available in the literature [104]. We also derive relations between the EC invariants for R and R_τ and those for D. In Section 5.3 the contour integrals for the R and R_τ are evaluated by using Taylor's theorem successively to evaluate D at a series of values of complex s around the unit circle contour of integration. A Simpson's rule numerical integration is then performed. The translation of D in complex s involves the effective charge beta-function and its derivatives. This function can be truncated or its leading-b terms resummed, as shown in the last chapter. In Section 5.4 fits to the experimental data for $\check{R}$ and $\check{R}_\tau$ are performed to determine α_s from fixed-order and resummed perturbation theory. In Section 5.5 we conclude by comparing the resulting values and estimates of the perturbative uncertainty with those suggested by other approaches.

This chapter has been previously summarised in reference [105].

5.2 Contour integral representation of Minkowski observables

The two quantities with which we shall be concerned in this chapter are the e^+e^- annihilation R-ratio and the R_τ ratio, defined analogously using the τ hadronic width. These quantities were discussed in Section 1.8.1 and 1.8.2, respectively. We now wish to elaborate in more detail on their contour integral representations.

We demonstrated in Section 1.8 that the two Minkowski quantities, R and R_τ can both be conveniently expressed in terms of the transverse part of the correlator $\Pi(s)$ of two vector currents in the Euclidean region. Moreover, $\hat{R}$, $\hat{R}_\tau$ and related Minkowski quantities such as spectral moments [94] can all be written in terms of a weighted contour integral of $\tilde{D}(se^{i\theta})$ around a circle in the complex s-plane [20].

Denoting such a generic Minkowski observable as $\hat{R}$ we have

$$\hat{R}(s_0) = \frac{1}{2\pi}\int_{-\pi}^{\pi} \mathrm{d}\theta\, W(\theta)\, \tilde{D}(s_0 \mathrm{e}^{i\theta}) \tag{5.1}$$

where $W(\theta)$ is a weight function which depends on the observable $\hat{R}$. For $\hat{R}$ we have $W(\theta) = 1$, and for $\hat{R}_\tau$

$$W_\tau(\theta) = (1 + 2\mathrm{e}^{i\theta} - 2\mathrm{e}^{3i\theta} - \mathrm{e}^{4i\theta})\,, \tag{5.2}$$

and $s_0 = m_\tau^2$.

A novel representation for $\hat{R}$ can be obtained by using Taylor's theorem to expand $\tilde{D}(se^{i\theta})$ around $s = s_0$. This yields

$$\hat{R}(s_0) = \frac{1}{2\pi}\int_{-\pi}^{\pi} \mathrm{d}\theta\, W(\theta) \left\{ \tilde{D}(s_0) + \sum_{n=1}^{\infty} i^n \frac{\theta^n}{n!} \frac{\mathrm{d}^n}{\mathrm{d}\ln s^n} \tilde{D}(s)\bigg|_{s=s_0} \right\}. \tag{5.3}$$

The derivatives in Eq.(5.3) can be recast in terms of the effective charge (EC) beta-function $\rho(\tilde{D})$ [42, 38], and its derivatives. $\rho(\tilde{D})$ is defined by

$$\begin{aligned} \frac{\mathrm{d}\tilde{D}(s)}{\mathrm{d}\ln s} &= -\frac{b}{2}\rho(\tilde{D}) \\ &\equiv -\frac{b}{2}(\tilde{D}^2 + c\tilde{D}^3 + \rho_2\tilde{D}^4 + \cdots + \rho_k\tilde{D}^{k+2} + \cdots)\,. \end{aligned} \tag{5.4}$$

Here b and c are first and second universal RS-invariant beta-function coefficients given in Eq.(2.5). The higher coefficients ρ_2, ρ_3, $\cdots$, in Eq.(5.4) are RS-invariants and may

be expressed in terms of the perturbative coefficients of $\tilde{D}$, d_k, together with the beta-function coefficients, c_k, which define the renormalization scheme employed to define the RG improved coupling a [37]. Thus

$$\frac{\mathrm{d}a(\mu^2)}{\mathrm{d}\ln\mu^2} = -\frac{b}{2}\left(a^2 + ca^3 + c_2a^4 + \cdots + c_ka^{k+2} + \cdots\right) . \tag{5.5}$$

The effective charge (EC) scheme corresponds to the choice of coupling $\tilde{D} = a$. Appendix B.2 gives the explicit expressions for the EC invariants ρ_k ($k = 1 \ldots 6$). We note that in Section 2.5, to which the reader is referred for additional discussion of the EC beta-function, the dependent energy variable was taken to be Q, whereas we are employing $s = Q^2$ in this chapter, hence there are additional factors of $\frac{1}{2}$ in Eq.(5.4) and Eq.(5.5) compared to Eq.(2.60) and Eq.(2.3).

Using Eq.(5.4) one can then show that the energy derivatives in Eq.(5.3) can be rewritten as

$$\frac{\mathrm{d}^n}{\mathrm{d}\ln s^n}\tilde{D}(s)\bigg|_{s=s_0} = \left(-\frac{b}{2}\right)^n \left[\rho(x)\frac{\mathrm{d}}{\mathrm{d}x}\right]^{n-1}\rho(x)\bigg|_{x=\tilde{D}(s_0)} , \; n > 0 . \tag{5.6}$$

Thus finally we can write Eq.(5.3) in the form

$$\hat{R}(s_0) = \tilde{D}(s_0) + \sum_{n=1}^{\infty}\left(\frac{-ib}{2}\right)^n \frac{w_n}{n!}\left[\rho(x)\frac{\mathrm{d}}{\mathrm{d}x}\right]^{n-1}\rho(x)\bigg|_{x=\tilde{D}(s_0)} . \tag{5.7}$$

Here w_n denotes moments of the weight function $W(\theta)$,

$$w_n = \frac{1}{2\pi}\int_{-\pi}^{\pi}\mathrm{d}\theta\,\theta^n\,W(\theta) . \tag{5.8}$$

For $\tilde{R}$ setting $W(\theta) = 1$ yields $w_n = \pi^n/(n+1)$ (n even), $w_n = 0$ (n odd). The first two terms in the sum of Eq.(5.7) are then

$$\tilde{R}(s_0) = \tilde{D}(s_0) - \frac{\pi^2b^2}{24}\rho\rho' + \frac{\pi^4b^4}{1920}\rho(\rho'^3 + 4\rho\rho'\rho'' + \rho^2\rho''') + \cdots . \tag{5.9}$$

Primes denote differentiation of $\rho(x)$ with respect to x, evaluated at $x = \tilde{D}(s_0)$. Successive terms are RS-invariants resulting from the resummation to all-orders of analytical continuation terms proportional to π^2b^2, π^4b^4, $\cdots$, respectively.

For $\tilde{R}_\tau$ the weight function $W_\tau(\theta)$ of Eq.(5.2) has moments $w_1^\tau = \frac{19i}{12}$, $w_2^\tau = \frac{\pi^2}{3} - \frac{265}{72}$, $\cdots$. Then Eq.(5.7) yields

$$\tilde{R}_\tau = \tilde{D}(m_\tau^2) + \frac{19b}{24}\rho - \left(\frac{\pi^2}{3} - \frac{265}{72}\right)\frac{b^2}{8}\rho\rho' + \cdots . \tag{5.10}$$

From Eq.(5.7) we see that Minkowski observables are naturally expressed in terms of the Euclidean Adler D-function and its EC beta-function. Given an all-orders definition of $\rho(x)$ one can discuss the radius of convergence of the sum in Eq.(5.7) in $\hat{D}(s_0)$. This is an interesting question which could be directly addressed using the leading-b resummation of ρ on which the RS-invariant resummations of Section 4.3 are based. However, one can anticipate a rather restricted radius of convergence by making the one-loop approximation $\rho(x) = x^2$. One then finds

$$\hat{R}_{\text{one-loop}} = \frac{2}{b\pi}\arctan(\frac{b\pi\hat{D}}{2}) \,, \tag{5.11}$$

for the result of resumming the analytical continuation terms which only involve the lowest beta-function coefficient. This suggests that the radius of convergence is limited by $\hat{D} < \frac{2}{b\pi}$ [94, 106]. For $N_f = 3$ this gives a radius of convergence $\frac{4}{9\pi} \simeq 0.141\cdots$, which is to be compared with $\hat{D}(m_\tau^2) \simeq 0.1$. So that the expansion will not be useful for evaluating $\hat{R}_\tau$ using the leading-b resummation of $\rho(x)$. As we shall discuss in the next section, however, we shall be able to make use of the Taylor's theorem approach to evaluate $\hat{D}(se^{i\theta})$ at closely spaced intervals around the integration contour using the resummed $\rho(x)$.

To conclude this section we note that the expansion of Eq.(5.7) is of use in straightforwardly relating the $\hat{R}$, $\hat{R}_\tau$ Minkowski perturbative coefficients r_k, r_k^τ to the Euclidean d_k coefficients of $\hat{D}$. The resulting calculated expressions are in agreement with the results available in the literature for $k \leq 5$ [104]. Details on the methodology and explicit expressions for $k \leq 6$ are included in Appendix C.1 and C.2, respectively.

In clarifying the connection between the various versions of fixed-order perturbation theory to be compared in Section 5.4 it will be useful to relate the EC RS-invariants ρ_k^R and $\rho_k^{R_\tau}$ corresponding to $\hat{R}$ and $\hat{R}_\tau$ to the ρ_k^D (hitherto ρ_k) connected with $\hat{D}$ [95]. The method used and expressions for ρ_k^R and $\rho_k^{R_\tau}$ ($k \leq 6$) are included in Appendix C.3

Having obtained the above expressions one can now calculate the numerical value of the contributions to $\rho(x)$ sub-leading in b which are omitted in $\hat{R}^{(L*)}$ and $\hat{R}_\tau^{(L*)}$. As in Section 4.5.1 we denote the sub-leading contribution to $\rho^{(L)}(x)$ by $\tilde{\rho}(x)$; the n^{th}-order truncated EC beta-functions $\rho^{(L**)R,R_\tau}$ then given by

$$\rho^{(L**)R,R_\tau}(x) = \rho^{(L*)R,R_\tau}(x) + \tilde{\rho}^{R,R_\tau}(x) \,. \tag{5.12}$$

Since ρ_2 is included exactly, potential sub-leading corrections start at order k ($k \geq 3$).

To look at the contribution order-by-order we denote the sub-leading contribution at order

N_f	Order n	$\rho_n^{(L)}$	$\tilde{\rho}_n$	$\rho_n^{(L**)}$
3	3	-81.97830	-148.0441	-230.0224
	4	-10.55325	+704.2099	+693.6567
	5	-7208.481	+7840.018	+631.5370
	6	+62312.32	+17182.86	+79495.18
4	3	-65.07708	-109.9478	-175.0249
	4	-7.756951	+934.7940	+927.0370
	5	-4905.971	+6490.257	+1584.286
	6	+39267.33	-140.9691	+39126.36
5	3	-50.67474	-76.19243	-126.8672
	4	-5.557025	+1084.924	+1079.367
	5	-3233.435	+5023.486	+1790.051
	6	+23809.94	-13980.97	+9838.970

Table 5.1: Numerical values of $\rho_n^{(L)}$, the correction $\tilde{\rho}_n$, sub-leading in b, and $\rho_n^{(L**)}$ for $\tilde{R}$ with $N_f = 3, 4, 5$.

Order n	$\rho_n^{(L)}$	$\tilde{\rho}_n$	$\rho_n^{(L**)}$
3	-34.01647	-95.23157	-129.2480
4	+439.4560	+1049.853	+1489.309
5	-6007.231	+154.3490	-5852.882
6	+102412.4	-28652.47	+73759.93

Table 5.2: Numerical values of $\rho_n^{(L)}$, the correction $\tilde{\rho}_n$, sub-leading in b, and $\rho_n^{(L**)}$ for $\tilde{R}_\tau$ with $N_f = 3$.

k by $\tilde{\rho}_k$ we then have

$$\rho_k^{(L**)} = \rho_k^{(L)} + \tilde{\rho}_k \ , \tag{5.13}$$

for $k \geq 3$. For $\tilde{R}$ we tabulate the values of $\rho_k^{(L)}$, $\tilde{\rho}_k$ and $\rho_k^{(L**)}$ for $N_f = 3, 4, 5$ in Table 5.1. The values for $\tilde{R}_\tau$ are tabulated in Table 5.2.

For both observables the sub-leading in b contributions are found to be strongly flavour-dependent and often greater in magnitude and/or of opposite sign to $\rho_k^{(L)}$. A partial resummation of the analytical continuation terms is therefore not an effective procedure to improve fixed-order perturbation theory. This further supports our proposal to resum the analytical continuation terms to all-orders.

5.3 Numerical evaluation of the contour integral

In this section we shall reformulate the Taylor's theorem expansion approach of the last section to obtain a tractable method for numerically evaluating the contour integral, appropriate not only when $\tilde{D}$ is truncated at fixed-order in perturbation theory but crucially also allowing us to perform the RS-invariant all-orders resummation $\tilde{D}^{(L*)}$ of Section 4.3.

5.3.1 Contour-improved RS-invariant leading-b resummations

We now turn to the problem of evaluating the improved resummations $\tilde{R}^{(L**)}$ and $\tilde{R}_\tau^{(L**)}$, advocated in Section 4.5.1, where the contour integration of Eq.(5.1) is performed with $D^{(L*)}(se^{i\theta})$ in the integrand,

$$\hat{R}^{(L**)}(s_0) = \frac{1}{2\pi}\int_{-\pi}^{\pi} \mathrm{d}\theta\, W(\theta)\, \tilde{D}^{(L*)}(s_0 \mathrm{e}^{i\theta})\,. \tag{5.14}$$

To perform the contour integration numerically one can split the range from $\theta = 0, \pi$ into K steps of size $\Delta\theta \equiv \frac{\pi}{K}$, and perform a sum over the integrand evaluated at $\theta_n \equiv n\Delta\theta$ $n = 0, 1, \cdots, K$. So that

$$\hat{R}(s_0) \simeq \frac{\Delta\theta}{2\pi}\Big[W(0)\tilde{D}(s_0) + 2\mathrm{Re}\sum_{n=1}^{K} W(\theta_n)\tilde{D}(s_n)\Big]\,, \tag{5.15}$$

where $s_n \equiv s_0 e^{in\Delta\theta}$. In practice we perform a Simpson's Rule evaluation.

An efficient strategy [107] is to start with the exact $\tilde{D}(s_0)$ and evolve $\tilde{D}(s_n)$ to $\tilde{D}(s_{n+1})$ using Taylor's theorem. Thus defining $x_n \equiv \tilde{D}(s_n)$ we have

$$\begin{aligned} x_{n+1} \;=\; & x_n - \frac{i\Delta\theta}{2} b\rho(x_n) - \frac{(\Delta\theta)^2}{8} b^2 \rho(x_n)\rho'(x_n) \\ & + \frac{i(\Delta\theta)^3}{48} b^3 \Big\{ \rho(x_n)(\rho'(x_n))^2 + (\rho(x_n))^2 \rho''(x_n) \Big\} \\ & + \frac{(\Delta\theta)^4}{384} b^4 \Big\{ \rho(x_n)(\rho'(x_n))^3 + 4(\rho(x_n))^2\rho'(x_n)\rho''(x_n) + \rho(x_n)^3\rho'''(x_n) \Big\} \\ & + O(\Delta\theta)^5 + \cdots\,, \end{aligned} \tag{5.16}$$

analogous to Eq.(5.7). If Eq.(5.16) is truncated by retaining its first m terms one anticipates an error $\sim 1/K^{m-2}$ in Eq.(5.15).

Determining $\hat{R}^{(L**)}$ with this approach is now relatively straightforward. For some given $\Lambda_{\overline{\rm MS}}$ one evaluates $\tilde{D}^{(L*)}(s_0)$ of Section 4.3.2 as we have reviewed. The truncated Eq.(5.16) is then used to obtain $x_1 = \tilde{D}^{(L*)}(s_1)$. This requires $\rho^{(L*)}(x_0)$ and some number of derivatives. $\rho^{(L)}(x_0)$ can be determined given the $\tilde{D}^{(L)}(F)$ expressions, Eq.(4.40) and Eq.(4.41) [76], and using the numerical inversion route of Eq.(4.85) and Eq.(4.86). $\rho^{(L)\prime}$, $\rho^{(L)\prime\prime}$, $\cdots$ can then be obtained by successive differentiation of Eq.(4.85) with respect to x. One finds

$$\begin{aligned}
\rho^{(L)} &= -\tilde{D}^{(L)\prime}(F(x)) \\
\rho^{(L)\prime}(x) &= -\frac{\tilde{D}^{(L)\prime\prime}(F(x))}{\tilde{D}^{(L)\prime}(F(x))} \\
\rho^{(L)\prime\prime}(x) &= \frac{\left(\tilde{D}^{(L)\prime\prime}(F(x))\right)^2}{\left(\tilde{D}^{(L)\prime}(F(x))\right)^3} - \frac{\tilde{D}^{(L)\prime\prime\prime}(F(x))}{\left(\tilde{D}^{(L)\prime}(F(x))\right)^2} \\
\rho^{(L)\prime\prime\prime}(x) &= 4\frac{\left(\tilde{D}^{(L)\prime\prime}(F(x))\right)\left(\tilde{D}^{(L)\prime\prime\prime}(F(x))\right)}{\left(\tilde{D}^{(L)\prime}(F(x))\right)^4} - \frac{\tilde{D}^{(L)\prime\prime\prime\prime}(F(x))}{\left(\tilde{D}^{(L)\prime}(F(x))\right)^3} - 3\frac{\left(\tilde{D}^{(L)\prime\prime}(F(x))\right)^3}{\left(\tilde{D}^{(L)\prime}(F(x))\right)^5} \\
&\vdots
\end{aligned} \tag{5.17}$$

where primes denote differentiation with respect to F. Thus, once $F(x)$ has been determined from Eq.(4.85) no further transcendental equations need to be solved and the explicit expressions for $\tilde{D}^{(L)}(F)$ can be repeatedly differentiated to obtain $\rho^{(L)\prime}$, $\rho^{(L)\prime\prime}$, $\cdots$. Finally $\rho^{(L*)}$, $\rho^{(L*)\prime}$, $\rho^{(L*)\prime\prime}$, $\cdots$, can be obtained using Eq.(4.87) and its derivatives. For instance

$$\begin{aligned}
\rho^{(L*)} &= \rho^{(L)}(x) + cx^3 + \rho_2^{(NL)}x^4 \\
\rho^{(L*)\prime}(x) &= \rho^{(L)\prime}(x) + 3cx^2 + 4\rho_2^{(NL)}x^3 \\
\rho^{(L*)\prime\prime}(x) &= \rho^{(L)\prime\prime}(x) + 6cx + 12\rho_2^{(NL)}x^2 \\
\rho^{(L*)\prime\prime\prime}(x) &= \rho^{(L)\prime\prime\prime}(x) + 6c + 24\rho_2^{(NL)}x \\
&\vdots
\end{aligned} \tag{5.18}$$

where $\rho_2^{(NL)} \equiv \rho_2 - \rho_2^{(L)}$. The only remaining difficulty is that x_1 is now complex, and so at subsequent steps it is unclear how to obtain $\rho^{(L*)}(x_n)$, since $\tilde{D}^{(L)}(F)$ is only defined for real F. One needs to replace the $\mathrm{Ei}(x)$ defined in Eq.(A.6) by the generalized exponential integral functions $\mathrm{Ei}(n,w)$ for complex w, used to evaluate $\tilde{R}^{(L)}$ and $\tilde{R}_\tau^{(L)}$ in Eq.(4.44,4.45) and Eq.(4.49,4.50) [76]. These are defined for $\mathrm{Re}\, w > 0$ in Eq.(A.8). For $\mathrm{Re}\, w < 0$ they are

defined in Eq.(A.9) by analytical continuation to arrive at a function analytic everywhere in the cut complex w-plane except at $w = 0$, and with a branch cut running along the negative real axis.

To define $\tilde{D}^{(L)}(F)$ correctly for complex F one needs to make the replacement

$$\mathrm{Ei}(-Fz_l) \to -\mathrm{Ei}(1, Fz_l) \tag{5.19}$$

in Eq.(4.40) [76] for $\tilde{D}^{(L)}(F)|_{\mathrm{UV}}$. In Eq.(4.41) [76] for $\tilde{D}^{(L)}(F)|_{\mathrm{IR}}$ one replaces

$$\mathrm{Ei}(Fz_l) \to -\mathrm{Ei}(1, -Fz_l) + i\pi \mathrm{sign}(\mathrm{Im}Fz_l). \tag{5.20}$$

In this way as F becomes real one avoids $\pm i\pi$ contributions from the discontinuity across the branch cut along the negative real axis and re-obtains $\tilde{D}^{(L)}(F)$ for real argument.

With $\tilde{D}^{(L)}(F)$ re-defined for complex arguments in this way $x_1, x_2, \cdots$, can be successively obtained. At each step one needs to solve the complex-valued transcendental equation

$$\tilde{D}^{(L)}(F_n) = x_n \ , \tag{5.21}$$

and F_n is then used to construct $\rho^{(L*)}(x_n)$ and its derivatives using Eq.(5.17).

Before proceeding to consider the results of evaluating these "contour-improved" RS-invariant resummations, we remark on their ease of evaluation. Initially one requires an input value, the RS-invariant resummation $D^{(L*)}(s_0)$, to be evaluated by the methods discussed in Section 4.3.3. To evaluate $R^{(L**)}(s_0)$ we again truncate the expression for $\tilde{D}^{(L)}$, Eq.(4.40) and Eq.(4.41), retaining terms up to and including $\ell \simeq 10$ in both UV_ℓ and IR_ℓ summations. The computing time is dominated by that required for the solution of Eq.(5.21), and is comparable to that needed for the conventional approach in fixed-order perturbation theory, where the complex-valued integrated beta-function equation is numerically solved at each step. Since $D^{(L*)}(F_n)$ is defined for complex arguments, the time needed to solve Eq.(5.21) is longer than that of the comparable Eq.(4.85) used to evaluate the input value $D^{(L*)}(s_0)$. In response to this one can include a larger number of terms in Eq.(5.16), reducing the number of discrete steps K. Repeated symbolic differentiation of $\rho^{(L)}(x)$ was made possible using MAPLE. Nonetheless, higher order derivatives of $\rho^{(L)}(x)$ become increasingly time-consuming to numerically evaluate. The number of discrete steps, K, required depends on the convergence of Eq.(5.16) and through this on the size of $x_0 = D^{(L*)}(s_0)$. Therefore observables at lower energy scales require a greater number of discrete steps due to the inferior convergence of Eq.(5.16).

To evaluate $\tilde{R}$ and $\tilde{R}_\tau$ to four significant figure accuracy retaining the first four terms in Eq.(5.16) we required 100 steps; with the first five terms this is reduced to only 25 steps.

Using MAPLE on a HEWLETT-PACKARD 712/80 it took $\sim$ 1.5 hours (4 terms) and $\sim$ 0.75 hours (5 terms) to perform the resummation.

We have checked that evaluating the contour integral with $\tilde{D}^{(L)}$ and $\rho^{(L)}$ reproduces values in numerical agreement with the expressions for $\tilde{R}^{(L)}$ and $\tilde{R}_\tau^{(L)}$, Eq.(4.43) and Eq.(4.48) [76].

5.3.2 Contour-improved EC fixed-order resummations

We can consider evaluating "contour-improved" fixed-order results in the EC scheme using the n^{th} order truncations $\tilde{D}^{(L*)}(s_0)$ of Eq.(4.89). In this case $\rho(x)$ is taken to be $\rho^{(L*)(n)}(x)$, Eq.(4.90), the truncation of $\rho^{(L*)}(x)$ retaining terms up to x^{n+2}. The input $\tilde{D}^{(L*)(n)}(s_0)$ is obtained by solving Eq.(4.80) with the truncated $\rho^{(L*)}(x)$.

To perform the contour integral is now straightforward. With an input value $D^{(L*)(n)}(s_0)$ we calculate Eq.(5.16) as before replacing $\rho(x)$ and its derivatives by Eq.(4.90) and

$$\begin{aligned}
\rho^{(L*)(n)\prime}(x) &= 2x + 3cx^2 + 4\rho_2 x^3 + \sum_{k=3}^{n}(k+2)\rho_k^{(L)}x^{k+1} \\
\rho^{(L*)(n)\prime\prime}(x) &= 2 + 6cx + 12\rho_2 x^2 + \sum_{k=3}^{n}(k+1)(k+2)\rho_k^{(L)}x^k) \qquad (5.22) \\
&\vdots
\end{aligned}$$

respectively. We shall denote these contour-improved fixed-order results by $\tilde{R}^{(L**)[n]}(EC)$ and $\tilde{R}_\tau^{(L**)[n]}(EC)$ for $n \geq 3$, and for $n = 1, 2$ where the exact ρ_k are used by $\tilde{R}^{[n]}(EC)$ and $\tilde{R}_\tau^{[n]}(EC)$.

The method obviously can also be used to evaluate the contour integral when $\tilde{D}$ is represented by fixed-order perturbation theory in the coupling $a(s_0e^{i\theta})$,

$$\tilde{D}(s_0e^{i\theta}) = a(s_0e^{i\theta}) + d_1a^2(s_0e^{i\theta}) + d_2a^3(s_0e^{i\theta}) \; . \qquad (5.23)$$

One can start with $a(s_0)$ and evolve $a(s_n)$ to $a(s_{n+1})$ using Eq.(5.16) with $\rho(x)$ replaced by the truncated beta-function in the corresponding RS,

$$B(x) = x^2 + cx^3 + c_2x^4 \; . \qquad (5.24)$$

The resummations can then be straightforwardly and rapidly evaluated. In particular there is no transcendental equation (5.21), which dominates the computing time required for the resummation, to solve in the case of fixed-order perturbation theory.

In the $\overline{\rm MS}$ scheme at NNLO this is equivalent in approach to the resummation procedure performed by Le Diberder and Pich for R_τ [94]. Perturbative uncertainties are then reduced to $d_{i>2}$ and $c_{i>2}$ with the analytical continuation terms g_i, π^{2n} terms containing b, c or c_2, resummed to all-orders. Note that the resulting expression is not a polynomial in $a(s)$, even though only the three-loop expression for $\hat{D}$ is used. In standard approaches [78, 95] the contour integral is performed numerically by solving the integrated beta-function equation with complex renormalization scale s_n for $a(s_n)$ at each integration step, and takes much longer to evaluate. Reference [95] considers in some detail the RS dependence of the contour integral.

In the next section we shall compare the "contour-improved" RS-invariant resummations $\check{R}^{(L**)}$ and $\check{R}_\tau^{(L**)}$, with "contour-improved" fixed-order results $\check{R}^{(L**)[n]}(EC)$ and $\check{R}_\tau^{(L**)[n]}(EC)$.

These "contour-improved" evaluations are to be compared with conventional fixed-order perturbative truncations $\check{R}^{(L**)(n)}(EC)$ and $\check{R}_\tau^{(L**)(n)}(EC)$ obtained by integrating up the n^{th}-order truncated EC beta-functions $\rho^{R,R_\tau(L**)}$, with coefficients $\rho_k^{R,R_\tau(L**)}$ obtained using Eq.(C.9) and (C.10) in Appendix C.3, with the exact ρ_2^D and using $\rho_k^{D(L)}$ for $k > 2$. By truncating ρ^{R,R_τ} one omits an infinite set of exactly-known and numerically important analytical continuation terms which are included in the "contour-improved" resummations.

5.4 Numerical results

5.4.1 The reliability of "contour-improved" FOPT

In Figures 5.1(a)-(c), for $\sqrt{s} = 91, 5, 1.5$ GeV, respectively, we compare the "contour-improved" resummation $\check{R}^{(L**)}(s_0)$ with the two versions of fixed-order perturbation theory, "contour-improved" $\check{R}^{(L**)[n]}(EC)$ and conventional $\check{R}^{(L**)(n)}(EC)$ (for $n \geq 2$), described in the last section. Values of $\Lambda_{\overline{\rm MS}}^{(5)} = 200$ MeV, $\Lambda_{\overline{\rm MS}}^{(4)} = 279$ MeV and $\Lambda_{\overline{\rm MS}}^{(3)} = 320$ MeV are used. These assume flavour thresholds at $m_b = 4.5$ GeV and $m_c = 1.25$ GeV.

As can be seen at all energies and in low orders the "contour-improved" fixed-order results (denoted "+") are significantly closer to the resummation $\check{R}^{(L**)}$ (horizontal line) than the conventional fixed-order results (denoted "×"). This is completely understandable since both the RS-invariant resummations and the contour-improved fixed-order results sum to all-orders known analytical continuation terms, as discussed above. The unnecessary truncation of these terms evidently greatly worsens the performance of $n = 2$ NNLO fixed-

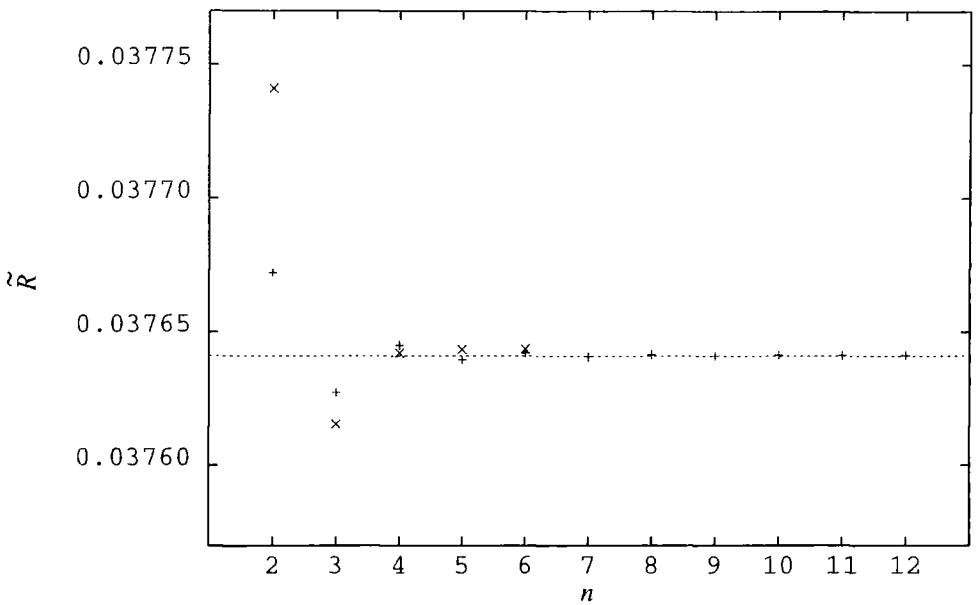

Figure 5.1(a): Comparison of two versions of fixed-order EC perturbation theory "contour-improved" $\tilde{R}^{(L**)[n]}(EC)$ ("+") and $\tilde{R}^{(L**)(n)}(EC)$ ("×") with the RS-invariant resummation $\tilde{R}^{(L**)}(s_0)$ (dashed line) at $\sqrt{s_0} = 91$ GeV.

order perturbation theory, whilst in higher orders both versions of fixed-order perturbation theory approach each other, and both track the RS-invariant resummation. Eventually, of course, both versions will breakdown as the leading UV_1 renormalon singularity asserts itself. Since $n = 2$ represents the highest order for which exact calculations exist at present, "contour-improvement" is clearly essential if reliable NNLO determinations of $\alpha_s(M_Z^2)$ are to be made.

In Figures 4.3(a)-4.3(c) of Chapter 4 we plotted $\tilde{D}^{(L*)}(s_0)$ (dashed line) and $\tilde{D}^{(L*)(n)}(EC)$ (denoted "+") at $\sqrt{s} = 91, 5, 1.5$ GeV, respectively. These represent the input values of $\tilde{D}(s_0)$ fed into the contour integration to produce the plots in Figures 5.1(a)-(c). For ease of comparsion they are plotted on the same vertical scales. In the Section 4.4.2 we noted that the fixed-order results in Figures 4.3(a)-4.3(c) show a clear oscillation above and below the resummed result. This is a reflection of the alternating sign factorial behaviour contributed by the leading UV_1 renormalon, which in the case of $\tilde{D}$ is a double pole, in the leading-b approximation. A similar oscillatory behaviour is also evident for the conventional fixed-order perturbative approximants for $\tilde{R}$ in Figures 5.1(a)-(c), but with much smaller amplitude. As explained in Section 4.4.2 this is because for $\tilde{R}$ the UV_1 singularity is softened to a single-pole, again in the leading-b approximation. As

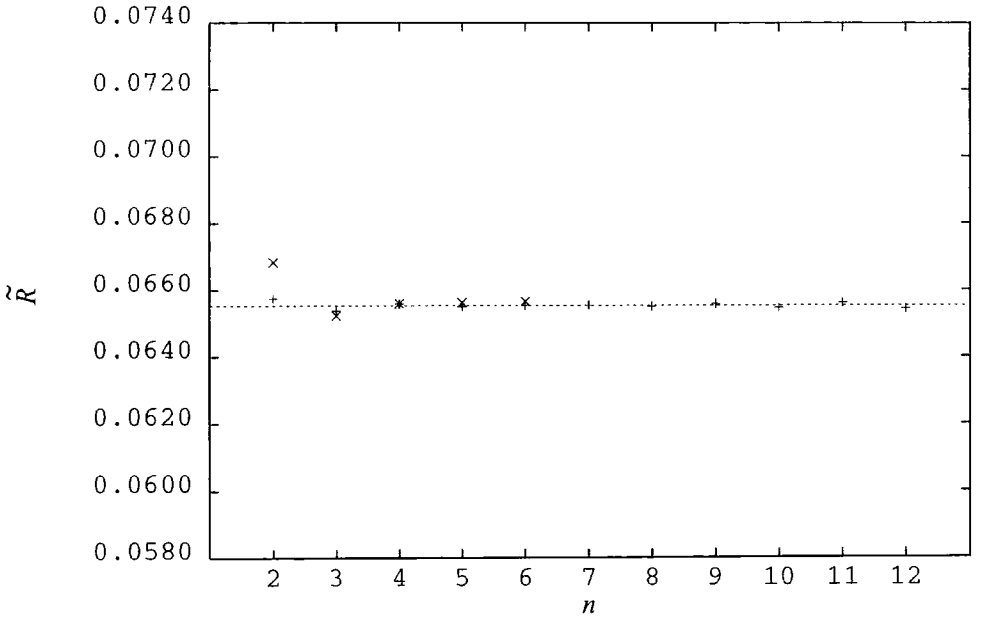

Figure 5.1(b): As for Figure 5.1(a) except at $\sqrt{s_0} = 5$ GeV.

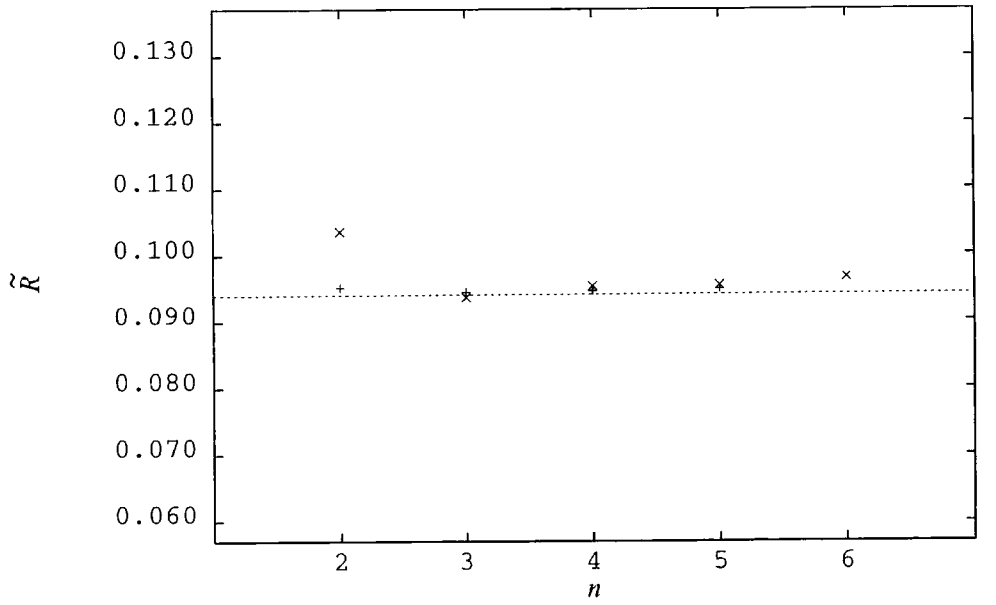

Figure 5.1(c): As for Figure 5.1(a) except at $\sqrt{s_0} = 1.5$ GeV

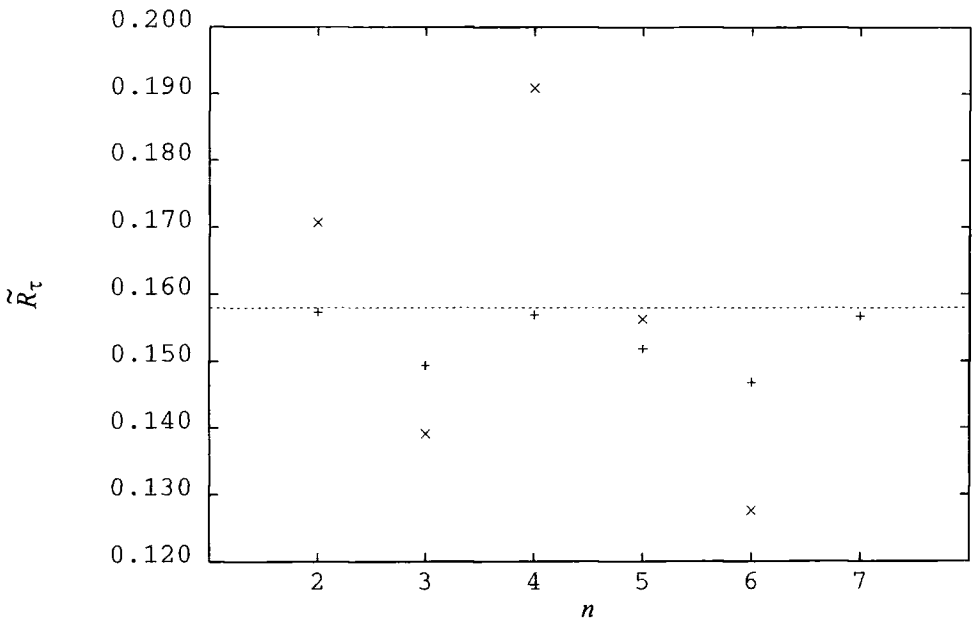

Figure 5.2: As for Figure 5.1(a) except for $\tilde{R}_\tau$ at $\sqrt{s_0} = 1.777$ GeV.

a result one expects $r_n/d_n \simeq \frac{1}{n}$ asymptotically [82, 64], and correspondingly $\rho_n^R/\rho_n^D \simeq \frac{1}{n}$. One intriguing effect of this is shown in Figure 5.1(c). We are unable to calculate the "contour-improved" fixed-order result $\tilde{R}^{(L**)[6]}(EC)$ since we lack the corresponding input value $D^{(L*)(6)}(EC)$. However, the conventional fixed-order perturbative truncation $\tilde{R}^{(L**)(6)}(EC)$ exists and can be calculated. This stems from the fact that perturbative coefficients for $D^{(L*)(n)}$ diverge faster than those of $R^{(L*)(n)}$ and as a result the perturbative series for $D^{(L*)(n)}$ breaks down more rapidly. Notice that the "contour-improved" fixed-order results which partially resum higher-order contributions do not exhibit the simple oscillatory behaviour observed for $D^{(L*)(n)}$. This contrasts with the situation that we were presented with in Figures 4.4(a)-4.4(c) of Section 4.4.2. There we observed that the fixed-order approximants $R^{(L*)(n)}$ did exhibit a simple oscillatory behaviour. Numerically this change is caused by the varying size of contributions to $\rho^{(L**)(n)}$ sub-leading in b; the exact numerical sign and magnitude of the sub-leading contributions is tabulated in Table 5.1.

In Figure 5.2 we give the analogous plot to Figures 5.1 for $\tilde{R}_\tau$, assuming $\Lambda_{\overline{\rm MS}}^{(3)} = 320$ MeV as before, $\sqrt{s_0} = 1.777$ GeV. If we compare with Figure 1(c) for $\tilde{R}$ at the comparable energy $\sqrt{s_0} = 1.5$ GeV, we see a deterioration in the behaviour of both versions of fixed-

order perturbation theory. The change of weight function from $W(\theta) = 1$ to $W_\tau = (1 + 2e^{i\theta} - 2e^{3i\theta} - e^{4i\theta})$ leads to much less convergent analytical continuation terms and the two versions of fixed-order perturbation theory no longer approach each other in higher orders. The contour-improved results are reasonably close to the resummation. This cannot be said of fixed-order results that only partially resum analytical continuation terms; they are a poor approximation to the resummed value. The simple oscillatory behaviour that was observed for $\hat{R}_\tau^{(L*)(n)}$ in Figure 4.5 has disappeared for $\hat{R}^{(L**)(n)}(EC)$ Again the "contour-improved" fixed-order results which partially resum higher-order contributions, $\hat{R}_\tau^{(L**)(n)}(EC)$, do not exhibit the simple oscillatory behaviour observed for $\hat{D}^{(L*)(n)}$ or for that matter $\hat{R}_\tau^{(L*)(n)}$ in Figure 4.5. This is again due to the sign and magnitude of sub-leading analytical continuation contributions, which are tabulated in Figure 5.2. Clearly "contour-improvement" is vital for reliable $\alpha_s(m_\tau^2)$ determinations.

5.4.2 Determining the uncertainty in $\Lambda_{\overline{\rm MS}}$ and α_s

We now wish to use the difference between the "contour-improved" $\hat{R}^{(L**)}$ and $\hat{R}^{[2]}(EC)$ to estimate the uncertainty with which $\alpha_s(M_Z^2)$ can be determined for the Minkowski observables. Our main interest will be in $\hat{R}_\tau$ which potentially gives the most accurate determination. To begin with, however, we consider $\hat{R}$ at $\sqrt{s} = M_Z$ (i.e. the hadronic decay width of the Z^0). As in our fits in Section 4.5.4 we shall take $\hat{R}(M_Z^2) = 0.040 \pm 0.004$. We obtain $\Lambda_{\overline{\rm MS}}^{(5)} = 298^{+235}_{-152}$ MeV and $\Lambda_{\overline{\rm MS}}^{(5)} = 297^{+233}_{-150}$ MeV for $\hat{R}^{(L**)}$ and $\hat{R}^{[2]}(EC)$, respectively. The fits to the three-loop NNLO $\overline{\rm MS}$ $\alpha_s(M_Z^2)$ are then $\alpha_s(M_Z^2) = 0.122 \pm 0.012$ from both $\hat{R}^{(L**)}$ and $\hat{R}^{[2]}(EC)$. This is also the same result as obtained in the Section 5.5.4 using $\hat{R}^{(L*)}$. So at this high energy scale the "contour-improvement" has little effect.

For R_τ we take $\hat{R}_\tau = 0.205 \pm 0.006$, as explained in Section 1.8.2. Fitting to the "contour-improved" RS-invariant resummation $\hat{R}_\tau^{(L**)}$ yields $\Lambda_{\overline{\rm MS}}^{(3)} = 429 \pm 12$ MeV and $\alpha_s(m_\tau^2) = 0.339 \pm 0.006$. Fitting to the "contour-improved" NNLO EC result $\hat{R}_\tau^{[2]}(EC)$ gives $\Lambda_{\overline{\rm MS}}^{(3)} = 450 \pm 16$ MeV and $\alpha_s(m_\tau^2) = 0.350 \pm 0.008$. To obtain $\alpha_s(M_Z^2)$ we evolved the three-loop (NNLO) coupling $\alpha_s^{\overline{\rm MS}}$ from $N_f = 3$ to $N_f = 5$ using Bernreuther-Wetzel matching [36], with quark masses at the bottom, middle and top of the range quoted in [41]. The results are tabulated in Table 5.3. Thus one can estimate an uncertainty $\delta\alpha_s(M_Z^2) \simeq 0.002$.

From Table 5.3 it can be noted that choosing running quark masses at the top or bottom of the range quoted in [41] creates a shift in $\alpha_s(M_Z^2)$ of $\sim$ 0.0008 or 0.7% from the central value. In the above analysis we use $s = m_q^2$ as the matching scale. To have some further estimate of the error involved in this process one could use $s = 4m_q^2$. This is

RS-invariant resummation	QCD parameter	Quark masses (GeV)		
		$m_c = 1.0$ $m_b = 4.1$	$m_c = 1.3$ $m_b = 4.3$	$m_c = 1.6$ $m_b = 4.5$
$\hat{R}_\tau^{(L**)}$	$\Lambda_{\overline{\rm MS}}^{(5)}$/MeV	301.5 ± 11.2	288.2 ± 10.5	278.6 ± 10.0
	$\alpha_s(M_Z^2)$	0.1222 ± 0.0007	0.1214 ± 0.0007	0.1207 ± 0.0007
$\hat{R}_\tau^{[2]}(EC)$	$\Lambda_{\overline{\rm MS}}^{(5)}$/MeV	320.6 ± 14.6	306.2 ± 13.6	295.9 ± 13.1
	$\alpha_s(M_Z^2)$	0.1234 ± 0.0009	0.1225 ± 0.0008	0.1218 ± 0.0008

Table 5.3: Values of $\Lambda_{\overline{\rm MS}}^{(5)}$ and 3-loop $\overline{\rm MS}$ $\alpha_s(M_Z^2)$, evolved from $\alpha_s(m_\tau^2)$ for a range of quark mass thresholds.

often motivated as the threshold energy scale required for virtual quark-antiquark pair production. It should be noted that this motivation is process-dependent and therefore not strictly relevant. Choosing this matching scale we have from Eq.(1.101)

$$a_{f-1}(2m) = a_f(2m) - \frac{\ln 4}{6} a_f(2m)^2 + \left(\frac{(\ln 4)^2}{36} - \frac{19 \ln 4}{24} + \frac{11}{72} \right) a_f(2m)^3 \,. \qquad (5.25)$$

With quark masses of $m_c = 1.3$ GeV and $m_b = 4.3$ GeV yields $\alpha_s(M_Z^2) = 0.1203 \pm 0.0008$ for $\hat{R}_\tau^{(L**)}$ and $\alpha_s(M_Z^2) = 0.1214 \pm 0.0007$ for $\hat{R}_\tau^{[2]}(EC)$; a downward shift in $\alpha_s(M_Z^2)$ of ~ 0.0011, or 0.8%. One can see that evolution through quark mass thresholds is somewhat arbitrary and creates an uncertainty $\delta\alpha_s(M_Z^2)$ comparable to that of unknown higher order perturbative corrections.

Using the recent calculation of the four-loop beta-function coefficient [49] and α_s^4 matching coefficients [110] reference [111] have studied in detail the induced errors in the evolution from $\alpha_s(m_\tau^2)$ to $\alpha_s(M_Z^2)$. By matching at α_s^4 the stability of the evolution with respect to changes in the threshold from $s = m_q^2$ to $s = 4m_q^2$ is greatly enhanced, since the residual dependences in the perturbative calculation are of order α_s^5. When consistent matching and running are used the error is reduced to $\delta\alpha_s(M_Z^2) < 0.0005$. Further it is found that the result with matching at α_s^4 is almost equivalent to matching at α_s^3 with $s = m_q^2$, for which choice there are no large logarithms.

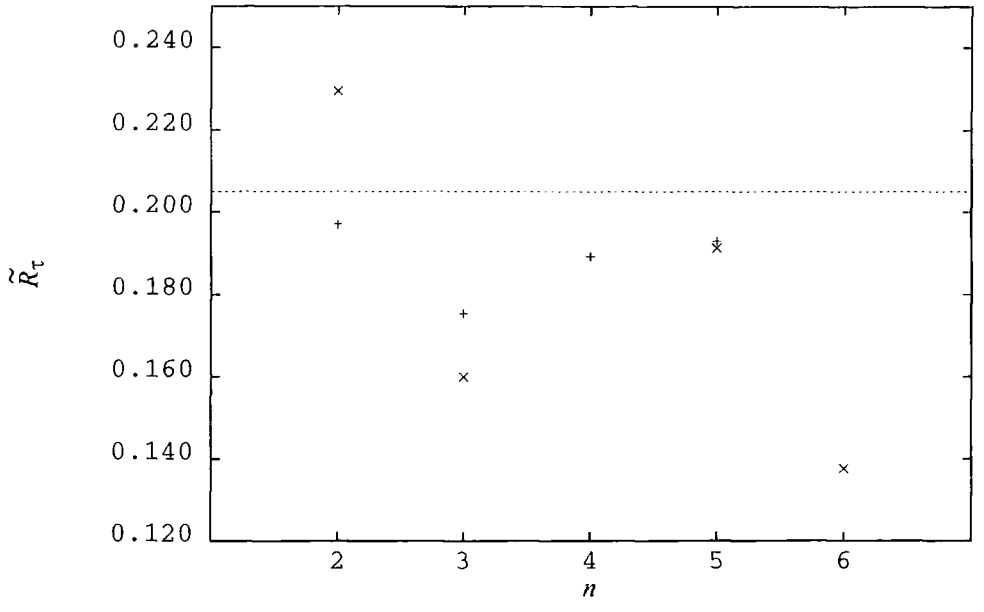

Figure 5.3(a): As for Figure 5.2(a) except $\tilde{R}_\tau^{(L**)}(EC)$ is fitted to $\tilde{R}_\tau^{data} = 0.205$ at $\sqrt{s_0} = 1.777$ GeV.

In Section 4.4.4 we fitted to the same value of $\tilde{R}_\tau$ using the RS-invariant resummation $\tilde{R}_\tau^{(L*)}$ which only includes analytical continuation terms at the leading-b level, and found $\alpha_s(m_\tau^2) = 0.328 \pm 0.005$, similarly fitting to NNLO EC fixed-order perturbation theory gave $\alpha_s(m_\tau^2) = 0.320 \pm 0.005$. In both cases the inclusion of exactly known analytical continuation terms involving $c, \rho_2, \cdots$, via the "contour-improvement" serves to significantly increase the fitted $\alpha_s(m_\tau^2)$, and hence slightly increase $\alpha_s(M_Z^2)$.

In Figure 5.3(a) we repeat the plot of Figure 5.2 but with the increased value of $\Lambda_{\overline{\rm MS}}^{(3)} = 429$ MeV, which results from fitting $\tilde{R}_\tau^{(L**)}$ to the data for $\tilde{R}_\tau$. A marked deterioration in the performance of both versions of fixed-order perturbation theory is evident, although the "contour-improved" fixed-order results are still significantly closer to the resummation. This serves as a warning that, at this low energy scale, relatively small changes in $m_\tau^2/(\Lambda_{\overline{\rm MS}}^{(3)})^2$ can produce significant changes in the accuracy of perturbation theory. Figure 5.3(b) represents the input values of $\tilde{D}(s_0)$ fed into the contour integration to produce the points in Figures 5.3(a). Notice how the simple oscillatory behaviour observed in $\tilde{D}(s_0)$ is destroyed by the analytical continuation terms.

In Figure 5.4 we extend the fits reported earlier. For $0.16 < \tilde{R}_\tau < 0.25$ we plot curves for the $\alpha_s(m_\tau^2)$ obtained by fitting $\tilde{R}_\tau^{(2)}(EC)$ (dotted curve), $\tilde{R}_\tau^{(L**)}$ (solid curve), $\tilde{R}_\tau^{[2]}(EC)$

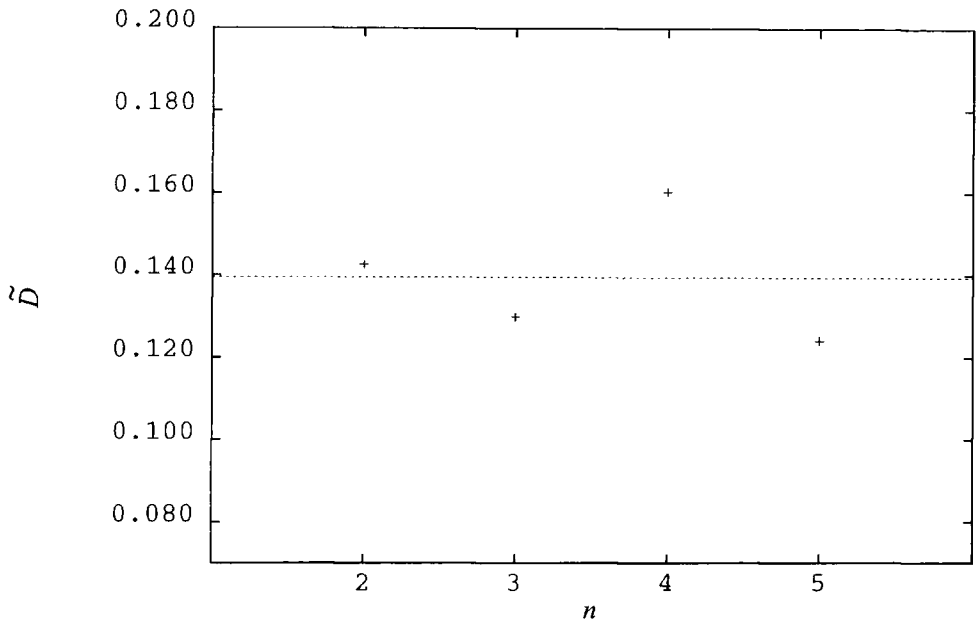

Figure 5.3(b): Comparison of fixed-order EC perturbation theory $\tilde{D}^{(L*)(n)}(EC)$ ("+") with the RS-invariant resummation $\tilde{D}^{(L*)}(s_0)$ (dashed line) at $\sqrt{s_0} = 91$ GeV with $\sqrt{s_0} = 1.777$ GeV and $\Lambda^{(3)}_{\overline{\rm MS}} = 429$ MeV.

(dashed curve), to this value. $\delta\alpha_s(m_\tau^2)$ can then be estimated for given $\tilde{R}_\tau$ from the difference between the lower two "contour-improved" curves. Clearly $\delta\alpha_s(m_\tau^2)$ increases very rapidly as $\tilde{R}_\tau$ increases. We are very fortunate that apparently $\tilde{R}_\tau \sim 0.2$, for which $\delta\alpha_s(m_\tau^2) \simeq 0.01$. We lie in a compromise region where the coupling $\alpha_s(m_\tau^2)$ is large enough that R_τ is sensitive to its value, but no so large that the perturbative expansion diverges.

We can compare the RS-invariant resummation $\tilde{R}_\tau^{(L**)}$ with the results obtained using a Le-Diberder Pich (LP) resummation [94], that is evaluating the contour integral with $\tilde{D}(m_\tau^2 e^{i\theta})$ as in Eq.(5.23). Fitting $\tilde{R}_\tau = 0.205 \pm 0.006$ to this $\tilde{R}_\tau^{[2]}(\overline{\rm MS})$ yields $\Lambda^{(3)}_{\overline{\rm MS}} = 469 \pm 16$ MeV and $\alpha_s(m_\tau^2) = 0.359 \pm 0.008$ in reasonable accord with the NNLO EC "contour-improved" value $\alpha_s(m_\tau^2) = 0.350 \pm 0.008$.

Fitting to conventional NNLO fixed-order perturbation theory in the $\overline{\rm MS}$ scheme $\tilde{R}_\tau^{(2)}(\overline{\rm MS})$, with $\mu = m_\tau$, yields $\alpha_s(m_\tau^2) = 0.342 \pm 0.006$. No special significance should be ascribed to the numerical coincidence that this is close to the RS-invariant resummation fit, $\alpha_s(m_\tau^2) = 0.339 \pm 0.006$. Crucially these $\overline{\rm MS}$ fits are strongly dependent on the assumed RS. In Figure 5.5 we show the $\tilde{R}_\tau$ versus $\alpha_s(m_\tau^2)$ plots with three choices of scale $\mu = 2m_\tau, m_\tau, \frac{1}{2}m_\tau$ (labelled 1, 2, 3, respectively). We also plot the curves for fitting to a

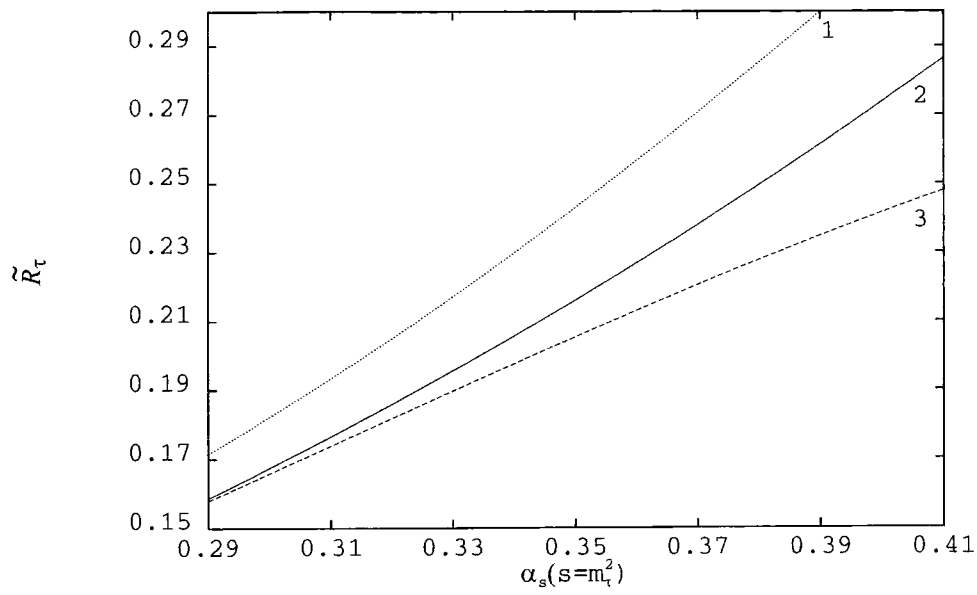

Figure 5.4: $\tilde{R}_\tau$ versus $\alpha_s(m_\tau^2)$ for $\tilde{R}_\tau^{(2)}(EC)$ (labelled 1), $\tilde{R}_\tau^{(L**)}$ (labelled 2) and $\tilde{R}_\tau^{[2]}(EC)$ (labelled 3).

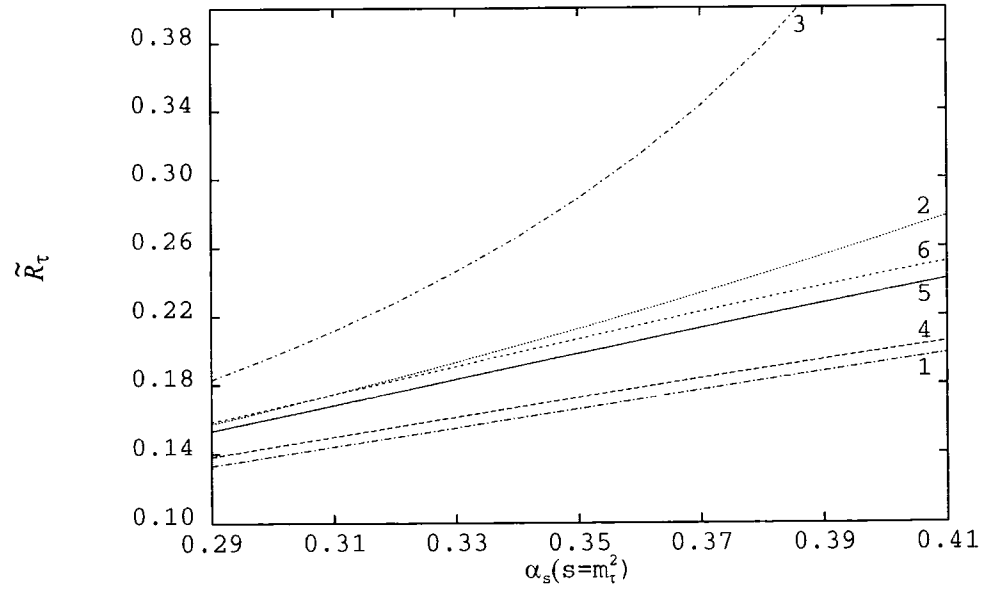

Figure 5.5: $\tilde{R}_\tau$ versus $\alpha_s(m_\tau^2)$ for $\tilde{R}_\tau^{(2)}(\overline{\rm MS})$ and $\tilde{R}_\tau^{[2]}(\overline{\rm MS})$, with three choices of scale $\mu = 2m_\tau, m_\tau, \frac{1}{2}m_\tau$; labelled (1, 2, 3) and (4, 5, 6) respectively.

LP resummation based on the NNLO $\overline{\rm MS}$ expansion of $\tilde{D}(m_\tau^2 e^{i\theta})$ in $a(4m_\tau^2 e^{i\theta})$, $a(m_\tau^2 e^{i\theta})$ and $a(\frac{1}{4}m_\tau^2 e^{i\theta})$ (labelled 4, 5, 6, respectively). As can be seen the $\tilde{R}_\tau^{(2)}(\overline{\rm MS})$ curves for different scales are very widely separated. Fitting to $\tilde{R}_\tau^{(2)}(\overline{\rm MS})$ to $\tilde{R}_\tau^{data} = 0.205$ with $\mu = 2m_\tau$ and $\frac{1}{2}m_\tau$ yields $\alpha_s(4m_\tau^2) = 0.278$ and $\alpha_s(\frac{1}{4}m_\tau^2) = 0.502$, for the two choices of RS. Evolving these all to m_τ using the three-loop $\overline{\rm MS}$ beta-function one obtains $\alpha_s(m_\tau^2) = 0.424$ and 0.305, respectively. For the LP resummation we find that $\alpha_s(4m_\tau^2) = 0.273$ and $\alpha_s(\frac{1}{4}m_\tau^2) = 0.659$. Evolving these to m_τ we find $\alpha_s(m_\tau^2) = 0.411$ and 0.348, respectively. The scale dependence of the LP resummations is seen to be much reduced compared to conventional fixed-order $\overline{\rm MS}$ perturbation theory, but is still significant.

5.4.3 Numerical parametrizations for $\tilde{R}_\tau^{(L**)}$, $\tilde{R}_\tau^{[2]}(EC)$ and $\tilde{R}_\tau^{[2]}(\overline{\rm MS})$

For convenience we now present simple numerical parametrizations for the contour-improved resummations $\tilde{R}_\tau^{(L**)}$, $\tilde{R}_\tau^{[2]}(EC)$ and LP (i.e. $\tilde{R}_\tau^{[2]}(\overline{\rm MS})$ based on an expansion in $a(m_\tau^2 e^{i\theta})$), in terms of $\alpha_s(m_\tau^2)$. We stress that $\alpha_s(m_\tau^2)$ denotes the 3-loop NNLO $\overline{\rm MS}$ coupling with scale $\mu = m_\tau$.

Given $x = \tilde{R}_\tau$ (data) the fitted $\alpha_s(m_\tau^2)$ is parametrized by

$$\alpha_s(m_\tau^2) = \pi x + A_2 x^2 + A_3 x^3 + A_4 x^4 \,. \tag{5.26}$$

The numerical coefficients A_i for the different "contour-improved" versions of perturbation theory are tabulated in Table 5.4. These coefficients give $\alpha_s(m_\tau^2)$ to a numerical accuracy of three significant figures over the range $0.16 \le \tilde{R}_\tau \le 0.25$ covered in Figure 5.5.

We also present reverse fits. Given $x = \alpha_s(m_\tau^2)$ the different approximations for $\tilde{R}_\tau$ are parametrized by

$$\tilde{R}_\tau = \frac{1}{\pi} x + \bar{A}_2 x^2 + \bar{A}_3 x^3 + \bar{A}_4 x^4 \,. \tag{5.27}$$

The numerical coefficients $\bar{A}_i$ are again tabulated in Table 5.4. $\tilde{R}_\tau$ is accurate to three significant figures over the range $0.29 < \alpha_s(m_\tau^2) < 0.41$.

5.4.4 The RS-dependence of the 'naive' resummation for R_τ

Finally in this section we wish to examine the performance of a straightforward leading-b resummation for $\tilde{R}_\tau$. To emphasize the associated RS ambiguity we shall evaluate it for three $\overline{\rm MS}$ scales $\mu = \lambda m_\tau$, where $\lambda = \frac{1}{2}, 1, 2$, as before. We then evaluate

$$\tilde{R}_\tau^{(L)}(F(a)) + r_1^{\tau(NL)} a^2 + r_2^{\tau(NL)} a^3 \,. \tag{5.28}$$

Perturbative approximation	A_i			$\bar{A}_i$		
	A_2	A_3	A_4	$\bar{A}_2$	$\bar{A}_3$	$\bar{A}_4$
$\check{R}_\tau^{(L**)}$	-13.23	+38.87	-47.44	+.6146	+.2099	+1.352
$\check{R}_\tau^{[2]}(EC)$	-13.61	+39.75	-36.71	+.09813	+4.504	-7.414
$\check{R}_\tau^{[2]}(\overline{\rm MS})$	-13.92	+45.55	-52.19	+.4319	+2.121	-3.823

Table 5.4: Numerical coefficients A_i and $\bar{A}_i$ to parametrize $\alpha_s(m_\tau^2)$, given $x = \tilde{R}_\tau$, and $\tilde{R}_\tau$, given $x = \alpha_s(m_\tau^2)$, respectively, for perturbative approximations $\tilde{R}_\tau^{(L**)}$, $\tilde{R}_\tau^{[2]}(EC)$ and $\tilde{R}_\tau^{[2]}(\overline{\rm MS})$.

Here a denotes the $\overline{\rm MS}$ coupling $a(\lambda^2 m_\tau^2)$, and

$$\begin{aligned} F(a) &\equiv \frac{1}{a} - b(\ln\lambda + \frac{5}{6}) \\ r_i^{\tau(NL)} &\equiv r_i^\tau - r_i^{\tau(L)} \ . \end{aligned}$$

$\check{R}_\tau^{(L)}(F)$ is given by the explicit expressions in Eq.(4.49) and (4.50) [76]. The extra terms ensure that at NLO and NNLO the exactly known r_1^τ, r_2^τ are included in the resummation.

Fitting Eq.(5.28) to $\tilde{R}_\tau = 0.205$ as before yields $\alpha_s(\frac{1}{4}m_\tau^2) = 0.475$, $\alpha_s(m_\tau^2) = 0.306$, and $\alpha_s(4m_\tau^2) = 0.233$, for the three choices of RS. Evolving these all to m_τ using the three-loop $\overline{\rm MS}$ beta-function, which is presumably appropriate since we are including the exact fixed-order results to NNLO, one obtains $\alpha_s(m_\tau^2) = 0.297, 0.306, 0.322$, respectively. Even if we restrict the beta-function to the one-loop leading-b level, as advocated in references [62, 69, 78], we obtain $\alpha_s(m_\tau^2) = 0.323, 0.306, 0.304$. Only if we leave out the NL correction terms in Eq.(5.28) and perform a pure leading-b resummation do we uniquely obtain $\alpha_s(m_\tau^2) = 0.305$ for all three RS's.

5.5 Summary and conclusions

The essential point which motivates our approach is that the basic ingredient out of which the Minkowski observables $\hat{R}$ are built is the EC beta-function $\rho(\tilde{D}(s))$ defined in Eq.(5.4). Using Eq.(1.60) one can see that this is proportional to $\frac{d^2}{d\ln s^2}\Pi(s)$, where $\Pi(s)$ is the fundamental correlator of two vector currents in the Euclidean region defined in Eq.(1.59). If one specifies $\rho(x)$, then given the NLO perturbative coefficient $d_1^{\overline{\rm MS}}(\mu^2 = s_0)$ and assuming some value of $\Lambda_{\overline{\rm MS}}$, $\tilde{D}(s_0)$ can be obtained unambiguously on solving Eq.(4.80). There is no scale dependence since $\tilde{D}(s_0)$ only involves the RS-invariant combination $\rho_0(s_0)$ in Eq.(2.76). Using Eq.(5.7) $\hat{R}(s_0)$ is then also uniquely specified given $\rho(x)$, where in practice the infinite sum is performed by numerically evaluating the contour integral, using

$\rho(x)$ to evolve $\check{D}(se^{i\theta})$ around the circular contour of integration, as described in Section 5.3.1

Of course, the function $\rho(x)$ is not known exactly. From NNLO calculations all that is known is the first three terms in its power series expansion,

$$\rho(x) = x^2 + cx^3 + \rho_2 x^4 + \cdots . \tag{5.29}$$

The uncertainty in predicting $\hat{R}(s_0)$ is then to be estimated by making some approximations for the unknown higher order terms indicated by the ellipsis in Eq.(5.29). We have chosen to approximate ρ_k by $\rho_k^{(L)}$ for $k \geq 3$. These leading-b contributions exactly reproduce ρ_k in the large-N_f limit, and, as shown in Section 4.2.1, for ρ_2 are a good approximation in the large-N (or $N_f \simeq 0$) limit.

Comparing the predictions for $\check{R}_\tau$ constructed from the NNLO $\rho(x)$ in Eq.(5.29) and the leading-b resummation indicates a moderate uncertainty $\delta\alpha_s(m_\tau^2) \simeq 0.01$ for $\check{R}_\tau \simeq 0.2$, which evolves up to $\delta\alpha_s(M_Z^2) \simeq 0.002$ and a central value $\alpha_s(M_Z^2) = 0.122$ in the $\overline{\text{MS}}$ scheme in line with other α_s measurements, which indicate a global average $\alpha_s(M_Z^2) = 0.118 \pm 0.005$ [34], as stated in Section 1.9.

Our reassuringly small uncertainty $\delta\alpha_s(m_\tau^2) \simeq 0.01$ is in stark contrast to other more pessimistic claims in the literature. Application of straightforward leading-b resummations compared to exact NNLO fixed-order perturbation theory leads to a claim of $\delta\alpha_s(m_\tau^2) \simeq 0.05$ in reference [79]. As we showed in Section 5.4.3, however, there is a matching problem if one wishes to include the exactly known NLO and NNLO coefficients. As a result the $\delta\alpha_s(m_\tau^2)$ estimate depends strongly on the renormalization scale chosen. This difficulty is avoided in our RS-invariant resummation approach, and originally motivated it.

In reference [108] an overall uncertainty of $\delta\alpha_s(m_\tau^2) \simeq 0.06$ is claimed. These authors use an LP resummation together with an acceleration technique applied to the perturbation series to lessen the influence of the leading UV_1 renormalon. The resulting uncertainty is dominated by the choice of renormalization scale μ. As we have pointed out above the only uncertainty in $\check{R}_\tau$ is due to our lack of knowledge of the uncalculated RS-invariants $\rho_3, \rho_4, \cdots$. Thus there is no scale dependence ambiguity. Since it is $\rho(x)$ which is ambiguous one could attempt to improve the convergence of this series. The corresponding Borel transform has a UV_1 renormalon and one could try to use acceleration methods. Crucially, however, the resulting uncertainties would have to do with real ambiguities associated with the singularities of the Borel transform of $\rho(x)$ in the Borel plane, and would not involve the unphysical and irrelevant renormalization scale μ. The same criticism applies to reference [109] which uses similar techniques to assess the perturbative

ambiguity in $\hat{R}$.

We should stress that these attempts to estimate the uncertainty in $\alpha_s(M_Z^2)$ have concentrated on approximating the contribution of uncalculated higher order terms in perturbation theory by performing a leading-b resummation. Strictly speaking power corrections cannot be estimated independently of this perturbative resummation, as we have attempted to do here, since their definition depends on the way in which the IR renormalon singularities are regulated. Fortunately, however, the dominant power corrections, estimated as in reference [78], come from the leading quark mass corrections proportional to m_τ^{-2}, which are not connected with the IR renormalons. The resummation is dominated by the leading UV_1 ultraviolet renormalon and so the ambiguity in the definition of the m_τ^{-6} and m_τ^{-8} power corrections should not be a serious source of extra uncertainty.

We therefore conclude that there is no reason to suppose that $\tilde{R}_\tau$ suffers from serious ambiguities due to $\mathrm{N^3LO}$ and higher terms which have yet to be exactly calculated. The techniques on which existing claims to this effect have been based are all severely RS-dependent, and their conclusions can be modified at will by making different ad hoc choices of renormalization scale.

Chapter 6

Conclusions

The purpose of this thesis has been to investigate the way in which we can utilize perturbation theory to broaden our understanding of Quantum Chromodynamics (QCD). By increasing the accuracy and reliability of perturbative calculations we strive to reinforce our confidence in QCD as the fundamental quantum field theory of strong interactions. Moreover, by refining the predictive power of perturbative QCD, we hope enhance our ability to uncover new phenomena and discover links between the perturbative and non-perturbative regimes of the theory.

To this aim considerable phenomenological activity is directed to the precision measurement of the renormalized QCD coupling $\alpha_s(M_Z^2)$ (or alternatively the fundamental dimensional transmutation mass parameter $\Lambda_{\overline{\rm MS}}$). Notwithstanding the many successes of renormalization group (RG) improved perturbation theory, applied at next-to-leading order (NLO) or more recently at next-to-NLO (NNLO), the accurate measurement of $\alpha_s(M_Z^2)$ is still plagued by a variety of problems.

To see this more clearly we focussed to an extent in the thesis on the specific, and highly relevant, example of the determination of $\alpha_s(M_Z^2)$ from the hadronic tau decay ratio R_τ. R_τ has many theoretical advantages as a observable with which to accurately measure $\alpha_s(M_Z^2)$: the existence of an exact NNLO calculation; small estimated non-perturbative power corrections; and a greatly reduced fractional error in $\alpha_s(M_Z^2)$ resulting from the evolution up in energy scale from $\alpha_s(m_\tau^2)$. These conspire to make R_τ potentially one of the most precise methods available for measuring $\alpha_s(M_Z^2)$.

Nonetheless, for low energy observables such as R_τ the QCD coupling α_s is sufficiently large to lead one to question the reliability of the perturbative prediction. Our concerns can be split into the following categories:

- The expectation of sizeable corrections from uncalculated N^3LO and higher orders in fixed-order perturbation theory.
- The knowledge that QCD perturbation theory is an asymptotic power series, and as such the next order calculation may well lead to no improvement, or even worse a deterioration, in the existing result.
- The potentially strong dependence of the prediction on the renormalization scale at NLO, and in higher orders on the renormalization scheme (RS). The extent of ambiguities connected with the violation of RS-invariance is often not fully appreciated.
- The possible ambiguities associated with the truncation at NNLO of the contour integral representation of R_τ.

Of course in reality these potential obstacles to an accurate determination of α_s are strongly entwined. In this thesis we have attempted to comment on these concerns and to provide a formalism for disentangling and quantifying each effect separately. In doing this we aim to provide a measure of confidence in the reliability of QCD perturbation theory.

The key point in our analysis is the existence in massless QCD of a set of RS-invariant quantities constructed from perturbative Feynman diagram calculations. Together these completely determine the physical observable.

To utilize this concept we introduced the effective charge (EC) formalism in Chapter 2. The EC formalism is a sophisticated extension of RG-improved perturbation theory, expressed in terms of a set of physically motivated RS-invariant quantities $\rho_0, \rho_2, \ldots, \rho_k, \ldots$. The information content of the Feynman diagram calculation is completely contained in this set of quantities. Furthermore, we can non-perturbatively identify each observable with an effective charge — an all-orders coupling. Consequently both coupling and beta-function are experimental observables. Given the EC beta-function $\rho(x)$ and a value for ρ_0, the observable R is unambiguously fixed. Our knowledge of $\rho(x)$ can be increased from perturbation theory and independently from measurements of the running of R, and then their consistency checked without the introduction of matching ambiguities.

Of course the technical difficulties of calculating higher-order QCD perturbative coefficients using Feynman diagrammatics are considerable. A present trend is to avoid explicit calculation and instead to improve the result by making use of some, necessarily approximate, all-orders resummation of the QCD perturbation series.

To resum perturbation theory we should use as many exact RS-invariants as are known — ρ_0 and ρ_2 for the observables discussed in this thesis — and approximate the remainder. In this way the maximum information is included in an RS-invariant manner. The exact QCD RG can be used to recover approximate fixed-order results in any RS if required. The accuracy of the resummation is then entirely dependent on how well the unknown RS invariants are approximated. The question is, of course, how one should approximate these unknown quantities.

A well motivated approach is provided by the "leading-b" expansion, where b is the first QCD beta-function coefficient, which we reviewed in Chapter 4. This approximation is sometimes referred to as "naive non-abelianization". The leading-b expansion is an attempt to generalize Dyson summation in the abelian theory of QED to the case of non-abelian QCD. Both the leading-b expansion and the analogous "large-N_f" in QED are motivated as an attempt to resum to all-orders the perturbative corrections contributed by the "renormalon" singularity structure in the Borel plane. As discussed in Chapter 3, renormalon singularities encode the large-order behaviour of the perturbative expansion coefficients induced by the insertion of a single chains of fermion vacuum polarization bubbles in QED.

Unfortunately, the resulting approximate perturbative coefficients obtained by inserting single chains of effective gluon vacuum polarization bubbles in QCD has an ambiguity. For instance in the background field method there is a quantum gauge (ξ_q) dependence. Crucially, however, the RS-invariants ρ_k are unambiguously determined. The ambiguity in the perturbative coefficients can be absorbed into the choice of renormalization scale and hence cancels in the RS-invariants.

Past 'naive' leading-b resummations have focussed on approximating the perturbative coefficients. Not only are these ambiguous (ξ_q-dependent) but in addition are RS-dependent so that the exact RG invariance is violated by the approximation. Any attempt to include the exact NLO and NNLO coefficients will introduce a sizeable matching ambiguity, as we demonstrated for the example of R_τ in Chapter 5.

In Chapter 4 we proposed an improvement of the renormalon-inspired leading-b resummation of QCD perturbation theory based on the EC formalism. The strategy is based on approximating the unknown RS-invariant EC beta-function coefficients by the portion containing the highest power of b, for SU(N) QCD with N_f quark flavours. The leading-b effective charge beta-function can be resummed using exact all-orders large-N_f results These leading-b contributions exactly reproduce ρ_k in the large-N_f limit, and for ρ_2 are a

good approximation in the large-N colour (or $N_f \simeq 0$) limit.

We then implemented the RS-invariant resummation programme in earnest for a number of QCD observables. The RS-invariant resummation was performed for the Adler D-function, e^+e^- R-ratio, hadronic tau-decay ratio R_τ, and DIS sum rules. We assessed the reliability of fixed-order perturbation theory for each of the observables by comparing the RS-invariant resummation with the exact NNLO results in the EC RS. This provides an assessment of the importance of unknown higher-order perturbative corrections. We discussed the deterioration in the accuracy of fixed-order perturbation theory as the energy scale was reduced.

For the Minkowski quantities, the R-ratio and R_τ, where large-order perturbative behaviour is dominated by a leading UV_1 renormalon singularity, the comparison indicated fixed-order perturbation theory to be very reliable. Comparison with fixed-order perturbation theory revealed impressive convergence to the resummed result for the e^+e^- R-ratio at LEP energies. As the energy scale was reduced the oscillatory behaviour of the fixed-order results above and below the resummed prediction became increasingly apparent, reflecting the alternating-sign factorial growth of the perturbative coefficients resulting from a dominant UV_1 renormalon singularity.

For R_τ, which is also UV_1 dominated, there was also a satisfactory approximation to the resummed value, although with much larger oscillations than for R at a comparable energy scale, and with an earlier breakdown of perturbation theory. This can be attributed to the IR_3 and IR_4 renormalon being double poles in the leading-b approximation.

In contrast for DIS sum rules, which have a leading IR_1 infra-red singularity, the performance is somewhat poor. Successive orders move steadily away from the resummed result, reflecting the fixed-sign factorial growth of the coefficients.

In Chapter 5 we considered the QCD Minkowski observables R and R_τ in more detail. We showed that the fundamental building block for these quantities is the vector correlator $\Pi(s)$, or equivalently the Euclidean Adler D-function. Once $\rho(x)$ and a value for ρ_0 are specified for D, R and R_τ are unambiguously determined on using a contour-integral representation for the Minkowski observables. An efficient numerical algorithm was presented for evaluating R, R_τ from a weighted contour integration of $D(se^{i\theta})$ around a circle in the complex squared energy s-plane, with $\rho(x)$ used to evolve in s around the contour of integration. In this way additional analytical continuation terms not captured in the original RS-invariant leading-b resummation are included exactly.

In Chapter 5 we used the difference between the "contour-improved" NNLO EC resummation and the "contour-improved" RS-invariant resummation to estimate the uncertainty in $\alpha_s(M_Z^2)$ due to uncalculated higher order corrections for R and R_τ. Furthermore, the comparison of these calculations with the original RS-invariant resummation and exact NNLO fixed-order results in the EC RS is indicative of the size of analytical continuation terms omitted in the conventional approach.

Comparing the predictions for $\check{R}_\tau$ constructed from the NNLO $\rho(x)$ and the leading-b resummation indicates a moderate uncertainty $\delta\alpha_s(m_\tau^2) \simeq 0.01$ for $\check{R}_\tau \simeq 0.2$, which evolves up to $\delta\alpha_s(M_Z^2) \simeq 0.002$ and a central value $\alpha_s(M_Z^2) = 0.122$ in the $\overline{\rm MS}$ scheme in line with the global average $\alpha_s(M_Z^2) = 0.118 \pm 0.005$. The significant effect of the analytical continuation terms, changing the central value of $\alpha_s(m_\tau^2)$ by 0.02, emphasised the potentially large contributions from higher-order beta-function coefficients. In our view it is essential to numerically perform the contour integral rather than truncate the expansion at NNLO.

Our reassuringly moderate uncertainty $\delta\alpha_s(m_\tau^2) \simeq 0.01$ sharply contrasts with other more pessimistic claims in the literature, which estimate the uncertainty in $\alpha_s(M_Z^2)$ to be same order as that quoted in determinations from jet observables at LEP and SLD.

As we have mentioned, however, there is a serious matching problem if one wishes to include the exactly known NLO and NNLO coefficients at the scale m_τ^2. The resulting uncertainty $\delta\alpha_s(m_\tau^2)$ is then strongly dependent on the choice of renormalization scale. Therefore the techniques on which existing claims have been based are all severely RS-dependent, and their conclusions can be modified at will by making different ad hoc choices of renormalization scale. In our view this makes the comparison of the 'naive' all-orders resummation with fixed-order perturbative theory misleading and invalidates the conclusions of these references.

We therefore see that there is no reason to suppose that $\check{R}_\tau$ suffers from serious ambiguities due to unknown higher order perturbative corrections.

We stress that this attempt to estimate the uncertainty in $\alpha_s(M_Z^2)$ has been performed in the conventional framework where the unknown higher-order perturbative corrections are assumed to be the dominant theoretical error. Of course in reality there are other uncertainties which are at least as important as that due to uncalculated higher order corrections deduced here. For instance the evolution from $\alpha_s(m_\tau^2)$ to $\alpha_s(M_Z^2)$ may introduce uncertainties of the same order due to the treatment of quark mass thresholds. More seriously there may be additional power corrections $O(m_\tau^{-2})$ of infra-red origin beyond

those suggested by the operator product expansion.

In conclusion, we have provided a framework based on the Effective Charge formalism for obtaining resummed results for a range of QCD observables from partial knowledge of their Borel transforms. The resulting resummation is RS-invariant, gauge-invariant and includes the exact next-to-leading order (NLO) and next-to-NLO (NNLO) coefficients in any RS. This framework should therefore provide a convenient starting point to obtain an objective measure of the reliability of QCD perturbation theory.

Appendix A

Special functions

A.1 Gamma function

The Gamma function is defined as

$$\Gamma(z) = \int_0^\infty \mathrm{d}t\; e^{-t} t^{z-1}\;, \quad \mathrm{Re}\; z > 0\;, \tag{A.1}$$

and has the properties

$$\begin{aligned} \Gamma(1+\epsilon) &= \epsilon\Gamma(\epsilon) \\ \Gamma(1+\epsilon) &= 1 - \gamma_E\;\epsilon + \left(\frac{\pi^2}{12} + \frac{1}{2}\gamma_E^2\right)\epsilon^2 + O(\epsilon^3)\;, \end{aligned} \tag{A.2}$$

where $\gamma_E = 0.57722\ldots$ is the Euler-Mascheroni constant.

A.2 Factorial function

The factorial function is defined as

$$n! = \int_0^\infty \mathrm{d}x\, x^n \mathrm{e}^{-x}\;. \tag{A.3}$$

For large n the factorial function may be approximated by the Stirling's formula

$$n! \sim \sqrt{2\pi n}\, \mathrm{e}^{n\ln n - n}\;. \tag{A.4}$$

A.3 Riemann zeta function

The Riemann zeta function is defined as

$$\zeta_n \equiv \sum_{k=1}^{\infty} \frac{1}{k^n}\;, \tag{A.5}$$

with $\zeta_3 = 1.20206\ldots$, $\zeta_5 = 1.03693\ldots$.

A.4 Exponential integral function

Exponential integral function

The exponential integral function, with negative argument, is defined as

$$\mathrm{Ei}(x) = -\int_{-x}^{\infty} \mathrm{d}t \frac{\mathrm{e}^{-t}}{t}\ , \quad (x < 0)\ . \tag{A.6}$$

For positive argument, one defines $\mathrm{Ei}(x)$ as a principal value

$$\mathrm{Ei}(x) = -\mathrm{PV}\int_{-x}^{\infty} \mathrm{d}t \frac{\mathrm{e}^{-t}}{t}\ , \quad (x > 0)\ . \tag{A.7}$$

Generalised exponential integral function

The generalised exponential integral function, with complex argument w, is defined for $\mathrm{Re}\, w > 0$ by

$$\mathrm{Ei}(n, w) = \int_{1}^{\infty} \mathrm{d}t \frac{\mathrm{e}^{-wt}}{t^n}\ , \quad (\mathrm{Re}\, w > 0)\ . \tag{A.8}$$

For $\mathrm{Re}\, w < 0$ one must make an analytical continuation to arrive at a function analytic everywhere in the cut complex w-plane, except at w=0; and with a branch cut running along the negative real axis [112]

$$\mathrm{Ei}(n, w) = \frac{(-w)^{n-1}}{(n-1)!}\left[-\ln w - \gamma_E + \sum_{m=1}^{n-1}\frac{1}{m}\right] - \sum_{\substack{m=0 \\ m\neq n-1}}^{\infty} \frac{(-w)^m}{(m-n+1)m!}\ , \quad (\mathrm{Re}\, w < 0)\ , \tag{A.9}$$

with γ_E=0.57722..., the Euler-Mascheroni constant. The $\ln w$ term in Eq.(A.9) means that $\mathrm{Ei}(n, w)$ is not a real function. For instance, for negative real w one has $\mathrm{Ei}(1, -x \pm i\epsilon)$=$\mathrm{Ei}(x) \pm i\pi$, where $\mathrm{Ei}(x)$ is the the principal value Eq.(A.7). To continue $\mathrm{Ei}(n, w)$ as a real function for $\mathrm{Re}\, w < 0$ one makes the replacement $\ln w \to \ln w + i\pi\, \mathrm{sign}(\mathrm{Im}\, w)$.

Interrelations

The following relationships are useful in connecting $\mathrm{Ei}(n, w)$ to $\mathrm{Ei}(x)$ [112]

$$\mathrm{Ei}(-x) = -\mathrm{Ei}(1, x)\ , \qquad (x > 0) \tag{A.10}$$

$$\mathrm{Ei}(x) \pm i\pi = -\mathrm{Ei}(1, -x \pm i\epsilon)\ , \quad (x > 0)\ . \tag{A.11}$$

Appendix B

Evaluation of ρ_k and $\rho_k^{(L)}$

In this Appendix we give details on the proof of Eq.(4.93), and then go on to list the expressions to sixth order for the reversion coefficients. We present the analytic expressions for the first six RS-invariants ρ_k and then tabulate the numerical values of the RS-invariants $\rho_k^{(L)}$ ($k = 2 \ldots 12$), in the leading-b approximation, for all five observables considered in Chapter 4.

B.1 Reversion of a power series

To prove Eq.(4.93) we follow the method of reference [89]. Consider a power series, $D(a)$, which starts at $O(a)$

$$D(a) = d_0 a + d_1 a^2 + \cdots + d_k a^{k+1} + \cdots , \tag{B.1}$$

then its inverse or reversed series, $a(D)$, is defined by

$$a(D) = K_1 D + K_2 D^2 + K_3 D^3 + \cdots + D^k K_k + \cdots . \tag{B.2}$$

We apply the calculus of residues to generate the reversion coefficients K_i. We start with the equality

$$a(D) = \frac{1}{2\pi i} \int_C \mathrm{d}t \frac{t(\mathrm{d}D/\mathrm{d}t)}{D(t) - D(a)} , \tag{B.3}$$

where t is a complex variable. One can verify Eq.(B.3) by calculating the residue of the integrand,

$$\begin{aligned} a_{-1} &= \lim_{t \to a} \frac{(t-a)t(\mathrm{d}D/\mathrm{d}t)}{D(t) - D(a)} \\ &= \lim_{t \to a} \frac{(t-a)t(\mathrm{d}D/\mathrm{d}t)}{D(a) + (t-a)(\mathrm{d}D/\mathrm{d}t) + (t-a)^2(\mathrm{d}^2D/\mathrm{d}t^2)/2! + \cdots - D(a)} \\ &= a(D) . \end{aligned} \tag{B.4}$$

The contour is chosen so that $D(t) \neq 0$ on and within the contour except for the zero of $D(t)$ at the origin; a is then restricted to keep $|D(a)| < |D(t)|$ over the entire contour. The integrand may now be expanded by the binomial theorem to yield

$$a(D) = \sum_{n=0}^{\infty} (D(a))^n \frac{1}{2\pi i} \oint \mathrm{d}t \frac{t(\mathrm{d}D/\mathrm{d}t)}{D(t)^{n+1}} \,. \tag{B.5}$$

Equating the coefficients of equal powers of $D(a)$ in Eq.(B.3) and Eq.(B.5) gives

$$K_n = \frac{1}{2\pi i} \oint \mathrm{d}t \frac{t(\mathrm{d}D/\mathrm{d}t)}{D(t)^{n+1}} \,. \tag{B.6}$$

Integrating Eq.(B.6) by parts we have

$$K_n = \frac{1}{2\pi n i} \oint \mathrm{d}t \frac{1}{D(t)^n} \,. \tag{B.7}$$

Finally one applies the residue theorem to obtain

$$K_n = \frac{1}{n!} \left[\frac{\mathrm{d}^{n-1}}{\mathrm{d}t^{n-1}} \left(\frac{t}{D(t)} \right) \right]_{t=0} \,. \tag{B.8}$$

Using Eq.(B.8) we evaluate the first six reversion coefficients, K_i, to be

$$\begin{aligned}
K_1 &= d_0^{-1} \\
K_2 &= -d_0^{-3} d_1 \\
K_3 &= d_0^{-4} (2 d_0^{-1} d_1^2 - d_2) \\
K_4 &= d_0^{-5} (-5 d_0^{-2} d_1^3 + 5 d_0^{-1} d_1 d_2 - d_3) \\
K_5 &= d_0^{-6} (14 d_0^{-3} d_1^4 - 21 d_0^{-2} d_1^2 d_2 + 3 d_0^{-1} d_2^2 + 6 d_0^{-1} d_1 d_3 - d_4) \\
K_6 &= d_0^{-7} (-42 d_0^{-4} d_1^5 + 84 d_0^{-3} d_1^3 d_2 - 28 d_0^{-2} d_1 d_2^2 - 28 d_0^{-2} d_1^2 d_3 \\
&\quad + 7 d_0^{-1} d_2 d_3 + 7 d_0^{-1} d_1 d_4 - d_5) \,.
\end{aligned} \tag{B.9}$$

Note the reversion coefficients are multinomials in d_i. For our purposes we can set $d_0 = 1$ so that $K_1 = 1$.

Another method of generating the RS-invariants ρ_k using reversion of series is given in reference [43]. The general form of the reversion coefficients was first obtained by McMahon

$$K_n = \sum \frac{(n+1)(n+2)\cdots(n+s)}{p!q!\ldots} (-1)^{s+1} d_i^p d_j^q \ldots \,, \tag{B.10}$$

where the sum is constrained by

$$pi + qj + \cdots = n - 1 \tag{B.11}$$

$$n \geq i \geq j \geq \cdots \geq 0 \tag{B.12}$$

and

$$s+1 \equiv p+q+\cdots \,. \tag{B.13}$$

Using Eq.(4.94) and Eq.(B.10) and equating powers of D an expression for the ρ_k in terms of the reversion coefficients is found

$$-(n+1)K_{n+1} + \sum_{r=0}^{n} c_r \sum_{\sigma_i=n+2} K_{i_1}K_{i_2}\cdots K_{i_3} - \sum_{i=1}^{n} iK_i\rho_{n+1-i} = 0, \quad n>1\,, \tag{B.14}$$

where $i = 1, 2, \cdots, n+1$, $K_1 \equiv 1$, $c_0 \equiv 1$, and $c_1 = c$. The notation $\sum_{\sigma_i=n+2}$ denotes the constrained sum, $i_1 + i_2 + \cdots = m$.

In addition to reversion of series other methods to calculate ρ_k have been promoted [44].

B.2 Exact expressions for ρ_k

Using the procedure outlined in Section 4.3.4 we can evaluate exact expressions for the RS-invariants ρ_k. The first six are given by

$$\begin{aligned}
\rho_1 &= c \\
\rho_2 &= c_2 + d_2 - cd_1 - d_1^2 \\
\rho_3 &= c_3 + 2d_3 - 4d_1d_2 - cd_1^2 - 2\rho_2 d_1 + 2d_1^3 \\
\rho_4 &= c_4 + 3d_4 - 4d_2^2 - 6d_1d_3 - 4d_1^4 + c(d_3 - 3d_1d_2 + d_1^3) \\
&\quad +11d_1^2d_2 - \rho_2(d_2 + 2d_1^2) - 3\rho_3 d_1 \\
\rho_5 &= c_5 + 4d_5 - 8d_1d_4 - 12d_2d_3 + 20d_1d_2^2 + 8d_1^5 - 28d_1^3d_2 + 16d_1^2d_3 \\
&\quad c(2d_4 - 4d_1d_3 + 6d_1^2d_2 - 3d_2^2 - 2d_1^4) - 4\rho_2 d_1 d_2 \\
&\quad -\rho_3(2d_2 + 4d_1^2) - 4\rho_4 d_1 \\
\rho_6 &= c_6 + 5d_6 - 10d_1d_5 - 16d_2d_4 + 21d_1^2d_4 - 73d_1^2d_2^2 - 40d_1^3d_3 + 68d_1^4d_2 \\
&\quad +58d_1d_2d_3 - 16d_1^6 + 12d_2^3 - 9d_3^2 - 5d_1\rho_5 - (3d_2 + 7d_1^2)\rho_4 \\
&\quad -(d_3 + 7d_1d_2 + 2d_1^3)\rho_3 + (d_4 - 4d_1d_3 + 2d_1^2d_2 - d_1^4 - 3d_2^2)\rho_2 \\
&\quad +c(3d_5 - 5d_1d_4 + 12d_1d_2^2 - 9d_2d_3 + 9d_1^2d_3 - 15d_1^3d_2 + 4d_1^5)
\end{aligned} \tag{B.15}$$

In addition there is the Q-dependent NLO RS-invariant

$$\rho_0 = \tau - d_1\,. \tag{B.16}$$

B.3 Numerical values of ρ_2 and $\rho_k^{(L)}$ for QCD observables

In section 4.4.4 we outlined the procedure used to numerically evaluate the RS-invariants $\rho_k^{(L)}$ appropriate in the leading-b resummation.

We start by tabulating the exactly calculable values of the NNLO RS-invariant ρ_2 for the five quantities considered in Chapters 4 and 5.

Observable	$N_f = 3$	$N_f = 4$	$N_f = 5$
$\tilde{D}$	+5.237828	-1.134306	-2.969366
$\tilde{R}$	-11.41713	-13.14463	-15.05506
$\tilde{R}_\tau$	-5.475723	–	–
$\tilde{K}$	+5.475683	+1.330399	-2.869499
$\tilde{U}$	+4.990119	+1.203003	-2.714981

Table B.1: Numerical values of ρ_2 for the five quantities resummed.

The following tables tabulate the numerical values of $\rho_k^{(L)}$ ($k = 2 \ldots 12$).

k	$\rho_k^{(k)}$	$\rho_k^{(L)}$		
		$N_f = 3$	$N_f = 4$	$N_f = 5$
2	+.6562246	+13.28855	+11.39279	+9.642856
3	−.8996256	−81.97838	−65.07708	−50.67474
4	+4.021468	+1640.053	+1212.103	+868.3423
5	−12.78539	−23592.64	−16056.75	−10582.71
6	+59.59474	+494860.8	+311846.2	+189089.5
7	−273.9652	-1.023724×10^7	-5.973332×10^6	-3.332203×10^6
8	+1479.987	$+2.488616 \times 10^8$	$+1.344522 \times 10^8$	$+6.900340 \times 10^7$
9	−8460.992	-6.402269×10^9	-3.202728×10^9	-1.512205×10^9
10	+53221.50	$+1.812225 \times 10^{11}$	$+8.394110 \times 10^{11}$	$+3.646304 \times 10^{10}$
11	−357704.1	-5.481022×10^{12}	-2.350716×10^{12}	-9.393412×10^{11}
12	$+2.584970 \times 10^6$	$+1.782402 \times 10^{14}$	$+7.078163 \times 10^{13}$	$+2.602403 \times 10^{13}$

Table B.2: Values of the RS-invariants $\rho_k^{(L)}$ for the Adler D-function.

k	$\rho_k^{(k)}$	$\rho_k^{(L)}$		
		$N_f = 3$	$N_f = 4$	$N_f = 5$
2	$-.1662425$	-3.366410	-2.886154	-2.442841
3	$-.8996256$	-81.97830	-65.07708	-50.67474
4	$-.0257357$	-10.55325	-7.756951	-5.557025
5	-3.906440	-7208.481	-4905.971	-3233.435
6	$+7.504104$	$+62312.32$	$+39267.33$	$+23809.94$
7	-44.20062	-1.651642×10^6	-963717.4	-537606.5
8	$+181.6950$	$+3.055224 \times 10^7$	$+1.650642 \times 10^7$	$+8.471407 \times 10^6$
9	-982.3713	-7.433413×10^8	-3.718557×10^8	-1.755759×10^8
10	$+5446.158$	$+1.854451 \times 10^{10}$	$+8.589696 \times 10^9$	$+3.731265 \times 10^9$
11	-33499.41	-5.133041×10^{11}	-2.201474×10^{11}	-8.797911×10^{10}
12	$+220963.8$	$+1.523601 \times 10^{13}$	6.050431×10^{12}	$+2.224540 \times 10^{12}$

Table B.3: Values of the RS-invariants $\rho_k^{(L)}$ for the R-ratio.

k	$\rho_k^{(k)}$	$\rho_k^{(L)}$
		$N_f = 3$
2	$+.1271603$	$+2.574996$
3	$-.3732946$	-34.01647
4	$+1.071680$	$+439.4560$
5	-3.255455	-6007.231
6	$+12.33325$	$+102412.4$
7	-52.12422	-1.947723×10^6
8	$+246.2552$	$+4.140812 \times 10^7$
9	-1279.663	-9.682960×10^8
10	$+7270.934$	$+2.475799 \times 10^{10}$
11	-44809.01	-6.865988×10^{11}
12	$+297851.1$	$+2.053758 \times 10^{13}$

Table B.4: Values of the RS-invariants $\rho_k^{(L)}$ for the R_τ-ratio; note $N_f = 3$.

k	$\rho_k^{(k)}$	$\rho_k^{(L)}$		
		$N_f = 3$	$N_f = 4$	$N_f = 5$
2	+.5972222	+12.09375	+10.36844	+8.775849
3	+.0185185	+1.687500	+1.339592	+1.043124
4	+3.803434	+1559.646	+1146.386	+821.2629
5	+.1450617	+267.6797	+182.1783	+120.0703
6	+48.91530	+406181.2	+255963.0	+155204.5
7	+2.529210	+94508.86	+55145.01	+30762.46
8	+1025.929	$+1.725112 \times 10^8$	$+9.320456 \times 10^7$	$+4.783326 \times 10^7$
9	+66.89162	$+5.061559 \times 10^7$	$+2.532040 \times 10^7$	$+1.195531 \times 10^7$
10	+31439.96	$+1.070550 \times 10^{11}$	$+4.958719 \times 10^{10}$	$+2.154010 \times 10^{10}$
11	+2472.913	$+3.789191 \times 10^{10}$	$+1.625119 \times 10^{10}$	$+6.494583 \times 10^9$
12	$+1.323278 \times 10^6$	$+9.124335 \times 10^{13}$	$+3.623399 \times 10^{13}$	$+1.332202 \times 10^{13}$

Table B.5: Values of the RS-invariants $\rho_k^{(L)}$ for the Polarized Bjorken (PBj) sum rule and Gross-Llewellyn Smith (GLS) sum rule.

k	$\rho_k^{(k)}$	$\rho_k^{(L)}$		
		$N_f = 3$	$N_f = 4$	$N_f = 5$
2	+.3750000	+7.593750	+6.510417	+5.510417
3	+.5000000	+45.56250	+36.16898	+28.16435
4	+1.828125	+749.6455	+551.0118	+394.7410
5	+5.250000	+9687.727	+6593.304	+4345.525
6	+21.59766	+179341.9	+113015.8	+68527.70
7	+89.50781	$+3.344634 \times 10^6$	$+1.951561 \times 10^6$	$+1.088672 \times 10^6$
8	+437.4719	$+7.356145 \times 10^7$	$+3.974296 \times 10^7$	$+2.039684 \times 10^7$
9	+2281.066	$+1.726039 \times 10^9$	$+8.634491 \times 10^8$	$+4.076873 \times 10^8$
10	+13173.68	$+4.485722 \times 10^{10}$	$+2.077757 \times 10^{10}$	$+9.025537 \times 10^9$
11	+81742.60	$+1.252524 \times 10^{12}$	$+5.371862 \times 10^{11}$	$+2.146897 \times 10^{11}$
12	+548481.3	$+3.781917 \times 10^{13}$	$+1.501851 \times 10^{13}$	$+5.521802 \times 10^{12}$

Table B.6: Values of the RS-invariants $\rho_k^{(L)}$ for the (unpolarized) Bjorken (Bj) sum rule.

Appendix C

RS-invariants for $\tilde{R}$, $\tilde{R}_T$ from $\tilde{D}$

This Appendix we sketch the method used to obtain the analytical continuation terms that link the RS-invariants for the two Minkowski observables $\tilde{R}$, $\tilde{R}_\tau$ to those of the Euclidean Adler D-function. We present the explicit expressions connecting $\rho_k^{R_\tau}$, ρ_k^R with ρ_k^D.

C.1 Power series expansion for $\hat{R}(s_0)$

To relate the $\hat{R}$, $\tilde{R}_\tau$ Minkowski perturbative coefficients r_k, r_k^τ to the Euclidean D-function d_k coefficients of $\tilde{D}$, we start with Eq.(5.7)

$$\hat{R}(s_0) = \tilde{D}(s_0) + \sum_{n=1}^{\infty} \left(\frac{-ib}{2}\right)^n \frac{w_n}{n!} \left[\rho(x)\frac{\mathrm{d}}{\mathrm{d}x}\right]^{n-1} \rho(x)\Big|_{x=\tilde{D}(s_0)} . \tag{C.1}$$

Here w_n denotes moments of the weight function $W(\theta)$,

$$w_n = \frac{1}{2\pi}\int_{-\pi}^{\pi} \mathrm{d}\theta\, \theta^n\, W(\theta)\,. \tag{C.2}$$

For $\tilde{R}$ we set $W(\theta) = 1$ in Eq.(C.2) to give

$$w_n = \frac{\pi^n}{n+1} \;\; (n \;\text{even}), \quad w_n = 0 \;\; (n \;\text{odd})\,. \tag{C.3}$$

Similarly, for $\tilde{R}_\tau$ we set $W_\tau(\theta) = (1 + 2\mathrm{e}^{i\theta} - 2\mathrm{e}^{3i\theta} - \mathrm{e}^{4i\theta})$ in Eq.(C.2) to give

$$\begin{aligned} w_1 &= \frac{19}{12}i \\ w_2 &= \frac{1}{3}\pi^2 - \frac{265}{72} \\ w_3 &= \frac{19}{12}i\pi^2 - \frac{3355}{288}i \end{aligned}$$

$$
\begin{aligned}
w_4 &= \frac{1}{5}\pi^4 - \frac{265}{36}\pi^2 + \frac{41041}{864} \\
w_5 &= \frac{19}{12}i\pi^4 - \frac{16775}{532}i\pi^2 + \frac{2479295}{10368}i \\
w_6 &= \frac{1}{7}\pi^6 - \frac{265}{24}\pi^4 + \frac{205205}{864}\pi^2 - \frac{29822525}{20736} \\
&\vdots
\end{aligned}
$$

Expanding Eq.(C.1) gives the power series expansion

$$
\begin{aligned}
\hat{R}(s_0) = \hat{D}(s_0) &- \frac{ib}{2}w_1\rho - \frac{b^2}{8}w_2\rho\rho' + \frac{ib^3}{48}w_3(\rho\rho'^2 + \rho\rho'') \\
&+ \frac{b^4}{384}w_4(\rho\rho'^3 + 4\rho^2\rho'\rho'' + \rho^3\rho''') \\
&- \frac{ib^5}{3840}w_5(\rho\rho'^4 + 11\rho^2\rho'^2\rho'' + 4\rho^3\rho'' + 7\rho^3\rho'\rho''' + \rho^4\rho'''') \\
&- \frac{b^6}{46080}w_6(\rho\rho'^5 + 26\rho^2\rho'^3\rho'' + 34\rho^3\rho'\rho''^2 + 32\rho^3\rho'^2\rho''' \\
&+ 15\rho^4\rho''\rho''' + 11\rho^4\rho'\rho'''' + \rho^5\rho''''') + \cdots . \qquad \text{(C.4)}
\end{aligned}
$$

Primes denote differentiation of $\rho(x)$ with respect to x, evaluated at $x = \hat{D}(s_0)$. Successive terms are RS-invariants resulting from the resummation to all-orders of analytical continuation terms proportional to $\pi^2 b^2$, $\pi^4 b^4$, $\cdots$, respectively.

To obtain the r_k, r_k^τ in terms of $d_{i\leq k}$ and $c_{i\leq k}$ we replace $\rho(x)$ and its derivatives with expressions in terms of $\hat{D}(s_0)$

$$
\begin{aligned}
\rho(x) &\to \rho(\hat{D}(s_0)) = \sum_{i=1}^{k} \rho_i \hat{D}(s_0)^{i+2} \\
\rho'(x) &\to \rho'(\hat{D}(s_0)) = \sum_{i=1}^{k} (i+2)\rho_i \hat{D}(s_0)^{i+1} \\
&\vdots
\end{aligned}
$$

On substituting

$$
\hat{D}(s_0) = a + d_1 a^2 + d_2 a^3 + \cdots + d_k a^{k+1} , \qquad \text{(C.5)}
$$

and isolating the coefficient of a^{k+1} one can directly obtain r_k, r_k^τ in terms of $d_{i\leq k}$, $\rho_{i\leq k}$ and c. The resulting calculated expressions for r_k, r_k^τ are then in agreement with the results available in the literature for $k \leq 5$ [104] on using Eq.(B.15) to re-express $\rho_{i\leq k}$ invariants in terms of beta-function coefficients $c_{i\leq k}$ and perturbative coefficients $d_{i\leq k}$.

C.2 Analytical continuation terms linking r_k^τ, r_k with d_k

For the R-ratio from Eq.(C.4) the first six relations are then

$$
\begin{aligned}
r_1 &= d_1 \\
r_2 &= d_2 - \frac{1}{12}\pi^2 b^2 \\
r_3 &= d_3 - \frac{1}{24}(6d_1 + 5c)\pi^2 b^2 \\
r_4 &= d_4 - \frac{1}{24}(12d_2 + 14cd_1 + 3c^2 + 6c_2)\pi^2 b^2 + \frac{1}{80}\pi^4 b^4 \\
r_5 &= d_5 - \frac{1}{24}(20d_3 + 27cd_2 + 8c^2 d_1 + 7cc_2 + 16c_2 d_1 + 7c_3)\pi^2 b^2 \\
&\quad + \frac{1}{960}(60d_1 + 77c)\pi^4 b^4 \\
r_6 &= d_6 - \frac{1}{24}(30d_4 + 44cd_3 + 15c^2 d_2 + 30c_2 d_2 + 18cc_2 d_1 + 18c_3 d_1 + 4c_2^2 + 8cc_3 + 8c_4)\pi^2 b^2 \\
&\quad + \frac{1}{480}(90d_2 + 171cd_1 + 85c^2 + 60c_2)\pi^4 b^4 - \frac{1}{448}\pi^6 b^6
\end{aligned}
\tag{C.6}
$$

For R_τ from Eq.(C.4) we obtain

$$
\begin{aligned}
r_1^\tau &= d_1 + I_1 b \\
r_2^\tau &= d_2 + (2d_1 + c)I_1 b + I_2 b^2 \\
r_3^\tau &= d_3 + (3d_2 + 2cd_1 + c_2)I_1 b + \frac{1}{2}(6d_1 + 5_c)I_2 b^2 + I_3 b^3 \\
r_4^\tau &= d_4 + (4d_3 + 3cd_2 + 2c_2 d_1 + c_3)I_1 b + \frac{1}{2}(12d_2 + 14cd_1 + 3c^2 + 6c_2)I_2 b^2 \\
&\quad + \frac{1}{3}(12d_1 + 13c)I_3 b^3 + I_4 b^4 \\
r_5^\tau &= d_5 + (5d_4 + 4cd_3 + 3c_2 d_2 + 2c_3 d_1 + c_4)I_1 b \\
&\quad + \frac{1}{2}(20d_3 + 27cd_2 + 8c^2 d_1 + 16c_2 d_1 + 7cc_2 + 7c_3)I_2 b^2 \\
&\quad + \frac{1}{6}(60d_2 + 94cd_1 + 35c^2 + 36c_2)I_3 b^3 + \frac{1}{12}(60d_1 + 77c)I_4 b^4 + I_5 b^5 \\
r_6^\tau &= d_6 + (6d_5 + 5cd_4 + 4c_2 d_3 + 3c_3 d_2 + 2c_4 d_1 + c_5)I_1 b \\
&\quad + \frac{1}{2}(30d_4 + 44cd_3 + 30c_2 d_2 + 15c^2 d_2 + 18c_3 d_1 + 18cc_2 d_1 + 4c_2^2 + 8cc_3 + 8c_4)I_2 b^2 \\
&\quad + \frac{1}{6}(120d_3 + 222cd_2 + 120c_2 d_1 + 118c^2 d_1 + 15c^3 + 48c_3 + 132cc_2)I_3 b^3 \\
&\quad + \frac{1}{6}(90d_2 + 171cd_1 + 85c^2 + 60c_2)I_4 b^4 \\
&\quad + \frac{1}{10}(60d_1 + 87c)I_5 b^5 + I_6 b^6
\end{aligned}
\tag{C.7}
$$

where for convenience we assign

$$\begin{aligned}
I_1 &= \frac{19}{24} \\
I_2 &= \frac{265}{288} - \frac{1}{12}\pi^2 \\
I_3 &= \frac{3355}{2304} - \frac{19}{96}\pi^2 \\
I_4 &= \frac{41041}{13824} - \frac{265}{576}\pi^2 + \frac{1}{80}\pi^4 \\
I_5 &= \frac{2479295}{331776} - \frac{16775}{13824}\pi^2 + \frac{19}{384}\pi^4 \\
I_6 &= \frac{29822525}{1327104} - \frac{205205}{55296}\pi^2 + \frac{265}{1536}\pi^4 - \frac{1}{448}\pi^6
\end{aligned}$$

The more complicated structure for R_τ is a direct result of the non-trivial weight function $W_\tau(\theta)$. Note Eq.(C.6) and Eq.(C.7) absorb all the effects of analytical continuation. The calculated expressions for $\tilde{R}$ and $\tilde{R}_\tau$ are in agreement with the results available in the literature for $k \leq 5$ [104],

C.3 Analytical continuation terms linking $\rho_k^{R_\tau}$, ρ_k^R with ρ_k^D

To relate the EC RS-invariants ρ_k^R and $\rho_k^{R_\tau}$ corresponding to $\tilde{R}$ and $\tilde{R}_\tau$ to the ρ_k^D connected with $\tilde{D}$ [95] we make use of Eq.(C.6) and Eq.(C.7). This is most easily accomplished by evaluating r_k and r_k^τ in the EC scheme for $\tilde{D}$, so that we can set $d_1 = d_2 = \cdots = 0$ in Eq.(C.6) and Eq.(C.7). These $r_k(d_i = 0)$ and $r_k^\tau(d_i = 0)$ are simply the coefficient of $\tilde{D}^{k+1}$ on the right-hand side of Eq.(C.1). One can then use the expressions in Eq.(B.15) for $\tilde{R}$, $\tilde{R}_\tau$ with $c_k = \rho_k^D$ to obtain the required relations.

For $\tilde{R}$ we can relate the Minkowski invariants ρ_k^R $(k \leq 6)$ to the corresponding Euclidean invariants ρ_k^D in the following manner

$$\begin{aligned}
\rho_2^R &= \rho_2^D - \frac{1}{12}b^2\pi^2 \\
\rho_3^R &= \rho_3^D - \frac{5}{12}cb^2\pi^2 \\
\rho_4^R &= \rho_4^D - \frac{1}{12}(8\rho_2^D + 7c^2)b^2\pi^2 + \frac{1}{360}b^4\pi^4 \\
\rho_5^R &= \rho_5^D - \frac{1}{12}(12\rho_3^D + 20\rho_2^D c + 3c^3)b^2\pi^2 + \frac{17}{360}cb^4\pi^4 \\
\rho_6^R &= \rho_6^D - \frac{1}{12}(17\rho_4^D + 28\rho_3^D c + 13(\rho_2^D)^2 + 12\rho_2^D c)b^2\pi^2
\end{aligned} \tag{C.8}$$

$$+\frac{1}{720}(99\rho_2^D + 137c^2)b^4\pi^4 - \frac{1}{20160}b^6\pi^6$$

Again, for $\hat{R}_\tau$ we have more complicated relations.

$$\begin{aligned}
\rho_2^{R_\tau} &= \rho_2^D + J_2 b^2 \\
\rho_3^{R_\tau} &= \rho_3^D + 5cJ_2 b^2 + J_3 b^3 \\
\rho_4^{R_\tau} &= \rho_4^D + (8\rho_2^D + 7c^2)J_2 b^2 + 7cJ_3 b^3 + J_4 b^4 \\
\rho_5^{R_\tau} &= \rho_5^D + (12\rho_3^D + 20\rho_2^D c + 3c^3)J_2 b^2 + (12\rho_2^D + 16c^2)J_3 b^3 \\
&\quad + \frac{1}{9}(83J_4 + 28J_2^2)cb^4 + J_5 b^5 \\
\rho_6^{R_\tau} &= \rho_6^D + (17\rho_4^D + 28\rho_3^D c\pi^2 + 13(\rho_2^D)^2 + 12\rho_2^D c^2)J_2 b^2 \\
&\quad + \frac{1}{2}(39\rho_3^D + 99\rho_2^D c + 30c^3)J_3 b^3 \\
&\quad + \frac{1}{36}(612\rho_2^D + 1081c^2)J_4 b^4 + \frac{1}{18}(234\rho_2^D + 277c^2)J_2^2 b^4 \\
&\quad + \frac{1}{8}(93J_5 + 60J_3 J_2)cb^5 + J_6 b^6
\end{aligned} \tag{C.9}$$

where for convenience we have assigned

$$\begin{aligned}
J_2 &= \frac{169}{576} - \frac{1}{12}\pi^2 \\
J_3 &= \frac{1819}{3456} \\
J_4 &= \frac{246779}{165888} - \frac{169}{864}\pi^2 + \frac{1}{360}\pi^4 \\
J_5 &= \frac{269203}{55296} - \frac{1819}{3456}\pi^2 \\
J_6 &= \frac{392305009}{21233664} - \frac{973531}{442368}\pi^2 + \frac{1859}{46080}\pi^4 - \frac{1}{20160}\pi^6
\end{aligned}$$

References

[1] T. Muta, *Foundations of Quantum Chromodynamics*, World Scientific Publishing (1987).

[2] M.R. Pennington, Reports in Progress of Physics, Vol. **46** (1983) 393.

[3] R.K. Ellis, W.J. Stirling and B.R. Webber, *QCD and Collider Physics*, Cambridge University Press (1996).

[4] R. D. Field, *Applications of Perturbative QCD*, Frontiers in Physics Series, Addison-Wesley Publishing (1989).

[5] M. Gell-Mann, in *QCD, 20 years later*, P.M. Zerwas and H.A. Kastrup (eds.), World Scientific Publishing (1993).

[6] M. Kaku, *Quantum Field Theory: A Modern Introduction*, Oxford University Press (1993).
L. H. Ryder, *Quantum Field Theory*, Cambridge University Press (1992).

[7] S. Weinberg, Phys. Rev. **118** (1960) 838.

[8] F. Bloch and A. Nordsieck, Phys. Rev. **52** (1937) 54.
T. Kinoshita, J. Math. Phys, **3** (1962) 650

[9] G. 't Hooft and M. Veltman, Nucl. Phys **B44** (1972) 199.

[10] J. Collins, *Renormalization*, Cambridge University Press (1992).

[11] M. Gell-Mann and F. Low, Phys. Rev. **95** (1954) 1300.

[12] E.C.G. Stueckelberg and A. Petermann, Helv. Phys. Acta **26** (1953) 449.

[13] D. Gross and F. Wilczek, Phys. Rev. Lett **26** (1973) 1343;
H.D. Politzer, Phys. Rev. Lett **26** (1973) 1346.

[14] K.G. Wilson, Phys. Rev. **179** (1969) 1499.

[15] M.A. Shifman, A.I. Vainshtein and V.I. Zakharov, Nucl. Phys. **B147** (1979) 385, 448, 519.

[16] G. Grunberg, Phys. Lett. **B325** (1994) 441.

[17] K.G. Chetyrkin, A.L. Kataev and F.V. Tkachov, Phys. Lett. **B85** (1979) 277;
M. Dine and J. Sapirstein, Phys. Rev. Lett. **43** (1979) 668;
W. Celmaster and R.J. Gonsalves, Phys. Lett. **B44** (1980) 560.

[18] S.G. Gorishny, A.L. Kataev and S.A. Larin, Phys. Lett. **B259** (1991) 144;
L.R. Surguladze and M.A. Samuel, Phys. Rev. Lett. **66** (1991) 560; **66** (1991) 2416 (E).

[19] A. Pich, "QCD tests from tau decays", talk given at 20th John Hopkins Workshop: Non-perturbative particle theory and experimental tests, Heidelberg, 1996.

[20] K. Schilder and M.D. Tran, Phys. Rev. **D29** (1984) 570.

[21] E. Braaten, Phys. Rev. Lett. **60** (1988) 1606; Phys. Rev. **D39** (1989) 1458.

[22] E. Braaten, S. Narison and A. Pich, Nucl. Phys. **B373** (1992) 581.

[23] K.G. Chetyrkin and A. Kwiatkowski, Z. Phys. **C59** (1993) 525.

[24] A. Hoecker, "Vector and axial-vector spectral function, talk given at TAU 96 conference, Colorado, 1996.

[25] P. Weber, "Review of tau lifetime measurements", talk given at TAU 96 conference, Colorado, 1996.

[26] W.J. Marciano and A. Sirlin, Phys. Rev. Lett. **61** (1988) 1815; **56** (1986) 22.

[27] E. Braaten and C.S. Li, Phys. Rev. **D42** (1990) 3888.

[28] S.G. Gorishny and S.A. Larin, Phys. Lett. **B172** (1986) 109;
E.B. Zijlstra and W. van Neerven, Phys. Lett. **B297** (1992) 377.

[29] S.A. Larin and J.A.M. Vermaseren, Phys. Lett. **B259** (1991) 345.

[30] J.D. Bjorken, Phys. Rev. **148** (1966) 1467; Phys. Rev. **D1** (1970) 1376.

[31] K.G. Chetyrkin, S.G. Gorishny, S.A. Larin and F.V. Tkachov, Phys. Lett. **B137** (1980) 230;

[32] S.A. Larin, F.V. Tkachov and J.A.M. Vermaseren, Phys. Rev. Lett **66** (1991) 862.

[33] D.J. Gross and C.H. Llewellyn Smith, Nucl. Phys. **B14** (1969) 337.

[34] P.N. Burrows, "Review of α_s measurements", Proc.XXVIII.Int.Conf. on High Energy Physics, Warsaw, July 1996. SLAC-PUB-7293 (1996).

[35] T. Applequist and J. Carazzone, Phys. Rev. **D11** (1975) 2856.

[36] W. Bernreuther and W. Wetzel, Nucl. Phys. **B197** (1982) 228.
S.A. Larin, T. van Ritbergen, and J.A.M. Vermaseren, Nucl. Phys **B438** (1995) 278.

[37] P.M. Stevenson, Phys. Rev. **D23** (1981) 2916.

[38] D.T. Barclay, C.J. Maxwell and M.T. Reader, Phys. Rev **D49** (1994) 3480.

[39] D.R.T. Jones, Nucl. Phys. **B75** (1974) 537;
W.E. Caswell, Phys. Lett. **33** (1974) 244.

[40] W. Celmaster and R.J. Gonslaves, Phys. Rev. **D20** (1979) 1420.

[41] Particle Data Group, R.M. Barnett *et al.*, Phys. Rev. **D54** (1996) 1.

[42] G. Grunberg, Phys. Lett. **B95** (1980) 70; Phys. Rev. **D29** (1984) 2315.

[43] C.J. Maxwell, Phys. Rev. **D29** (1984) 2884.

[44] P.M. Stevenson, Phys. Rev. **D33** (1986) 3130 .

[45] J.A. Nicholls, Ph.D. thesis, "Optimization and the convergence of perturbation series", Durham (1990) (unpublished).

[46] W.A. Bardeen, A.J. Buras, D.W. Duke and T. Muta, Phys. Rev. **18** (1978) 3998.

[47] W. Celmaster and R.J. Gonsalves, Phys. Rev. **D21** (1980) 3112 .

[48] O.V. Tarasov, A.A. Vladimirov, and A.Yu. Zharkov, Phys. Lett **B93** (1980) 429.
S.A. Larin and J.A.M. Vermaseren, Phys. Lett. **B 303** (1993) 334.

[49] S.A. Larin, T. Van Ritbergen and J.A.M. Vermaseren, [hep-ph/9701390].

[50] G.'t Hooft, in *Deeper pathways in high-energy physics*, B. Kursunoglu, A. Perlmutter and W. Scott (eds.), Orbis Scientiae, Coral Gables (1977);
in *The Whys of Subnuclear Physics*, Erice lectures 1977, A. Zichichi (ed.), Plenum, New York (1977).

[51] S.J. Brodsky, G.P. Lepage and P.B. Mackenzie, Phys. Rev. **D28** (1983) 228.

[52] G. Grunberg and A.L. Kataev, Phys. Lett **B279** (1992) 352.

[53] C.J. Maxwell, Durham preprint DTP/97/46 [hep-ph/9706365].

[54] M. Beneke, Phys. Lett. **B307** (1993) 154.

[55] P.M. Stevenson, Nucl. Phys. **B231** (1984) 65.

[56] Current Physics – Sources and Comments, vol. 7, *Large-Order Behaviour of Perturbation Theory*, J.C. Gillou and J. Zinn-Justin (eds.), (1990).

[57] J. Fischer, PRA-HEP 97/06 [hep-ph/9704351].

[58] F. Dyson, Phys. Rev. **85** (1952) 631.

[59] G.H. Hardy, *Divergent Series*, Oxford University Press (1949).

[60] D.T. Barclay, Liverpool preprint [hep-ph/9609275].

[61] B. Lautrup, Phys. Lett. **B69** (1977) 109.

[62] M. Beneke and V.M. Braun, Phys. Lett. **B348** (1995) 513.

[63] A.I. Vainshtein and V.I. Zakharov, Phys. Rev. Lett **73** (1994) 1207.

[64] M. Beneke, Nucl. Phys. **B405** (1993) 424.

[65] D.J. Broadhurst, Z. Phys. **C58** (1993) 339.

[66] D.J. Broadhurst and A.L. Kataev, Phys. Lett. **B315** (1993) 179.

[67] M. Beneke and V.M. Braun, Nucl. Phys. **B426** (1994) 301.

[68] M. Neubert and C. Sachrajda, Nucl. Phys. **B438** (1995) 235.

[69] P. Ball, M. Beneke and V.M. Braun, Nucl. Phys. **B452** (1995) 563.

[70] H. Kawai, T. Kinoshita and Y. Okamoto, Phys. Lett. **B260** (1991) 193.

[71] G. Parisi, in *Hadron Structure and Lepton-Hadron Interactions*, Proceedings, Cargèse, 1977, M. Lévy (ed.), Plenum (1979); Phys. Lett. **B76** (1978) 65; Phys. Rep. **49** (1979) 215; Nucl. Phys. **B150** (1979) 163.

[72] C.M. Bender and T.T. Wu, Phys. Rev. Lett. **37** (1976) 117.

[73] A.H. Mueller, in *QCD, 20 years later*, P.M. Zerwas and H.A. Kastrup (eds.). World Scientific Publishing, Singapore, 1993.

[74] A.H. Mueller, Nucl. Phys. **B250** (1985) 327.

[75] F. David, Nucl. Phys. **B234** (1984) 237; **B263** (1986) 637.

[76] C.N. Lovett-Turner and C.J. Maxwell, Nucl. Phys. **B452** (1995) 188.

[77] M. Neubert, Phys. Rev. **D51** (1995) 5924.

[78] M. Neubert, Nucl. Phys. **B463** (1996) 511

[79] M. Girone and M. Neubert, Phys. Rev. Lett. **76** (1996) 3061.

[80] N.J. Watson, Phys. Lett. **B349** (1995) 155; CPT-96-P-3347 [hep-ph/9606381].

[81] A. Denner, S. Dittmaier and G. Weiglein, Phys. Lett. **B333** (1994) 420;
S. Hashimoto, J. Kodaira, Y. Yashui and K. Sasaki, Phys. Rev. **D50** (1994) 7066;
J. Papavassiliou, Phys. Rev. **D51** (1995) 856.

[82] C.N. Lovett–Turner and C.J. Maxwell, Nucl. Phys. **B432** (1994) 147.

[83] M. Beneke, V.M. Braun and N. Kivel, NORDITA 97/17-P [hep-ph/9703389].
C.J. Maxwell, Durham University preprint DTP/97/40 [hep-ph/9706231]

[84] J. Chyla, Phys. Lett. **B356** (1995) 341.

[85] C.J. Maxwell and D.G. Tonge, Nucl. Phys. **B481** (1996) 681.

[86] G. Grunberg, Phys. Rev. **D46** (1992) 2228.

[87] D.J. Broadhurst, private communication.

[88] D.J. Broadhurst and A.G. Grozin, Phys. Rev. **D52** (1995) 4082.

[89] G. Arfken, *Mathematical Methods for Physicists*. Second Edition, Academic Press Inc. (1985).

[90] LEP Collaborations Joint Report. CERN-PPE/93-157 (1993).

[91] R. Marshall, Z. Phys. **C43** (1989) 595.

[92] CCFR-NuTeV collaboration. Contribution to 30th Rencontres de Moriond: QCD and High Energy Hadronic Interactions, Meribel Les Allues, France, 19-25 March 1995, [hep-ex/9506010].

[93] V.M. Braun and A.V. Kolesnichenko, Nucl. Phys. **B283** (1987) 723.

[94] F. Le Diberder and A. Pich, Phys. Lett. **B286** (1992) 147; F. Le Diberder and A. Pich, Phys. Lett. **B289** (1992) 165.

[95] P. Raczka and A. Szymacha, Phys. Rev. **D54** (1996) 3073; Z. Phys. **C70** (1996) 125.

[96] G. Auberson and G. Mennessier, J. Math. Phys. **22** (1981) 2472; Commun. Math. Phys. **100** (1985) 439.

[97] A.C. Mattingly and P.M. Stevenson, Phys. Rev. **D49** (1994) 437.

[98] P.M. Stevenson, Phys. Lett **B331** (1994) 187.

[99] Yu.L. Dokshitzer, G. Marchesini and B.R. Webber, Nucl. Phys. **B469** (1996) 93

[100] G.'t Hooft. Commun. Math. Phys. **86** (1982) 449.

[101] ALEPH Collaboration, D. Buskulic et al, Phys. Lett. **B307** (1993) 209.

[102] CLEO Collaboration, T. Coan et al, Phys. Lett. **B356** (1995) 580.

[103] A.A. Pivovarov, Z. Phys. **C53** (1992) 461.

[104] A.L. Kataev and V.V. Starshenko, Mod. Phys. Lett. **A10** (1995) 235.

[105] C.J. Maxwell and D.G. Tonge. Durham Preprint DTP/97/30 [hep-ph/9705314].

[106] S. Groote, J.G. Korner and A.A. Pivovarov, [hep-ph/9703268].

[107] A. Pich, private communication. This approach is used in the computer program written by F. Le Diberder and widely applied in experimental analyses.

[108] G. Altarelli, P. Nason and G. Ridolfi, Z. Phys. **C68** (1995) 257.

[109] D.E. Soper and L.R. Surguladze, Phys. Rev. **D54** (1996) 4566.

[110] K.G. Chetyrkin, B.A. Kniehl and M. Steinhauser, [hep-ph/9706430].

[111] G. Rodrigo, A. Pich and A. Santamaria, [hep-ph/9707474].

[112] *Handbook of Mathematical Functions*, Milton Abramowitz and Irene A.Stegan (eds.), Dover (1970).